Investigation of the mechanisms of the G2/M phase transition in human cells – the role of Greatwall kinase

CLARE VESELY

A thesis submitted to the University of Sussex for the degree of Doctor of Philosophy

MAY 2013

Genome Damage and Stability Centre
University of Sussex

DECLARATION

I hereby declare that this thesis has not been submitted in this or any other form to any other university for the award of a degree. The work described here is my own except where otherwise stated.

Clare Vesely
May 2013

ACKNOWLEDGMENTS

I would like to acknowledge and thank everyone who has helped me get this far. My family and friends who provided invaluable support and advice. Helfrid for offering me the opportunity to undertake my PhD in his laboratory and for mentoring me and offering guidance throughout all the ups and downs along the way, and everyone in the Hochegger laboratory who also offered their time and assistance to make this work possible. I would also like to thank our collaborators: Dr. Anthony Oliver (from the Genome Damage and Stability Centre) for all his help with understanding Greatwall structurally, and Dr. Victoria Haley (from the Brighton and Sussex Medical School) for her help with the human cancer cell lines.

In particular I would like to note the amazing role of my unquestioningly supportive parents, Sheila and John, wonderful partner, Rich, and incredible sisters' Ann and Louise, who all never wavered in their belief that I could overcome anything I set my mind to and achieve my goals.

My work throughout my PhD was supported by the Medical Research Council.

University of Sussex

Clare Vesely - Doctor of Philosophy

Investigation of the mechanisms of the G2/M phase transition in human cells – the role of Greatwall kinase

SUMMARY

Understanding the mechanisms and factors that govern cell cycle control is key to developing more effective treatments for human diseases, such as cancer. The human MASTL gene encodes an AGC family kinase, Greatwall kinase, that is conserved among higher eukaryotes. The protein contains an unusual bifurcated kinase domain separated by a stretch of nonconserved amino acids. In *Drosophila*, mutations in Greatwall cause the failure of chromosomes to condense resulting in a delayed entry in to and progression through mitosis. In mitotic *Xenopus* egg extracts, immunodepletion of Greatwall results in exit from M phase, characterised by the decondensation of the chromosomes and the reforming of the nuclear envelope. The addition of purified Greatwall to egg extracts immunodepleted for Greatwall causes precocious phosphorylation of Cdc25 and premature entry into mitosis. These reports indicate that Greatwall plays an important role in the control of mitosis but little is known about the function of Greatwall kinase in human cells, its structure, or control of its activity.

This project aimed to elucidate the role of this novel kinase in human cells. To this end, the gene has been cloned and antibodies generated to allow the study of human Greatwall kinase. RNAi-mediated knockdown of Greatwall in HeLa cells caused aberrant mitotic progression and apoptosis. To gain further insight into the mechanism of Greatwall activation, the Greatwall kinase structure was modelled and key motifs of the kinase fold identified. In particular, a key activating phosphorylation was identified, and a specific antibody raised to this site, allowing investigation of the regulation of Greatwall activity at mitotic entry and exit. The use of chemical genetics to attempt to specifically inhibit the kinase in human cells is described. Finally, evidence is presented that Greatwall kinase may represent a promising new biomarker and drug target for cancer therapy.

TABLE OF CONTENTS

ABBREVIATIONS

3D	3-dimensional
A	Alanine
aa	Amino acid
AAV	Adeno-associated viral
ADP	Adenosine diphosphate
ANOVA	Single factor analysis of variance
APC/C	Anaphase-promoting complex/cyclosome
APS	Ammonium persulphate
Arpp19	cAMP-regulated phospho-protein 19
as	ATP-analogue sensitive
ATM	Ataxia telangiectasia mutated kinase
ATP	Adenosine triphosphate
ATR	Ataxia telangiectasia and Rad-3-related kinase
att	Attachment site
bp	Base pairs
BSA	Bovine serum albumin
Bub	Budding uninhibited by benzimidazole
C	Cysteine
C-lobe	Carboxy-terminal lobe
Ca^{2+}	Calcium
$CaCl_2$	Calcium chloride
CAK	CDK-activating kinase
cAMP	Cyclic adenosine monophosphate
Cdc	Cell division cycle
Cdh1	Cell division cycle homologue 1
CDK	Cyclin dependant kinase
CDPK1	Calcium-dependant protein kinase 1
cDNA	Complimentary DNA
cGMP	Cyclic guanosine monophosphate
Chfr	Checkpoint protein with an FHA domain and RING finger

CKI	CDK-inhibitors
cm	Centimetre
CO_2	Carbon dioxide
CPC	Chromosome passenger complex
CSF	Cytostatic factor
D	Aspartic acid
D-box	Destruction box
DAPI	4', 6-diamidino-2-phenylindole
dCTP	Deoxy cytosine triphosphate
ddH_2O	Double distilled water
DDK	Dbf4-dependant kinase
DMEM	Dulbecco's modified eagle's medium
DNA	Deoxyribonucleic acid
DSBs	Double strand breaks
E	Glutamic acid
E.coli	*Escherichia coli*
ECL	Enhanced chemiluminescence
EDTA	Ethylene diamine tetraacetic acid
EGTA	Ethylene glycol tetraacetic acid
Emi2	Endogenous meiotic inhibitor 2
Ensa	α-Endosulfine
es	Electrophile-sensitive
F	Phenylalanine
FACS	Fluorescence assisted cell sorting
FCS	Foetal calf serum
G	Glycine
g	Grams
GDSC	Genome damage and stability centre
GFP	Green fluorescent protein
GVBD	Germinal vesicle breakdown
HAT	Histone acetyltransferase
HBSS	HEPES-buffered saline solution
HCl	Hydrogen chloride

HEK	Human embryonic kidney cells
HRP	Horseradish peroxidase
hTERT	Human telomerase reverse transcriptase
HTP	High-throughput
Inc.	Incorporation
INCENP	Inner centromere protein
INK	Inhibitors of CDK
IP	Immunoprecipitation
IPTG	Isopropylthio-β-galactoside
IR	Ionising radiation
ITRs	Inverted terminal repeats
K	Lysine
K^+	Potassium
KCl	Potassium chloride
Kb	Kilo base
kDa	Kilo daltons
KNL1	Kinetochore-null 1
λ phosphatase	Lambda phosphatase
L	Litre
LB	Lauria Bertani medium
Ltd	Limited
M	Methionine
M phase	Maturation phase
Mad	Mitotic arrest deficient
MAP	Mitogen activated protein
MAST	Microtubule associated serine/threonine
MASTL	Microtubule associated serine/threonine-like
MAT1	Ménage à trois-1
MBP	Myelin basic protein
MCM	Mini-chromosome maintenance
Mdm2	Murine double mutant 2
Mg^{2+}	Magnesium
$MgCl_2$	Magnesium chloride

ml	Millilitre
mM	Millimolar
mm	Millimetre
$MnCl_2$	Manganese chloride
MOI	Multiplicity of infection
MPF	Maturation promoting factor
MPM-2	Mitotic protein monoclonal 2
Mps1	Monopolar spindle 1
mRNA	Messenger RNA
MS	Mass spectrometry
N/A	Not applicable
N-lobe	Amino-terminal lobe
NaCl	Sodium chloride
NaF	Sodium fluoride
NaOH	Sodium hydroxide
Na_3VO_4	Sodium orthovanadate
NCBI	National centre for biotechnology information
NCMR	Non-conserved middle region
NEBD	Nuclear envelope breakdown
NF-κB	Nuclear factor-kappa B
NF-Y	Nuclear transcription factor Y
ng	Nanogram
Ni-NTA	Nickel-nitrilotriacetic acid
NL	The Netherlands
nM	Nanomolar
ORC	Origin recognition complex
PAGE	Polyacrylamide gel electrophoresis
PCAF	p300/CBP-associated factor
PCNA	Proliferating cell nuclear antigen
PCR	Polymerase chain reaction
PDK1	3-phosphoinositide-dependant kinase 1
PHYRE	Protein homology/analogy recognition engine
PI	Propidium iodide

PKA	cAMP-activated protein kinase
PKC	Protein kinase C
PKG	cGMP-dependant protein kinase
PLK1	Polo-like kinase 1
Plx	*Xenopus* PLK
PP1	Protein phosphatase 1
PP2A	Protein phosphatase 2A
pRB	Retinoblastoma protein
pre-RC	Pre-replication complex
PTM	Post-translational modification
R	Arginine
r.p.m.	Revolutions per minute
RFP	Red fluorescent protein
RISC	RNA-induced silencing complex
RNA	Ribonucleic acid
RNAi	RNA interference
RPA	Replication protein A
RPE	Human retinal pigmented epithelium cells
RT PCR	Reverse-transcriptase PCR
S	Serine
S6K	p70 ribosomal S6 kinase
SAC	Spindle assembly checkpoint
Scant	*Scott of the Antarctic*
SDS	Sodium dodecyl sulphate
Ser	Serine
siRNA	Short interfering RNA
Smc	Structural maintenance of chromosomes
sogg	Suppressors of the glycine gatekeeper
SPI/II	Artificial splice transcript I/II
SSC	Saline-sodium citrate
STLC	S-trityl-L-cysteine
T	Threonine
TEMED	N,N,N',N'-tetramethylethylenediamine

Thr	Threonine
Tyr	Tyrosine
µg	Microgram
µl	Microlitre
µM	Micromolar
UK	United Kingdom
USA	United States of America
UTR	Untranslated region
UV	Ultra violet
V	Valine
w/v	Weight per volume
WT	Wildtype
Y	Tyrosine
YFP	Yellow fluorescent protein

CHAPTER 1. Introduction

1.1 The mammalian cell cycle

In 1665 the term ‘cell’ was coined by Robert Hooke who observed small regular units he described as like those monks would live in while studying a slice of cork under a microscope. This term is still used today. It is now known that cells probably first arose on earth around 3.5 billion years ago. Our current understanding of the origins of life informs us that simple primordial cells were formed by spontaneous chemical reactions. Over time they evolved, out-reproducing their competitors, and eventually covering the earth and altering its atmosphere, ultimately giving rise to life itself (Turner 1890; Alberts 2002).

That all living things are comprised of these basic living units and that one cell gives rise to another cell by making a copy of itself and dividing is a theory, known as cell theory, first formed by ideas from Theodor Schwann, Matthias Jakob Schleiden and Rudolf Virchow in the early 17th century. This theory describes the processes that are common to and critical for all organisms and are fundamental for life to exist (Turner 1890).

The cell cycle describes the process by which cells can grow and proliferate to pass on genetic material from one generation to the next. In general it can be broken down into four distinct phases: interphase, comprising G1, G2 and S phases, and mitosis (Howard *et al.* 1951). In interphase cells replicate their DNA during S phase at the end of which their DNA content is precisely duplicated. This is separated by two gap phases known as G1 and G2. In G1 new cells grow, coordinate external signals and prepare to synthesise their DNA. After this, in G2 the final stage of interphase, cells complete DNA replication and prepare to enter mitosis (Alberts 2002; Morgan 2007).

The cell then commits to enter mitosis where it divides its replicated chromosomes. Mitosis is divided into distinct phases: In prophase the chromosomes begin to condense and the nuclear envelope is broken down. Next, in prometaphase and then metaphase, the mitotic spindle is assembled and the chromosomes are aligned on the metaphase plate and attached under tension to each spindle pole. After this, in anaphase, the sister chromatids are separated to each spindle pole, and telophase is the final stage in

which a new nuclear envelope begins to form and the chromosomes start to decondense. Upon completion of mitosis the cell cleaves in two to form two daughter cells by the process of cytokinesis (Alberts 2002; Morgan 2007).

Studies of cell cycle control mechanisms in a wide variety of eukaryotes have revealed that the cell cycle is highly conserved throughout evolution, and is in many respects common to all eukaryotic organisms. It has become increasingly clear that in mammalian cells this continuous sequence of cell proliferation is highly controlled in its timing and sequence, and that this is tightly regulated by complex signalling networks which comprise of the activation and inhibition of many different effector proteins and signalling molecules.

1.2 Cell cycle checkpoints and transitions

To prevent aberrant cell proliferation and genomic instability a number of checkpoints exist. These cell cycle checkpoints ensure that a cell will only transition into the next cell cycle phase once the previous one has been completed successfully. The G1/S checkpoint, or restriction point, serves to shift cells between the quiescent phase and proliferative state. This monitors if a cell is ready to enter S phase and replicate its DNA by assessing the presence of DNA damage and growth factors. The restriction point is the time after which a cell is committed to enter S phase and replicate its DNA even if growth factors are removed (Pardee 1974; Elledge 1996). During the course of the cell cycle the DNA damage response continues to monitor and sense DNA damage, only allowing cell cycle progression if conditions are favourable. The DNA damage checkpoint can arrest the cell cycle in mid S phase (intra-S phase checkpoint) or in late G2 (G2/M checkpoint) (Zhu *et al.* 2004b; Ciccia *et al.* 2010). The cell cycle can also be arrested at the G2/M transition by the stress response that is activated by a range of stress agents. Once a certain point, known as antephase, has been reached the cell is then committed to continue into mitosis (Pines *et al.* 2001). A final checkpoint known as the spindle assembly checkpoint (SAC) acts to ensure accurate chromosome segregation and must be satisfied in late metaphase before the cell can successfully segregate its chromosomes and divide (Musacchio *et al.* 2007). These checkpoints act as surveillance mechanisms and fail-safes to ensure that genomic stability is maintained and that aberrant

cells are not propagated. Mutation or misregulation of checkpoint signalling is common in human diseases such as cancer (Malumbres *et al.* 2009a).

1.3 Molecular models of cell cycle control: ordering the cell cycle

To ensure cell cycle fidelity each phase must occur at the right time in the correct order and this is stringently monitored by the checkpoints. A key question for scientists was what was the molecular mechanism of these phase transitions? Cell cycle regulation was initially studied using two principle model systems: genetic manipulations in yeast and biochemical analysis of early embryonic cell cycles using frog (*Xenopus*) eggs. This led to the formation of two seemingly distinct models for control of the cell cycle: the domino model favoured by the yeast genetists and the clock model favoured by the frog biochemists. In the later decades of the last century the molecular mechanisms were unpicked and found to display elements common to both models allowing the two to be reconciled (Hartwell 1978; Hara *et al.* 1980).

In the 1970s, Leland Hartwell and Paul Nurse pioneered the search for temperature sensitive mutants that disturbed the cell cycle of budding yeast (*Sacchromyces cerevisiae*) and fission yeast (*Schizosaccharomyces pombe*). These mutants were identified by their arrest at distinct stages of the cell cycle. This pointed to genes that were responsible for control of the cell division cycle. These mutants were called Cell division cycle (Cdc) mutants or, depending on their size at the time of cell cycle arrest, Wee mutants. From the phenotypes displayed by these mutants much could be deduced about the role of the gene affected. From these studies the functions of normal wildtype genes required for cell cycle regulation were determined. One gene named Cdc28 in *Sacchromyces cerevisiae* and Cdc2 in *Schizosaccharomyces pombe* was identified to be of critical importance in the control of the cell cycle in these organisms. It was essential for the cell cycle, for Start (the yeast equivalent of the restriction point) and for the control of mitosis. Additionally, Wee1 and Cdc25 were identified as important regulators of Cdc2/Cdc28 (these are discussed in more detail later in this chapter). Experiments using these mutants revealed that if a cell lacks a gene required for initiating or completing a particular cell cycle phase, that phase becomes restrictive and prevents a cell proceeding to later cell cycle phases. This was referred to as the ‘domino model’ of cell cycle regulation as each cell cycle phase is dependent on the proper completion of

the prior phase. This underlies the concept of checkpoint pathways, as the sequential order of the cell cycle is dependant on these signalling events to ensure the fidelity of phase transitions (Hartwell *et al.* 1970; Nurse *et al.* 1976; Beach *et al.* 1982; Hartwell *et al.* 1989; Parker *et al.* 1992; Hoffmann *et al.* 1993).

In *Xenopus* egg extracts the rapid early embryonic divisions do not have gap phases. No cell growth occurs as the eggs undergo cycles of S phase and M phase in rapid succession. This provides a useful system to functionally analyse and purify the factors that drive a cell into mitosis. In 1971, Masui *et al*. postulated the existence of a cytoplasmic biochemical activity that was sufficient to induce entry into M (maturation) phase in *Xenopus* oocytes (Masui *et al.* 1971). They called this activity Maturation Promoting Factor (MPF). In the following decades further cell cycle analysis suggested a mechanism for cell cycle control that was very different to the yeast domino model. Studies pointed to a ticking 'clock' mechanism regulated by a biochemical component, the MPF, present in the cytoplasm that served as a cell cycle engine to drive the cell from one phase to another based on a strict timing mechanism (Smith *et al.* 1971; Hara *et al.* 1980).

Genetic cross-species complementation assays in yeast had confirmed that Cdc2 and Cdc28 were functionally equivalent proteins. This indicated that Cdc2 was a master cell cycle regulator in yeast much like the MPF in *Xenopus*. It took almost two decades for this activity to be purified but in 1987 a breakthrough study was published by Melanie Lee and Paul Nurse that used another cross-species complementation assay. Here they identified the human homologue of Cdc2 and aptly named it CDC2 because it could replace the function of Cdc2 in fission yeast (Lee *et al.* 1987). During this time further illuminating studies in *Xenopus* had defined the MPF as a complex of a cyclin and a catalytic kinase subunit (Dunphy *et al.* 1988). Since Cdc2 and CDC2 were highly evolutionarily conserved proteins that resembled protein kinases, examination of their relationship to the MPF was a logical progression. A final cross-species complementation study revealed that the kinase subunit of MPF in frogs was the same kinase as yeast Cdc2. This allowed for the formation of a final unifying theory of cell cycle control in which the same protein kinase acts as a master controller of mitotic transition. Finally the MPF was identified as a complex of Cyclin Dependent Kinase 1 (CDK1, or CDC2) and its regulatory subunit, cyclin B (Cdc13), which drives entry from G2 into mitosis (Lee *et al.* 1987; Dabauvalle *et al.* 1988; Dunphy *et al.* 1988; Labbe *et al.* 1988; Lohka *et al.* 1988; Langan *et al.* 1989; Minshull *et al.* 1989a; Murray *et al.* 1989; Gautier *et al.* 1990).

These numerous studies in yeast and other organisms have led to the current understanding that the cyclin-CDK complexes are the molecular motors that serve to drive a cell though the different stages of the cell cycle. This brought together the two divergent models of cell cycle regulation. These proteins are remarkably conserved from yeast to humans and govern phase transitions in a sequential order. This has led to a new understanding of the control of the cell cycle as like that of an automatic washing machine: the washing machine model. In this model the cell cycle is likened to a wash cycle. There are a series of stages through which a complete wash cycle must progress i.e. washing the clothes, rinsing them, spinning them dry. Here each phase must be completed in turn before entry into the next phase is permitted. This is analogous to the cell cycle during which the individual stages of cell growth, DNA synthesis and mitosis must be ordered and completed correctly. In both cases a central control mechanism triggers each process in a set sequence (Nurse *et al.* 1976; Felix *et al.* 1989; Hunt 1989; Hunt *et al.* 1992; Hochegger *et al.* 2001).

It is now known that cyclin-CDKs are regulated by highly interconnected control systems. These include feedback loops and other regulatory interactions leading to switch-like activation and inactivation of the cyclin-CDK complexes at different stages of the cell cycle. These regulatory interactions coordinate with one another to ensure the correct order and timing of activation/inactivation and will be discussed here in more detail in the following sections. This system is robust and adaptable relying on multiple mechanisms and cellular inputs to respond to different conditions or component failures (Minshull *et al.* 1989b; Doree *et al.* 2002).

1.4 Cyclins and Cyclin Dependent Kinases (CDKs) controlling the cell cycle

Cyclins were discovered in 1982 by R. Timothy Hunt while studying the cell cycle of sea urchins (Evans *et al.* 1983; Pines *et al.* 1987; Hunt 2004). They were originally named cyclins as their concentration varies in a cyclical fashion during the cell cycle. It is these oscillating levels of cyclins, namely fluctuations in cyclin gene expression and their subsequent destruction by proteolysis, that drive the cell cycle by inducing oscillations in CDK activity (Minshull *et al.* 1990). While CDK levels remain fairly constant throughout the cell cycle, it is the cyclic rise and fall of these cyclins and the subsequent CDK activity that is key to satisfy the checkpoints that exist to monitor

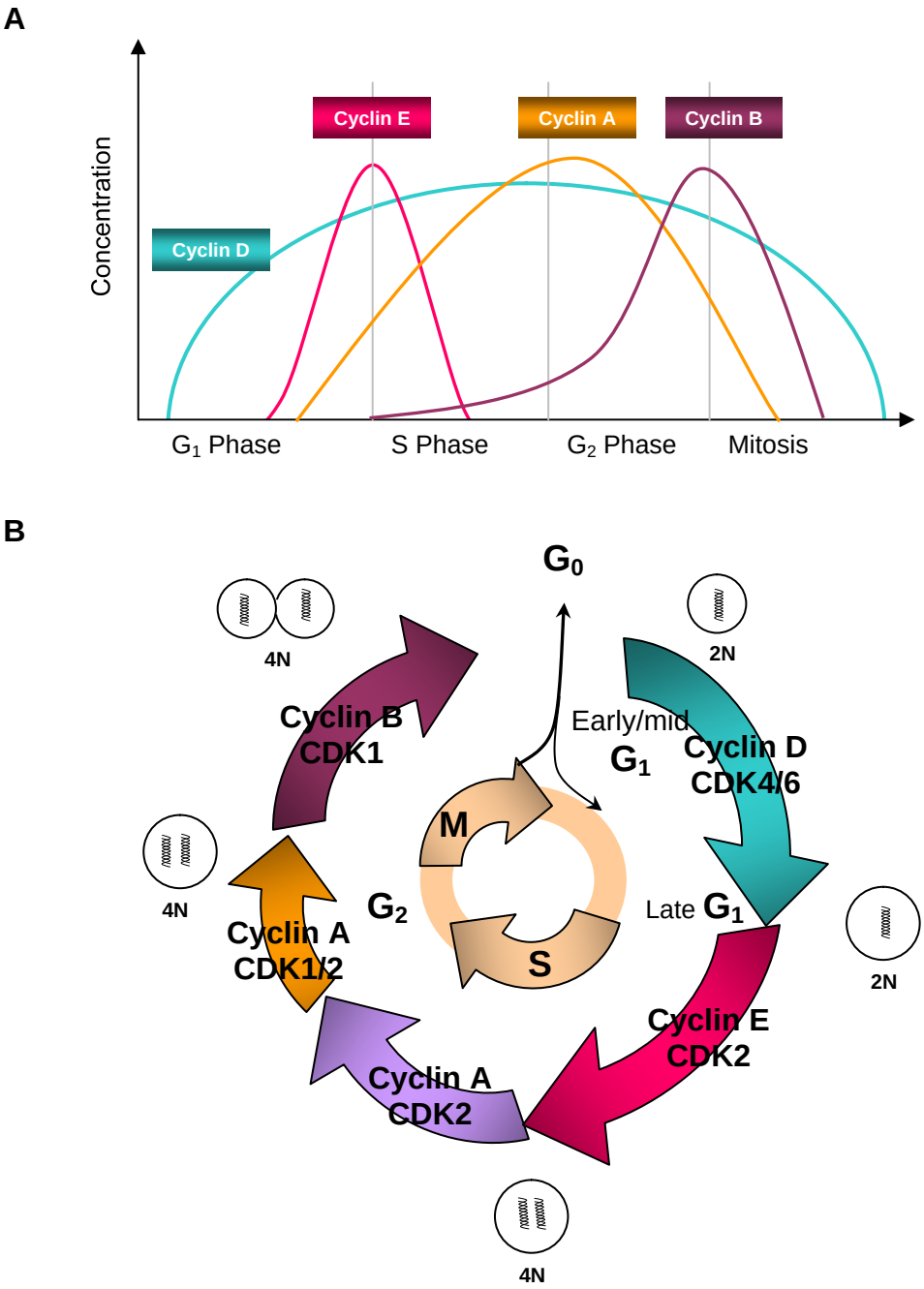

Figure 1.1 Control of the mammalian cell cycle by cyclin-CDKs

(A) Cyclin expression during the cell cycle. D-type cyclin levels are relatively stable throughout the cell cycle but have an important role in early G1. E-type cyclins are expressed at G1/S to drive S phase entry. A-type cyclins allow progression into mitosis from S phase and B-type cyclins are responsible for mitosis. Adapted from Arcadian (2007). **(B)** Cell cycle control by cyclin-CDKs. Schematic representation of mammalian cyclin-CDK complexes involved in progression throughout the different phases of the cell cycle. These are master regulators of the cell cycle. Adapted from Malumbres (2010).

and licence cell cycle progression (**Figure 1.1 A**). It should be noted that now cyclins are classified according to their conserved cyclin box structure and not all cyclins alter in level through the cell cycle (Fung *et al.* 2005; Hochegger *et al.* 2008; Malumbres *et al.* 2009a).

A cyclin forms a complex with a CDK beginning its activation. The active site of CDKs is a small cleft between the small amino-terminal lobe and the larger carboxy-terminal lobe. In 1993 the publication of the crystal structure of CDK2 revealed that cyclin-unbound CDKs have a helix-loop segment that forms the activation- or T-loop and interferes with substrate and ATP-binding (De Bondt *et al.* 1993). Upon binding a cyclin, conformational changes occur to rearrange the T-loop so the active site is no longer blocked and key amino acid residues are moved into place for optimal ATP binding. Cyclins themselves have no enzymatic activity but have binding sites for interactors and substrates as well as serving to target the CDKs to specific subcellular locations (Evans *et al.* 1983; Doree *et al.* 2002; Petri *et al.* 2007).

These cyclin-induced conformational changes of CDKs are important for activity but, in addition, other post-translational modifications of CDKs are required for full activity. An activating phosphorylation on a threonine adjacent to the active site is put on by a CDK-activating kinase (CAK) that is necessary for full activation (Jeffrey *et al.* 1995). The identity of the CAK that performs the phosphorylation varies between organisms, in humans it is a trimeric complex of ménage à trois-1 (MAT1), CDK7 and its cyclin, cyclin H (Kaldis *et al.* 1998). CAK activity is not regulated in a cell cycle dependant manner and remains high throughout all cell cycle phases. The timing of the phosphorylation also varies. For example, in budding yeast it occurs before cyclin binding while in mammalian cells it can only occur after the cyclin has bound. In both it is the cyclin binding that is the limiting step for CDK activation (Makela *et al.* 1994; Russo *et al.* 1996b; Brown *et al.* 1999; Lolli *et al.* 2005).

An additional layer of control occurs in G1 through cyclin dependant kinase inhibitors (CKIs) (Sherr *et al.* 1999). These small polypeptides bind to CDK-cyclin complexes usually in G1, in response to exogenous signals or in response to DNA damage signalling, blocking the kinase activity. There are two families of CKIs in mammals, Inhibitors of CDK4 (INK4) and Cip/Kip family. Discovered in 1993 the INK4 family includes INK4A, INK4B, INK4C and INK4D (Canepa *et al.* 2007). They specifically bind and inhibit the cyclin D binding CDKs, CDK4 and 6, as monomers. The crystal structure of CDK6 bound to INK4 indicated that they bind and cause distortion of

the kinase preventing cyclin or ATP binding (Jeffrey *et al.* 2000). The Cip/Kip family of CKIs include p21, p27 and p57. These regulators can be activating as well as inhibitory regulators of the CDKs (Russo *et al.* 1996a). They negatively regulate cyclin E-CDK2, cyclin A-CDK2, and cyclin B–CDK1 complexes by binding to both the cyclin and the CDK. They also bind to cyclin D-CDK4/6 in early G1 and positively regulate them by mediating the formation of the complexes (LaBaer *et al.* 1997). The outcome of this is the titration of the Cip/Kip family CKIs from cyclin E-CDK2 in G1 allowing its eventual activation to drive cells from G1 into S phase. The active CDK2 feeds back and phosphorylates the CKI targeting it for degradation (Sherr *et al.* 1995). The CKIs ultimately serve as tumour suppressors to restrict proliferation by preventing phosphorylation of the retinoblastoma protein (pRB) in G1 until mitogenic signals cause increased D cyclin expression to achieve sufficient CDK activity to phosphorylate the pocket proteins. Thereby, releasing the EF2s transcription factors to induce gene expression required for cell cycle progression (Sherr *et al.* 1999).

In humans, it is currently known that there are 20 different CDKs that interact with at least 29 cyclins and cyclin-related proteins. Of these, however, only 10 cyclins are known to have a direct role in driving the cell cycle; three D-type, two E-type, two A-type and three B-type cyclins. Four CDKs, CDK1, 2, 4, and 6 are known to have key roles in cell cycle control (Fung *et al.* 2005; Malumbres *et al.* 2009a).

Broadly, there are three interphase CDKs: CDK2, CDK4 and CDK6, and one mitotic CDK: CDK1. Mitogenic signals are first sensed as described previously by expression of the D-type cyclins (cyclin D1, D2 and D3) that bind CDK4 and CDK6 in G1. The formation of the active cyclin D-CDK4/6 complexes causes the partial inactivation of the pocket proteins (pRB, p107 and p130) to allow expression of E-type cyclins (cyclin E1 and E2). These preferentially bind to CDK2, activating CDK2 to further phosphorylate the pocket proteins fully inactivating them. The availability of the E-type cyclins is tightly controlled during the cell cycle and is limited specifically to the early stages of DNA synthesis. For this reason, combined with evidence that inhibition of CDK2 inhibited the cell cycle in human tumour cell lines, it was thought that active cyclin E-CDK2 complexes were a requirement to drive the G1/S transition. During the late stages of DNA synthesis CDK2 is activated by the A-type cyclins (cyclin A1 in germ cells and A2 in somatic cells). These cyclin A-CDK2 complexes drive entry into mitosis from S phase during G2 and at the end of interphase induce expression of the B-type cyclins (cyclin B1, B2 and B3). Cyclin A also associates with CDK1 to facilitate

mitotic entry and is degraded upon nuclear envelope breakdown (NEBD). It is cyclin B-CDK1 active complexes that drive forward commitment to enter and progress through mitosis (**Figure 1.1 B**) (Fung *et al.* 2005; Malumbres *et al.* 2009a; Malumbres *et al.* 2009b).

This classical model that there is a specific CDK to drive each phase of the cell cycle has been recently cast into doubt by genetic studies in mice. That CDK2, 4, and 6 are not essential for the cell cycle in most cell types has been established by the systematic knockout of CDK loci in the mouse germline (Santamaria *et al.* 2007). These studies determined that these CDKs are instead required for development specifically in highly specialised cell types. CDK4 is required for proliferation of pancreatic β-cells and pituitary lactrophs during post-natal development (Rane *et al.* 1999; Tsutsui *et al.* 1999). CDK6 leads to minor problems in cells of erythroid lineage (Malumbres *et al.* 2004). CDK2 knockout mice are viable and do not display any cell cycle defect in somatic cells but are infertile. Thus CDK2 is essential only in meiosis (Berthet *et al.* 2003; Ortega *et al.* 2003; Duensing *et al.* 2006).

CDK1 is the only CDK that is essential for the mammalian cell cycle in mouse embryonic fibroblasts. Knockout mouse models have shown that loss of CDK1 is lethal, with embryos experiencing a cell cycle arrest preventing development beyond the two cell stage (Santamaria *et al.* 2007; Adhikari *et al.* 2012b; Diril *et al.* 2012). Even expression of CDK2 from the CDK1 gene locus, examined by replacement of one gene for the other by homologous recombination, still resulted in early embryonic lethality (Satyanarayana *et al.* 2008).

Ablation of D-type cyclins causes specific developmental defects due to their differential expression, while if all three D-type cyclins are ablated heamatopoitetic defects cause embryonic lethality. This is similar to the phenotype seen for mice lacking CDK4 and 6 and provides evidence that these G1 kinases are functionally activated by the D-type cyclins (Kozar *et al.* 2004; Malumbres *et al.* 2004). Knockout models of cyclin E1 and E2 are also embryonic lethal due to defects in the endoreduplication of trophoblast cells (Geng *et al.* 2003; Parisi *et al.* 2003). Ablation of cyclin A2 causes early embryonic lethality indicating its main role is to activate CDK1, while A1 knockout mice are viable (Murphy *et al.* 1997). Cyclin B1 is essential and mice in which this gene has been ablated die in utero. Mice lacking cyclin B2 develop normally but are less fertile and smaller than wildtype mice (Brandeis *et al.* 1998). Cyclin B3 knockout has not yet been carried out.

Thus it is likely that there is a level of redundancy between the cyclins and their CDK partners. Their essential and overlapping roles are still to be completely elucidated but it is clear that in control of the cell cycle the temporal and spatial control of cyclins and their associated CDKs has many complex layers of regulation. This has led to a minimal-threshold model of cell cycle control replacing the classical model. In this model the differences between interphase and mitotic CDKs is not due to substrate specificity necessarily, but rather result from different localisation and a higher threshold activity required for mitosis than for interphase (Hochegger *et al.* 2008; Malumbres *et al.* 2009a).

1.5 Initiation of cell cycle entry by CDKs

Most adult cells are fully differentiated and in a quiescent state. This resting state is often referred to as G0 and cells in G1 can enter this state in response to extracellular factors signalling that continuation through the cell cycle is not appropriate. Once the cell cycle has been exited they express very few or none of the genes required for the cell cycle. Thus, in order to enter the cell cycle the transcriptional and translational machinery required to specifically express these genes must be activated. In the rapid early divisions of embryogenesis these genes are already active. A repression mechanism acts to suppress these in cells that terminally differentiate during organogenesis (Classon *et al.* 2002; Malumbres 2011). This occurs via pRB and other pocket protein family members p107 and p130. These are transcriptional regulators that repress a wide array of genes including those of cell cycle regulators (Knudsen *et al.* 2006). When hypophosphorylated pRB is active and binds and inhibits the E2F family of transcription factors. These complexes sequester the EF2 transcriptional activators in an inactive form preventing the expression of genes necessary to continue through the cell cycle and enter S phase (Infante *et al.* 2008). In addition, cell cycle gene expression is repressed via pRB-mediated recruitment of polycomb-group proteins, repressor complexes, like the SWI/SNF complex, histone deacetylases and methylases to these genes (Sif *et al.* 1998; Macaluso *et al.* 2006; Sauvageau *et al.* 2008).

In order for the cell cycle to be reactivated this repression must therefore be lifted. Mitogenic signals received by the cell serve to lift pRB-mediated gene repression via activation of the CDKs. These proteins are present even in quiescent cells but are kept inactive due to the absence of their cyclin activators. Mitogenic signalling pathway

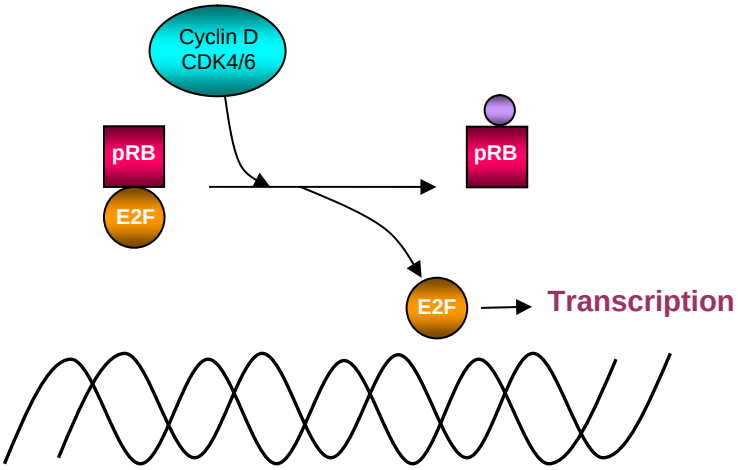

Figure 1.2 Cyclin D-CDK4/6 activation of E2F in G1

Schematic drawing of E2F activation by cyclin-CDK. CDK4 or CDK6 complexed with cyclin D phosphorylates pRB. This then releases E2F to transcribe genes needed to drive cell cycle progression. Phosphorylation is represented by a violet sphere. Adapted from Schafer (1998).

activation leads to the induction of expression of the D and E cyclins that form active complexes with their CDK4/6 and CDK2 binding partners respectively, which can then phosphorylate pRB, inactivating it. This allows the induction of transcription of genes required for cell cycle progression and subsequent cell cycle phases (**Figure 1.2**) (Bandara *et al.* 1991; Schafer 1998; Malumbres 2011).

1.6 S phase

In the next stage of the cell cycle, cyclin E-CDK2 and cyclin A-CDK2 complexes are key to drive cells out of G1 and to carry out DNA replication in S phase. CDK activity is not only critical for DNA replication but also to ensure that replication of the genome occurs only once per cell cycle (Woo *et al.* 2003).

Cyclin E-CDK2 activity peaks during S phase entry, where it has two main functions (Woo *et al.* 2003). Firstly it participates in the release of E2F from pRB, to enable E2F to exhibit transcriptional control of a number of genes required for S phase and driving S phase entry (Lundberg *et al.* 1998). It is thought that the irreversible

inactivation of pRB by cyclin E-CDK2 renders cells independent of mitogenic signals and corresponds to the restriction point (Malumbres *et al.* 2001). Secondly, it phosphorylates components required for the initiation of DNA replication.

Replication of the genomic DNA during S phase is a well choreographed, highly ordered process involving numerous different proteins (Bell *et al.* 2002; Tanaka *et al.* 2010). In eukaryotes, DNA replication is initiated at multiple locations along each chromosome. These are referred to as replication origins (Mendez *et al.* 2003). The replication process begins prior to S phase with the ordered assembly of a multiprotein complex at the replication origins referred to as the pre-replication complex (pre-RC) (Mendez *et al.* 2000; Diffley 2004). Firstly, the Origin Recognition Complex (ORC) proteins associate with the DNA at origin sites and form a platform to recruit Cdc6 and Cdt1 (Mendez *et al.* 2003; Diffley 2004). The recruitment of these two proteins is a critical step in the formation of the pre-RC and both are required for the subsequent loading of six Mini-Chromosome Maintenance (MCM) 2 to 7 proteins (Mendez *et al.* 2000). The MCM2-7 proteins form important components of the pre-RC replicative helicase activity that unwinds the DNA at the origin sites forming templates for DNA polymerase (Pacek *et al.* 2004). These origins are then said to be licensed but the helicase is still inactive and initiating activation requires the additional binding of multiple cofactors and two kinases; Dbf4-dependant kinase (DDK) and CDK (Masai *et al.* 2000; Diffley 2004). The activation of the pre-RC and initiation of DNA replication is known as origin firing. Cdc45 is among the cofactors required for DNA replication to begin. It interacts with the pre-RC and induces loading of RPA and DNA polymerase α to initiate origin firing (Mimura *et al.* 1998; Zou *et al.* 2000). Phosphorylations by cyclin-CDK2 and DDK are essential for Cdc45 loading onto the origins, although it is not clear whether it is cyclin E or A that is involved there is evidence that both can functionally compensate for each other in S phase (Woo *et al.* 2003; Hochegger *et al.* 2008; Zhao *et al.* 2012). The expression of cyclin E peaks before cyclin A at the beginning of S phase indicating that cyclin E-CDK2 complexes likely dominate in early S phase and are replaced by cyclin A-CDK2 complexes later in S phase (Zhao *et al.* 2012). Other specific targets of DDK and CDK2 are still to be fully elucidated in human nuclei but they likely include the MCM2-7 complex, RecQ4, TOPBP1 and Treslin (Tanaka *et al.* 1997; Garcia *et al.* 2005; Xu *et al.* 2009; Kumagai *et al.* 2010). Together, these two kinase activities regulate the formation of the initiation complex and the initiation of replication of licensed origins at the beginning of S phase.

Once replication has begun, bidirectional replication forks are established and both DDK and cyclin E-CDK2 are dispensable for the completion of S phase (Bousset *et al.* 1998; Tanaka *et al.* 2010). They are therefore exclusively required for the initiation of DNA replication. The inactivation of pRB promotes transcription genes required for subsequent cell cycle stages, including cyclin A and B, and cyclin A-CDK2 activity increases as S phase progresses (Schulze *et al.* 1995; Woo *et al.* 2003). Cyclin A-CDK2 complexes phosphorylate numerous targets required for completion and exit from S phase. These include targets that promote activation of pre-RC complexes and also targets that allow elongation and inhibit the formation of new pre-RC complexes (Lundberg *et al.* 1998; Harbour *et al.* 1999; Arata *et al.* 2000; Malumbres *et al.* 2001). Cyclin A has been shown to be associated with replicating DNA and to colocalise with replication foci (Fotedar *et al.* 1991; Cardoso *et al.* 1993). Cyclin A-CDK2 complexes have also been shown to phosphorylate several components of the replication machinery including DNA polymerase α and the processivity factor Proliferating Cell Nuclear Antigen (PCNA) (Nasheuer *et al.* 1991; Prosperi *et al.* 1994).

In 1970 cell-fusion experiments carried out by Johnson and Rao indicated the presence of a re-replication block (Rao *et al.* 1970). The results indicated that only G1 cells are competent to carry out replication of their DNA, while cells that have already completed this process, i.e. G2 cells, were unable to re-replicate their DNA. This re-replication block is key to limit replication to only once per cell cycle preventing genomic instability. It is now understood that this occurs due to the two step nature of the activation of DNA replication (Mendez *et al.* 2003; Woo *et al.* 2003; Remus *et al.* 2009). CDK activity is relatively low in G1 and is permissive to pre-RC assembly and origin licensing (step one). As CDK activity increases in S phase, and cyclin A-CDK2 complexes predominate, DNA replication is initiated and the pre-RCs are activated (step two). At this stage the high CDK activity inhibits the formation of further pre-RC complexes preventing their reformation and remains high until the end of mitosis. CDK activity is therefore critical to ensuring that genomic DNA is replicated exactly once per cell cycle and is thus transmitted stably over generations. CDK inhibition of pre-RC formation is mediated in several ways. The CDK initiation of origin firing disassembles the pre-RC leaving an unlicensed origin and high CDK activity then inhibits the formation of new pre-RC by several mechanisms (Nguyen *et al.* 2001; Takeda *et al.* 2005). These include the phosphorylation of free Cdc6 causing its export from the nucleus and the phosphorylation of the ORC complex and Cdt1, leading to their

dissociation from the chromatin and/or degradation (Delmolino *et al.* 2001; Li *et al.* 2002; Sugimoto *et al.* 2004).

The end of S phase is signified by the completion of DNA replication and the cell then moves into the next cell cycle phase, G2, in which the cell prepares to divide its newly synthesised chromosomes.

1.7 The G2/M transition - activation of MPF via control of cyclin B

Of the three B cyclins known, cyclins B1 and B2 are expressed in most cycling cells. They are differently localised, with cyclin B1 being found on the microtubules and cyclin B2 found associated with the Golgi apparatus. Cyclin B3 expression is restricted to developing germ cells and the testis in adults, where it is degraded shortly after cyclin B1 (Brandeis *et al.* 1998; Nguyen *et al.* 2002).

Cyclin B levels first begin to rise in S phase. Its levels slowly increase throughout G2 and then climb to high levels, peaking in late G2, and remain high in early mitosis. Cyclin B must be present at sufficient levels for the formation of an active MPF at the end of G2 phase to drive mitotic entry (Fung *et al.* 2005).

The expression of the cyclins required to drive cells from S phase into mitosis must be repressed until the correct time, at which point their expression must then be rapidly activated. In order to achieve this, the levels of this protein are temporally restricted throughout the cell cycle by tight control of transcription and subsequent proteolysis (Felix *et al.* 1989; Lindqvist *et al.* 2009).

This transcriptional control is accomplished via several transcriptional control elements. The promoters of cyclins A2, B1 and B2 contain CCAAT-boxes. These invariant DNA sequences are found downstream of the origin of replication of genes and bind transcription factors required for a gene to be transcribed in sufficient quantities. These are bound by the trimeric nuclear transcription factor Y (NF-Y), activating cyclin gene transcription (Katula *et al.* 1997; Kramer *et al.* 1997). In addition, the coactivator p300 binds to the promoters of cyclins B1 and B2 and synergises with NF-Y to further enhance their transcription. Their promoters also contain E2F binding elements that can be positive or negative acting. For cyclin B1, E2F1, 2, and 3 bind to the positive acting site and E2F4 binds to the negative acting site, inhibiting transcription. Another element, the cell cycle genes homology region (CHR), is

important for the repression of cyclin A2, B1 and B2 in G1 (Wasner *et al.* 2003). The transcription factor B-MYB positively regulates transcription of cyclin A2 and B1 and its activity is enhanced by phosphorylation by cyclin A-CDK2 in S phase. B-MYB is in fact itself regulated by E2F transcription factors which induce its expression at G1/S (Joaquin *et al.* 2003b; Joaquin *et al.* 2003a; Zhu *et al.* 2004a). Cyclin B1 expression is also activated by the forkhead transcription factor FOXM1. This transcription factor is essential for timely entry into mitosis as it stimulates the expression of numerous G2-specific genes (Laoukili *et al.* 2005). In fact many of these elements, CCAAT boxes, NF-Y and B-MYB binding and CHR are present in genes involved in the control of the G2/M transition, including genes for CDK1 and Cdc25. During mitosis the cyclin B1 gene remains in an open chromatin conformation and its promoter remains bound by NF-Y allowing its expression during mitosis (Sciortino *et al.* 2001). All these transcription factors, NF-Y, B-MYB and FOXM1 are controlled by CDK activity. These led to the efficient transcription of cyclin B only once the activity of cyclin A-CDK2 has built up sufficiently during S phase and G2 (Bolognese *et al.* 1999; Salsi *et al.* 2003; Fung *et al.* 2005).

Control of destruction of cyclin B is mediated through the destruction box (D-box) (Klotzbucher *et al.* 1996). This is a short N-terminal sequence that targets the mitotic cyclins to the E3 ubiquitin ligase, the anaphase-promoting complex/cyclosome (APC/C) (Acquaviva *et al.* 2006). This multi-subunit complex is crucial for allowing progression through the cell cycle. The APC/C has two activating/adaptor subunits, the cell division cycle protein 20 (Cdc20) and cell division cycle homologue 1 (Cdh1). In mitosis, APC/C^{Cdc20} is critical for the transition from metaphase to anaphase and APC/C^{Cdh1} becomes active in late mitosis into G1 phase. The APC/C acts by targeting its substrate proteins to the 26S proteasome for degradation in a highly regulated and specific manner. The mutation or deletion of the D-box from the N-terminus of these cyclins leads to inhibition of cyclin degradation. The ubiquitin-mediated proteolysis of the cyclin B begins at the metaphase/anaphase transition, once APC/C^{Cdc20} becomes active after correct chromosome alignment has been achieved and the mitotic checkpoint known as the spindle assembly checkpoint (SAC) has been satisfied. The active APC/C continues to promote cyclin B degradation until S phase when its levels can begin to rise again. In this manner, high cyclin B levels and thus MPF activity are regulated by protein expression and proteolysis during the cell cycle (Pfleger *et al.* 2000; Sudakin *et al.* 2001; Yamano *et al.* 2004).

The cellular localisation of cyclin B is also regulated (Takizawa *et al.* 2000). Cyclin B is shuttled between the cytoplasm and the nucleus. In S phase and the majority of G2 phase its export from the nucleus outweighs import, making cyclin B predominantly cytoplasmic (Pines *et al.* 1991). Cyclin B localisation accumulates during G2 at the centrosomes as they mature (Pines *et al.* 1991; Jackman *et al.* 2003). Maturation of the centrosomes is also signified by an increased concentration of other proteins required for mitotic entry and gamma tubulin. This subcellular shuttling of cyclin B likely contributes to formation of active MPF by concentrating cyclin B in specific cellular compartments. In prophase, cyclin B rapidly accumulates in the nucleus allowing CDK activity and mitotic progression (Hagting *et al.* 1998; Toyoshima *et al.* 1998; Yang *et al.* 1998).

1.8 The cyclin B-CDK1 positive feedback loop

The presence of cyclin B at sufficient levels is important for the formation of an active MPF to drive mitotic entry but additionally CDK1 must be phosphorylated by the CAK on Thr161 in the T loop to create an active kinase (Tassan *et al.* 1994). Further inhibitory phosphorylations elsewhere in CDK1 act to keep it inactive until it is required to drive progression into mitosis, at which point it becomes dephosphorylated and active. These inhibitory phosphorylations, unlike the activating phosphorylation put on by CAK, are vital for the regulation of the cell cycle. These form the basis of the feedback loops that ultimately control activation of the MPF and mitotic entry (Lindqvist *et al.* 2009).

The highly conserved kinase, Wee1, phosphorylates CDK1 on tyrosine 15 inhibiting it (Parker *et al.* 1992). The Wee1 protein was so named because its functional loss in yeast cells produces a smaller than normal daughter cell after division as mitosis is induced prematurely (Nurse *et al.* 1980). This phenotype indicates its role in dictating cell size in these cells and in coordinating cell size with cell cycle progression, preventing cells that are too small from entering mitosis and dividing. A second membrane-associated kinase, Myt1, that is related to Wee1 is found also in vertebrates and phosphorylates CDK1 on threonine 14 as well as tyrosine 15 also inhibiting it (Mueller *et al.* 1995; Fattaey *et al.* 1997). Wee1 is predominantly nuclear or associated with the centrosomes while Myt1 is found associated with membrane bound structures in the cytoplasm (Baldin *et al.* 1995; Liu *et al.* 1997).

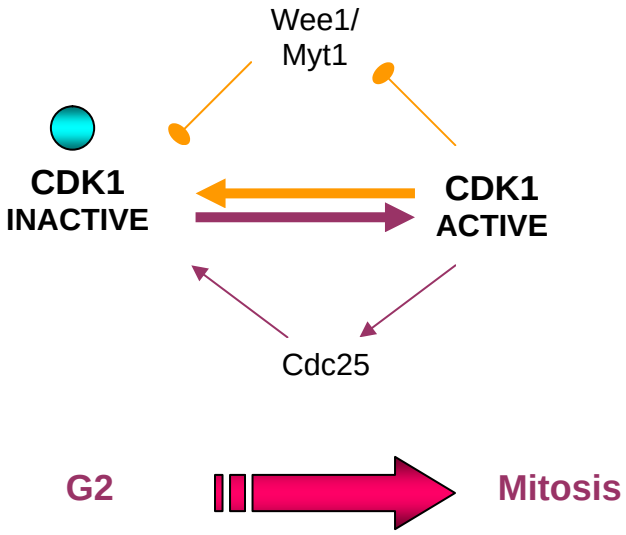

Figure 1.3 The cyclin B-CDK1 positive feedback loop

Schematic representation of the cyclin B-CDK1 positive feedback loop that functions to rapidly escalate the activation of CDK1 to promote and maintain mitotic entry. CDK1 is kept inactive prior to mitotic entry in G2 by inhibitory phosphorylations on Thr14 and Tyr15 added by Wee1 and Myt1, represented by the aqua sphere. It is activated when these are removed by the phosphatase Cdc25 at the G2/M transition. Active CDK1 can then phosphorylate and inactivate Wee1 and Myt1, and phosphorylate and activate Cdc25. This creates a positive feedback loop that serves to rapidly drive up CDK1 activity and promote mitotic entry. Activating modifications are shown as purple arrows and inhibitory modifications are shown in orange.

Phosphatases from the Cdc25 family remove these inhibitory phosphorylations therefore activating the CDK1 again (Dutcher *et al.* 1982; Kumagai *et al.* 1991; Kumagai *et al.* 1992). These are dual specificity phosphatases that can dephosphorylate both serine and threonine residues as well as tyrosine residues (Dunphy *et al.* 1991). Knockout mouse models of Cdc25B and C, both separately and together, are viable but Cdc25A deletion is lethal (Chen *et al.* 2001; Ferguson *et al.* 2005). In G2 phase, Cdc25A, B and C shuttle between the nucleus and the cytoplasm but Cdc25A is predominantly nuclear and is critical for unperturbed cell cycle progression and cell cycle arrest in response to checkpoint signalling (Jinno *et al.* 1994). Cdc25B and C appear to primarily regulate progression from G2 into mitosis, Cdc25A is active in all stages of the cell cycle. Cdc25A can bind to different cyclins and dephosphorylate CDKs *in vitro* and is transcriptionally controlled by the transcription factor c-Myc as well as by E2F. Cdc25B

and C are also targeted to the centrosomes in G2 and Cdc25B is implicated in the initial activation of cyclin B-CDK1 here (Hoffmann *et al.* 1994; Gabrielli *et al.* 1996; Jackman *et al.* 2003; Lindqvist *et al.* 2005; Boutros *et al.* 2006).

These regulatory proteins, Cdc25, Wee1 and Myt1 are themselves directly regulated by CDK1 phosphorylation. Once cyclin B-CDK1 complexes are active they feedback and promote Wee1 and Myt1 inactivation and further activation of Cdc25 creating a positive feedback loop that rapidly drives up CDK1 activity. Phosphorylation of Wee1 by CDK1 begins a cascade that targets it for degradation, while the phosphorylation of Myt1 ultimately inhibits its kinase activity (Booher *et al.* 1997; Nakajima *et al.* 2003; Watanabe *et al.* 2004; Watanabe *et al.* 2005). Phosphorylation by CDK1 of Cdc25C activates it, stabilises Cdc25A and causes relocalisation of Cdc25B (Hoffmann *et al.* 1993; Baldin *et al.* 2002; Mailand *et al.* 2002b). Thus, CDK1 activation at the end of G2 phase deactivates its inactivators and activates its activators. Together these interactions form a positive feedback loop to drive up high levels of cyclin B-CDK1 activation very rapidly. Once activation of cyclin B-CDK1 has reached a sufficient threshold nuclear lamina is disassembled and the nuclear envelope is broken down. The cell is then committed to enter mitosis. It is the balance between these activating and inhibitory mechanisms that ultimately controls entry into mitosis to complete the cell cycle (**Figure 1.3**) (O'Farrell 2001; Boutros *et al.* 2006; Hochegger *et al.* 2008; Lindqvist *et al.* 2009).

1.9 Further feedback loops controlling mitotic entry

There are in addition multiple layers of feedback regulation that serve to add layers of complexity to the biochemical signal to enter mitosis.

In numerous CDK substrates phosphorylation by CDK1 creates docking sites for Polo-Like Kinase 1 (PLK1) (Elia *et al.* 2003a; Elia *et al.* 2003b). This serine/threonine kinase was first identified in *Drosophila* as a mutant phenotype that caused aberrant mitosis and ablation of PLK1 from the mouse genome is lethal (Sunkel *et al.* 1988; Lu *et al.* 2008). It is now known to function as a key regulator of the G2/M transition and to play important roles in centrosome function, bipolar spindle formation and cytokinesis as well as in meiosis (van Vugt *et al.* 2004c). At the G2/M transition Wee1 phosphorylation by CDK1 mediates PLK1 recruitment and subsequent phosphorylation of Wee1 by PLK1

(Watanabe *et al.* 2005). This dual phosphorylation forms a phospho-degron that targets it for ubiquitin-mediated destruction (Freire *et al.* 2006). PLK1 phosphorylation of Myt1 inhibits its kinase activity and phosphorylation of Cdc25C promotes its concentration in the nucleus (Nakajima *et al.* 2003). Functional activation of Cdc25B by PLK1 has recently been demonstrated. Phosphorylation of Cdc25B by PLK1 causes it to relocate to the nucleus (Toyoshima-Morimoto *et al.* 2002). The overexpression of Cdc25B that drives cells prematurely into mitosis could be overcome by the inhibition of PLK1 (Lobjois *et al.* 2009). At present it is not clear if PLK1 can directly phosphorylate Cdc25A. PKL1 can phosphorylate cyclin B in its nuclear export sequence (NES) on serine 147 or near it on serine 133 but the significance of these phosphorylations is again unclear (Toyoshima-Morimoto *et al.* 2001; Yuan *et al.* 2002; Gavet *et al.* 2010a). What is clear is that PLK1 acts in concert with CDK1 to amplify and modulate mitotic entry signalling. Two CDK1 consensus phosphorylation sites have been shown to be phosphorylated on mitotic PLK1 (Gavet *et al.* 2010b). Although the function of these phosphorylations is not known, it is likely that CDK1 additionally directly phosphorylates and regulates PLK1 itself (van Vugt *et al.* 2004b; Daub *et al.* 2008; Gavet *et al.* 2010b). The need for PLK1 activity to allow mitotic entry was seemingly confirmed by the injection of anti-PLK antibodies into non-transformed human cells resulting in a late G2 block preventing entry into mitosis (Lane *et al.* 1996). However, when performed in transformed human cells the same block was not duplicated and later studies using specific PLK1 inhibitors suggested that PLK1 is not required for mitotic entry but for maintaining centrosome and kinetochore function (Lane *et al.* 1996; Lenart *et al.* 2007). PLK1 inhibition resulted in prophase entry but a delay of the transition to prometaphase. Thus, the relative role of PLK1 in the commitment to mitotic entry remains to be clearly deciphered.

Consistent with its proposed mitotic roles, PLK1 is localised to the centrosomes and the kinetochores. This is likely influenced by the presence of its phosphorylated target substrates (Hanisch *et al.* 2006; Qi *et al.* 2006). It is activated by a phosphorylation in its T-loop on threonine 210 by Aurora A (Macurek *et al.* 2008). The serine/threonine kinases, the Aurora kinase family includes, Aurora A, B and C (Nigg 2001). Aurora A localises to the centrosomes from the end of S phase and likely first activates PLK1 here (Seki *et al.* 2008). Aurora A has an important role in formation of a stable bipolar spindle and fidelity of chromosome segregation (Eyers *et al.* 2003; Girdler *et al.* 2006; Barr *et al.* 2007). It is degraded at the end of mitosis/ beginning of G1 by the APC/C^{Cdh1}. Aurora B

is localised to the kinetochores in early mitosis where it forms a component of the chromosome passenger complex (CPC) required for proper chromosome alignment at the metaphase plate. It then moves onto the spindle and eventually the midbody during cytokinesis where it is required for completion of abscission. It is also responsible for the mitotic phosphorylation of serine 10 and probably serine 28 of histone H3. This indicates it likely has additional functions via epigenetic modification of chromatin (Carmena *et al.* 2003; Ruchaud *et al.* 2007; Sabbattini *et al.* 2007; Kelly *et al.* 2009). Much less is known about the role of Aurora C. It is expressed at high levels in the testis and has a specific role in spermatogenesis (Dieterich *et al.* 2007). Its role in mitosis is largely unknown but it has been reported to bind members of the CPC and rescue the loss of function of Aurora B in cultured cells (Sasai *et al.* 2004). Knockout mouse models of Aurora A and B are embryonic lethal but Aurora $C^{-/-}$ mice are viable with minor defects in spermatogenesis (although it should be noted that there may be multiple Aurora C loci in the mouse genome) (Kimmins *et al.* 2007; Cowley *et al.* 2009; Malumbres 2011).

Aurora A is activated by autophosphorylation of threonine 288 in its T-loop (Walter *et al.* 2000; Littlepage *et al.* 2002). It must then bind to its cofactor Bora to allow it to phosphorylate PLK1 on threonine 210 (Seki *et al.* 2008). In turn, PLK1 has been shown to regulate Aurora A activity and localisation in mitosis, indicating that there is considerable cross talk amongst these two mitotic kinases (Scutt *et al.* 2009; Lens *et al.* 2010). Additionally, although Bora has been shown to bind PLK1 even if CDK1 is absent, CDK1 phosphorylation of Bora enhances its binding of PLK1 (Hutterer *et al.* 2006). In this way CDK1 may enhance the Aurora A-mediated activation of PLK. This adds a layer of positive feedback with CDK1 stimulating its own activation via the stimulation of PLK1 activation. Aurora A has been found to directly phosphorylate Cdc25B at the centrosome at the G2/M transition, implicating it in the initial activation of cyclin B-CDK1 here in concert with PLK1 (Dutertre *et al.* 2004; Cazales *et al.* 2005). Furthermore, there is some evidence that Aurora A is itself required for mitotic entry. The injection of anti-Aurora A antibodies delayed entry into mitosis in human cells suggesting it may play a role in the initiation of mitosis possibly by facilitating the translocation of cyclin B-CDK1 to the nucleus allowing full activation to be achieved (Marumoto *et al.* 2002). The precise mechanisms of these signalling networks remain to be completely understood but it is clear that layered feedback loops exist governing cyclin B-CDK1 activation ensuring that PLK1 and Aurora A are activated with correct

timing to facilitate centrosome maturation and bipolar spindle formation concomitantly with cyclin B-CDK1 activation and timely mitotic entry (Lindqvist *et al.* 2009).

The centrosomes are the microtubule nucleating centres of the cell and are important for mitotic spindle formation and chromosome stability (Abal *et al.* 2002; Chevrier *et al.* 2002). They are duplicated in each S phase and separated during the G2/M transition to form the mitotic spindle poles. Although the exact mechanisms of the centrosome cycle remain to be elucidated, it is important for timely disjunction, separation and positioning to form the spindle poles. CDK1, PLK1 and the motor protein Eg5 all play a role in this control (Blangy *et al.* 1995; Smith *et al.* 2011). Increasing evidence suggests that signalling at the centrosomes must be tightly controlled at the G2/M transition to mediate coordination of control networks facilitating commitment to mitotic entry (Hagan 2008). As mentioned previously, important mitotic regulators are recruited and concentrated at the centrosome in late G2, including cyclin B, PLK1, Mps1, Aurora A, Cdc25B and C (Bornens 2002; Blagden *et al.* 2003; Tyler *et al.* 2007; Hagan 2008; Tyler *et al.* 2009). This implies an important additional role for the centrosome mediating the signalling feedback loops required for timely mitotic entry.

The concentration of the many proteins required for the mitotic entry network is further compounded by the activation of transcription factor FOXM1 by PLK1 (Fu *et al.* 2008). This forms an addition layer of feedback in which CDK1-dependent activation of PLK1 via Aurora A/Bora serves to ultimately stimulate further cyclin B-CDK1 activation.

1.10 The mitotic entry network

Thus there are multiple feedback loops that act in concert to form a complex mitotic entry signalling network that allows the required level of cyclin B-CDK1 activation to be achieved. This forms a bistable switch-like mechanism in which once sufficient cyclin B-CDK1 activity has built up the whole cellular pool of cyclin B-CDK1 is rapidly activated (O'Farrell 2001). To protect against inappropriate triggering of this system, Wee1 and Cdc25 act as highly sensitised substrates for cyclin B-CDK1 activity. Low levels of cyclin B-CDK1 activity are only able to phosphorylate Wee1 on sites that do not inhibit its activity. Once CDK1 activity has built up to a higher level it can phosphorylate Wee1 and cause its inhibition (Kim *et al.* 2007). At the same time Cdc25

can be rapidly activated by a relatively low level of CDK1 activity (Trunnell *et al.* 2011). This results in the requirement for a threshold level of CDK1 activity to be achieved before the amplification loop is triggered. But once this level has been reached the switch is triggered and CDK1 activation is rapid and complete (Pines *et al.* 2011).

In addition to the proteins and feedback loops discussed here it is likely that many additional components and signalling networks are also involved. These have been indicated by recent proteomic studies that have revealed that several thousand proteins become phosphorylated during mitotic entry. Many of these components and signalling networks are still to be elucidated (Daub *et al.* 2008; Dephoure *et al.* 2008).

Additionally, the relative contribution of each of the known components or feedback loops of the mitotic entry signalling network is not yet well resolved. Studies using RNA interference (RNAi) mediated depletion or chemical inhibition of individual components imply that there is at least some redundancy in these signalling networks (Lindqvist *et al.* 2009). Surprisingly even centrosomes themselves are not essential for mitosis in all cells. Human HeLa cells continued normally through the cell cycle after their removal by laser ablation (La Terra *et al.* 2005). Although not all components of the network are absolutely required for mitotic entry there is evidence that all components are needed in order for a cell to enter mitosis with correct timing and for proper coordination of all mitotic events. A CDK1 mutant that cannot be inhibited by Wee1 or Myt1 led to abnormal mitosis and the expression of active cyclin A-CDK2 by injection led to the effective ablation of G2 phase and caused cells to display mitotic abnormalities (Furuno *et al.* 1999; Pomerening *et al.* 2008). This implies that although there is redundancy in the network all components and feedback loops must function in concert with correct timing to allow error free cell division.

1.11 Antephase

In mammalian mitosis cyclin A-CDK is required for cells to enter and progress through prophase (Furuno *et al.* 1999; Fung *et al.* 2007). Here the nucleoli are disassembled, the chromosomes condense and cyclin B-CDK1 is activated. Once activation of cyclin B-CDK1 has been achieved it is then required to allow progression into metaphase. It is required for completion of chromosome condensation, NEBD and completing the formation of the mitotic spindle (Rieder 2011). The period in which the

chromosomes begin to condense at the end of G2, just before a cell becomes committed to enter mitosis regardless of environmental conditions, is termed antephase (Chin *et al.* 2010). Until the rapid accumulation of active cyclin B-CDK1 in the nucleus the process of prophase chromosome condensation can still be reversed (Rieder *et al.* 2000). Once this point is passed, however, a cell has committed to enter mitosis and only death can prevent it from breaking down its nuclear envelope and entering mitosis (Mazia 1961; Pines *et al.* 2001). The point of no return, when a cell cannot reverse mitotic entry, occurs approximately 10 minutes before NEBD at the time when cyclin B-CDK1 accumulates in the nucleus. Before this, various insults can cause the cell cycle to arrest, preventing or delaying entry into mitosis. This can be triggered by two main checkpoint control pathways; the DNA damage checkpoint pathway and the stress response pathway (Mikhailov *et al.* 2005; Bartek *et al.* 2007). Both checkpoint control pathways ultimately act to inhibit cyclin B-CDK1 activation until conditions are favourable for the cell to enter mitosis. The DNA damage checkpoint will be discussed in more detail later in this chapter. The stress response checkpoint pathway is also known as the antephase checkpoint and can be triggered by ultra violet (UV) light exposure, heat shock, osmotic shock and mitotic stress (Matsusaka *et al.* 2004). This pathway is based on two proteins; the E3 ubiquitin ligase 'Checkpoint protein with an FHA domain and RING finger' (Chfr) and the Mitogen Activated Protein (MAP) kinase family member p38 kinase (Alonso *et al.* 2000; Nebreda *et al.* 2000; Matsusaka *et al.* 2004). Chfr is necessary to activate the checkpoint in response to mitotic stress, such as microtubule spindle poisons, and is thought to act upstream of p38 (Scolnick *et al.* 2000; Chaturvedi *et al.* 2002). Once p38 is activated by stress stimuli or Chfr signalling, it activates a signalling cascade that promotes Cdc25B binding to the 14-3-3 protein, sequestering it in the cytoplasm, slowing cyclin B-CDK1 activation and delaying mitotic entry (Conklin *et al.* 1995; Karlsson-Rosenthal *et al.* 2006). It can also produce a more sustained block by phosphorylating p53 causing it to dissociate from Murine double mutant 2 (Mdm2) and induce the expression of the CDK inhibitor p21 (Alberts 2002; Bulavin *et al.* 2002; Kang *et al.* 2002; Mikhailov *et al.* 2005).

1.12 Mitosis

Once a cell has committed to enter mitosis the nuclear envelope is broken down. This allows the dynamic microtubule arrays emanating from the mature separating centrosomes to interact with the chromosomes to form a bipolar spindle (Rieder 2011). On each replicated chromosome or sister chromatid, a kinetochore must attach to an opposing spindle pole. They must do this in a manner that results in each being attached to just one opposing pole. This 'amphitelic' or biorientated attachment ensures faithful segregation of the chromosomes in anaphase with one copy of each being delivered to the two resulting daughter cells. During the process of forming the bipolar spindle sister kinetochores can become erroneously attached. These attachments are rapidly dealt with by a correction mechanism based on Aurora B at the inner kinetochore. This is important to prevent chromosome missegregation and the production of aneuploid progeny (Rieder *et al.* 1995; Scutt *et al.* 2009; Xu *et al.* 2010; Hegarat *et al.* 2011).

The kinetochores are multiprotein complexes that form at the centromeres of sister chromatids. Key regulators at the kinetochores are Aurora B kinase and its antagonising phosphatase Protein Phosphatase 1 (PP1). Aurora B with Inner Centromere Protein (INCENP), survivin and borealin comprises the chromosome passenger complex (CPC) (Vader *et al.* 2006; Ruchaud *et al.* 2007). Aurora B is only fully active when it is recruited to the centromeres as part of the CPC. PP1γ is recruited to the outer kinetochore by kinetochore-null 1 (KNL1) and inactivates Aurora B as it comes into contact with it. This forms a gradient of Aurora B activity that is high at the centromere decreasing towards the outer kinetochore. This is further propagated by Aurora B feeding back and phosphorylating PP1γ, preventing its binding to KNL1. When a microtubule is first captured by the kinetochore improper attachments fail to push the kinetochore away from the centromere and high Aurora B activity destabilises it. Correct end-on attachment pushes the kinetochore away from the centromere and high Aurora B activity allowing the attachment to be stabilised (Cimini 2007; Kelly *et al.* 2009; Maresca *et al.* 2009; Liu *et al.* 2010; Rosenberg *et al.* 2011).

To minimise chromosome missegregation cells have evolved the spindle assembly checkpoint (SAC). This delays anaphase onset until all 92 kinetochores of a human cell have achieved biorientation and attached to a single pole that is opposite to the pole their sister kinetochore has attached to (Rieder *et al.* 1995). This is mediated by targeting the APC/C activator/adaptor Cdc20. When Cdc20 binds to the APC/C it allows

it to recognise specific substrates, including cyclin B and securin, and targets them for degradation (Izawa *et al.* 2011). The SAC proteins Mitotic Arrest Deficient (Mad) proteins, Budding Uninhibited by Benzimidazole (Bub) proteins and Monopolar Spindle 1 (Mps1) kinase accumulate at unattached kinetochores and the APC/C and Cdc20 also accumulate here (Chen *et al.* 1996; Abrieu *et al.* 2001; Kallio *et al.* 2002; Acquaviva *et al.* 2004; Musacchio *et al.* 2007). The mechanism by which the SAC proteins target Cdc20 has been, and still is to some extent, controversial. The current dominant model focuses on Mad2 and its ability to exist in two conformations, an open conformation (O-Mad2) and a closed conformation (C-Mad2). C-Mad2 can catalyse O-Mad2 binding to Cdc20 after which it is converted to the closed conformation (Luo *et al.* 2002; De Antoni *et al.* 2005). C-Mad2 is stably bound to unattached kinetochores via Mad1 where it can continuously promote O-Mad2 binding to Cdc20 via an Mps1 dependant mechanism. The Mad2-Cdc20 complex is then sequestered by binding to the BubR1-Bub3 complex preventing Cdc20 from associating with and activating the APC/C (Sudakin *et al.* 2001; Nilsson *et al.* 2008; Hewitt *et al.* 2010; Bolanos-Garcia *et al.* 2011). Upon microtubule binding two mechanisms are thought to silence the SAC: the dissociation of Mps1 and the Mad1-Mad2 complex removal via dynein-mediated microtubule-dependant transport (Howell *et al.* 2001; Jelluma *et al.* 2010).

Aurora B has also been suggested to play a role in SAC signalling independently of its role in error correction (Santaguida *et al.* 2011). It is proposed that Aurora B prevents PP1γ binding to KNL1 at kinetochores and that this KNL1 mediated PP1γ recruitment is required for silencing of the SAC. This therefore is only achieved once microtubule binding pushes the kinetochore away from the centromere allowing it to move away from high Aurora B activity enabling PP1γ recruitment. PP1γ can then dephosphorylate checkpoint components silencing the SAC (Vanoosthuyse *et al.* 2009).

The chromosomes are aligned at the spindle equator forming the metaphase plate, and once correct biorientation is achieved, anaphase is initiated and the sister chromatids are separated. This can only occur once the SAC has been silenced and this only happens once the last unattached kinetochore has been stably attached. Even a single unattached kinetochore can delay anaphase for several hours (Rieder *et al.* 1994). Once the checkpoint activity is extinguished Cdc20 is released and the APC/C is activated (Fang *et al.* 1998a; Fang *et al.* 1998b). APC/C^{Cdc20} then initiates anaphase by targeting securin and cyclin B for ubiquitin-mediated degradation. These are both inhibitors of separase. Securin is a small protein that binds and sequesters separase while cyclin B-CDK1

inhibits it by direct binding and phosphorylation. Once they are degraded CDK1 is inactivated and separase is activated. Separase is a cysteine protease which cleaves the centromeric cohesin ring. Cohesin is the protein complex responsible for tethering the sister chromatids together preventing premature segregation. It is loaded onto the chromosomes in S phase along their entire length. The majority of cohesin molecules found along the chromatid arms are removed in prophase by the phosphorylation of the Smc3 cohesin complex subunit by PLK1 and Aurora B. This results in dissociation of the cohesin complex from the DNA, except at the centromere where it is protected by Shugoshin. This keeps the centromeric cohesin intact and ensures sister chromatids remain together until anaphase onset. Once activated separase cleaves the kleisin subunit of the cohesin ring complex resulting in the complete loss of cohesion between the sister chromatids (Hornig *et al.* 2004; Hauf *et al.* 2005; McGuinness *et al.* 2005; Kitajima *et al.* 2006; Tang *et al.* 2006).

The sister chromatids then migrate to their facing pole during early anaphase, or anaphase A. Pole-ward movement occurs predominantly via the shortening of the kinetochore microtubules. In late anaphase, or anaphase B, the spindle lengthens and elongates, moving the spindle poles apart along with the centrosomes to where the two daughter cells will be formed. This process requires kinesin and dynein motor proteins as well as microtubule dynamics (Brust-Mascher *et al.* 2004). The inactivation of CDK1 and activation of mitotic phosphatases lead to the removal of inhibitory phosphorylations on Cdh1. It can then bind and activate the APC/C. APC/C^{Cdh1} targets important substrates for degradation to allow mitotic exit. Targets of active APC/C^{Cdh1} include PLK1 and Aurora B, mitotic cyclins and also Cdc20 (Li *et al.* 2009). This results in predominant APC/C^{Cdh1} activity. It remains active into G1 and maintains low levels of CDK activity by degrading cyclins until mitogenic-mediated increases in CDK activity phosphorylate and inactive Cdh1 (Li *et al.* 2009).

During telophase a nuclear envelope reforms around each set of sister chromatids and nucleoli reappear. Next, cytokinesis ensures complete segregation of the two sets of chromosomes. The astral microtubules emanating from the spindle poles send signals to the cortex or midzone activating the assembly of an actin and myosin contractile ring. Here the cleavage furrow develops and ingresses until the midbody is formed. At the end of cytokinesis the midbody is physically cleaved in two by abscission and two daughter cells are formed (Minshull *et al.* 1989a; Guse *et al.* 2005; Murthy *et al.* 2005; Brennan *et al.* 2007; Neef *et al.* 2007).

1.13 Phosphatases regulating mitosis

Since the discovery of the CDKs, kinases have been hailed as the master regulators of mitosis. Recently, however, the role of the phosphatases that reverse the kinase signalling events is beginning to be highlighted and appreciated as a crucial aspect of the control of mitotic entry and exit (Bollen *et al.* 2009). Studies are now revealing that the timely ordering of mitotic events, in fact, appears to be a result of a delicate interplay between both the kinases and their counteracting phosphatases (Domingo-Sananes *et al.* 2011). They have long been thought of as silencing signalling events by ubiquitous and broad acting dephosphorylation. This viewpoint is now being challenged and phosphatases are emerging as highly specific inhibitors of precise signalling pathways that are critical for control of mitotic events (De Wulf *et al.* 2009; Domingo-Sananes *et al.* 2011). In keeping with this developing appreciation for the important role of phosphatases in carefully counterbalancing kinase activity to control cellular activities, recent work has highlighted the importance of several key phosphatases in mitotic processes.

The dual-specificity Cdc25 phosphatases are required for mitotic entry, as has been described in some detail here already. These important phosphatases are required to remove inhibitory phosphorylation of CDKs to activate their activity throughout the cell cycle and crucially to activate the MPF at the G2/M transition to drive mitotic entry (Kumagai *et al.* 1991; Lindqvist *et al.* 2005; Domingo-Sananes *et al.* 2011).

Another well characterised mitotic phosphatase is Cdc14. This is another dual-specificity phosphatase that controls mitotic exit in budding yeast. Its release from the nucleolus in anaphase promotes dephosphorylation of CDK1 substrates and mitotic exit (Visintin *et al.* 1998). There are two human isoforms of Cdc14, A and B (Li *et al.* 2000). These target proteins that are phosphorylated by proline-directed kinases. Cdc14A has been implicated in centrosome separation, mitotic spindle formation and chromosome segregation (Kaiser *et al.* 2002; Mailand *et al.* 2002a). Cdc14B is sequestered in the nucleolus of interphase human cells and released in mitosis and has been implicated in assembly and disassembly of the mitotic spindle and promoting mitotic exit (Dryden *et al.* 2003; Cho *et al.* 2005; Rodier *et al.* 2008). Very recently Cdc14B has also been shown to dephosphorylate and inhibit Cdc25 inactivating CDK1 in anaphase; implicating Cdc14B as having an important role in promoting mitotic progression (Tumurbaatar *et al.* 2011).

The conserved serine/threonine phosphatases PP1 and Protein Phosphatase 2A (PP2A) have also recently been highlighted as important regulators of mitotic events. PP1 has been discussed here where relevant, highlighting its emerging role in mitotic events. Roles have been described for PP1 in the inhibition of Aurora A activity until MPF activation to promote ordered mitotic entry, in antagonising Aurora B activity at the kinetochore in metaphase, and participation in the SAC. In addition to these, PP1 has been reported to be required for chromatin decondensation and timely dephosphorylation of mitotic phospho-proteins and nuclear envelope reassembly (with PP2A) at mitotic exit (Thompson *et al.* 1997; Vagnarelli *et al.* 2006; Wu *et al.* 2009; Schmitz *et al.* 2010).

PP2A has been implicated in prevention of precocious separation of chromosomes in anaphase. PP2A, in complex with its regulatory B56 subunit, is recruited to the centromeres by Shugoshin and keeps cohesion subunits in an unphosphorylated state, counteracting PLK1 phosphorylation (Kitajima *et al.* 2006; Tang *et al.* 2006). Also PP2A, in complex with is regulatory B55α subunit, has been implicated in Golgi reassembly after mitotic exit (Schmitz *et al.* 2010). Additionally, PP2A has recently emerged as an important part of the signalling network required to allow proper mitotic entry and progression (Mochida *et al.* 2009; Lorca *et al.* 2012).

It has long been a source of debate in the literature as to which phosphatase is the key counterbalancing phosphatase of mitotic CDK substrates. It has been known since the late 1980s that okadaic acid, a specific phosphatase inhibitor, could drive *Xenopus* oocytes into M phase (Goris *et al.* 1989; Felix *et al.* 1990). Pointing to the important role for phosphatases in control of cell proliferation in general and igniting the hunt for phosphatases responsible for permitting entry into and exit from mitosis. Although it is now known that Cdc14 is the key phosphatase responsible for the completion of mitosis in budding yeast (Visintin *et al.* 1998), for a long time the identity of phosphatase(s) involved in higher eukaryotes remained elusive. However, recent work has significantly moved our understanding forward. In particular, findings by Mochida *et al.* (2007; 2009) that PP2A activity oscillates inversely to CDK1 activity throughout the cell cycle (i.e. it is high during interphase and low during mitosis) and that the depletion of its B55δ isoform from *Xenopus* egg extracts significantly advanced entry into mitosis, suggested that it might be counterbalancing CDK1 activity. Although, mitotic exit was not notably blocked by its specific depletion, indicating that in higher eukaryotes regulation of mitosis is likely complex (this is discussed further in

Chapter 5) (Mochida *et al.* 2009). This work coincided with the work described throughout the remainder of this chapter and throughout this thesis, and considerably contributed to the emergence of a new picture of the regulation of mitotic entry and progression.

1.14 The Greatwall kinase

In February 2004 a report was published by Yu *et al*. describing a novel kinase that could play a previously unknown role in the mitotic entry network (Yu *et al.* 2004). They reported that this kinase was required for proper chromosome condensation and mitotic progression in flies (*Drosophila*). Subsequent work would find that this highly conserved kinase played a key role at the G2/M transition in all cells and would ultimately change the way people thought about mitotic entry.

1.15 Greatwall discovery in *Drosophila*

In 2004, Yu *et al.* published the finding of mutations in a gene encoding a novel nuclear protein that resulted in the production of an inactive kinase in *Drosophila*. Expression of the inactive kinase led to failure of the chromosomes to condense and delayed entry into and progression through mitosis. These mutations were isolated in a *Drosophila* gene, previously uncharacterised, that caused larval brains to have an elevated mitotic index indicative of mitotic arrest combined with irregular chromosome condensation (**Figure 1.4 A**). They named this gene *Greatwall* (*gwl*) as the mutant phenotype indicated a significant role for this protein in protecting chromosome structure (Yu *et al.* 2004).

The *gwl* gene encodes an AGC family kinase that is conserved in insects and vertebrates. The AGC kinases are a diverse family of serine/threonine kinases that target amino acids for phosphorylation that are surrounded by basic amino acids (Tamaskovic *et al.* 2003). The Greatwall protein is composed of a bifurcated kinase domain that is split by a region of ~ 500 amino acids. In a comparison of *Drosophila* and human Greatwall an overall amino acid sequence identity of 59% was identified. The homology between these proteins extended beyond the kinase domain and included short amino acid

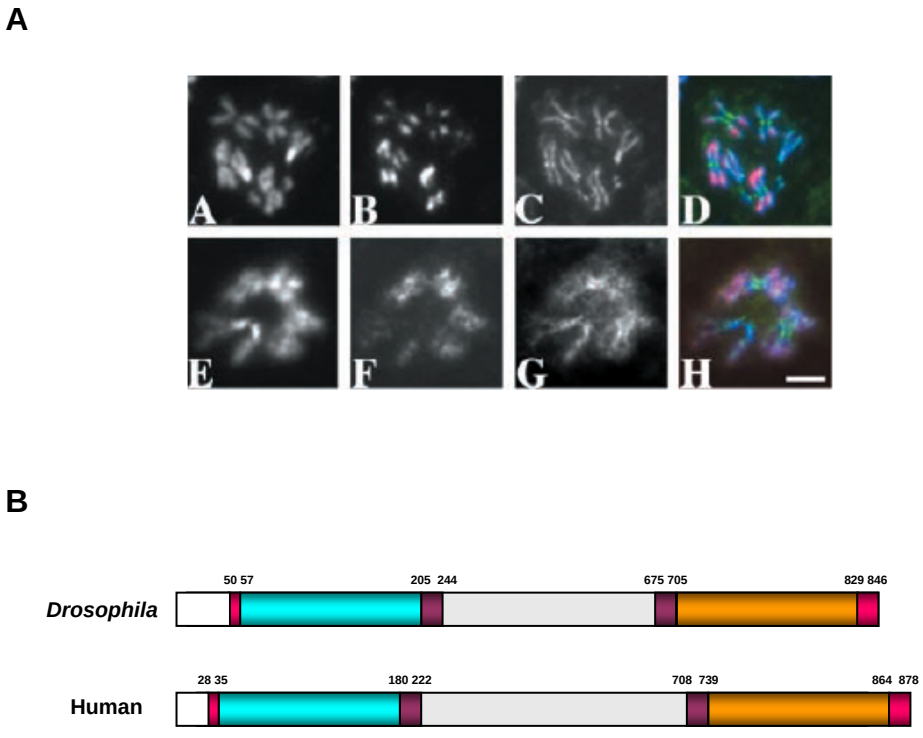

Figure 1.4 Greatwall, a novel cell cycle regulator

(A) The Greatwall mutant phenotype. Immunofluorescent staining of chromosomes from wildtype and *gwl* mutants. Taken from Yu *et al.* (2004). Here the condensin component Barren is stained green, phospho-histone H3 is stained red and the DNA signal is blue. Greatwall wildtype neuroblasts are shown in panels A to D, while *gwl* mutant neuroblasts are shown in panels E to H. **(B)** Schematic drawing of the structure of the Greatwall proteins. Taken from Yu *et al.* (2004). The conserved kinases in *Drosophila* and human Greatwall are compared. The bifurcated kinase domains are indicated, with the N-terminal portion indicated in aqua and the C-terminal portion indicated in orange with the inserted unrelated amino acids that show a limited degree of homology shown in grey. The sections indicated in pink and purple are less well conserved regions found in all Greatwall kinases but not in other kinases. Four of the mutant Greatwall alleles identified encoded missense mutations within the conserved amino acids of the serine/threonine kinase catalytic domain, while the fifth allele encoded a nonsense mutation that truncated the protein (Yu *et al.* 2004).

sequences flanking the split kinase domain sections (**Figure 1.4 B**) (Yu *et al.* 2004).

In *Drosophila*, once DNA replication has been completed, the activation of cell cycle regulators leads to chromosome condensation. Late in G2 the activation of cyclin A-CDK induces the initial stages of chromosome condensation and later, at early

prophase, the nuclear accumulation and activation of cyclin B-CDK1 triggers the breakdown of the nuclear envelope.

The defect most notable in the larval brains containing the mutated *gwl* was the undercondensation of their chromosomes. This was observed by immunofluorescent staining when the mutant larval brains had been treated with colchicine. Aberrantly condensed chromosomes appeared to clearly have two sister chromatids and to still recruit phospho-histone H3 and the condensin component Barren, indicating that the chromosome condensation apparatus was unaffected (**Figure 1.4 A**) (Yu *et al.* 2004).

The progression of the cell cycle was stalled in mitosis in the fixed brains of all of the five identified mutant *gwl* alleles. The proportion of the cells in mitosis was 2.5-fold higher and the proportion of cells in anaphase or telophase was decreased by 85-90 %, indicating that a non-functional Greatwall kinase leads to the delay or arrest of cell cycle progression prior to anaphase onset. Cells that had progressed into anaphase or telophase displayed lagging chromosomes or chromosome bridges but spindles at all stages of mitosis were morphologically normal. In live cell imaging experiments of neuroblast cells from mutant and control flies expressing GFP-tagged histone H2AvD, progression through prophase was delayed and lasted >10 times longer than wildtype controls. The progression into metaphase was also delayed after NEBD in *gwl* mutant cells with 20% never achieving a stable metaphase. This was not due to spindle defects as was seen to occur even in the presence of the spindle poison colchicine. Additionally, 30 % of the colchicine-treated *gwl* mutant cells failed to condense their chromosomes properly or achieve NEBD for periods longer than four hours. Therefore, the Greatwall gene is clearly implicated in late G2/M for chromosome condensation and timely NEBD in flies. The delay seen in metaphase is likely due to the activation of the spindle checkpoint, as sister chromatids were never separated in *gwl* mutant cells after NEBD and they showed elevated levels of cyclin B that would be expected if the checkpoint was active. In support of this, immunofluorescent staining showed that Bub1, the key checkpoint protein, localised to and accumulated on *gwl* mutant kinetochores (Yu *et al.* 2004).

These defects seen in the *gwl* mutant flies were not a consequence of DNA replication problems. BrdU incorporation was normal as compared with control flies and all mitotic cells had double the DNA content of interphase cells. The mutant phenotype might have arisen as a consequence of an early G2/M phase checkpoint reversing the progression of chromosome condensation and NEBD. This was ruled out using caffeine at concentrations that disrupts normal checkpoints activated in response to DNA damage

and would lead to the shortening of the period of chromosome condensation before NEBD if such a checkpoint had been activated by the loss of functioning Greatwall. This did not occur in live cell imaging experiments; instead Greatwall deficient cells never achieved NEBD when caffeine treated.

The phenotype analysis attributed to the defective Greatwall mutations was validated by RNAi knockdown of the *gwl* gene in tissue culture *Drosophila* cells. In these cells the chromosomes were again undercondensed and showed an increased mitotic index with a decreased proportion of cells in anaphase/telophase.

Greatwall antibodies were used as immunofluorescent probes to characterise the cellular localisation of Greatwall kinase. It was visualised in the nucleus of interphase cells and throughout the cells in mitosis with no notable chromosome or spindle localisation. This localisation was confirmed by expression of a GFP-tagged Greatwall, leading the authors to conclude that it does not play a structural role on the chromosomes themselves (Yu *et al.* 2004).

1.16 Greatwall kinase and cyclin B-CDK1

In 2006, the same group published a second paper examining the role of Greatwall in *Xenopus* egg extracts taking advantage of its conservation in all vertebrates (Yu *et al.* 2006). Antibodies raised against the *Xenopus* Greatwall detected a band of approximately 98 kilo Daltons (kDa) that shifted up significantly in mitotic extracts. This shift was likely due to phosphorylation as it was lost upon lambda (λ) phosphatase treatment. This mitotic hyperphosphorylated form of the Greatwall showed activity in [γ-^{32}P]ATP incorporation assays while Greatwall from interphase extracts did not. Thus, the hyperphosphorylated mitotic Greatwall represents the active form of the kinase. A much reduced activity was seen with a mutant kinase dead version of Greatwall that has two mutated residues, G41S and D173A, predicted to be essential for an active kinase domain, indicating that this mitotic activity is likely due, at least in part, to autophosphorylation.

Depletion of Greatwall from Cytostatic Factor (CSF) *Xenopus* egg extracts resulted in exit from M phase and reversion to interphase. This was characterised by decondensation of the chromosomes and reforming of the nuclear envelope of demembranated sperm nuclei in CSF extracts. MPF activity rapidly returned to

interphase levels. Concurrently the phosphorylation of other proteins Wee1, Myt1, Cdc25, Plx (*Xenopus* PLK) and MAP kinase, which should become phosphorylated upon mitotic entry, were also rapidly lost. This was not due to the degradation of cyclin B as its protein levels remained constant. Additionally, the introduction of a non-degradable form of cyclin B failed to rescue this phenotype and was not able to hold the CSF extracts in M phase in the absence of Greatwall. This reversion to interphase can be explained by the accumulation of inhibitory phosphorylations on CDK1 inactivating it, thus preventing sufficiently high levels of MPF activity necessary to promote and sustain mitosis (Yu *et al.* 2006).

The addition of Ca^{2+} to control extracts induces mitotic exit and initiation of a new round of S phase but this was not seen in Greatwall depleted extracts, indicating that exit from mitosis seen in the absence of Greatwall is not a normal exit. Further more, when pre-treated/activated recombinant Greatwall, hyperphosphorylated by incubation in CSF extracts, was reintroduced to the depleted extracts, M phase was restored. A pre-treated kinase dead version of the Greatwall (G41S and D173A) was unable to rescue this phenotype, indicating a role of Greatwall in maintenance of M phase in these extracts.

In cycling *Xenopus* extracts the loss of the Greatwall kinase results in a phenotype that is strikingly similar to the phenotype reported in flies. The depletion of Greatwall led to the prevention of entry into mitosis specifically at the G2/M phase transition with no apparent effects on DNA replication or on the activation of the DNA damage checkpoints. This block was again rescued by the addition of wildtype Greatwall but not kinase dead Greatwall.

Mass spectral analysis of recombinant Greatwall phosphorylated *in vitro* by MPF revealed five sites that were potentially phosphorylated by CDK1 and conserved in vertebrates. Sequential mutation (from a serine or threonine to alanine) revealed only one mutation, T748A, which was unable to rescue the depleted CSF extracts to M phase. This suggests that there is at least one CDK1 phosphorylation site in Greatwall that is important for its activation. To further support the interaction of the Greatwall protein with MPF complex, it was found that only MPF pre-treated recombinant Greatwall was autophosphorylated in [γ-^{32}P]ATP incorporation assays. Untreated recombinant Greatwall and kinase dead Greatwall did not autophosphorylate *in vitro* and were unable to rescue the CSF extracts to M phase. This leads to the conclusion that MPF is an important activator of Greatwall or may perform a priming phosphorylation necessary to achieve high activity (Yu *et al.* 2006).

How Greatwall might fit into the mitotic entry network is hinted at by the use of constitutively active CDK1, CDK1AF, in which Thr14 and Tyr15 are replaced by non-phosphorylatable residues alanine and phenylalanine, preventing inhibition by Wee1 and Myt1 (Krek *et al.* 1991; Pomerening *et al.* 2008). Introduction of CDK1AF compensated for the loss of Greatwall in restoring M phase in CSF extracts, although a five-fold higher amount was required in comparison with endogenous CDK1. This implies that Greatwall forms part of an autoregulatory loop that generates and maintains high MPF activity to support mitosis. Interaction with the MPF is unlikely to occur via regulation of Wee1 or Myt1. Wee1 and Myt1 are negatively controlled in CFS extracts by the MAP kinase pathway. The MAP kinase pathway remained active after the MPF was inactivated suggesting that the deregulation of the pathway was not due to aberrant activity of Wee1 or Myt1. As described in flies, caffeine failed to overcome the cell cycle block seen in Greatwall depleted cycling extracts and cannot therefore be a result of a G2 arrest due to activation of a DNA damage checkpoint. A weak interaction of Greatwall with Plx in co-immunoprecipitation experiments was observed and active Greatwall failed to phosphorylate Cdc25 in *in vitro* kinase assays. The role that PLK1 plays in the regulation of Greatwall still remains to be clarified *in vivo* but potentially Greatwall acts through PLK1 to contribute to Cdc25 activation, thus acting as an upstream trigger of MPF activity (Jackson 2006; Yu *et al.* 2006).

1.17 Greatwall kinase and Cdc25

A third paper published by Zhao *et al*. in 2008 investigated the potential role of Greatwall in the regulation of the phosphatase Cdc25 in *Xenopus* egg extracts (Zhao *et al.* 2008). In cycling egg extracts Cdc25C was phospho-shifted on immunoblots but not in Greatwall depleted extracts. The maintenance of the mitotic phosphorylation on Cdc25C was dependent on the presence of Greatwall but did not rely on the presence of PLK1 which was removed by immunodepletion, or on CDK1 activity which was inhibited by roscovitine. This suggests that Greatwall might be a key regulator of Cdc25 activity.

Greatwall purified from M phase arrested insect Sf9 cells has the required mitotic phosphorylations to be active and was added to cycling egg extracts immunodepleted for Greatwall. This resulted in precocious phosphorylation of Cdc25C and a premature entry into mitosis advanced by as much as an hour when compared to normally cycling

extracts. An effect that was not seen when activated kinase dead Greatwall (G41S) was added or when wildtype non-activated Greatwall was added, indicating that activated (hyperphosphorylated) Greatwall is sufficient to promote premature entry into mitosis (Zhao *et al.* 2008).

In meiotic maturation of progesterone stimulated *Xenopus* oocytes, Greatwall was expressed at a steady level in prophase I to metaphase II and became hyperphosphorylated upon entry into M phase. Active Greatwall was injected into immature oocytes arrested in G2 and induced maturation indicative of entry into meiotic M phase. The breakdown of the germinal vesicle began three hours later despite the absence of progesterone and was almost complete after seven hours. This effect was not seen with the activated kinase dead form of Greatwall, indicating that active Greatwall is sufficient to promote premature entry of oocytes into meiosis even in the absence of progesterone.

Further, activated Greatwall induced phosphorylation of Cdc25C in the absence of activity of CDK1, Plx or MAP kinase or in the presence of an activator of cAMP-activated protein kinase (PKA) that normally blocks mitotic entry. Interestingly, the observed G2 arrest caused by Greatwall depletion could be overcome by the addition of the potent phosphatase inhibitor, okadaic acid. This suggests that Greatwall and okadaic acid are inducing similar effects on cell cycle control and raises the possibility that Greatwall antagonises the activity of an unknown okadaic acid-sensitive phosphatase.

In this proposed model the unidentified phosphatase would act to remove specific mitotic phosphorylations on key mitotic proteins to prevent the activation of MPF to sufficient levels necessary for M phase entry. Greatwall would act to inhibit this crucial okadaic acid-sensitive phosphatase that would otherwise inhibit M phase induction by the removal of M-phase-specific modifications from mitotic phospho-proteins including Cdc25. This phosphatase must be turned off by Greatwall activity to allow accumulation of phosphorylations mediated by a variety of mitotic kinases on Cdc25 and other proteins to achieve entry into and maintain progression through mitosis (Zhao *et al.* 2008).

1.18 Greatwall antagonises PP2A

The existence of a key phosphatase that specifically counteracts M phase entry has long been postulated to exist (Goris *et al.* 1989; Picard *et al.* 1989; Picard *et al.* 1991;

Mochida *et al.* 2007). The identity of this unknown phosphatase that is regulated by Greatwall and acts to counteract M phase entry was determined by two papers published in 2009.

This was investigated by Vigneron *et al*. (2009) through depletion of Greatwall in *Xenopus* CSF extracts. This depletion caused MPF inactivation, indicated by the rapid (within five minutes) dephosphorylation of its substrates early mitotic inhibitor 2 (Emi2), Cdc27 and Cdc25 and its re-phosphorylation on Tyr15. This was accompanied by DNA decondensation as previously described. This phenotype was rescued by wildtype but not a kinase dead Greatwall. Co-depletion with Wee1 or Myt1 individually or together failed to reverse this phenotype although a small delay of MPF inactivation was observed in Greatwall and Wee1 depleted extracts. Interestingly the triple depletion of Wee1, Myt1, and Greatwall caused mitotic exit despite the lack of Tyr15 phosphorylation on MPF and its activity in kinase assays remaining at a high level. That Greatwall depletion promoted mitotic exit even in the presence of high cyclin B-CDK1 levels suggests its primary role is to regulate a phosphatase activity rather than to regulate the MPF feedback loop directly (Vigneron *et al.* 2009).

Another study by Castilho *et al*. (2009) supported these findings. Tagged 25-amino acid peptides, each containing a single CDK phospho-site, were *in vitro* phosphorylated by cyclin A-CDK2 and added to extracts depleted of Greatwall. In this experiment four of the seven CDK phospho-sites tested were rapidly dephosphorylated in the depleted extracts but not in untreated or mock-depleted extracts. This dephosphorylation was okadaic acid sensitive and further confirmed that Greatwall acts by inhibiting a phosphatase that is directed against CDK phospho-sites. Further, once Greatwall is active, its suppression of the anti-CDK phosphatase is independent of MFP activity. This was demonstrated by the loss of phosphatase inhibition, indicated by dephosphorylation of CDK-phosphorylated PP1γ, before the loss of MPF H1 kinase activity in Greatwall depleted extracts. Additionally the supplementation of constitutively active CDK1AF did not prevent phosphatase activation in these depleted extracts (Castilho *et al.* 2009).

The Greatwall depletion phenotype could be rescued in CSF extracts by the addition of microcystin, a potent PP1 and PP2A dual inhibitor (Vigneron *et al.* 2009). Greatwall was depleted from CSF extracts and microcystin was subsequently added and analysis carried out after addition at 0, 30 and 60 minutes. Initially, the characteristic phosphorylation of MPF on Tyr15 and dephosphorylation of MPF substrates was

observed, but was reversed after 30 minutes. The MPF lost Tyr15 phosphorylation once more and its substrates were again phosphorylated. This clearly implies a role for PP1 or PP2A in the reversal of the phenotype seen in the absence of Greatwall. To elucidate which of these two phosphatases was the crucial Greatwall regulated phosphatase, okadaic acid was used. It was found that a dose of 500 nM okadaic acid was the minimum dose required to reverse the Greatwall depletion phenotype. At this concentration okadaic acid has been described to only inhibit 20% of PP1 but 70% of PP2A, indicating that it is PP2A that is responsible for the reversion of the Greatwall depletion phenotype (Felix *et al.* 1990; Favre *et al.* 1997). In support of this, the PP1 inhibitor, Inhibitor 2, failed to rescue the effect of loss of Greatwall (Vigneron *et al.* 2009). The addition of an active form of PP2A also, after Greatwall depletion and okadaic acid addition, again restored mitotic exit. Furthermore, a yellow fluorescent protein (YFP) -tagged Greatwall co-immunoprecipitated from HEK 293 cells with PP2A subunits and vice versa. The same result was obtained from CSF extracts with endogenous proteins. The physical interaction of Greatwall with PP2A subunits suggests that Greatwall binds to PP2A in cells and that it is this phosphatase that may be the target of Greatwall regulation for entry into and maintenance of mitosis. To confirm that Greatwall can inhibit PP2A activity, c-Mos, a known PP2A substrate that is phosphorylated by active MPF activity, was used in *in vitro* kinase assays (Vigneron *et al.* 2009). C-Mos was initially incubated with immunoprecipitated MPF from CSF extracts and incubated with [γ-^{32}P]ATP. The radiolabeled c-Mos was then incubated with immunoprecipitated PP2A from CSF extracts that had or had not been depleted for Greatwall. The PP2A phosphatase activity was shown to be three-fold less from extracts containing Greatwall i.e. the dephosphorylation of c-Mos was three-fold less in these extracts. Thus, dephosphorylation of MPF substrates by PP2A is regulated by Greatwall in mitotic *Xenopus* egg extracts (Castilho *et al.* 2009; Vigneron *et al.* 2009).

PP2A is a highly abundant serine/threonine phosphatase conserved throughout eukaryotes. It is known to have roles in numerous cellular processes including cell division, cytoskeleton organisation, gene regulation and protein synthesis (Janssens *et al.* 2008; De Wulf *et al.* 2009). The basis for this broad functional diversity can be attributed to its complex structure and regulation. It is a holoenzyme that is comprised of a structural scaffold A subunit (also known as PR65) and a catalytic C subunit. Both A and C subunits have two isoforms, α and β, and this core PP2A structure can exist independently or complex with variable regulatory B subunits. Substrate specificity

and/or subcellular localisation are regulated by the B subunits. These are comprised of structurally unrelated subfamilies: B/B55/PR55, B'/B56/PR61, B''/PR72 and B'''/PR93/PR110. In turn each subfamily has many different structurally related isoforms. This huge variety of B subunits with the two isoforms of the A and C subunits result in over 70 possible PP2A holoenzymes that could each have different specificities and functions (Xu *et al.* 2006; Janssens *et al.* 2008).

The PP2A-B55 family, in particular the δ isoform (B55δ), has been previously shown to specifically dephosphorylate CDK phospho-sites *in vitro* and *in vivo* and to be critical for entry into mitosis, although exit from mitosis likely requires the action of additional phosphatases (Mochida *et al.* 2009). That the B55δ isoform accounts for as much as 70% of total B55 subunits present in *Xenopus* egg combined with these findings suggest that PP2A-B55δ could be the target of Greatwall activity. Its immunodepletion from CSF extracts that were also Greatwall depleted, rescued the mitotic exit defect seen upon Greatwall depletion alone. It is therefore likely that it is the PP2A-B55δ that is the major phosphatase regulated by Greatwall, although it is possible that other less abundant B55 subunits are also targets of Greatwall regulation. In addition, this interaction is unlikely to be direct as *in vitro* kinase assays provided no indication that Greatwall was able to phosphorylate any component of the PP2A holoenzyme (Castilho *et al.* 2009).

Further experiments carried out by Lorca *et al.* (2010) supported this idea. They found that, in concert with the MPF autoregulatory feedback loop, the Greatwall mediated inhibition of PP2A was required to promote correct first embryonic cell division in *Xenopus* egg extracts.

Thus, entry into mitosis requires not only sufficient levels of MPF activation, but additionally, the Greatwall regulated suppression of a phosphatase, PP2A, that would otherwise remove necessary MPF phosphorylations. This provides a new insight into the regulation of mitotic entry, implicating not only CDK kinase activity but also counterbalancing phosphatase activity as critical to allow proper entry into and progression through mitosis.

1.19 Greatwall substrates

In 2010 two groups established α-Endosulfine (Ensa) and cyclic adenosine monophosphate (cAMP)-regulated phospho-protein 19 (Arpp19) as the elusive substrates

of Greatwall that mediate its inhibition of PP2A. Using the kinase substrate tracking and elucidation (KESTREL) method (Cohen *et al.* 2006), Mochida *et al.* (2010) identified Greatwall substrate, Ensa, from interphase *Xenopus* egg extracts, while Gharbi-Ayachi *et al.* (2010) identified Arpp19 using biochemical fractionation of CSF *Xenopus* egg extracts and *in vitro* Greatwall kinase assays; Both reported Arpp19 and Ensa identification as substrates of Greatwall.

Arpp19 was first identified as a major substrate for PKA. It was found to be conserved in all vertebrates but absent in invertebrates. Arpp19 is ubiquitously expressed in all tissues but its levels decrease with development. In adult tissues Arpp19 was only found expressed in the brain and pancreas. Interestingly it was also found to be highly expressed in nine (all that were tested) malignant cell lines (Girault *et al.* 1990). Ensa is a close relative of Arpp19 and was first identified as an endogenous ligand of the sulfonylurea receptor K^+ channels in the pancreas. Its expression was also found throughout the central nervous system (Virsolvy-Vergine *et al.* 1992; Peyrollier *et al.* 1996). In *Drosophila*, oocytes with mutant Ensa display a prolonged prophase and fail to progress to metaphase despite high MPF activity (Von Stetina *et al.* 2008). Targeted mutagenesis identified a single serine, serine 62 in Arpp19 and serine 67 in Ensa, as the site phosphorylated by Greatwall (Gharbi-Ayachi *et al.* 2010; Mochida *et al.* 2010). Additionally, cyclin A-CDK2 phosphorylated Arpp19 (at serine 28) and Ensa (at threonine 28) as did PKA (on serine 109 in both) (Mochida *et al.* 2010).

Greatwall phosphorylated Arpp19 and Ensa were able to strongly inhibit the PP2A-B55δ holoenzyme in *in vitro* phosphatase assays. The non-phosphorylated forms or forms phosphorylated with CDK or PKA were not inhibitory (Mochida *et al.* 2010). Mochida *et al*. (2010) reported that in *Xenopus* egg extracts only Ensa was detected at significant levels by immunoblotting and the majority of this was phosphorylated in mitotic extracts in a serine 67 dependent manner. In cycling extracts, Ensa depletion resulted in failure to enter mitosis despite high MPF activity as judged by H1 kinase activity. Add back of wildtype Ensa rescued induction of mitosis but an S67A Ensa mutant that could not be phosphorylated by Greatwall did not (Mochida *et al.* 2010). Accordingly, the addition of thio-phosphorylated Ensa or Arpp19 to interphase egg extracts that have been previously depleted of Greatwall, allowed the loss of Greatwall phenotype to be rescued and induced mitotic entry (Gharbi-Ayachi *et al.* 2010). This was not seen if Ensa and Arpp19 were not thio-phosphorylated as phosphorylated forms were rapidly dephosphorylated and could not induce mitotic entry in the absence of Greatwall.

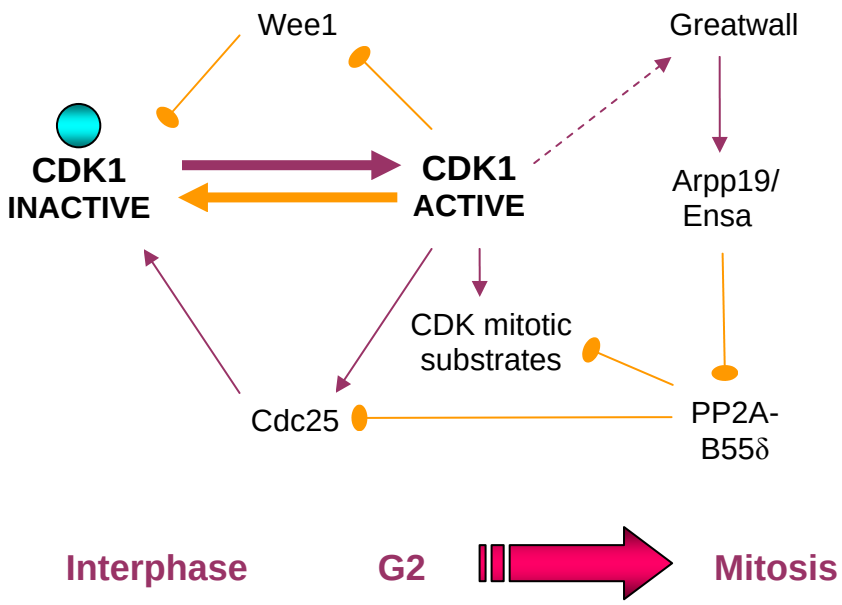

Figure 1.5 The Greatwall pathway

Schematic representation of the potential role of Greatwall in mitotic entry and maintenance in mammalian cells. Greatwall is activated in late G2 and phosphorylates its targets, Ensa and/or Arpp19, crucially inactivating PP2A-B55δ. This prevents PP2A antagonising CDK phosphorylation, allowing mitotic phosphorylations to accumulate on targets and activation of the CDK positive feedback loop to drive cells into mitosis. Further potential interactions have been omitted for simplicity in this model. Activating modifications are shown as purple arrows and all inhibitory modifications are shown in orange. The unconfirmed activation of Greatwall by CDK1 is indicated with a dashed line.

This suggests that endogenous Greatwall phosphorylation of Ensa and Arpp19 counterbalances their dephosphorylation. Phosphorylated Ensa and Arpp19 on serine 67/62 was seen to increase with Greatwall phosphorylation at mitotic entry and decrease with Greatwall dephosphorylation at mitotic exit. However, in contrast to Mochida *et al.* (2010), the second group found that only depletion of Arpp19, and not Ensa, prevented cycling egg extracts entry into mitosis and exit from mitosis in CSF extracts. Add back of thio-phosphorylated protein rescued mitotic entry in cycling extracts and okadaic acid-mediated PP2A inhibition overcame the mitotic exit phenotype in CSF extracts (Gharbi-Ayachi *et al.* 2010). It not clear why the two groups found differing importance of Arpp19 and Ensa in their preparations. It is possible that the high sequence identity between Arpp19 and Ensa (88% between the human proteins) has meant that the

experiments and antibodies used were not rigorous enough to distinguish between them. Furthermore, that Arpp19 is present in far lower concentrations in these extracts could mean that its importance was effectively masked in the first study. Whether Arpp19 has a distinct role in this pathway to Ensa remains to be established (Haccard *et al.* 2011), but it is clear that both these proteins can act downstream of Greatwall to inhibit PP2A to allow correct mitotic entry and progression. Therefore, at the G2/M transition the activation of Greatwall, possibly by CDK1 itself, leads to the phosphorylation of Arpp19/Ensa which then inhibits PP2A-B55δ. This allows CDK1 activity to predominate and drive entry into mitosis (**Figure 1.5**).

1.20 Greatwall in recovery from the DNA damage checkpoint

As mentioned previously, many cell cycle control proteins are implicated in eliciting cell cycle arrest in response to assaults by DNA damaging agents. This response is known as the DNA damage checkpoint and serves to arrest cells in response to DNA damage before entry into mitosis. Such agents include UV light, mutagenic chemicals, or ionising radiation (IR) that can come from exogenous sources, i.e. UV light emitted by the sun. DNA damage can also be a result of endogenous cellular processes that include oxidation, alkylation or hydrolysis of bases, bulky adduct formation and mismatch of bases due to replication errors. This response engages repair machineries to restore the DNA and elicits the arrest of cell cycle progression to allow this repair via complex networks of signal transduction (Zhou *et al.* 2000).

The cell cycle arrest is mediated by master kinases ataxia telangiectasia mutated (ATM) kinase and ataxia telangiectasia and Rad-3-related (ATR) kinase. ATM primarily responds to direct DNA damage (DNA double strand breaks and disruptions in chromatin structure) while ATR is critical for response to stalled replication forks during DNA synthesis (Kastan *et al.* 2004). These conditions often occur together so ATM and ATR are often active simultaneously and perform in concert to elicit DNA damage checkpoint activation (Harrison *et al.* 2006; Cimprich *et al.* 2008).

In response to double strand breaks (DSBs), ATM homodimers autophosphorylate and dissociate. The active ATM monomer can then phosphorylate numerous substrates including p38, p53 and structural maintenance of chromosomes 1 (Smc1) (Yazdi *et al.* 2002). P38 phosphorylation promotes the 14-3-3 protein

sequestering Cdc25B (Thornton *et al.* 2009). Thus the DNA damage checkpoint pathway overlaps with the stress response checkpoint pathway. ATR is recruited and activated by the presence of single stranded DNA at stalled forks and has been suggested to be required for S phase even in the absence of DNA damage. Crucially ATM and ATR phosphorylate and activate checkpoint effectors Chk1 and Chk2. Phosphorylation of Cdc25A mediated by Chk1 and Chk2 on serine 123 leads to its rapid degradation in response to checkpoint activation and the Cdc25 phosphatases are major targets of the DNA damage checkpoint response. Overexpression of Cdc25A causes a bypass of the IR-induced S and G2 checkpoints, as well as the DNA replication checkpoint (Shreeram *et al.* 2008). Phosphorylation of p53 by Chk2 activates it leading to expression of the CDK inhibitor p21. Additionally, cyclin B1 and B2 are transcriptionally repressed when cells are arrested in G2 in response to DNA damage checkpoint signalling. This repression is dependant on the presence of functional transcriptional control elements including the NF-Y binding motif and CCAAAT box (Fung *et al.* 2005). Thus DNA damage checkpoint signalling acts to inhibit CDK activity until cell cycle progression is favourable (Kastan *et al.* 2004).

This signalling must be turned off upon satisfaction of DNA repair. This process of checkpoint recovery involves the deactivation of the checkpoint mediators and subsequent activation of activators of cell cycle progression. Work carried out by Peng *et al.* (2010) suggested a novel role for Greatwall in recovery from DNA damage. They utilised an elegant *in vitro* system in which the addition of double stranded oligonucleotides to *Xenopus* egg extracts mimics DNA damage and elicits the DNA damage response, indicated by Chk1 phosphorylation. The subsequent removal of these double stranded oligonucleotides mimics DNA repair and allows the study of recovery from this signalling response. In this system, immunodepletion of Greatwall amplified the response to DNA damage, inhibiting recovery, while addition of wildtype but not kinase dead Greatwall actually inhibited the DNA damage response, speeding recovery up. Moreover, Greatwall was directly inhibited by DNA damage checkpoint activation raising an interesting possibility that it might be a target of ATM/ATR or Chk1/Chk2 (Medema 2010). Thus indicating that Greatwall might be an important target of the DNA damage checkpoint and that its reactivation is then required to allow recovery from the checkpoint (Peng *et al.* 2010).

PLK1 is known to play an important role in DNA damage checkpoint recovery (van Vugt *et al.* 2001; van Vugt *et al.* 2004a; van Vugt *et al.* 2004b). It phosphorylates

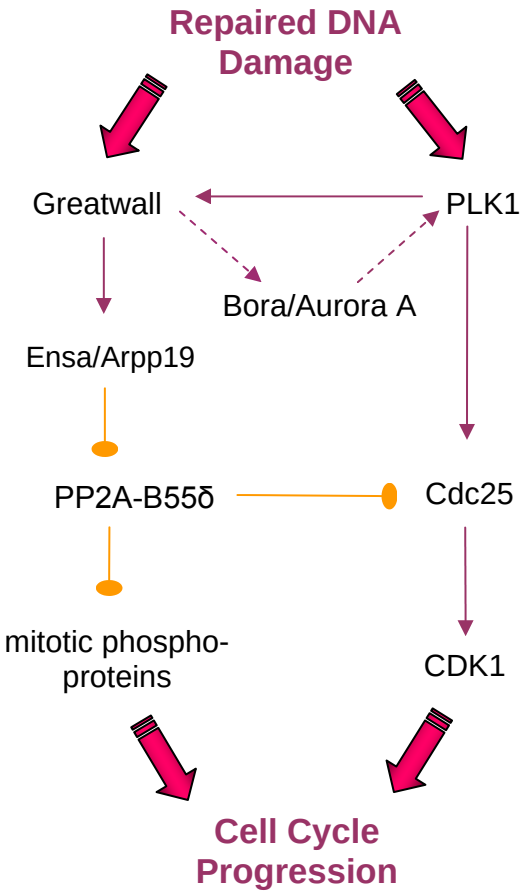

Figure 1.6 Greatwall promotes cell cycle restart after a DNA damage-mediated cell cycle arrest

Schematic representation of Greatwall as a new regulator that promotes recovery from the DNA damage checkpoint arrest. Once DNA has been repaired, PLK1 is activated and phosphorylates and activates its targets, including Cdc25 (promoting activation of CDK1) and Greatwall (promoting inhibition of PP2A). This leads to activation of CDK1 to allow cell cycle progression into mitosis. Furthermore, Greatwall itself is activated upon checkpoint recovery leading to inhibition of PP2A independently of PLK1. In addition it can likely activate PLK1 by activation of the Bora/Aurora A complex. Evidence that Greatwall directly interacts with PLK1 via a binding motif in its N-terminal domain but does not directly phosphorylate it suggests that this interaction might serve to mediate Aurora A-Greatwall interactions (Peng *et al.* 2011). Therefore PLK1 and Greatwall function in a synergistic manner to promote checkpoint recovery and mitotic entry after a DNA damage-mediated cell cycle arrest. Activating modifications are shown as purple arrows and all inhibitory modifications are shown in orange. Proposed unconfirmed interactions are indicated with dashed lines.

substrates required for maintenance of checkpoint activation and CDK inhibition and targets them for proteolysis. These include Wee1 and Claspin (Mamely *et al.* 2006).

Claspin is an adaptor protein that is required to allow ATR/Chk1 interaction and subsequent Chk1 activation in response to DNA damage (Freire *et al.* 2006; Cimprich *et al.* 2008). After a damage-mediated cell cycle arrest PLK1 is critical to allow re-entry into the cell cycle and progression into mitosis (Bartek *et al.* 2007; Clemenson *et al.* 2009). A recent report by Peng *et al.* (2011) found evidence of a functional relationship between Greatwall and PLK1 in checkpoint recovery in *Xenopus* egg extracts. Here depletion of Greatwall or Plx significantly delayed the deactivation of checkpoint signalling in a manner that was not synergistic. Further, pre-activated Greatwall addition to the extracts promoted checkpoint inactivation in the absence of Plx, suggesting that their roles in this process are distinct from one another. The depletion of Greatwall, however, abolished Plx activation and depletion of Plx abolished Greatwall activation. They were also reported to directly interact via a Plx binding motif in the Greatwall N-terminal and Plx was able to phosphorylate Greatwall *in vitro*. This implies that they may act in a coordinative positive feedback manner to activate one another to drive recovery and cell cycle re-entry after DNA damage repair. This was supported by the fact that pre-phosphorylated Greatwall by Plx exhibited stronger activity in promoting checkpoint recovery. Plx was not phosphorylated *in vitro* by Greatwall. However, Greatwall was required for Aurora A activation during checkpoint recovery and the reconstitution of wildtype Aurora A activity in Greatwall depleted extracts restored Plx activation. Thus it is probable that Greatwall regulates Plx activation indirectly, through the activation of Aurora A. This might represent a specific pathway required to allow proper mitotic entry after a DNA damage provoked cell cycle arrest that is not as significant for unperturbed normal cell cycle progression (**Figure 1.6**) (Macurek *et al.* 2008; Peng *et al.* 2011).

1.21 Greatwall in development

A novel role for Greatwall in development was proposed by Archambault *et al.*'s (2007) work in *Drosophila*. They first identified Greatwall as a gain of function mutation in an allele of *Drosophila* Greatwall (*gwl)* called *Scant* (*Scott of the Antarctic*). When this was heterozygous with one wildtype and one mutant copy of *polo* (the *Drosophila* gene for PLK1), *Scant* led to female production of embryos with greatly reduced viability. The gene defined by the *Scant* mutation encodes an allele of *gwl* that carries a K97M point mutation to produce a hyperactive form of Greatwall. The severity of the dominant *Scant*

mutant phenotype was increased in direct proportion to the decrease in Polo (*Drosophila* PLK1) function. The primary and only phenotype seen in these mutants was premature centrosome detachment that led to spindle abnormalities and aberrant subsequent mitoses. Thus the Polo-Greatwall balance is important to maintain centrosome-nuclear proximity. The same effect was observed when a transgenic *Scant* Greatwall mutant was expressed in females that were Polo deficient (Archambault *et al.* 2007).

These effects were only seen when the overexpression or hyperactivation (as in *Scant*) of Greatwall was combined with reduced levels of Polo. *In vitro* kinase assays with Myc-tagged Greatwall or *Scant* Greatwall expressed in *Drosophila* culture cells showed that the *Scant* Greatwall had increased activity with altered specificity as compared with wildtype activity *in vivo*. This suggests that Greatwall and Polo have antagonistic activities in early developing *Drosophila* embryos (Archambault *et al.* 2007; Boke *et al.* 2011).

Additionally, *Scant* Greatwall rescued the effects of Greatwall loss of function identified by Yu *et al*. (2004), even when expressed at low levels (Archambault *et al.* 2007). Further study of loss of function mutants of Greatwall showed that it was required for proper chromosome structure and segregation in mitosis as well as meiosis. One mutant resulted in the loss of Greatwall in vitellogenesis (building up of the egg's contents) leading to the failure of meiosis I due to premature sister chromatid separation, implicating Greatwall in the cohesion of sister chromatids in female meiosis I (Archambault *et al.* 2007).

In *Xenopus* oocytes co-immunoprecipitation shows that Greatwall complexes with PP2A-B55 in G2 (interphase) oocytes and dissociates in progesterone-treated M phase (germinal vesicle breakdown; GVBD) oocytes (Yamamoto *et al.* 2011). A kinase dead Greatwall could also associate with PP2A in interphase and release it in M phase so the kinase activity of Greatwall is not required. A K71M mutant Greatwall, the *Xenopus* equivalent of *Drosophila Scant*, showed very reduced but constitutive gain of activity against Ensa. Kinase assays revealed that *Scant* Greatwall but not wildtype Greatwall had interphase activity toward Ensa. It was able to promote M phase in oocytes but took several hours longer than progesterone-mediated GVBD, suggesting its low activity levels are limiting. *Scant* Greatwall in *Xenopus* displayed only a two-fold increase in activity (at best) and it is likely that the increased activity seen in *Drosophila Scant* might have resulted from the cell cycle arrest of the cultured cells leading to a high concentration of protein in the preparation. That addition of proteasome inhibitor,

MG132, led to increased levels and accelerated M phase entry suggests that Scant has reduced stability (Yamano *et al.* 2004).

In 2011, two co-published reports investigated the functional relationship between Greatwall and Polo in Drosophila further. Wang *et al.* (2011) carried out a genetic screen that identified an inter-dependence between Polo and PP2A B-type subunit Twins. Reducing both Polo and PP2A-Twins from the maternal contribution led to embryonic lethality. PP2A-Twins collaborated with Polo to ensure centrosome attachment to the nuclei. Polo was required for centrosome cohesion to the nuclei in prophase while PP2A-Twins was required for centrosome attachment during mitotic exit. Therefore, proper regulation of mitotic events by Polo and PP2A-Twins play an important role in promoting mitotic entry and exit. Consistent with other studies they found that Greatwall antagonised PP2A-Twins in metaphase of meiosis I and in early mitotic cycles, suggesting an important pathway connecting Polo and Greatwall in control of M phase in flies (Wang *et al.* 2011).

Another genetic screen carried out by Rangone *et al.* (2011) identified mutants in a *Drosophila* protein Endos, the single *Drosophila* orthologue of Arpp19/Ensa. These mutants potently suppressed the embryonic lethality that occurs with *Scant* Greatwall in combination with reduced Polo function. That the loss of Greatwall and Endos function in mitosis was very similar and reduced Endos function suppresses the phenotype seen in Polo/Twins heterozygous double mutants suggests Endos is activated by Greatwall and inhibits PP2A. This is further supported because the Endos depletion phenotype in cultured cells is rescued by co-depletion of catalytic subunit of PP2A or the Twins regulatory subunit (Rangone *et al.* 2011).

The mutation of the catalytic subunit of PP2A or the Twins subunit synergises with *Scant* Greatwall when maternal dosage of Polo is low. This is suppressed by reduction of Endos. This observation leads to a model for Greatwall and Polo genetic interaction in which, during mitotic entry, Greatwall is active and inhibits PP2A-Twins via Endos. This sustains CDK phosphorylations that enable Polo to bind to phosphorylated partners mediating its functions in early mitosis. Once CDK activity is decreased in anaphase, Polo then binds to partners via their dephosphorylated CDK sites. These sites must be dephosphorylated by PP2A-B55/Twins. In this model the activating *Scant* mutation of Greatwall would lead to inappropriate inhibition of PP2A in interphase reducing the levels of Polo complexed to its dephosphorylated partners. One of these partners would include a substrate required to maintain cohesion of the centrosome with

the nuclear envelope. The mechanism of this cohesion still remains to be elucidated but, as the other functions of Polo are normal, this would require the highest level of Polo activity. Thus, if Polo activity is reduced in combination with increased Greatwall-mediated PP2A inhibition in interphase, sufficient dephosphorylation of Polo interphase partner(s) is prevented and their association is abolished (Rangone *et al.* 2011).

This suggests that sophisticated and precise control of mitotic entry and exit is critical during embryonic cycles. It points to a conserved pathway in which Polo, Greatwall and PP2A-Twins are key regulators. Overall this indicates that Greatwall kinase potentially plays multiple roles in both mitotic and meiotic progression, fulfilling crucial functions in different cell cycles of a developing animal (Archambault *et al.* 2007).

1.22 Aims of this dissertation

At the beginning of this project the human Greatwall homologue had not been characterised and the aim was to investigate the role of this novel protein kinase in human cells. The fact that this unusual kinase has such an important function in flies and is conserved in mammals led us to believe that it might play an as yet unknown but critical role in human cells. This project aimed to address this and to characterise Greatwall in human cells.

This study of human Greatwall includes cloning the gene, analysis of Greatwall depletion and overexpression phenotypes, using structural modelling to determine its activation mechanisms, investigating its activation regulation within the cell cycle, attempting a chemical genetics approach to specifically inhibit the kinase, and assessing its potential as a key anti-cancer drug target and clinical biomarker. Overall this thesis describes insights into the function and regulation of human Greatwall kinase.

CHAPTER 2. Materials and methods

2.1 Materials

2.1.1 Chemicals and biochemicals

All chemicals were obtained from Fisher Scientific (Leicestershire, UK) or Sigma-Aldrich (Missouri, USA) unless otherwise stated. Recombinant cyclin A-CDK2 was a kind gift from Tim Hunt (Clare Hall Laboratories, Hertfordshire, UK) and the myelin basic protein (MBP; dephosphorylated) substrate was purchased from Merck Millipore (Billerica, USA). Complete Protease Inhibitors and PhoSTOP Phosphatase Inhibitor Cocktails were from Roche Diagnostics (West Sussex, UK). Prolong® Gold mounting solution with DAPI was purchased from Invitrogen (Paisley, UK). Bio-Rad Protein Assay Reagent was obtained from Bio-Rad (Hertfordshire, UK). The CDK inhibitor, RO-3306, and phosphatase inhibitor, okadaic acid, were purchased from Merck Chemicals (Nottingham, UK). The PLK inhibitor, BI2536, was purchased from Axon Medchem (Gronigen, NL). The phosphatase inhibitor, Tautomycetin, and the Eg5 inhibitor, S-trityl-L-cysteine (STLC), were both purchased from Tocris Bioscience (Bristol, UK). All restriction enzymes used were from New England Biolabs (Beverly, USA). All buffers and chemicals were made up in double distilled water (ddH_2O) unless otherwise stated.

2.1.2 Cell culture

Transformed human cervical epithelial cancer HeLa cells, transformed human colorectal epithelial carcinoma HCT116 cells, transformed Human Embryonic epithelial Kidney (HEK) 293T cells, non-transformed human Telomerase Reverse Transcriptase (hTERT) immortalised human Retinal Pigmented Epithelium (RPE) cells, and non-transformed hTERT immortalised human fibroblast 1BRhTERT and 48BRhTERT cell lines were used. Cells were obtained from laboratory stocks. The HeLa cell derivatives,

HeLa Kyoto cells, were also used and were a kind gift from Dr Mark Petronczki (Clare Hall Laboratories, Hertfordshire, UK). AAV-293 cells (Invitrogen) derived from HEK 293 were used for viral replication and packaging. Culture vessels and plates used were from Corning (New York, USA).

2.1.3 Antibodies

Primary antibodies used for this study are listed in **Table 2.1.1**. Alexa-flour®-conjugated secondary antibodies for immuunostaining; Alexa488 anti-rabbit, Alexa488 anti-mouse and Alexa594 anti-rabbit were purchased from Invitrogen. Horseradish peroxidase- (HRP-) conjugated rabbit or mouse polyclonal secondary antibodies for immunoblotting were from Dakocytomation (Cambridge, UK).

Table 2.1.1 Primary antibodies used in experiments

Optimal antibody concentrations were determined by titration. Dilutions used for immunoblotting (IB) or for immunofluorescence (IF) are listed.

Primary Antibody	***Raised In***	***Dilution for IB***	***Dilution for IF***	***Source***
Anti-Greatwall	Rabbit	1:200	1:100	GenScript (Piscataway, USA)
Anti-pT194 Greatwall	Rabbit	1:1,000	1:500	Eurogentec (Southampton, UK)
Anti-α Tubulin (DM1A)	Mouse	1:10,000	1:2,000	Abcam (Cambridge, UK)
Anti-Flag M2	Mouse	1:250	N/A	Sigma-Aldrich (Missouri, USA)
Anti-Myc (9E10)	Mouse	1:500	N/A	Abcam (Cambridge, UK)
Anti-phospho-(Ser) CDK substrates	Rabbit	1:5000	N/A	Cell Signaling Technology (Beverly, USA)
Anti-Ensa	Rabbit	1:250	N/A	Cell Signaling Technology
Anti-phospho-Ensa (Ser67) Arpp19 (Ser62)	Rabbit	1:250	N/A	Cell Signaling Technology

2.1.4 Primers

DNA sequences were obtained from the National Centre for Biotechnology Information website (NCBI; http://www.ncbi.nlm.nih.gov/) and primers were designed according to requirements using Lasergene SequBuilder 10.1 DNASTAR (Madison, USA). Primers were ordered from Eurofins MWG Operon (Ebersberg, Germany) or GATC Biotech (London, UK). The primers used in this study are listed in **Table 2.1.2**.

Table 2.1.2 Primers used for this work

Primer	***Sequence (5'-3')***
His-tag F+R *Primer pair to clone N-terminal 100 amino acids of Greatwall cDNA in frame with a His-tag in pET28*	ATT ACC ATG GAT CCC ACC GCG GGA A AGA TCT CGA GCA GTG AAT AAT ACA AAT GGA CAA TGA ATG GGC
GW F+R *Primer pair to clone full-length Greatwall cDNA*	ATG GAT CCC ACC GCG GGA AGC AAG AAG GAG CTA CAG ACT AAA TCC AGA TAC GGT CAG GTG
GWEntry F+R *Primer pair to clone full-length Greatwall cDNA into pDONR211*	GGG GAC AAG TTT GTA CAA AAA AGC AGG CTT AAT GGA TCC CAC CGC GGG AAG C GGG GAC CAC TTT GTA CAA GAA AGC TGG GTC CTA CAG ACT AAA TCC AGA TAC GG
M110A *Mutagenesis primer pair*	CAA TGT CTA CTT GGT AGC GGA ATA TCT TAT TGG GG CCC CAA TAA GAT ATT CCG CTA CCA AGT AGA CAT TG
T193A *Mutagenesis primer pair*	GGA TAT CCT TGC AAC ACC ATC AAT GGC GCC ATT GAT GGT GTT GCA AGG ATA TCC
T194A *Mutagenesis primer pair*	GGA TAT CCT TAC AGC ACC ATC AAT GGC GCC ATT GAT GGT GCT GTA AGG ATA TCC
T193A/T194A *Mutagenesis primer pair*	GAT GGA TAT CCT TGC AGC ACC ATC AAT GGC GCC ATT GAT GGT GCT GCA AGG ATA TCC ATC
T740S *Mutagenesis primer pair*	CGA ATT CTA GGA TCC CCA GAC TAC CTT G CAA GGT AGT CTG GGG ATC CTA GAA TTC G

T740A *Mutagenesis primer pair*	**CGA ATT CTA GGA GCC CCA GAC TAC CTT G** **CAA GGT AGT CTG GGG CTC CTA GAA TTC G**
S874A *Mutagenesis primer pair*	**CAG CAC CTG ACC GTA GCT GGA TTT AGT CTG TAG** **CTA CAG ACT AAA TCC AGC TAC GGT CAG GTG CTG**
S877A *Mutagenesis primer pair*	**CCG TAT CTG GAT TTG CTC TGT AGG ACC CAG** **CTG GGT CCT ACA GAG CAA ATC CAG ATA CGG**
S874A/S877A *Mutagenesis primer pair*	**CAG CAC CTG ACC GTA GCT GGA TTT GCT CTG TAG GAC CCA GC** **GCT GGG TCC TAC AGA GCA AAT CCA GCT ACG GTC AGG TGC TG**
S874T *Mutagenesis primer pair*	**CAG CAC CTG ACC GTA ACA GGA TTT AGT CTG TAG** **CTA CAG ACT AAA TCC TGT TAC GGT CAG GTG CTG**
T194D *Mutagenesis primer pair*	**GGA TAT CCT TAC AGA CCC ATC AAT GGC** **GCC ATT GAT GGG TCT GTA AGG ATA TCC**
S874D *Mutagenesis primer pair*	**CAG CAC CTG ACC GTA GAT GGA TTT AGT CTG TAG** **CTA CAG ACT AAA TCC ATC TAC GGT CAG GTG CTG**
T194E *Mutagenesis primer pair*	**GGA TAT CCT TAC AGA ACC ATC AAT GGC** **GCC ATT GAT GGT TCT GTA AGG ATA TCC**
S874E *Mutagenesis primer pair*	**CAG CAC CTG ACC GTA GAA GGA TTT AGT CTG TAG** **CTA CAG ACT AAA TCC TTC TAC GGT CAG GTG CTG**
S101D *Mutagenesis primer pair*	**GTA TTA TTC ACT GCA GGA TGC AAA CAA TGT CTA C** **GTA GAC ATT GTT TGC ATC CTG CAG TGA ATA ATA C**
T206E *Mutagenesis primer pair*	**CAA GAT TAT TCA AGA GAG CCA GGA CAA GTG TTA TCG C** **GCG ATA ACA CTT GTC CTG GCT CTC TTG AAT AAT CTT G**
S370A *Mutagenesis primer pair*	**GGA GTT AGC TCT TGC ACC CAT TCA TAA CAG C** **GCT GTT ATG AAT GGG TGC AAG AGC TAA CTC C**

K72M *Mutagenesis primer pair*	**GCA GAC ATG ATC AAC ATG AAT ATG ACT CAT CAG G** **CCT GAT GAG TCA TAT TCA TGT TGA TCA TGT CTG C**
T194S *Mutagenesis primer pair*	**GGA TAT CCT TAC ATC ACC ATC AAT GGC** **GCC ATT GAT GGT GAT GTA AGG ATA TCC**
Left Arm_attB4 F *5' primer to amplify Greatwall genomic DNA with the attB4 sequence for the left recombination arm for gene targeting*	**GGG GAC AAC TTT GTA TAG AAA AGT TGT GAG ACT CTG TCT CAA AAT AAA ATA ACA TG**
Left Arm_attB1_NdeI R *3' primer to amplify Greatwall genomic DNA with the attB1 for the left recombination arm to introduce an additional NdeI site for gene targeting*	**GGG GAC TGC TTT TTT GTA CAA ACT TGC ATA TGA TTA CAG TTA CAA TAT TTG GCA TGG CTC TG**
Right Arm_attB2 F *5' primer to amplify Greatwall genomic DNA with the attB2 sequence for the right recombination arm introducing the M110A mutation in exon 3 for gene targeting*	**GGG GAC AGC TTT CTT GTA CAA AGT GGC TTT TTT GAA AGG TAG CGG AAT ATC TTA TTG GGG G**
Right Arm_attB3 R *3' primer to amplify Greatwall genomic DNA with the attB3 sequence for the right recombination arm for gene targeting*	**GGG GAC AAC TTT GTA TAA TAA AGT TGC TGG TCT CAA ACT CCC GAC CTC AGG TGA TC**
Primer A *Forward primer situated at the beginning of exon 3 of the Greatwall allele used to detect wildtype Greatwall alleles*	**GGG GAC AGC TTT CTT GTA CAA AGT GGC TTT TTT GAA AGG TAG C**
Primer B *Reverse primer situated in exon 4 of the Greatwall allele used to detect wildtype and targeted alleles*	**CTC ATT AGA AAT AAG CAT ATT GTC CGG TTT C**

Primer C *Forward primer situated in the selection cassette and mutated (M110A) region of exon 3 in targeted Greatwall alleles used to detect the presence of targeted alleles*	**CAC AAT ATT AAA TTC TTT TTT GAA AGG TAA T**
Primer D *Forward primer situated in the puromycin resistance gene of targeted Greatwall alleles used to detect the presence of the resistance gene*	**CTA ATT CCA TCA GAA GCT GGT CG**
Southern Probe *Used for Southern blotting*	**CCA ATG ATA CCA AAG ATA ATC TAG** **GTT GGA TGT TTT AAA AAA GTA CTT**
Y59V *Mutagenesis primer pair*	**GAA AGG CGG CAA ATT GGT TGC AGT AAA GGT TG** **CAA CCT TTA CTG CAA CCA ATT TGC CGC CTT TC**
Y59T *Mutagenesis primer pair*	**GAA AGG CGG CAA ATT GAC TGC AGT AAA GGT TG** **CAA CCT TTA CTG CAG TCA ATT TGC CGC CTT TC**
V61I *Mutagenesis primer pair*	**GGC AGA AAG GCG GCA AAT TGT ATG CAA TAA AGG TTG** **CAA CCT TTA TTG CAT ACA ATT TGC CGC CTT TCT GCC**
Y107V *Mutagenesis primer pair*	**GCA GTC TGC AAA CAA TGT CGT CTT GGT AAT GG** **CCA TTA CCA AGA CGA CAT TGT TTG CAG ACT GC**
Y107T *Mutagenesis primer pair*	**GCA GTC TGC AAA CAA TGT CAC CTT GGT AAT GG** **CCA TTA CCA AGG TGA CAT TGT TTG CAG ACT GC**

2.1.5 Vectors

Vectors used in this work and their sources are listed in **Table 2.1.3**.

Table 2.1.3 List of vectors used

Vector	*Source*	*Notes*
pET28a(+)	Novagen (Merk KGaA, Darmstadt, Germnay)	For expression of N-terminal His-tagged 100 amino acid Greatwall fragment.
pCR®II-TOPO	Invitrogen (Paisley, UK)	For cloning of Greatwall full-length cDNA.
pDONR™221	Invitrogen	For cloning of Greatwall full-length cDNA and use with the Multisite Gateway® system from Invitrogen.
deltaT-FLAG-DEST	A kind gift from Stephan Geley (Biocenter, Innsbruck Medial University, Austria)	Expression vector for N-terminal flag-tagged Greatwall and mutants.
deltaT-Myc-DEST	A kind gift from Stephan Geley	Expression vector for N-terminal myc-tagged Greatwall and mutants.
pEGFP-C3	Clontech Laboratories (Mountain View, USA)	Expression vector for GFP.
bML4(puroR)	A kind gift from Shunichi Takeda (Kyoto University, Japan)	Used for co-transfection with flag-tagged Greatwall to provide puromycin resistance and indicate integration events.
SPI	GenScript (Piscataway, USA)	Minimal kinase construct containing artificial splice transcript I in pUC57.
SPII	GenScript	Minimal kinase construct containing artificial splice transcript II in pUC57.

pDONR™ P4-P1R	Invitrogen	Left homology arm donor vector for gene targeting using Gateway® technology (Iiizumi *et al.* 2006).
pDONR™ P2R-P3	Invitrogen	Right homology arm donor vector for gene targeting using Gateway® technology (Iiizumi *et al.* 2006).
pAAV-dest	A kind gift from Professor Alan Lehman (University of Sussex, UK)	Destination vector with Gateway® *att* site-containing cassette for recombination inserted into the pAAV-MCS vector (Invitrogen) using NotI restriction sites.
pHelper	Invitrogen	For production of infectious viral particles containing the Greatwall gene targeting vector in AAV-293 cells.
pAAV-RC	Invitrogen	For production of infectious viral particles containing the Greatwall gene targeting vector in AAV-293 cells.
Puro entry clone	A kind gift from Shunichi Takeda	Puromycin resistance gene subcloned into the donor vector pDONR™221 (Iiizumi *et al.* 2006).
Ad-CMV-Cre	Vector BioLabs (Philadelphia, USA)	For excision of puromycin resistance gene.
pDEST™14	Invitrogen	Destination vector used for *in vitro* translation of Greatwall cDNA.

2.2 Methods

2.2.1 Bacterial cultures and plasmid preparation

Individual colonies were picked from an LB (Luria Bertani medium; 0.5% yeast extract, 1% tryptone and 171 mM sodium chloride (NaCl)) agar plate containing appropriate selective antibiotics (kanamycin was used at 50 µg/ml and ampicillin was used at 100 µg/ml). To prepare small amounts of plasmid deoxyribonucleic acid (DNA), 3 ml LB cultures containing the appropriate selective antibiotics were incubated overnight at 225 revolutions per minute (r.p.m.) / 37˚C. Cells were harvested by centrifugation at 4000 r.p.m. for 5 minutes. The plasmid DNA was then purified from the cells using the alkaline lysis method following the manufacturer's protocol with the QIAprep Spin Miniprep Kit using a microcentrifuge from QIAGEN (West Sussex, UK). Plasmid DNA was eluted in 50 µl ddH_2O and the concentration analysed by measuring the absorbance at 260 nm on a spectrophotometer and confirmed by restriction digestion and sequencing. Restriction digests were performed according to manufacturer's instructions and as recommended by the New England Biolabs website (https://www.neb.com/) and analysed by agarose gel electrophoresis. DNA was sent to GATC Biotech for sequencing and then analysed using Lasergene SequBuilder 10.1 DNASTAR.

For preparation of larger quantities of plasmid DNA for transfection into human cells, 5 ml starter cultures were grown for 8 hours at 225 r.p.m. / 37˚C. Then 100 µl of the starter cultures were used to inoculate 100 ml LB containing appropriate selective antibiotics which were incubated at 225 r.p.m. / 37˚C overnight. Cells were harvested by centrifugation at 4000 r.p.m. / 4˚C for 20 minutes. The plasmid DNA was then purified from the pelletted cells again using the alkaline lysis method following the manufacturer's protocol with the QIAFilter Plasmid Midi Kit from QIAGEN. The concentration of the purified plasmid DNA was then measured and the presence of the expected plasmid DNA confirmed by restriction digestion and sequencing.

2.2.2 Transformation of plasmid DNA in bacteria

Competent DH5α *Escherichia coli* (*E.coli*) cells were thawed on ice and 50 µl used per transformation. Between 50 to 100 ng of plasmid DNA was used and 50 µl competent cells were added to the DNA and mixed gently, then incubated on ice for 20 minutes. The tubes were next incubated at 42˚C for 45 seconds to heat shock the cells before being returned to ice for 2 minutes. 1 ml of warmed LB was then added to the cells and mixed gently. The tubes were incubated for a further hour in a water bath at 37˚C. After this 50 to 200 µl of the samples were plated onto LB agar plates with appropriate selection antibiotics and placed at 37˚C overnight. For transformations of mutagenesis PCR products the entire suspension was spun down and the supernatant removed to leave a 50 µl concentrated suspension which was then plated onto LB agar plates (LB medium and 15 g/L agar).

2.2.3 Cloning, PCR and RT-PCR

As mentioned previously, all DNA extractions were performed using QIAprep Spin Miniprep from QIAGEN and all restriction digests were performed using enzymes and buffers from New England Biolabs. All ribonucleic acid (RNA) extractions were performed using the RNeasy Mini Kit from QIAGEN. Polymerase chain reactions (PCRs) were performed using the Phusion High-Fidelity PCR Kit from Finnzymes (Waltham, USA). Ligations were performed using the Ligation high Ver.2 from TOYOBO (Osaka, Japan). Reverse-transcriptase PCRs (RT PCRs) were performed using the SuperScript™ III One-Step RT-PCR System from Invitrogen. Greatwall cDNA was amplified from HeLa cell messenger RNA (mRNA) using primers GW F+R (detailed in section **2.1.4**) and cloned into the pCR®II-TOPO cloning vector using the TOPO-TA Cloning Kit from Invitrogen. In all cases the manufacturer's recommended protocols were followed and the presence of the expected DNA sequences confirmed by restriction digestion and sequencing.

2.2.4 Agarose gel electrophoresis and gel extraction

DNA was separated using 1% agarose gels by electrophoresis in TAE (40 mM Tris base, 1 mM ethylene diamine tetraacetic acid (EDTA) and 20 mM acetic acid) and visualised using the gel imaging system InGenius LHR from Syngene (Cambridge, UK). The size of the DNA fragments was confirmed by parallel loading of 1Kb/+ DNA ladder from New England Biolabs. When required, DNA was purified using the QIAquick Gel Extraction Kit from QIAGEN following the manufacturer's recommended protocol and eluted in ddH_2O.

2.2.5 Gateway cloning

In this work the MultiSite Gateway® technology from Invitrogen was used instead of traditional cloning methods to manipulate the cDNA of Greatwall. This technology takes advantage of the lambda phage recombination system to allow transfer of cloned DNA between vectors via site specific *att* recombination sequences (**Figure 2.2.1**). Recombination is conservative and does not require any DNA synthesis. Once DNA has been cloned in this system the DNA can then be transferred from an entry clone into numerous other destination vectors, i.e. vectors for protein expression or to tag the protein.

In order to create an entry clone containing the cDNA of Greatwall, the appropriate *att* recombination sequences were added by PCR to either end of the cDNA (that had been previously subcloned into the pCR®II-TOPO cloning vector) using the primers GWEntry F+R (listed in section **2.1.4**). A BP reaction was then performed using the Gateway® BP Clonase II Enzyme Mix (Invitrogen) to move the cDNA into the pDONR™221 vector (Invitrogen) following the manufacturer's recommended protocol, creating a Greatwall entry clone (**Figure 2.2.1 A**). This was then subsequently used for a further cloning step by performing an LR reaction using the Gateway® LR Clonase II Enzyme Mix (Invitrogen) following the manufacturer's recommended protocol with various destination vectors to yield the vectors detailed throughout this work (**Figure 2.2.1 B and C**). Details of all reactions can be found in the Gateway® Technology with Clonase II Manual available on the Invitrogen website (www.invitrogen.com).

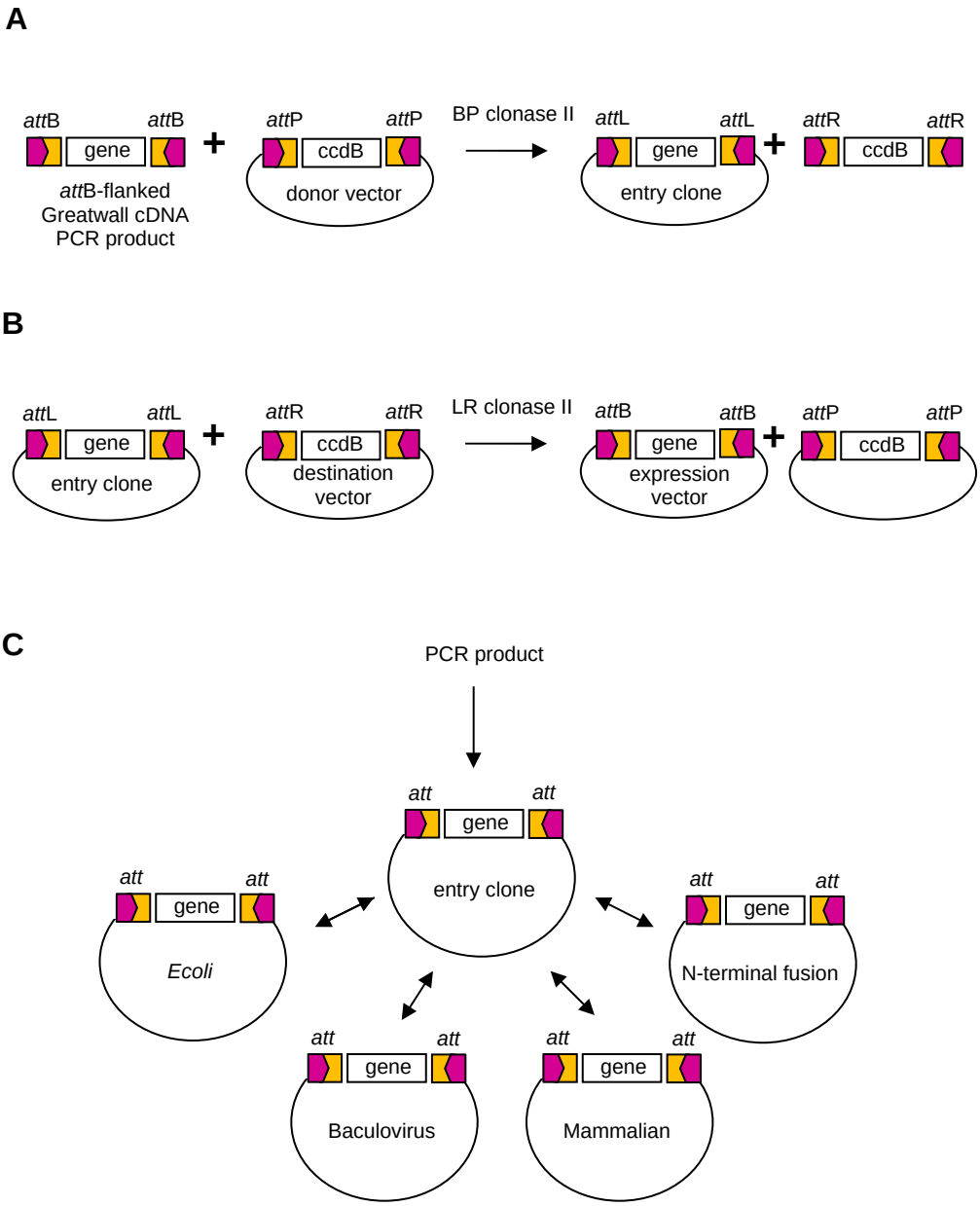

Figure 2.2.1 Cloning using Gateway® technology

(A) In the BP reaction, BP Clonase facilitates recombination of the *att*B substrate (which can be an *att*B-flanked PCR product, as was used for Greatwall, or a linearised *att*B expression clone) with the *att*P substrate (the donor vector). This creates an *att*L entry clone that can then be used in the MultiSite Gateway® system. **(B)** In the LR reaction, LR Clonase facilitates recombination of the *att*L substrate (the entry clone) with an *att*R substrate (any destination vector). In this manner the cloned DNA can be effectively transferred into multiple vectors, as was used for Greatwall cloning. **(C)** This technology provides a rapid and efficient way to move a cloned DNA sequence into multiple vector systems. Adapted from the Gateway® Technology with Clonase II Manual from Invitrogen (www.invitrogen.com).

In this manner I created N-terminally flag- and myc-tagged Greatwall constructs by performing LR reactions with the Greatwall entry clone and the destination vectors; deltaT-FLAG-DEST and deltaT-Myc-DEST respectively. I also cloned Greatwall cDNA into the Gateway® pDEST™14 expression vector. This allowed *in vitro* expression of the cDNA in a rabbit reticulocyte lysate system using the TNT® Quick Coupled Transcription/Translation System from Promega (Madison, USA) following the manufacturer's recommended protocol.

2.2.6 Site-directed mutagenesis

Primers were designed using Lasergene SequBuilder 10.1 DNASTAR and properties checked using the Multifunctional Oligo Property Scan Tool provided by Eurofins MWG Operon website (http://www.eurofinsgenomics.eu.). In general, the codon that required the minimum base changes possible was chosen to mutate the target amino acids. Primers were usually designed with the bases to be mutated in the centre of the primer sequence with approximately 15 bases either side of the mutated bases with a guanine (G) or cytosine (C) base at the termini of the primer.

The mutagenesis was carried out using the QuickChange® XL Site-Directed Mutagenesis Kit from STRATAGENE (California, USA) following the manufacturer's protocol. The unmutated template DNA was removed by digestion with the restriction enzyme DpnI as recommended and 5 µl of the reaction was taken for transformation into DH5α *E.coli* cells.

2.2.7 Immunoblotting

Cells were lysed in SDS-sample buffer (0.01% (w/v) bromophenol blue, 62.5 mM Tris-hydrogen chloride (HCl) [pH6.8], 7% (w/v) sodium dodecyl sulphate (SDS), 5% β-mercaptoethanol and 20% (w/v) sucrose) and sonicated at high power with 0.5 second intervals using a Bioruptor (Diagenode, Cambridge, UK) for 10 minutes in a chilled ultrasonic bath at 4ºC. Samples were then boiled at 95ºC for 5 minutes and run on SDS-polyacrylamide gels by electrophoresis using the Bio-Rad Mini Protean III System from Bio-Rad, in Running buffer (25 mM Tris base, 192 mM glycine and 3.5

mM SDS) along with a ColourPlus Prestained Protein Marker (Broad-range, New England Biolabs). Stacking gels comprised 5% bisacrylamide, 125 mM Tris-HCl [pH 6.8], 0.1% SDS, 0.1% ammonium persulphate (APS) and 0.1% N,N,N',N'-tetramethylethylenediamine (TEMED). Resolving gels comprised 10% bisacrylamide, 375 mM Tris-HCl [pH 8.8], 0.1 % SDS, 0.1% APS and 0.05% TEMED. Protein was transferred by electro-blotting onto a Hybond^{TM} C+ membrane (Amersham Biosciences, Piscataway, USA) using Trans-Blot Semi-Dry Transfer Cell (Bio-Rad) in Semi-dry Transfer buffer (48 mM Tris base, 39 mM glycine, 0.04% SDS and 20% methanol). Protein bands were then visualised using Ponceau S solution (0.1% (w/v) in 5% acetic acid). The membranes were washed in PBS (137 mM NaCl, 0.3 mM potassium chloride (KCl), 10 mM disodium hydrogen phosphate (Na_2HPO_4), 1.7 mM monopotassium phosphate (KH_2PO_4) and pH to 7.4 with HCl) with 0.1% NP40 and blocked in 5% milk (Marvel with PBS-0.1% NP40) for 1 hour at room temperature. Antibodies were diluted in 5% milk or 5% bovine serum albumin (BSA; with PBS-0.1% NP40) and secondary HRP-conjugated rabbit or mouse polyclonal secondary antibodies were used at recommended concentrations. Proteins were visualised using the Enhanced Chemiluminescence (ECL) Advance Western Blotting Detection Kit (Amersham) following the manufacturer's protocol. The membrane was exposed to Hyperfilm ECL (Amersham) and processed using an automatic X-ray film processor (Xograph, Gloucestershire, UK).

2.2.8 Antibody generation

Antibodies against the Greatwall protein were produced by cloning the N-terminal 100 amino acids (aa) of Greatwall into the pET28a(+) expression vector from Novagen using XhoI and NcoI restriction enzymes. The N-terminal fragment was expressed from this vector with a C-terminal 6 x His-tag from this vector in *E.coli* BL21 cells using 1 mM isopropylthio-β-galactoside (IPTG) and purified under denaturing conditions using nickel-nitrilotriacetic acid (Ni-NTA) agarose beads from QIAGEN in an empty PD-10 Desalting Column from Amersham. This was carried out following the batch purification protocol under denaturing conditions in 6 M Urea detailed in The QIAexpressionist handbook available from QIAGEN. The purified recombinant protein fragment was then sent to GenScript to raise antibodies in rabbit.

The 4th immunisation sera was then purified by running out 4 x 5 µg of the purified recombinant protein fragment in SDS-sample buffer on a 15% SDS-polyacrylamide gel by electrophoresis and transferred onto a Hybond C+ membrane (as described in section **2.2.8**). The protein bands were then visualised using Ponceau S solution and individually cut out. These were then blocked in 5% milk for 1 hour at room temperature and then washed briefly two times with PBS-0.1% NP40. After this they were incubated at 4ºC for 72 hours with 0.5 ml 4th immunisation sera with end over end rotation. The membranes were then washed five times with PBS-0.1% NP40 and the antibodies eluted from the membrane in 150 µl freshly prepared chilled Elution buffer (0.5 M NaCl, 50 mM glycine, 0.5% Tween-20, 0.1 mg/ml BSA and pH to 2-3 with HCl) while vortexing for 20 seconds. Next 25 µl of 1 M Tris [pH 8.8] was added to neutralise the buffer and the elute removed and taken into a new tube. This was then repeated. Next, the elute was then pooled and 10% Thimerosal added at 1:1000. Finally, the elute was concentrated by centrifugation for 20 minutes through a Vivaspin 2 ml column from Satorius Biotech (Gottingen, Germany) at 3000 r.p.m. / 4ºC. The purified and concentrated 4th immunisation sera (anti-Greatwall) antibodies were then stored in 20 µl aliquots at - 80ºC.

Phospho-specific antibodies against the phosphorylated threonine 194 of human Greatwall were generated in rabbit by Eurogentec (antigen code: Greatwall-EP110355-KLH-MBS) using the peptide sequence the peptide sequence CMMDILTT(PO_3H_2)PSMAK (EP110355) and CMMDILTTPSMAK (EP110356). The purified antibody sera was used for this work and stored at -20˚C.

2.2.9 Cell culture and inhibitor treatments

Cells were cultured in Dulbecco's Modified Eagle's Medium (DMEM) supplemented with 2 mM L-glutamine, 10% foetal calf serum (FCS) and 1% Penicillin G (sodium salt)-Streptomycin in saline solution in a 37˚C, 5% carbon dioxide (CO_2) incubator. Trypsin-EDTA was used to passage cells. Frozen stocks were made in FCS with 10% dimethyl sulfoxide.

Cells were treated with 1 mM of Thymidine, 10 µM RO-3306, or 10 µM of BI2536 for 24 hours. Cells were treated with 75 ng/ml Nocodazole or 5 µM of STLC for 16 hours. Cells were also treated with phosphatase inhibitors: 5 µM Tautomycetin

and 1 µM okadaic acid (for further details see section **2.2.23**). For these treatments the media was aspirated and replaced with drug containing media, and mixed thoroughly by pipetting.

2.2.10 Double Thymidine block and release

HeLa cells were seeded at 1 x 10^5 cells in a 6-well plate in 1 ml medium and incubated at 37˚C overnight. The cells were then treated with 1 mM Thymidine for 24 hours. Treatment was carried out by aspirating the medium and replacing it with drug-containing medium, except for control cells for which the medium was replaced with fresh (drug-free) medium. After 24 hours the Thymidine was washed away by the addition of 5 ml of warmed PBS which was swirled and then removed for five repeats. Finally, 1 ml of fresh medium was added and the cells allowed to recover for 12 hours at 37˚C. The cells were then treated again with 1 mM Thymidine for a further 12 hours in the same manner as before. An initial sample (at time zero) was taken of the blocked cells. The Thymidine was washed away, as above, for all the other cells and they were released from their cell cycle block by the addition of 1 ml fresh drug-free medium. Samples were then collected every hour for a 10 to 12 hour period. Samples were collected by trypsiniation and resuspended in 1 ml PBS. 150 µl of the cell suspension was then taken and the cells fixed in 70% ethanol for analysis by fluorescence assisted cell sorting (FACS). The remaining cells were resuspended in 50 µl SDS-sample buffer for analysis by immunoblot.

2.2.11 FACS analysis

Cells were fixed in 70% ethanol for at least 16 hours at 4^{o}C. Cells were then centrifuged at 1500 r.p.m. for 3 minutes and rinsed in 0.5 ml of 3% BSA-PBS. After this they were re-centrifuged and resuspended in 3% BSA-PBS with 5 µg/ml propidium iodide (PI) and 1 µg/ml RNase. These were analysed on a BD FACSCanto machine from BD Biosciences (Oxford, UK) and FACS Diva software (BD Biosciences) was used to plot PI area versus cell counts.

2.2.12 Transfection

Cells were transfected with DNA at 60 to 80% confluency using FuGene® 6 Transfection Reagent (Roche Diagnostics) using the 3:2 ratio of reagent to DNA in serum-free DMEM without antibiotics as per the manufacturer's instructions. Cells were then grown at 37^{o}C for 48 to 72 hours before lysates were collected.

2.2.13 Generation of stable cell lines

HEK 293T cells were seeded at 1 x 10^5 cells in a 6-well plate and co-transfected the next day with 5 µg of flag-tagged Greatwall cDNA in deltaT-FLAG-DEST and 1 µg bML4(puroR) for selection of incorporation events using puromycin with FuGene® 6 Transfection Reagent as described in section **2.2.12**. Cells were selected 48 hours later with addition of medium containing 3 µg/ml puromycin. Selection pressure was maintained over two weeks by the addition of fresh puromycin-containing medium every 3 to 4 days. Surviving clones were trypsinised using 3 mm cloning disks and expanded into 6-well plates in puromycin-containing medium. Once cells were 80% to 90% confluent half of the cells were frozen and the other half taken for analysis by immunoblotting. Clones found to be expressing flag-Greatwall were then woken up and expanded for experiments.

2.2.14 Growth curves

Flag-Greatwall expressing HEK 293T clones number 1 and 7 at passage 1 were seeded at 5 x 10^4 cells in 1 ml medium in 24-well plates. Cells were then assessed and data collected for growth curves using the IncuCyte system from Essen Biosciences (Hertfordshire, UK). This phase-contrast compact microscope can be placed inside the cell culture incubator to allow direct long-term monitoring and data collection of cell growth. Nine different points from 6 wells of a 24-well plate were measured every 3 hours for 255 hours. Growth curves were then plotted using Microsoft® Office Excel 2003 from Microsoft (Reading, UK).

2.2.15 siRNA transfection

Cells with 60% to 80% confluency were transfected with 6 µl HiPerFect Transfection Reagent (QIAGEN) as per manufacturer's instructions, using 5 to 100 nM RNA. Cells were then grown at 37^{o}C for 48 to 72 hours before lysates were collected. Control siRNA used was AllStars Negative Control siRNA from QIAGEN, control siRNA against Eg5 was Hs_KIF11_8 FlexiTube siRNA from QIAGEN (target sequence: CTCGGGAAGCTGGAAATATAA). Greatwall siRNA was Hs_MASTL_6 FlexiTube siRNA (target sequence: ACGCCTTATTCTAGCAAATTA) and Hs_MASTL_7 FlexiTube siRNA (target sequence: CAGGACAAGTGTTATCGCTTA) also from QIAGEN.

2.2.16 Immunoflourescent staining of cells

Prior to fixation, cells were seeded onto glass cover slips. Once cells had reached 60% to 80% confluency, the media was aspirated and the cells washed briefly with warmed PBS. The cells were then fixed in ice cold methanol at -20˚C for 10 minutes. The fixed cells were next washed with PBS three times for 5 minutes and then permeabilised using PBS-0.1% NP40 for 20 minutes. After this, the cells were blocked for 30 minutes at room temperature in 5% BSA-PBS and incubated for 1 hour with primary antibodies made up in 5% BSA-PBS. The cells were then washed with PBS three times for 5 minutes and incubated with secondary antibodies diluted in 5% BSA-PBS for 1 hour at room temperature. The cells were washed again with PBS before being mounted onto standard laboratory slides face down with 10 µl of Prolong® Gold mounting solution with DAPI and allowed to set for at least 16 hours at 4˚C. Images of cells were taken using a Delta Vision® microscope from Applied Precision (Washington, USA) with a x100 or x60 oil immersion objective (Olympus, Essex, UK). Z-series of 0.3 µm stacks were acquired using SoftWoRx software version 3.7.1 from Applied Precision and deconvolution performed using Huygens Professional Deconvolution Software Version 3.5 from Scientific Volume Imaging (Hilversum, NL). Maximum intensity projections were obtained in Omero Version Beta 4.1.1 (The OME Consortium, UK) and exported as Tiff files.

2.2.17 Quantification of multinuclear cells

HeLa cells were treated with 25 nM control or Greatwall siRNA for 72 hours after which cells were fixed and stained using anti-α Tubulin antibodies to visualise the cells and DAPI to visualise the nuclei. Z-series of 0.3 µm stacks were acquired and the maximum intensity projections were obtained in Omero Version Beta 4.1.1. The number of cells retaining a single nuclei or that had become multinucleate were counted. For this 75 to 100 cells from three separate siRNA experiments were counted. The data was then exported into Microsoft® Office Excel 2003 and plotted.

2.2.18 Transfection of flag-tagged Greatwall and mutants

Cells were seeded into 10 cm^3 culture dishes at 1 x 10^6 in 10 ml medium. Cells were transfected the next day using the calcium phosphate precipitation method. For this 10 µg of plasmid DNA was added to 61 µl of 2 M calcium chloride ($CaCl_2$) and sterile water added to 500 µl. This solution was added drop wise to 500 µl of 2 × HEPES-Buffered Saline Solution (HBSS) (12 mM dextrose, 50 mM HEPES, 10 mM KCl, 280 mM NaCl, 1.5 mM disodium hydrogen phosphate dihydrate ($Na_2HPO_4.2H_2O$), pH to 7 with HCl) while bubbling gently using a glass Pasteur pipette and electronic pipette to mix. The 1 ml solution was then immediately added drop wise to the cells and swirled to mix. The next day the precipitate-containing medium was removed, the cells washed with PBS and fresh medium added back. Samples were collected the following day.

2.2.19 Immunoprecipitation of flag-tagged Greatwall and mutants

HEK 293 cells were plated in 10 cm^3 culture dishes at 1 x 10^6 cells in 10 ml medium. Cells were transfected with plasmids using the calcium phosphate method as described in section **2.2.19**. The next day (16 hours later) the medium was removed, the cells were washed once with 5 ml PBS and fresh medium or drug-containing medium added and swirled to coat cells.

The following day, after the appropriate incubation time with drug treatments if required (see figure legends for details of individual experiments), cells were harvested by trypsinisation (2 x plates per condition). The cells were resuspended in 500 µl of chilled Lysis buffer (20 mM Tris-HCl [pH7.5], 137 mM NaCl, 10% glycerol, 0.5% NP-40, 2 mM EDTA with one tablet of Complete Protease Inhibitors Cocktail and PhoSTOP Phosphatase Inhibitor Cocktail per 50 ml) and incubated on ice for 20 minutes. The cell lysates were then spun down at 13000 r.p.m. / 4˚C for 15 minutes and the elute transferred to new tubes. Protein was equalised using the Bio-Rad Protein Assay Reagent (Bio-Rad) and measuring absorbance at 600 nm. A 50 µl sample of the equalised whole cell lysate was kept and SDS-sample buffer added for evaluation by immunoblotting. The Anti-flag M2 Magnetic beads were prepared by washing two times with Immunoprecipitation (IP) buffer (20 mM Tris-HCl [pH7.5], 137 mM NaCl, 10% glycerol, 0.5% NP-40, 2 mM EDTA, 10 mM sodium fluoride (NaF) and 1 mM sodium orthovanadate (Na_3VO_4)) on a chilled magnetic stand. The equalised whole cell lysates were then incubated with 20 µl of the beads resuspended in IP buffer for 1 hour with end over end rotation at 4˚C to capture the flag-Greatwall protein. After this, the supernatant was removed from the beads using the chilled magnetic stand and the beads were then washed two times in High Salt IP buffer (20 mM Tris-HCl [pH7.5], 500 mM NaCl, 10% glycerol, 0.5% NP-40, 2 mM EDTA, 10 mM NaF and 1 mM Na_3VO_4). Next, the beads were resuspended in 1 ml of chilled Kinase buffer (50 mM MOPS [pH7.5], 5 mM magnesium chloride ($MgCl_2$), 0.4 mM EDTA, 0.4 mM ethylene glycol tetraacetic acid (EGTA) with one tablet of Complete Protease Inhibitors Cocktail and PhoSTOP Phosphatase Inhibitor Cocktail per 50 ml with 1:1000 β-mercaptoethanol added as per use) and 100 µl (10%) of the beads removed and resuspended in 25 µl SDS-sample buffer for analysis by immunoblotting. Beads resuspended in 0.9 ml Kinase buffer were then prepared for kinase assays.

2.2.20 Kinase assays with immunoprecipitated flag-tagged proteins

Beads were split in half and each half then resuspended in 30 µl Kinase buffer or Kinase buffer containing 20 µg of the Myelin Basic Protein (MBP) substrate. To start reactions, 10 µl of 100 µM ATP including 0.1 MBq [γ-^{32}P]ATP (made up in Kinase buffer) from PerkinElmer (Massachusetts, USA) was added. Reactions were incubated

at 37˚C for 20 minutes and were terminated by the addition of 25 µl SDS-sample buffer and boiling at 95˚C for 5 minutes. The phosphorylation was then analysed by running 15 µl of each reaction out on a 15% SDS-polyacrylamide gel by electrophoresis (as described in section **2.2.8**). The gel was dried and transferred to a lead-lined cassette. Based on the intensity of the radioactive signal, the blot was exposed on the Storm 840 PhosphorImager (Molecular Dynamics; California, USA) and the autoradiograph exported as a Tiff file.

2.2.21 Quantification of kinase assays

The levels of flag-tagged Greatwall protein recovered in each immunoprecipitate were measured using densitometry of the ECL film taken with ImageJ software (Wayne Rasband, National Institutes of Health, USA). The corresponding phosphorylation of the MBP induced by Greatwall in the kinase reaction were also measured using densitometry of the autoradiograph using ImageJ software. Finally, the activity levels were corrected by the amount of protein present in each immunoprecipitate and represented as a percentage of the phosphorylation compared with that of the wildtype form. This data was then exported into Microsoft® Office Excel 2003 and plotted. All kinase assays were repeated twice unless otherwise stated.

2.2.22 Kinase assays with recombinant cyclin A-CDK2

Immunoprecipitations were performed as described in section **2.2.19**. Beads were split in half and each half resuspended in 30 µl Kinase buffer or Kinase buffer containing 40 ng/µl recombinant cyclin A-CDK2. To start reactions 10 µl of 100 µM ATP (made up in Kinase buffer) was added. Reactions were incubated at 37˚C for 20 minutes and were terminated by the addition of 25 µl SDS-sample buffer and boiling at 95˚C for 5 minutes. Where required, instead of terminating the reaction, 1 µl of Lambda Protein Phosphatase with Protein MetalloPhosphatases buffer and manganese chloride ($MnCl_2$) from New England Biolabs were added to the tube as per the manufacturer's recommended protocol and incubated at 30˚C for 30 minutes. The reactions were then

stopped by addition of 15 µl SDS-sample buffer and boiling at 95˚C for 5 minutes. The phosphorylation was then analysed by immunoblotting (as described in section **2.2.8**).

2.2.23 Phosphatase treatments

Cells that were 70 to 90% confluent in 125 cm^3 culture flasks were treated with the 5 µM of the Eg5 inhibitor, STLC, for 16 hours to arrest cells in mitosis. A mitotic shake off was then performed and the cells collected and centrifuged at 1500 r.p.m. for 5 minutes before being resuspended in 5 µM STLC-containing medium alone or medium that also contained 5 µM Tautomycetin or 1 µM okadaic acid. Cells were incubated at 37˚C for one hour after which a time zero sample was taken. Samples were collected by centrifugation at 2000 r.p.m. for 2 minutes and immediately resuspended in SDS-sample buffer. They were then transferred to ice before being sonicated and boiled at 95˚C for 5 minutes at the end of the experiment. To the remaining cells 10 µM RO-3306 was added to inhibit CDK1 (Vassilev *et al.* 2006) and the cells incubated again at 37˚C. Samples were then taken at different time points after the addition of RO-3306.

2.2.24 Sequence alignments

All sequences alignments were carried out using CLUSTAL 2.1 multiple sequence alignment (Larkin *et al.* 2007) using the Sequence Alignment Tool on the European Bioinformatics Institute website (http://www.ebi.ac.uk/) (Goujon *et al.* 2010).

2.2.25 Structural modelling

The structural model of Greatwall was created in collaboration with Dr. Anthony Oliver from the Genome Damage and Stability Centre (GDSC) at the University of Sussex and was produced using the computational protein structure prediction engine, the Protein Homology/analogY Recognition Engine (PHYRE) (Kelley *et al.* 2009). This allowed generation of a 3-dimensional (3D) model based on protein threading (or fold recognition). Structural prediction for proteins that have no

homologues with known structures are made in this case by aligning, or ‘threading’, amino acids from the target sequence onto a template structure and then evaluating how well the target matches the template. In this manner a ‘best-fit’ template was selected from known structures and a model of the target sequence structure was built. The catalytic core of Greatwall was modeled in this manner using the α isoform of PKC, another AGC family kinase, as the best-fit template. All molecular graphics figures were produced with the help of Dr. Anthony Oliver using the MacPyMOL Molecular Graphics System from DeLano Scientific (www.delanoscientific.com/).

2.2.26 Phospho-site analysis

Phosphorylation site mapping analysis of Greatwall was performed using PhosphoSitePlus® from Cell Signaling Technology (http://www.phosphosite.org). This is an online systems biology resource for the study of protein post-translational modifications (PTMs) that provides an extensive, manually curated database indicating phosphorylation sites and other PTMs that have been identified from both high-throughput and low-throughput articles and reports (Hornbeck *et al.* 2012). The output of this analysis indicated likely modified (phosphorylated) residues of human Greatwall and informed this study.

2.2.27 Gateway cloning to make an analogue sensitive Greatwall kinase

The MultiSite Gateway® technology from Invitrogen was used instead of traditional cloning methods to create a gene targeting vector to introduce the M110A mutation in the ATP-binding site of the Greatwall kinase. The targeting strategy involved the generation of right and left homologous arms to target the Greatwall genomic locus to introduce the mutation into exon 3 of the gene (Iiizumi *et al.* 2006). This is described in detail in **Chapter 6**. The MultiSite Gateway® Three-Fragment Vector Construction Kit from Invitrogen was used and manufacturer's protocols from the MultiSite Gateway® Technology Manual Version E were followed.

2.2.28 Adeno-associated viral (AAV) vectors and infection

The destination vector, pAAV-dest, used for Greatwall gene targeting contained the Gateway *att* site-containing cassette for recombination inserted into the pAAV-MCS vector using NotI restriction sites. Adeno-associated viruses are replication deficient parvoviruses that require co-transfection with helper adenoviruses for productive infection. The pAAV-MCS vector was co-transfected with the pHelper and pAAV-RC vectors in AAV-293 cells using the calcium phosphate precipitation method (described in section **2.2.18**) to allow the production of infectious viral particles containing the gene targeting vector. Viral particles were produced and HCT116 cells were infected as described in the Stratagene AAV Helper-Free System Instruction Manual A.02 and in Kohli *et al*. (2004). Selection was performed in complete DMEM with 2 µg/ml puromycin.

2.2.29 Deletion of puromycin cassette in targeted clones

This was carried out using the Ad-CMV-Cre virus from Vector BioLabs (Philadelphia, USA) at 100 multiplicity of infection (MOI) in 2 ml medium in a 6-well culture plate for 24 hours. Cells were then diluted in DMEM in 96-well culture plates and clones screened using double selection in medium with and without puromycin at 2 µg/ml.

2.2.30 Extraction of genomic DNA

Cells were trypsinised, pelleted and resuspended in Lysis buffer (200 mM NaCl, 20 mM EDTA, 40 mM EGTA, 40 mM Tris-HCl [pH8.0], 0.5% SDS, 0.5% 2-Mercaptoethanol and 200 µg/ml Proteinase K), then incubated overnight at 55^{o}C. The next day 250 µl of 6 M NaCl was added and the samples vortexed for 10 seconds then incubated on ice for 30 minutes. Next, these were then centrifuged at 13,000 r.p.m. for 30 minutes after which the supernatant was decanted and 1 volume of 100% ethanol was added. These were then centrifuged again at 13,000 r.p.m. for 10 minutes. The

DNA pellet was washed with 70% ethanol, air-dried and re-suspended in 20 µl of TE (10 mM Tris-HCl [pH 8.0] and 1 mM EDTA [pH 8.0]).

2.2.31 Southern blotting

Once genomic DNA had been extracted, the concentration was measured and 30 µg was digested overnight using the NdeI restriction enzyme and then run on a 0.7% agarose gel in TAE. The gel was depurinated using HCl solution (0.25 M HCl) for 15 minutes and placed in Denaturation buffer (1.5 M NaCl and 0.5 M sodium hydroxide (NaOH)) for 30 minutes with gentle shaking. The gel was washed two times for 30 minutes in Neutralisation buffer (1.5 M NaCl and 0.5 M Tris-HCl [pH 7.5]). The DNA was transferred overnight at room temperature using capillary blotting apparatus with 20 x Saline-Sodium Citrate (SSC) buffer (3 M NaCl and 300 mM trisodium citrate and pH to 7 with HCl) onto a Hybond™ Nylon Membrane from Amersham. The DNA on the membrane was then cross-linked using a UV-Stratalinker 2400 (Stratagene). The 371 bp probe was labelled using the Ready-to-go DNA labelling beads from Amersham. For this 50 ng of DNA in 45 µl of TE was denatured by heating for 5 minutes at 95^{o}C and immediately placed on ice for 2 minutes. The denatured DNA was added to the tube containing the reaction mix beads with 1.85 MBq of [α-^{32}P]dCTP (PerkinElmer). The tubes were incubated at 37^{o}C for 1 hour and the labelled probe was purified using the DyeEx 2.0 spin kit from QIAGEN following the manufacturer's protocol. Prior to use, the labelled probe was again denatured at 95^{o}C for 5 minutes. The membrane was pre-hybridised using 10 ml of warmed ExpressHyb^{TM} Hybridisation Solution (BD Biosciences) at 68^{o}C for 30 minutes with continuous rotation. The denatured radiolabeled probe was added to the hybridisation solution overnight at 68°C with continuous rotation. The membrane was washed with 2 x SSC buffer for 15 minutes and 2 x SDS-SSC buffer (2 x SSC with 0.1% SDS) for 30 minutes. The blot was transferred to a lead-lined cassette and, based on the intensity of the radioactive signal, the blot was exposed on the Storm 840 PhosphorImager. The autoradiograph was then exported as a Tiff file.

2.2.32 Human lung and breast cancer cell lines

Samples were prepared by collection of 1 x 10^5 cells in 100 µl SDS-sample buffer by Dr. Victoria Haley from the Trafford Centre at the Brighton and Sussex Medical School. These were then sonicated and boiled at 95˚C for 5 minutes, and run out on an SDS-polyacrylamide gel. They were then analysed by immunoblotting and the levels of the Greatwall protein present in each cell line sample was measured using densitometry of the ECL film taken with ImageJ software. These levels were normalised against the levels of the α tubulin protein present in each cell line sample, also measured using densitometry of the ECL film again taken with ImageJ software. The data was then exported into Microsoft® Office Excel 2003 and plotted. This quantification was carried out by Dr. Victoria Haley (Trafford Centre, Brighton and Sussex Medical School, Sussex, UK).

CHAPTER 3. Making tools to investigate and characterise Greatwall in human cells

3.1 Introduction

The gene encoding the human homologue of Greatwall was first identified by Gandhi *et al.* in 2003. This gene, called *FLJ14813*, was within the region of chromosome 10p that in 2000 Drachman *et al.* had mapped to autosomal dominant nonsyndromic thrombocytopenia, also known as thrombocytopenia-2 (Drachman *et al.* 2000). A novel missense mutation in this gene segregated perfectly with thrombocytopenia in their cohort of 51 family members. All the thrombocytopenic family members carried a substitution of guanidine to cytosine at position 565 of this gene that predicted a substitution of glutamic acid to aspartic acid (E167D) in exon four. This disorder is characterised by decreased numbers of normal platelets that results in a mild bleeding tendency (Gandhi *et al.* 2003). Platelet function and morphology is normal in these patients suggesting it results from defective platelet production or release. They described the gene product as a putative kinase similar to a novel gene described in *Drosophila* called Greatwall (Yu *et al.* 2004) and postulated that this mutation, although subtle, might be responsible for the disorder in these patients. A follow up study in 2009 in zebrafish linked the disorder to a reduction in expression levels of the gene (Johnson *et al.* 2009). It is unclear how this defect could fit with the emerging model of Greatwall function but suggests a role for Greatwall in the development of megakaryocytes in humans that could be similar to the defect seen in *Xenopus* oocytes.

In 2002 Manning *et al.* catalogued the protein kinase complement of the human genome; the human kinome (Manning *et al.* 2002). In this study they identified the same gene but categorised it as Microtubule Associated Serine/Threonine-Like (MASTL) kinase, as a distantly related family member of the Microtubule Associated Serine/Threonine kinases (MAST kinases) (Walden *et al.* 1993; Garland *et al.* 2008). This family of AGC kinases comprise MAST1 to 4 and MASTL. They are characterised by the presence of a kinase domain, a Domain of Unknown Function 1908 (DUF1908) and a PDZ scaffolding/membrane-targeting domain (Manning *et al.* 2002; Pearce *et al.*

2010). MAST 1 and 2 are found expressed in multiple tissues in the rodent brain. MAST3 and 4 are expressed more selectively in the brain and are found in the striatum and oligodendrocytes respectively (Garland *et al.* 2008). MAST1 to 3 have been reported to bind to the tumour suppressor protein PTEN to mediate its signalling (Valiente *et al.* 2005) and missense mutations in MAST3 have been linked to increased risk of inflammatory bowel disease, due to its loss promoting aberrant signalling from nuclear factor-kappa B (NF-κB) (Labbe *et al.* 2008). Although relatively little is currently known about their biological functions, this family of proteins are proposed to play a structural role that facilitates signal transduction and plasticity throughout the central nervous system (Valiente *et al.* 2005; Garland *et al.* 2008; Labbe *et al.* 2008). Recently the identification of functional gene fusions in several breast cancers that result in MAST1 and 2 overexpression and increased proliferation have also been described (Robinson *et al.* 2011).

In contrast to the other members of the MAST family, MASTL was not found expressed in the rodent brain (Garland *et al.* 2008). Its expression appeared to be exclusive to the heart and testis in the rat tissues examined. Moreover, it bears little homology to the other MAST kinase family members. MASTL lacks a DUF1908 or PDZ domain and is far shorter than the other MAST family kinases (**Figure 3.1 A**) (Pearce *et al.* 2010). Human MAST1 to 4 are large enzymes of 1,309 to 2,444 amino acids with conventional small T-loops (31 amino acids in length for MAST1), while human MASTL is 879 amino acids and the kinase domain is split by a large region of ~540 amino acids. The exact function of this large insertion between the two halves of the kinase domain has yet to be determined but could represent an as yet uncharacterised large T-loop (discussed further in the next Chapter). This large insertion of amino acids separating the kinase domain N- and C-termini is replicated in the *Drosophila* and *Xenopus* Greatwall kinases and these proteins share 50.2% and 65.7% sequence homology respectively with human MASTL, while its homology with MAST1 is only 10.4% (**Figure 3.1 B**) (Burgess *et al.* 2010). This evident lack of similarity to any of the other MAST family kinases, supported by recent studies of human MASTL described later in this chapter, led to the conclusion that MASTL is not a true member of the MAST family, and that it is instead the functional human orthologue of *Drosophila* and *Xenopus* Greatwall kinase. This was subsequently confirmed by Burgess *et al.* in 2010 when they cloned and expressed human MASTL complimentary DNA (cDNA) in *Xenopus* CSF egg extracts (Burgess *et al.* 2010). Using

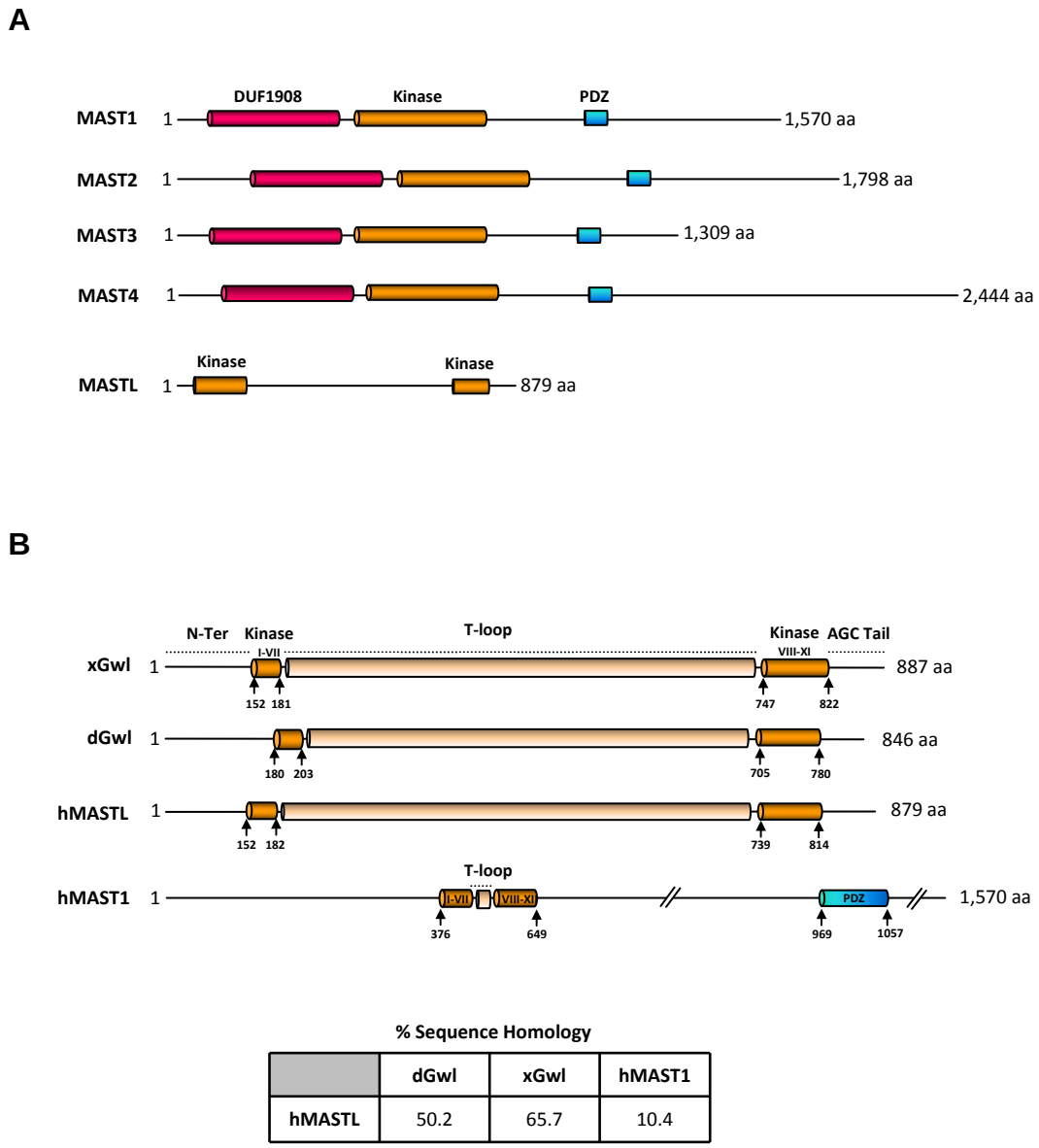

% Sequence Homology

	dGwl	xGwl	hMAST1
hMASTL	50.2	65.7	10.4

Figure 3.1 MASTL is the human homologue of Greatwall

(A) Schematic drawing of the domain structures of the human MAST kinase family. Copied from Pearce *et al.* (2010). Human MASTL does not contain either a DUF1908 or PDZ domain and is far shorter than the other MAST family members. **(B)** Schematic drawing to show sequence homology between *Xenopus* Greatwall (xGwl), *Drosophila* Greatwall (dGwl), human MASTL (hMASTL) and human MAST1 (hMAST1). Copied from Burgess *et al.* (2010). The kinase domains of xGwl, dGwl and hMASTL are separated by long inserted regions of >500 amino acids, while hMAST1 has a conventional T-loop of ~30 amino acids. Neither xGwl, dGwl nor hMASTL contains a PDZ domain and hMASTL shows much higher sequence homology with xGwl and dGwl than when compared with hMAST1 (see table).

extracts that had been depleted of their endogenous Greatwall the expression of MASTL cDNA, at endogenous levels, rescued the mitotic state while expression of a kinase dead MASTL did not. For the purpose of this study this MATSL gene product will be referred to as Greatwall kinase from this point onward.

3.2 Making tools to investigate human Greatwall

At the onset of my work on this thesis little was known about the functions of human Greatwall kinase and no tools existed to allow detection or analysis of Greatwall in human cells. Thus, in order to begin to research this novel kinase I needed to develop tools to allow me to undertake its analysis. During this investigation of human Greatwall other studies, now published, also described the important role of this kinase in the cell cycle in human cells and these will be discussed in detail at the end of this chapter and where relevant.

3.2.1 Antibody generation

To initiate this study of human Greatwall kinase I first raised antibodies against an N-terminal fragment of the protein cDNA encoding the N-terminal 1 to 100 amino acids (aa). This was obtained by PCR amplification from HeLa cell mRNA in a two step RT-PCR **Figure 3.2 A**). This was carried out with primers that introduced XhoI and NcoI restriction sites at the N- and C-termini respectively, allowing it to be directionally cloned into the pET28 bacterial expression vector. Using this strategy, I expressed the Greatwall N-terminus with a C-terminal His-tag of six histidine residues in *E.coli* BL21 cells and purified it under denaturing conditions in 6M urea using nickel-nitrilotriacetic acid (Ni-NTA) beads. The purified recombinant protein fragment was then used to raise antibodies in rabbit using a commercial service.

Antibodies were raised in two rabbits (A and B) and the 4th immunisation sera from both rabbits were tested by immunoblotting. I expressed the human Greatwall protein (from cloned full-length cDNA) in a rabbit reticulocyte system in a T7 expression vector (pDEST14). This *in vitro* translated Greatwall was run out on an SDS-PAGE gel with HeLa cell lysates from asynchronous and mitotically arrested cells

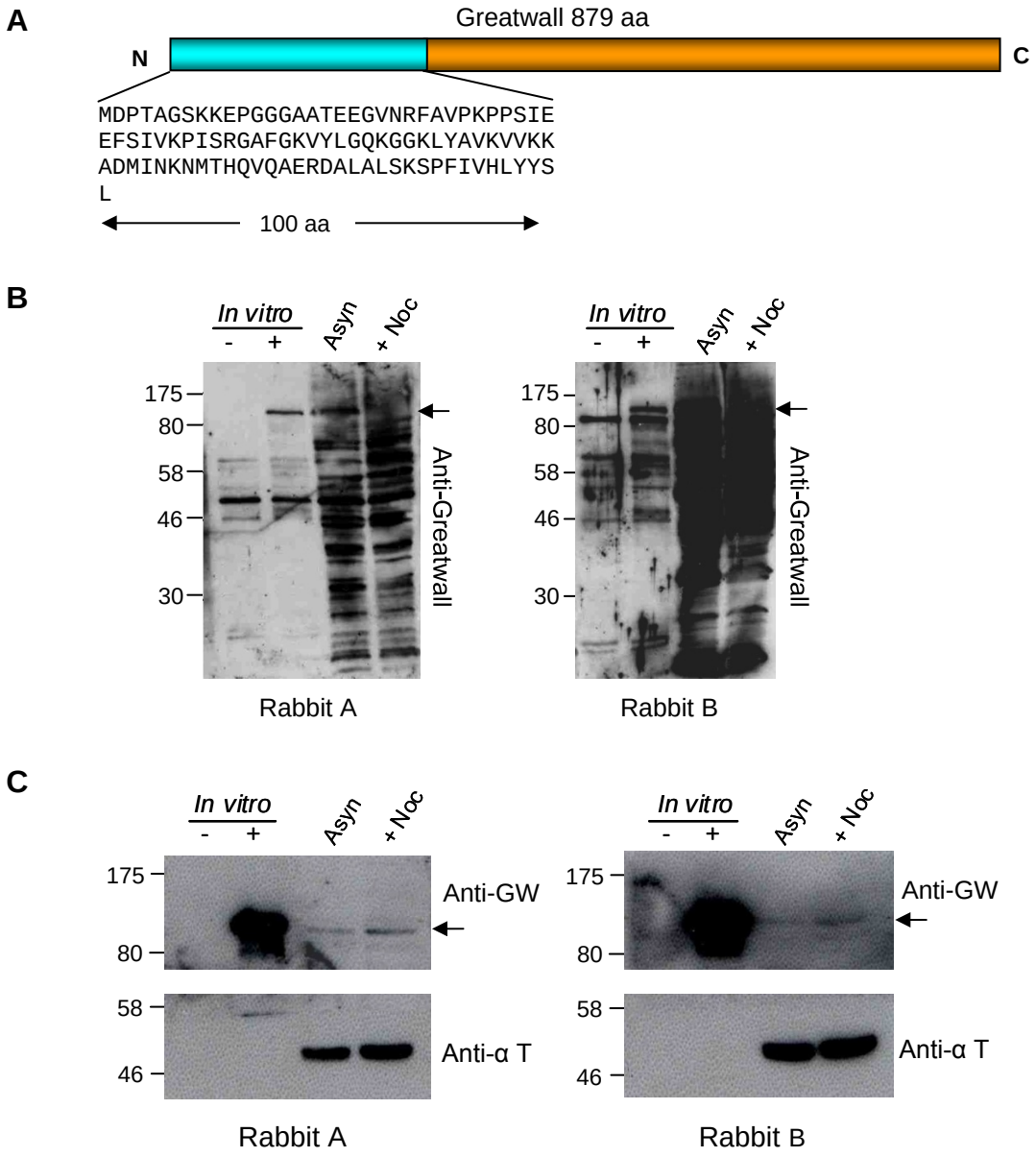

Figure 3.2 Making tools to investigate Greatwall in human cells

(A) Schematic representation of the Greatwall protein. The N-terminal 100 aa indicated were used to create an antigen peptide subsequently used for antibody generation in rabbit. **(B)** SDS-PAGE analysis of the 4th immunisation sera from rabbit (rabbits A and B). Loaded in the first lanes are *in vitro* translations in a rabbit reticulocyte system alone (-) or in the presence of Greatwall cDNA expressed from pDEST14 (+). Loaded in the next lanes are HeLa cell lysates from asynchronous cells (Asyn) or cells that have been treated with Nocodazole (+ Noc). The *in vitro* translated human Greatwall kinase and HeLa endogenous Greatwall kinase is seen at its predicted size of ~110 kDa (indicated by the arrow), other bands are non-specific background signal. **(C)** The same SDS-PAGE analysis was performed using the concentrated and purified antibody sera (anti-GW). Far fewer non-specific bands are observed. The *in vitro* translated and endogenous Greatwall kinase is seen as a band at ~110 kDa (indicated by the arrow). An anti-α Tubulin antibody (anti-α T) was used as a loading control here.

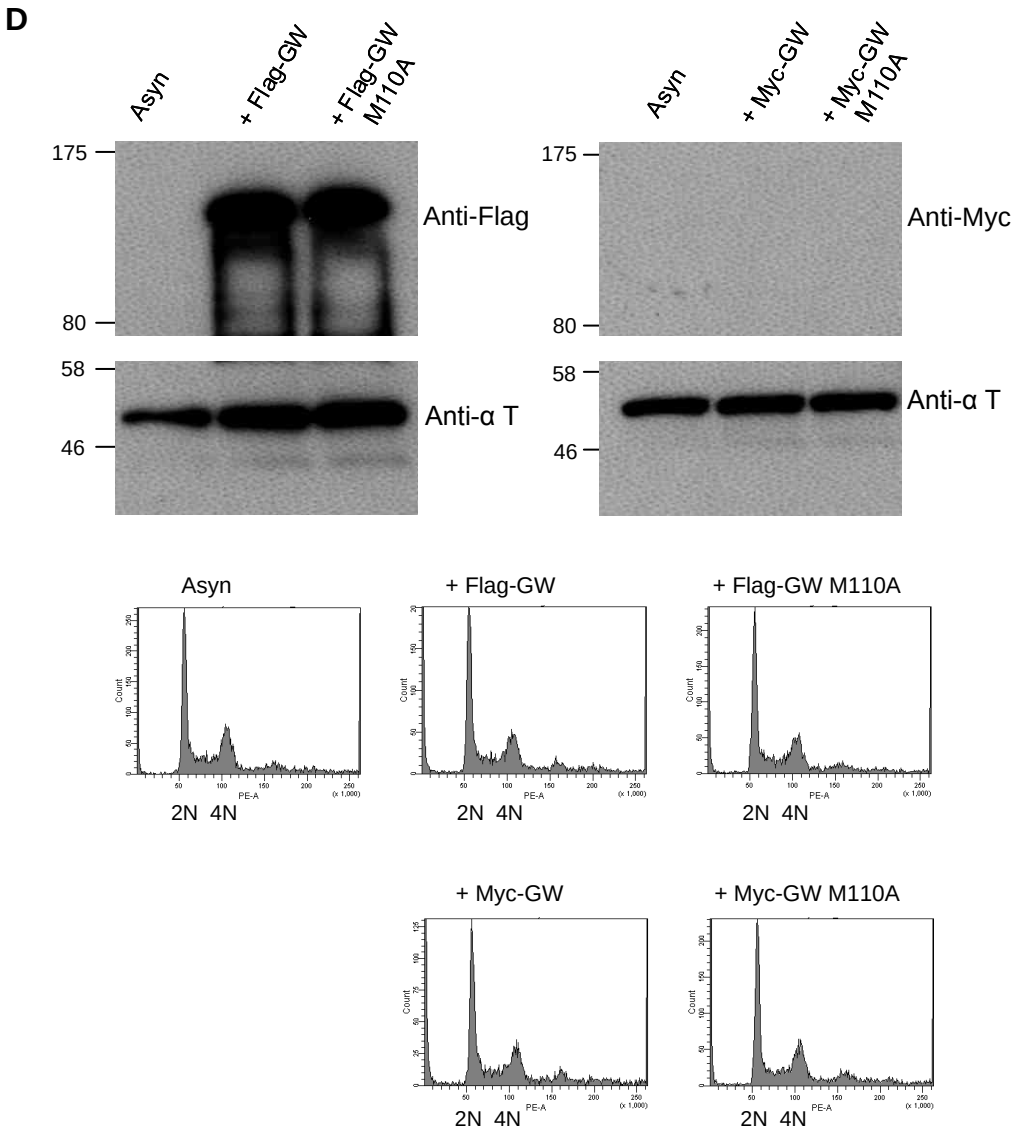

(D) SDS-PAGE analysis of flag- and myc-tagged Greatwall constructs expressed in HEK 293T cells. Loaded in the first lane is asynchronous (Asyn) HEK 293T cell lysate and subsequent lanes contain lysates from HEK 293T cells transfected with myc- (Myc-) or flag-tagged Greatwall (Flag-GW) or a Greatwall mutant (Flag-GW-M110A), as indicated. Anti-Flag or anti-Myc antibodies were used to detect the expressed tagged constructs and an anti-α Tubulin (anti-α T) antibody was used as a loading control. The cell cycle (FACS/PI) profiles for these HEK 293T cell samples transfected with the constructs (myc- or flag-tagged Greatwall or Greatwall M110A) as indicated are shown beneath.

using the spindle poison Nocodazole (**Figure 3.2 B**). These were then transferred to a nitrocellulose membrane and probed with the rabbit anti-Greatwall antibodies. Both antibodies clearly detected the *in vitro* translated Greatwall in the rabbit reticulocyte lysates, but high background signal was seen on the resulting immunoblots, especially

in the whole cell lysates. To remove this high non-specific background signal the antibodies were further purified by incubation with the His-tagged N-terminal Greatwall protein fragment run out on an SDS-PAGE gel and transferred to a nitrocellulose membrane. Specific antibodies were then eluted from the membrane and concentrated. The concentrated purified antibody sera was then used to probe fresh immunoblots for Greatwall. This resulted in much cleaner blots showing a single specific band at ~110 kDa, corresponding to the predicted size of the human Greatwall protein. This band was identified at the same position in the *in vitro* translation reaction in which the cloned Greatwall cDNA was expressed but not in the translation sample without any Greatwall cDNA. This indicates that the band detected by these antibodies is human Greatwall kinase and this protein is present in human (HeLa) cell lysates.

3.2.2 Tagging Greatwall

I cloned the cDNA of human Greatwall for use as a tool to investigate Greatwall, principally to allow tagged versions of the protein to be produced. In order to clone Greatwall, I prepared mRNA from HeLa cells and carried out a two step RT-PCR to amplify the cDNA of the Greatwall (MASTL) gene product. A DNA fragment of the expected 2367 bp size was obtained and was subsequently purified from an agarose gel and cloned into a TOPO cloning vector. This was confirmed by sequence analysis (**Appendix A** contains a full alignment of the cloned sequence with human Greatwall cDNA sequence) and used for subsequent cloning using Gateway® Technology from Invitrogen (Hartley *et al.* 2000). This is a universal cloning system that is based on the site-specific recombination properties of bacteriophage lambda that provides an efficient way in which to move DNA sequences into multiple vector systems (for a detailed explanation of this technology see **Chapter 6** section **6.3**).

Tagging of human Greatwall cDNA to create fluorescently tagged proteins proved unsuccessful. Constructs created with green fluorescent protein (GFP), red fluorescent protein (RFP) or mCherry at the C-terminus or at the N-terminus of Greatwall failed to express. The addition of multiple myc-tags at the N-terminus also failed to be expressed. It is likely that these results can be explained because the Greatwall kinase domain is bifurcated and must fold correctly to bring the two sections of its kinase domain together to form a fully active kinase. The presence of a tag at

either the N-terminus or C-terminus of the protein thus might interfere with this folding and result in an unfolded protein that is subsequently degraded by the cell. For this reason the size and/or nature of the attached tag is therefore critical and the GFP, RFP, mCherry and multiple myc-tags were likely incompatible with the correct folding of the protein to produce a tagged and functional kinase. Finally, the expression of N-terminal flag-tagged Greatwall cDNA was achieved in HEK 293T cells (**Figure 3.2 D**). Of all tags tested only this small flag-tag on the N-terminus was amenable to permitting correct protein folding, preventing any adverse effects from the tag on the tertiary structure of the protein, and allowing the functional kinase to be expressed.

In addition to the flag-tagged wildtype cDNA, I introduced a methionine to alanine substitution at position 110 (M110A) into this flag-tagged cDNA (Greatwall M110A) that should render the protein ATP-analogue sensitive (discussed in more detail in **Chapter 6**). This Greatwall M110A mutant was also successfully expressed by transient transfection in HEK 293T cells. The cell cycle (FACS) profiles for HEK 293T cells transfected with either the wildtype or Greatwall M110A appeared normal. This implies that these cells were capable of growing and proceeded to cycle normally despite the presence of the ectopically expressed Greatwall proteins (**Figure 3.2 D**).

3.3 Characterisation in human cell lines

Expression of Greatwall kinase was detected in several human cell lines. The protein was detected by immunoblotting in human HeLa, HCT116, HEK 293T and RPE cells (**Figure 3.3 A**). I compared Greatwall levels in different cell cycle states including asynchronous cells, early S phase (treated with Thymidine), G2 phase (treated with the CDK1 inhibitor RO-3306,), and in mitotic cells (treated with the microtubule poison Nocodazole). Greatwall protein levels were slightly increased in S phase in the HeLa cells, something that was repeatedly seen after a Thymidine block in these cells. The reason for this is not clear but is possibly as a result of the DNA replication block causing cells with significant levels of Greatwall to build up in this cell cycle phase. The RPE cells were not evaluated for Greatwall in S phase as they did not arrest in response to Thymidine treatment. In the other cell lines Greatwall levels appeared unchanged in S phase, while Greatwall levels seemed to be decreased in late G2 and mitosis. This may be due to post-translational modifications (PTMs) of the protein in

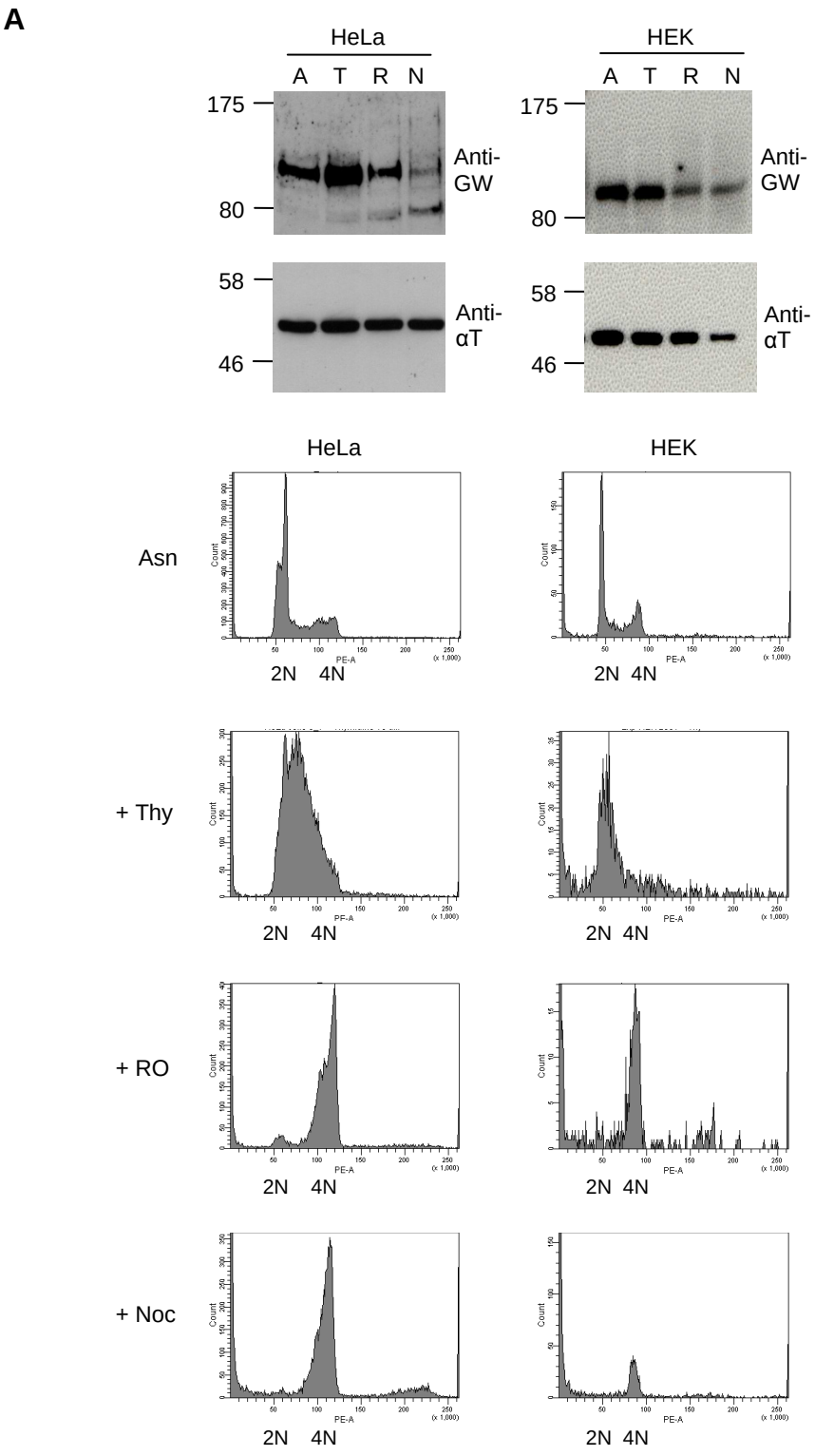

Figure 3.3 Greatwall characterisation in human cells

(A) SDS-PAGE analysis of HeLa, HEK 293T, HCT116 and RPE cell lysates from asynchronous (A) cells or cells that had been treated with Thymidine (T), RO-3306 (R) or Nocodazole (N). The anti-Greatwall antibody (the purified 4th immunisation sera from rabbit A; anti-GW) was used to probe for human

A cont.

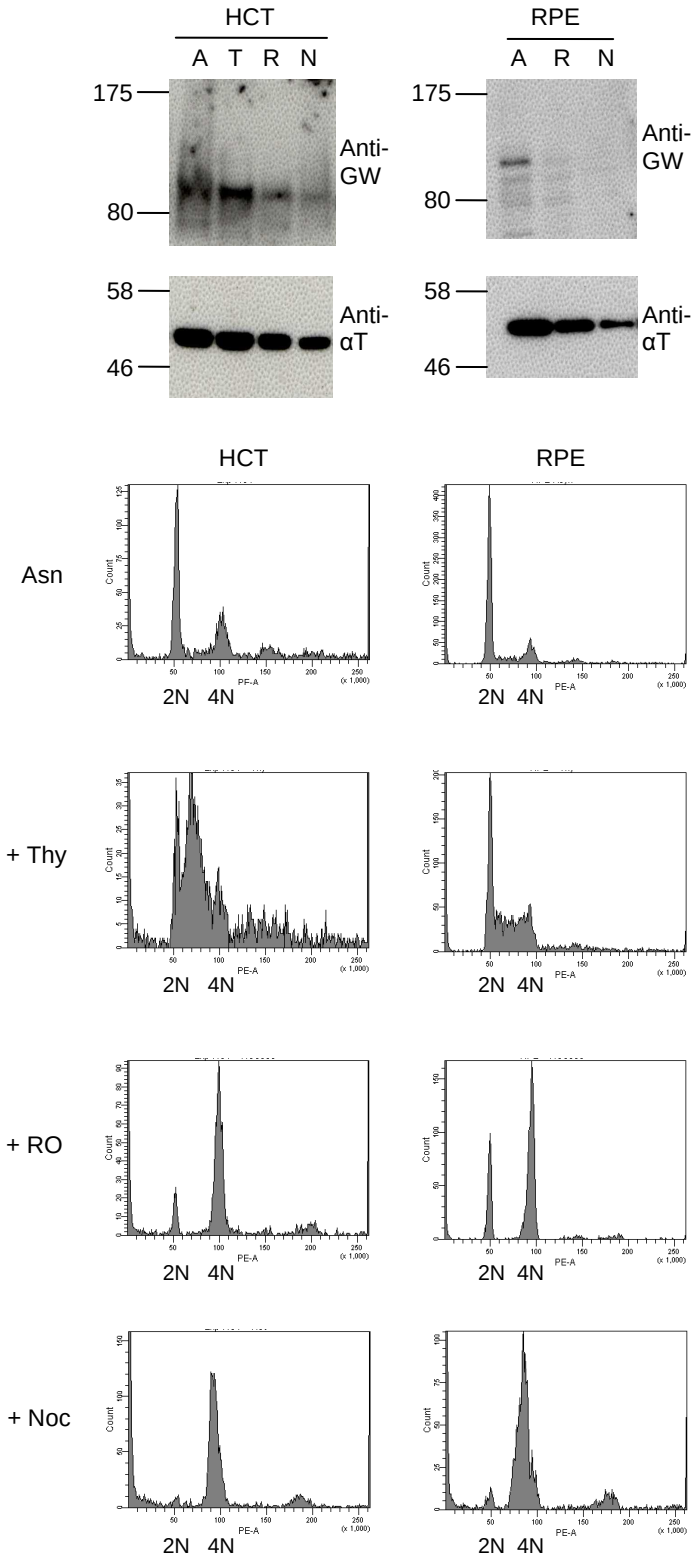

Greatwall protein levels and an anti-α Tubulin antibody (anti-α Tub) was used as a loading control. The cell cycle (FACS/PI) profiles for HeLa, HEK 293T, HCT116 and RPE cells from asynchronous (Asn) cells, cells that had been treated with Thymidine (+ Thy), RO3306 (+ RO) or Nocodazole (+ Noc) are shown beneath. **(B)** SDS-PAGE analysis of HeLa cells synchronised by a double Thymidine block and

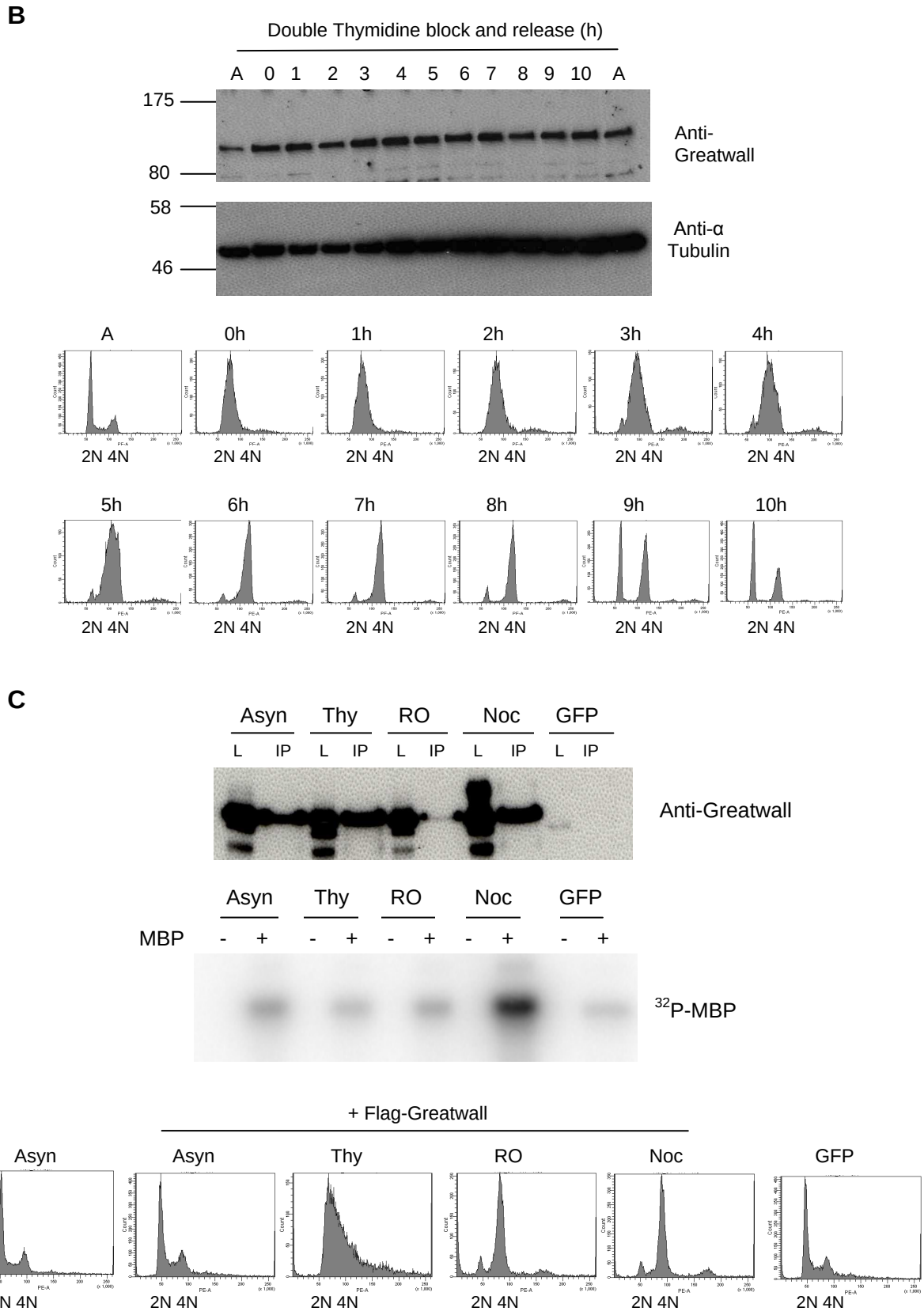

then released for 10 hours. Samples were analysed using the anti-Greatwall antibody to probe for human Greatwall protein levels and an anti-α Tubulin antibody was used as a loading control. The cell cycle (FACS/PI) profile of these cells at each hour time point are shown in the lower panel. Asynchronous (A)

cells were analysed as well for comparison. **(C)** Flag-tagged Greatwall was expressed and immunoprecipitated from HEK 293T asynchronous cells (Asyn) or cells that had been treated with Thymidine (Thy), RO-3306 (RO), or with Nocodazole (Noc). Asynchronous cell lysates transfected with GFP (GFP) were analysed as well for comparison. The top panel shows the immunoblot indicating the expression of the flag-tagged protein from the cell lysates (L) or the immunoprecipitation (IP) detected using the anti-Greatwall antibody. An *in vitro* kinase assay was performed and the autoradiograph is shown in the second panel. The cell cycle (FACS/PI) profiles for all the cell lysates and untransfected cells are shown in the bottom panel.

late G2 (at the G2/M transition) and mitosis, resulting in a poor transfer and a smear of shifted bands with lower electrophoretic mobility. Therefore, Greatwall levels are likely not decreased in late G2 or mitosis but the presence of activating PTMs prevented its detection. In the G2 cells this could alternatively be a result of Greatwall protein levels being kept at a low level until activation of CDK1 allows the cells to activate and increase (or stabilise) Greatwall levels to allow progression into mitosis.

How Greatwall protein levels alter throughout the cell cycle was further analysed using synchronised cells. HeLa cells were synchronised by a double Thymidine block, then released and subsequently followed through their cell cycle for 10 hours. During this time samples were taken every hour and analysed for Greatwall levels by immunoblotting (**Figure 3.3 B**). Greatwall expression levels remained relatively stable, indicating that during the cell cycle Greatwall kinase levels largely remain constant and that its predominant mode of regulation might be via PTMs controlling the initiation and inhibition of its activity. These observations are supported by work carried out by Burgess *et al.* (2010) and Voets *et al.* (2010) who also observed that Greatwall protein levels were stable during the cell cycle and that it became phosphorylated upon mitotic entry.

The transient overexpression of flag-tagged Greatwall in human HEK 293T cells allowed analysis of the activity of Greatwall in different cell cycle phases. Flag-Greatwall was transfected into HEK 293T cells and allowed to express for 24 hours. The media was then replaced with fresh media or drug-containing media and the cells incubated for 24 hours or overnight and then harvested. Flag-Greatwall was immunoprecipitated using magnetic beads coated with an anti-flag antibody and the purified kinase was then taken into an *in vitro* kinase assay using recombinant Myelin Basic Protein (MBP) as a substrate. The lysates and immunoprecipitates were assessed

for flag-Greatwall expression by immunoblotting and Greatwall kinase activity against MBP was visualised on an autoradiograph (**Figure 3.3 C**). Interestingly, the levels of exogenous protein again appeared reduced in G2 cells arrested using the CDK1 inhibitor RO-3306 as I previously also observed for the endogenous protein. The lysates of the mitotically arrested cells exhibited an additional shifted band of higher molecular weight Greatwall, confirming that Greatwall is modified in mitosis and the overexpression of the flag construct allowed it to be detected here. The activity of Greatwall was low overall in the asynchronous population and in S phase cells but was increased in mitotically arrested cells, as judged by the autoradiographs shown in **Figure 3.3 C**. Greatwall's overall low activity from an asynchronous cell population is likely due to the small percentage of mitotic cells present. It has little or no activity in S phase arrested cells. It is difficult to conclude if Greatwall is active in the late G2 RO-3306-mediated block as it was always only immunoprecipitated at very low levels. This indicates that it might be unstable or modified so it cannot be assessed well by immunoprecipitation in G2 in the absence of CDK1 activity. In the mitotic cells it was shown to have high activity. That Greatwall is maximally active only in mitosis was also reported by Voets *et al.* (2010). They observed a mitotic mobility shift that was concomitant with the phosphorylation of APC/C subunit APC3 and was diminished by treatment with λ phosphatase. This was also enhanced by treatment with okadaic acid. This suggests that Greatwall is subject to an activating phosphorylation event in mitosis similar to that seen for *Xenopus* Greatwall.

3.4 Greatwall depletion leads to G2/M delay, mitotic defects and cytokinesis failure

Short interfering (si) RNA was used to target Greatwall mRNA to the RNA-induced silencing complex (RISC) to achieve post-transcriptional gene silencing. HeLa cells were transfected with Greatwall siRNA at 5 nM to 100 nM concentration. These cells were then analysed 72 hours later by SDS-PAGE and FACS (**Figure 3.4 A**).

The immunoblot indicates that Greatwall levels had decreased below detectable levels in cell lysates that had been treated with Greatwall siRNA as compared with asynchronous untreated cell lysates. In lysates from cells treated with control non-coding siRNA, Greatwall levels remained comparable with those seen in the untreated cells ruling out this being a non-specific effect of the siRNA treatment. The

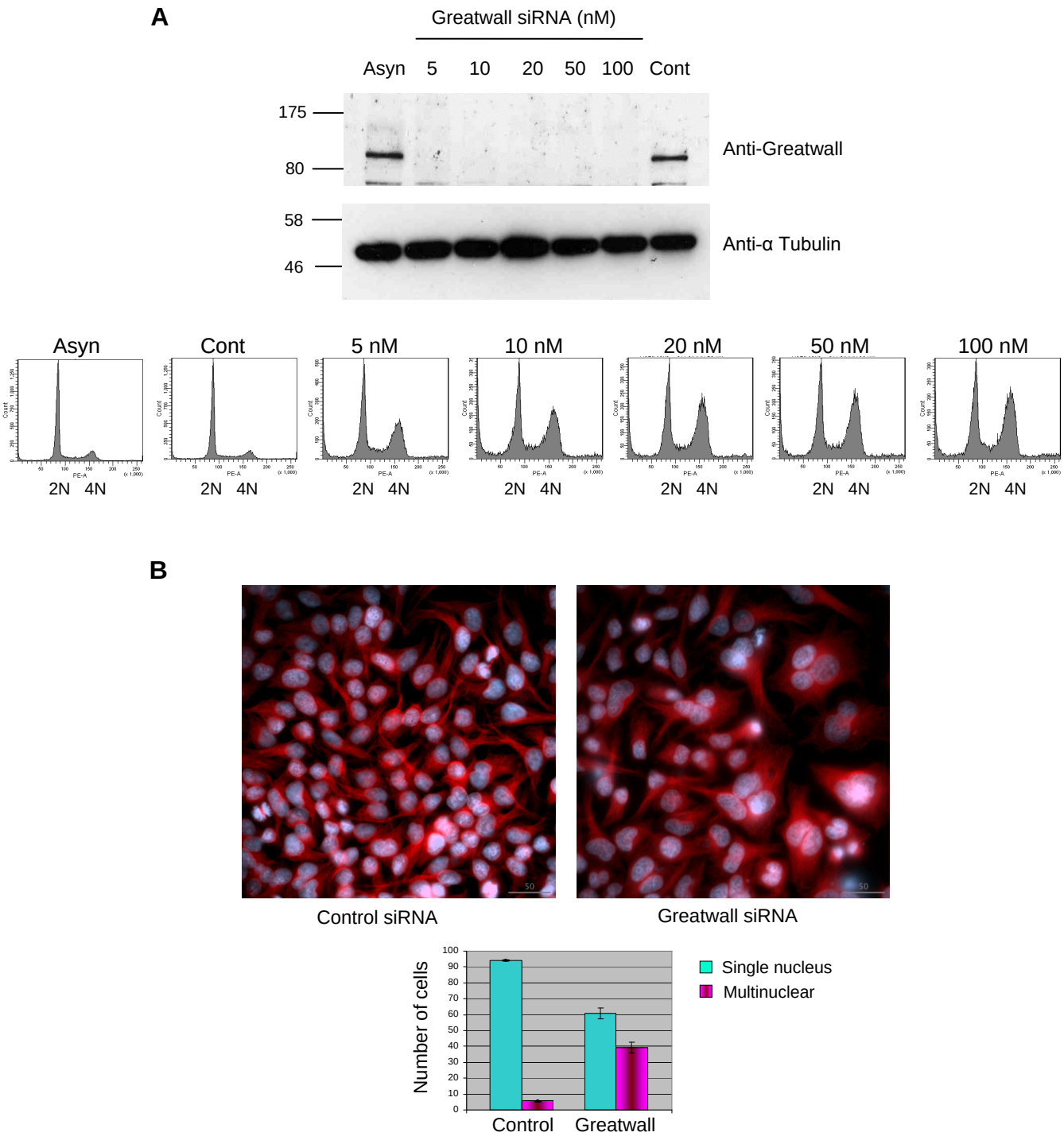

Figure 3.4 Greatwall depletion in human cells

(A) SDS-PAGE analysis of HeLa cells that had been treated with Greatwall siRNA. Lysate from asynchronous (Asyn) cells is loaded in the first lane followed by lysates from cells that had been treated with 5, 10, 20, 50 and 100 nM Greatwall siRNA for 72 hours. Loaded in the final lane is lysate from cells that were treated with 100 nM control (scrambled) siRNA (Cont) for 72 hours. The anti-Greatwall antibody (anti-Greatwall) was used to probe for human Greatwall protein levels and an anti-α Tubulin antibody was used as a loading control. The cell cycle (FACS/PI) profiles for the asynchronous, control

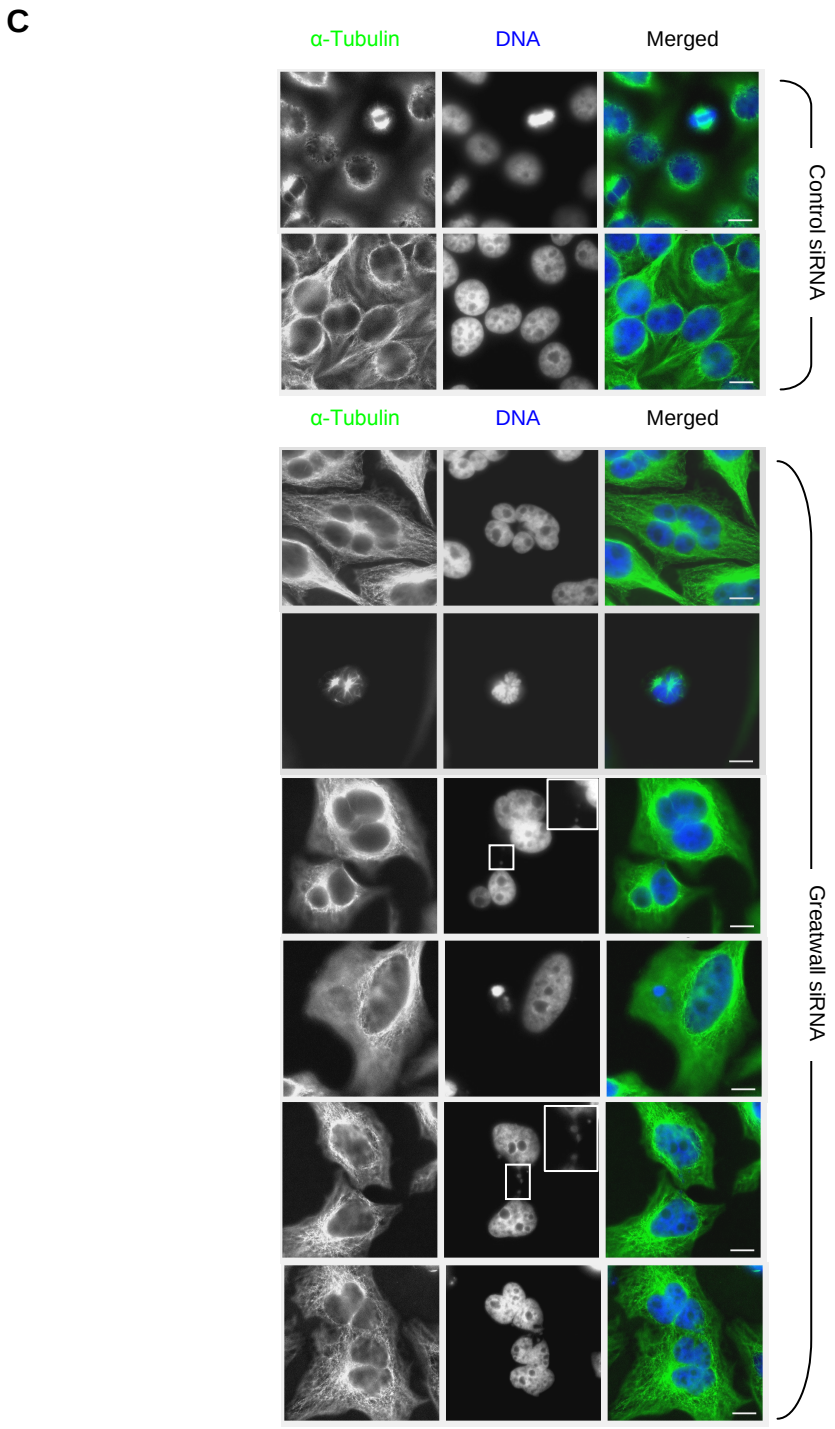

or Greatwall siRNA treated cells are shown beneath. **(B)** Images showing HeLa cells depleted of Greatwall. Cells were treated with 25 nM Greatwall or control siRNA for 72 hours. HeLa cells were probed with an anti-α Tubulin antibody (red) and the DNA stained with DAPI (pale blue). The maximum projection from 0.3μm Z-sections are shown with scale bars of 50 μm. Quantification of the number of cells retaining single nuclei or that had become multinucleate is shown beneath. For this 75-100 cells from three separate siRNA experiments were counted. **(C)** Representative images showing defects in HeLa cells depleted of Greatwall. Cells were treated with 25 nM Greatwall or control siRNA for 72

hours. HeLa cells were probed with an anti-α Tubulin antibody (green) and the DNA stained with DAPI (blue). The maximum projection from 0.3μm Z-sections are shown with scale bars of 10 μm. The inserts are magnified images of the DNA bridges seen.

corresponding cell cycle (FACS) profiles indicated that depletion of Greatwall resulted in accumulation of the G2/M population of the cells, suggesting that human Greatwall, similar to its *Xenopus* and *Drosophila* counterparts, is required for cell cycle progression through mitosis.

Immunofluorescence analysis of the Greatwall depleted HeLa cells indicated numerous defects (**Figure 3.4 B** and **C**). The images shown are from cells that had been treated with Greatwall siRNA for 72 hours. At this time many of the cells had already died and were subsequently washed away during the fixation treatment. A large proportion of the cells that survived fixation appeared to have become multinucleate, while cells treated with control siRNA exhibited few multinucleate cells (**Figure 3.4 B**). Control siRNA treated cells showed only 5.7% polyploid cells while 39.3% of the Greatwall depleted population had a 4n DNA content or greater. A similar accumulation (40%) of cells with ≥4n DNA content and an increased cell death after Greatwall depletion were also reported by both Burgess *et al.* (2010) and Voets *et al.* (2010). It is therefore conceivable that the accumulation of cells with 4n DNA content 72 hours after Greatwall depletion was not only a result of an increased population of cells arrested at G2/M and an increased mitotic index, but also the result of the accumulation of multinuclear cells in which cytokinesis has failed. We also observed signs of abnormal and aborted mitoses in the Greatwall depleted cells as well as DNA bridges between daughter cells, further indicating a failure to complete mitosis and carry out efficient cytokinesis (Figure **3.4 C**). These observations have been subsequently supported by the work of Burgess *et al*. (2010) and Voets *et al*. (2010) who carried out in depth investigations, which are discussed in detail at the end of this chapter.

3.5 Greatwall overexpression

As a tool for Greatwall analysis stable HEK 293T cell lines overexpressing flag-tagged Greatwall were generated. The presence of flag-Greatwall in two cell lines,

Clone 1 (C1) and Clone 7 (C7), was confirmed by immunoblotting (**Figure 3.5 A**) and by immunoprecipitation using anti-flag magnetic beads (**Figure 3.5 B**).

Both cell lines expressed Greatwall at much higher levels than the endogenous protein. C1 had 6-fold overexpression and C7 had 13-fold overexpression as compared to endogenous Greatwall levels in HEK 293T cells. These cell lines were assessed for any cell cycle perturbation that might result from this increase in Greatwall expression. The cell cycle (FACS) profiles for both cell lines were normal and growth curves for the cell lines showed that they grew at the same rate (**Figure 3.5 B and C**). A single factor analysis of variance (ANOVA) was performed on the growth data (shown in **Appendix B**) which showed no significant main effect ($F(2, 255) = 0.14$, $p = 0.87$), indicating that there is no significant difference between the growth of the wildtype HEK 293T cells and the two cell lines' growth. Thus, no adverse effects of Greatwall overexpression were observed in either cell line, even at these elevated expression levels. Greatwall overexpression from our observations with these stable cell lines and from transient overexpression by transfection seems well tolerated in human cells. Its activity here is likely highly regulated and, as such, simply overexpressing Greatwall might not have a relevant effect on the cell cycle. A more detailed investigation, perhaps using additional cell lines and with Greatwall mutants with aberrant activity that cannot be regulated, could be more informative as to possible phenotypes associated with inappropriate (high) Greatwall activity.

The C7 cell line was used to assess Greatwall activity in an *in vitro* kinase assay. The cells were treated with the CDK1 inhibitor RO-3306 to arrest them in G2, the PLK1 inhibitor BI2536 to arrest them in mitosis or with both drugs for 24 hours. Flag-Greatwall was then immunoprecipitated and taken into an *in vitro* kinase assay with recombinant MBP as a substrate (**Figure 3.5 D**). Greatwall had high activity in the mitotic BI2536-treated lysates and was phospho-shifted on the immunoblot. These data supports findings in *Xenopus* (Yu *et al.* 2006) that Greatwall is phosphorylated and active in mitosis. The activation of Greatwall in mitosis appears independent of PLK1 activity. Where the cells were treated with RO-3306 and BI2536 together the FACS profile indicates that the cells arrested in G2 and therefore Greatwall was likely not active, although its levels again appear lower in the immunoprecipitate upon RO-3306 treatment as previously discussed. The high overexpression of Greatwall in these cells did not effect its activation, further supporting the hypothesis that Greatwall activation

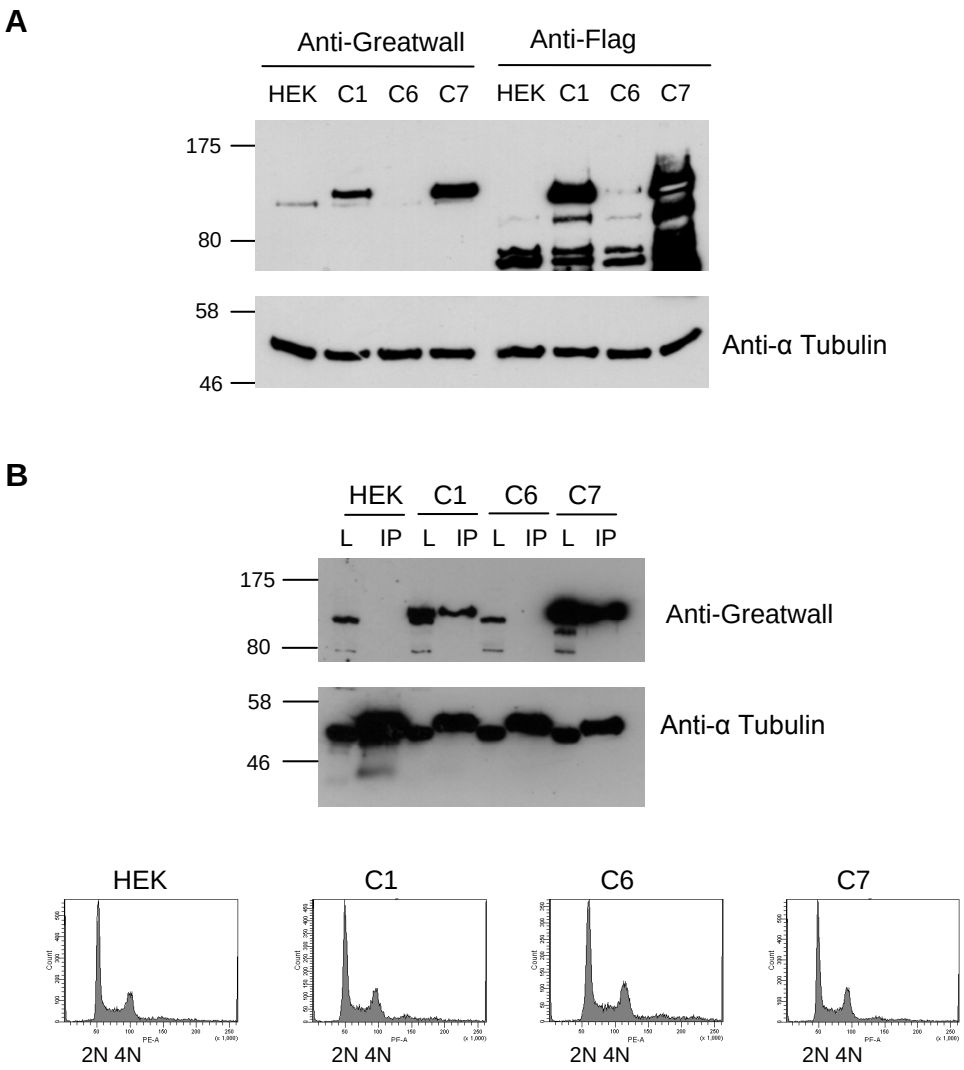

Figure 3.5 Greatwall overexpression in human cells

(A) SDS-PAGE analysis of HEK 293T (HEK) and stable cell lines, C1, C6 and C7 indicating their expression of flag-Greatwall at passage 1. The anti-Greatwall antibody (anti-Greatwall) and an anti-Flag antibody was used to probe for flag-Greatwall protein levels in these clones and an anti-α Tubulin antibody was used as a loading control. C1 and C7 highly overexpress flag-Greatwall while C6 was not targeted **(B)** Flag-tagged Greatwall immunoprecipitated from HEK 293T (HEK) and stable cell line clones, C1, C6 and C7. The immunoblot indicates the expression of the flag-tagged protein from the cell lysates (L) or the immunoprecipitation (IP) detected using the anti-Greatwall antibody (anti-Greatwall), and an anti-α Tubulin antibody (anti-α Tub) was used as a loading control. The cell cycle (FACS/PI) profiles for the HEK 293T and stable cell lines are shown beneath. **(C)** Growth curves of HEK 293T and stable cell lines C1 and C7. These were generated using an IncuCyte (ESSEN Biosciences). Nine different points from 6 wells of a 24-well plate were measured every 3 hours for 255 hours. **(D)** Stable cell line C7 was used to investigate Greatwall activity. Flag-tagged Greatwall was immunoprecipitated from asynchronous (Asyn) cells or cells that had been treated with RO-3306 (RO) or BI2536 (BI) or both

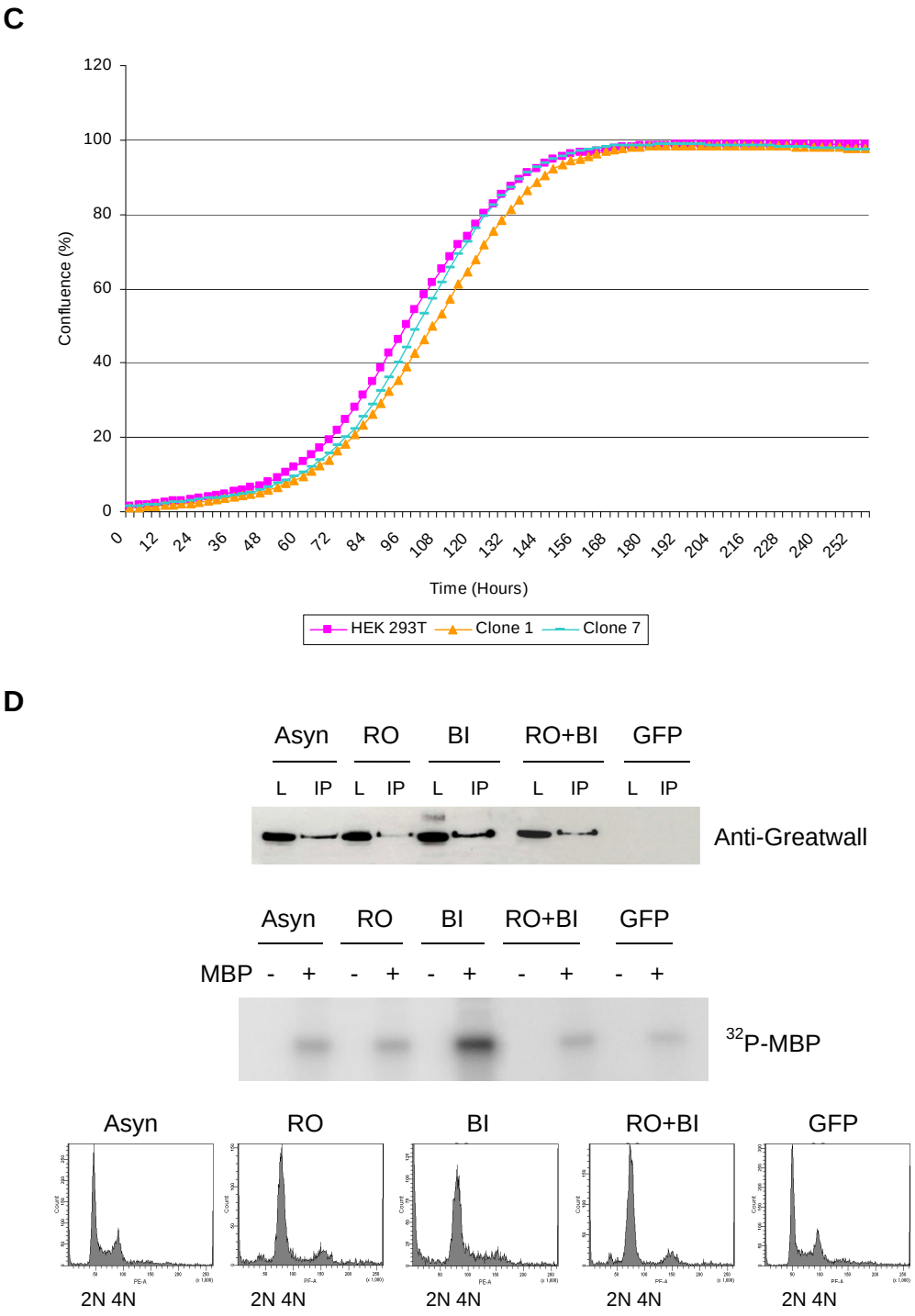

drugs (RO+BI). Asynchronous cell lysates transfected with GFP (GFP) were analysed as well for comparison. The top panel shows the immunoblot indicating the expression of the flag-tagged protein from the cell lysates (L) or the immunoprecipitation (IP) detected using the anti-Greatwall antibody. An *in vitro* kinase assay was performed using MBP as a substrate. The autoradiograph is shown in the second panel. The cell cycle (FACS/PI) profiles for all the cell lysates are shown in the bottom panel.

is highly regulated by PTMs and that this restricts its activity specifically to mitosis in human cells.

3.6 Conclusions and discussion

Here I generated tools that allowed the characterisation of Greatwall in human cells. Rabbit polyclonal antibodies were produced that detected human Greatwall at ~110 kDa on immunoblots of human cell lysates. Human Greatwall cDNA was cloned, flag-tagged and expressed in human cell lines, and *in vitro* kinase assays to analyse Greatwall activity were developed. These tools allowed the investigation of human Greatwall expression and activity.

I found that Greatwall protein levels remain relatively constant throughout the cell cycle. It is instead tightly regulated by post-translational modifications that activate it at the G2/M transition in the presence of CDK1 activity. Depletion of Greatwall in human cells causes a delay or arrest in G2. Cells that do enter mitosis exhibit multiple defects and either die due to mitotic catastrophe or exhibit chromosomal alignment defects, segregation defects, cytokinesis defects and aberrant mitotic exit that leads to multinucleate cells. Conversely Greatwall overexpression is well tolerated in human HEK 293T cells and points to the regulation of Greatwall activity by PTMs as key for its function.

While work on this thesis was underway Burgess *et al.* (2010) and Voets *et al.* (2010) published detailed characterisations of Greatwall localisation and its depletion phenotypes in human cells, that are in agreement with my findings. These studies characterised Greatwall localisation and described the effects of Greatwall depletion in human cells in greater depth than is explored here. The publication of these reports led to a decision to investigate other aspects of human Greatwall biology in this work.

Briefly, as reported from work in *Drosophila*, their investigations of human Greatwall found that the kinase is predominantly present in the nucleus of interphase cells (Yu *et al.* 2004; Burgess *et al.* 2010; Voets *et al.* 2010). Although they additionally observed persistent partial cytoplasmic localisation as well as localisation at the centrosomes of G1, S and G2 phase cells (Burgess *et al.* 2010; Voets *et al.* 2010). Mitotic cells display an enhanced signal that spreads diffusely throughout the cell upon nuclear envelope breakdown but is excluded from the chromosomes. Greatwall is also

concentrated at spindle poles in early mitosis and Burgess *et al.* (2010) also observed that Greatwall emanated out along the spindle fibers as the cells entered mitosis. Once cells are in anaphase Greatwall leaves the spindle becoming increasingly diffuse throughout the cell. During telophase and cytokinesis it localises in the nucleus as the nuclear envelope reforms, although a small proportion localises to the cleavage furrow and midzone microtubules where it is also occasionally detected at the midbody (Burgess *et al.* 2010; Voets *et al.* 2010).

These studies also confirmed that Greatwall depleted cells released from an S phase block induced using Thymidine showed delayed entry into mitosis and then further delayed progression into anaphase (Burgess *et al.* 2010; Voets *et al.* 2010). In mitosis, cells depleted of Greatwall showed significant chromosome abnormalities. In metaphase cells displayed under-condensed chromatin scattered along the spindle or, in cases where they had managed to condense their chromosomes, they failed to correctly align them on the metaphase plate. Many cells arrested in metaphase for long periods after which they died or performed an aberrant anaphase. This delay was likely due to activation of the SAC as the checkpoint proteins (BubR1 and Aurora B) were localised to the kinetochores in these cells (Burgess *et al.* 2010). Few cells were observed in anaphase, but those that were had lagging chromosomes and displayed chromosome bridges. The spindles appearance was relatively normal in these cells, although in some cases the spindles were slightly elongated with lower numbers of microtubules and were observed by live cell imaging to rotate dynamically several times within the cell. The defects seen in cells that had exited mitosis are indicative of a cytokinesis failure. DNA bridges trapped in the cleavage furrow suggest problems with abscission that ultimately lead to retraction of the cleavage furrow and formation of 4n cells, suggesting a role for Greatwall in sister chromatid separation (Burgess *et al.* 2010; Voets *et al.* 2010).

The severity of the depletion phenotype observed correlated with the level of depletion achieved. As the level of Greatwall knockdown increased the ability of cells to remain in and perform efficient mitosis decreased. In synchronised cells depleted of Greatwall, progression through S phase occurred with normal kinetics but showed delayed entry into mitosis that corresponded to the level of Greatwall depletion. In the most severe cases, in which Greatwall knockdown was greatest, the delay in entry into mitosis was greatest, indicating that increasing Greatwall depletion results in an increased G2 arrest (Burgess *et al.* 2010; Voets *et al.* 2010).

Immunoblotting revealed that Greatwall depletion did not prevent the loss of

inhibitory phosphorylation on CDK1 in mitotic cells but did enhance mitotic phosphatase activity. This was shown by the diminished presence of mitotic phospho-epitopes in Greatwall depleted mitotic cells (Voets *et al.* 2010). The double depletion by siRNA of Greatwall and PP2A resulted in rescue of mitotic phospho-epitopes. Also the addition of okadaic acid to Greatwall depleted synchronised cells rescued the delayed mitotic entry defect and allowed depleted cells to enter mitosis with normal kinetics (Burgess *et al.* 2010). Thus indicating that increased PP2A phosphatase activity mediates the Greatwall knockdown phenotype.

Taken together, these data indicates that Greatwall is required in human cells to regulate PP2A activity to promote and maintain mitosis. This role for human Greatwall fits well with the current understanding of *Drosophila* and *Xenopus* Greatwall function and indicates that human Greatwall is their functional homologue.

Greatwall interacts with PP2A via its substrates Arpp19 and Ensa in *Xenopus* (Gharbi-Ayachi *et al.* 2010; Mochida *et al.* 2010). Accordingly, Arpp19 knockdown using siRNA in HeLa cells released from a Thymidine block into Nocodazole showed a 50% decrease in the number of mitotic cells compared with controls (Gharbi-Ayachi *et al.* 2010). This suggests that this pathway is highly conserved and that Greatwall regulates mitotic entry by Arpp19/Ensa mediated inhibition of PP2A.

Historically, entry into mitosis has been thought to be regulated exclusively by CDK1 activation and positive feedback loops. The emergence of the role of Greatwall in mitotic entry has highlighted that in fact it is the balance of CDK activation and phosphatase inhibition that coordinate to allow timely and proficient mitotic entry. The data and studies cited here indicate that Greatwall is a highly evolutionary conserved regulator of mitosis in higher eukaryotes including humans.

CHAPTER 4. Understanding the mechanisms of activation of Greatwall

4.1 Introduction

Protein kinases are key signalling enzymes that make up two percent of the proteins encoded in eukaryotic genomes and represent the third most common protein domain in the human genome (Hunter *et al.* 1997; Plowman *et al.* 1999; Morrison *et al.* 2000; Manning *et al.* 2002). In order to classify and distinguish between kinases they are grouped into distinct families based on their catalytic domain amino acid sequences (Hanks *et al.* 1991).

Greatwall is a member of the AGC kinase family (Hanks *et al.* 1995; Yu *et al.* 2004). An alignment of its N- and C- lobes with other AGC kinases is shown in **Table 4.1**. This is a diverse family of serine/threonine kinases that phosphorylate target amino acids C-terminal to basic amino acids (Hanks *et al.* 1995). These were first described in 1995 as a family of kinases that are related to cAMP-dependant protein kinase 1 (PKA), cGMP-dependant protein kinase (PKG) and protein kinase C (PKC). There are at least 60 AGC kinases and in many cases multiple isoforms and splice variants exist that add to the complexity in this family (Hanks *et al.* 1995; Manning *et al.* 2002; Pearce *et al.* 2010). The AGC kinase family phosphorylate a vast array of cellular substrates and regulate numerous cellular processes including cell division, survival, metabolism, transmembrane ion flux, migrative behaviour and differentiation (Sturgill *et al.* 1988; Kobayashi *et al.* 1999; Park *et al.* 1999; Flynn *et al.* 2000; Williams *et al.* 2000). Intricate and diverse mechanisms control their activity. These are often mediated by key functional domains outside of the catalytic core. These are critical to facilitate AGC kinases localisation and association with their activators and substrates (Frodin *et al.* 2000; Williams *et al.* 2000; Frodin *et al.* 2002). The phosphorylated targets of these kinases are often distinct as well as overlapping. The AGC kinases are further divided into 21 subfamilies based on their homology outside of the kinase domain (Pearce *et al.* 2010). One of these is the MAST kinase family that includes Greatwall (as described in **Chapter 3**).

The vast array of important cellular functions that these kinases are involved in means that, conversely, deregulation of these enzymes can lead to human diseases such

Table 4.1 Multiple sequence alignment

```
Greatwall       ----------------------------------------------------------------------------------------------------
PKA             ----------------------------------------------------------MGNAAAAKKGSEQES--------VKEFLAKAKE 25
AKT             ----------------------------------------------------------MSDVAIVKEGWLHKRGEYIKTWRPRYFLLKNDG 33
PKCalpha        MADVFPGNDSTASQDVANRFARKGALRQKNVHEVKDHKFIARFFKQPTFCSHCTDFIWGFGKQGFQCQVCCFVVHKRCHEFVTFSCPGADKGPDTDDPRSKHKFKIHTYGSPTFCDHCGS 120
PKCbeta         MADPAAGPPPSEGEESTVRFARKGALRQKNVHEVKNHKFTARFFKQPTFCSHCTDFIWGFGKQGFQCQVCCFVVHKRCHEFVTFSCPGADKGPASDDPRSKHKFKIHTYSSPTFCDHCGS 120
PKCgamma        MAGLGPGVGDSEG-GPRPLFCRKGALRQKVVHEVKSHKFTARFFKQPTFCSHCTDFIWGIGKQGLQCQVCSFVVHRRCHEFVTFECPGAGKGPQTDDPRNKHKFRLHSYSSPTFCDHCGS 119
AuroraA         ------------------------------------------------------MDRSKENCISGPVKATAPVGGPKRVLVTQQFPCQNPLPVNSGQAQRVLCPSNSSQRIPLQAQK 63
NDR1            ----------------------------------------------------------------------MAMTGSTPCSSMSNHTKERVTMTKVTLENFYSNLIAQHEER 41
PDK1            ----------------------------------------------------------------------MARTTSQLYDAVPIQSSVVLCSCPSPSMVRTQTE 34


Greatwall       --MD--------------------------------------------------------------------PTAGSKKEPGGGAATEEGVNRIAVPKPP---------------- 30
PKA             DFL---------------------------------------------------------------------KKWESPAQNTAH---------------------- 40
AKT             TFIGYKERPQDVDQREAPLNNFSVAQC-----------------------QLMKTERPRPNTFIIRCLQWTTVIERTFHVETPEEREEWTTAIQTVADGLKKQEEEEMDFRSGSPSDN 128
PKCalpha        LLYGLIHQGMKCDTCDMNVHKQCVINVPSLCGMDHTEKRGRIYLKAEVAD-EKLHVTVRDAKNLIPMDPNGLSDPYVKLKLIPDPKNESKQKTKTIRSTLNPQWNESFTFKLKPSDKDRR 239
PKCbeta         LLYGLIHQGMKCDTCMMNVHKRCVMNVPSLCGTDHTERRGRIYIQAHIDR-DVLIVLVRDAKNLVPMDPNGLSDPYVKLKLIPDPKSESKQKTKTIKCSLNPEWNETFRFQLKESDKDRR 239
PKCgamma        LLYGLVHQGMKCSCCEMNVHRRCVRSVPSLCGVDHTERRGRLQLEIRAPTADEIHVTVGEARNLIPMDPNGLSDPYVKLKLIPDPRNLTKQKTRTVKATLNPVWNETFVFNLKPGDVERR 239
AuroraA         LVSSHKP-----------------------------------------------------------VQNQKQKQLQATSVPHPVSRPLNNTQKSKQPLPSAPENNPEEELASKQKNEE 122
NDR1            EMRQ-------------------------------------------------------------------KKLEKVMEEEGLKDEEKRLRRSAHARKETEFLRLKRT------- 82
PDK1            SSTP-------------------------------------------------------------PGIPGGSRQGPAMDGTAAEPRPGAGSLQHAQPPPQPR---------------- 75
                                                                                                .


Greatwall       ----------------------------------------------------------------------------------------------------SIEEFSIVKP 40
PKA             ----------------------------------------------------------------------------------------------------LDQFERIKT 49
AKT             SGAEEMEVSLAKPK-------------------------------------------------------------------------------------HRVTMNEFEYLKL 155
PKCalpha        LSVEIWDWDRTTRNDFMGSLSFGVSELMKMPASGWYKLLNQEEGEYYNVPIPEGD-------EEGNMELRQKFEKAKLGP---AGNKVISPSEDRKQPS-----NNLDRVKLTDFNFLMV 344
PKCbeta         LSVEIWDWDLTSRNDFMGSLSFGISELQKASVDGWFKLLSQEEGEYFNVPVPPEG-------SEANEELRQKFERAKISQGTKVPEEKTTNTVSKFDNN-----GNRDRMKLTDFNFLMV 347
PKCgamma        LSVEVWDWDRTSRNDFMGAMSFGVSELLKAPVDGWYKLLNQEEGEYYNVPVADADNCSLLQKFEACNYPLELYERVRMGP---SSSPIPSPSPSPTDPKRCFFGASPGRLHISDFSFLMV 356
AuroraA         SKKR---------------------------------------------------------------------------------------------------QWALEDFEIGRP 138
NDR1            ----------------------------------------------------------------------------------------------------RLGLEDFESLKV 94
PDK1            ----------------------------------------------------------------------------------------------------KKRPEDFKFGKI 87
                                                                                                                      :*.

Greatwall       ISRGAFGKVYLGQKG--GKLYAVKVVKKADMINKNMTHQVQAERDALALSKS------PFIVHLYYSLQSANNVYLVMEYLIGGDVKSLLHIYGYFDEEMAVKYISEVALALDYLHR-HG 151
PKA             LGTGSFGRVMLVKHKETGNHYAMKILDKQKVVKLKQIEHTLNEKRILQAVNF------PFLVKLEFSFKDNSNLYMVMEYVPGGEMFSHLRRIGRFSEPHARFYAAQIVLTFEYLHS-LD 162
AKT             LGKGTFGKVILVKEKATGRYYAMKILKKEVIVAKDEVAHTLTENRVLQNSRH------PFLTALKYSFQTHDRLCFVMEYANGGELFFHLSRERVFSEDRARFYGAEIVSALDYLHSEKN 269
PKCalpha        LGKGSFGKVMLADRKGTEELYAIKILKKDVVIQDDDVECTMVEKRVLALLDK-----PPFLTQLHSCFQTVDRLYFVMEYVNGGDLMYHIQQVGKFKEPQAVFYAAEISIGLFFLHK-RG 458
PKCbeta         LGKGSFGKVMLSERKGTDELYAVKILKKDVVIQDDDVECTMVEKRVLALPGK-----PPFLTQLHSCFQTMDRLYFVMEYVNGGDLMYHIQQVGRFKEPHAVFYAAEIAIGLFFLQS-KG 461
PKCgamma        LGKGSFGKVMLAERRGSDELYAIKILKKDVIVQDDDVDCTLVEKRVLALGGRGPGGRPHFLTQLHSTFQTPDRLYFVMEYVTGGDLMYHIQQLGKFKEPHAAFYAAEIAIGLFFLHN-QG 475
AuroraA         LGKGKFGNVYLAREKQSKFILALKVLFKAQLEKAGVEHQLRREVEIQSHLRH------PNILRLYGYFHDATRVYLILEYAPLGTVYRELQKLSKFDEQRTATYITELANALSYCHS-KR 251
NDR1            IGRGAFGEVRLVQKKDTGHVYAMKILRKADMLEKEQVGHIRAERDILVEADS------LWVVKMFYSFQDKLNLYLIMEFLPGGDMMTLLMKKDTLTEEETQFYIAETVLAIDSIHQ-LG 207
PDK1            LGEGSFSTVVLARELATSREYAIKILEKRHIIKENKVPYVTRERDVMSRLDH------PFFVKLYFTFQDDEKLYFGLSYAKNGELLKYIRKIGSFDETCTRFYTAEIVSALEYLHG-KG 200
                :. * *. * *  .       *:*:: *  :           *                .  :   ::   .: : :.:   * :   :     : *  :  * ::    :   :
```

Here the AGC kinases PKA, AKT/PKB, PKC isoforms α, β and γ, NDR1 and PDK1 are aligned with Greatwall kinase (the insertion between the N- and C-lobes has been removed here). Key mitotic kinase Aurora A has been aligned also. The kinase fold N-lobe (aqua font) and C-lobe (orange font) as well as the hydrophobic motif (pink font) are indicated. Key residues are indicated in purple font and highlighted.

as diabetes and cancer (Cho *et al.* 2001; Sano *et al.* 2003; Carpten *et al.* 2007; Maurer *et al.* 2009). Protein kinases have recently emerged as major targets for drug development and comprise almost a third of newly validated targets by the pharmaceutical industry (Cohen 2002). This makes the AGC family of kinases important potential new targets of great relevance to our understanding of health and disease.

That Greatwall has been implicated in human disease and seemingly has critical importance in control of entry into and progression through mitosis, makes it an attractive target. Key to understanding how it functions is to unlock the mechanisms controlling its activity. In this chapter I use structural modeling, phosphorylation site mapping and mutagenic analysis to gain insight into the mechanisms that regulate Greatwall.

4.2 The structure of AGC kinases

The kinase core of AGC kinases is a bilobal kinase fold that comprises a small amino-terminal lobe (N-lobe) and a larger carboxy-terminal lobe (C-lobe). This gives the catalytic core of these kinases a characteristic 'bean-like' structure. The kinase domain can be further split into 12 subdomains that are defined by possessing characteristic patterns of conserved residues that are not interrupted by large amino acid insertions. The N-lobe is comprised of kinase subdomains I-IV and has a predominantly anti-parallel β-sheet structure. It serves primarily to anchor and orientate the nucleotide. The C-lobe contains subdomains VIA-XI and has a predominantly α-helical structure. This lobe is responsible mainly for binding the substrate and initiating phospho-transfer. Subdomain V residues span the lobes (Hanks *et al.* 1995; Pearce *et al.* 2010).

The two lobes sandwich a molecule of ATP in the cleft between them. ATP binds via the glycine rich loop in the N-lobe (Hirai *et al.* 2000). The ATP molecule then serves as the phosphate donor. Its adenine ring lies deep in the cleft directing the γ-phosphate outward which is transferred to the acceptor hydroxyl group of a specific serine or threonine residue of the substrate protein (**Figure 4.1**). It is common for protein kinases to posses N-terminal and C-terminal extensions from the catalytic core that can fold back into the core forming important and specific interactions. The AGC kinases possess such extensions that serve to promote both their activation and their stability (Hanks *et al.* 1995; Huse *et al.* 2002; Pearce *et al.* 2010).

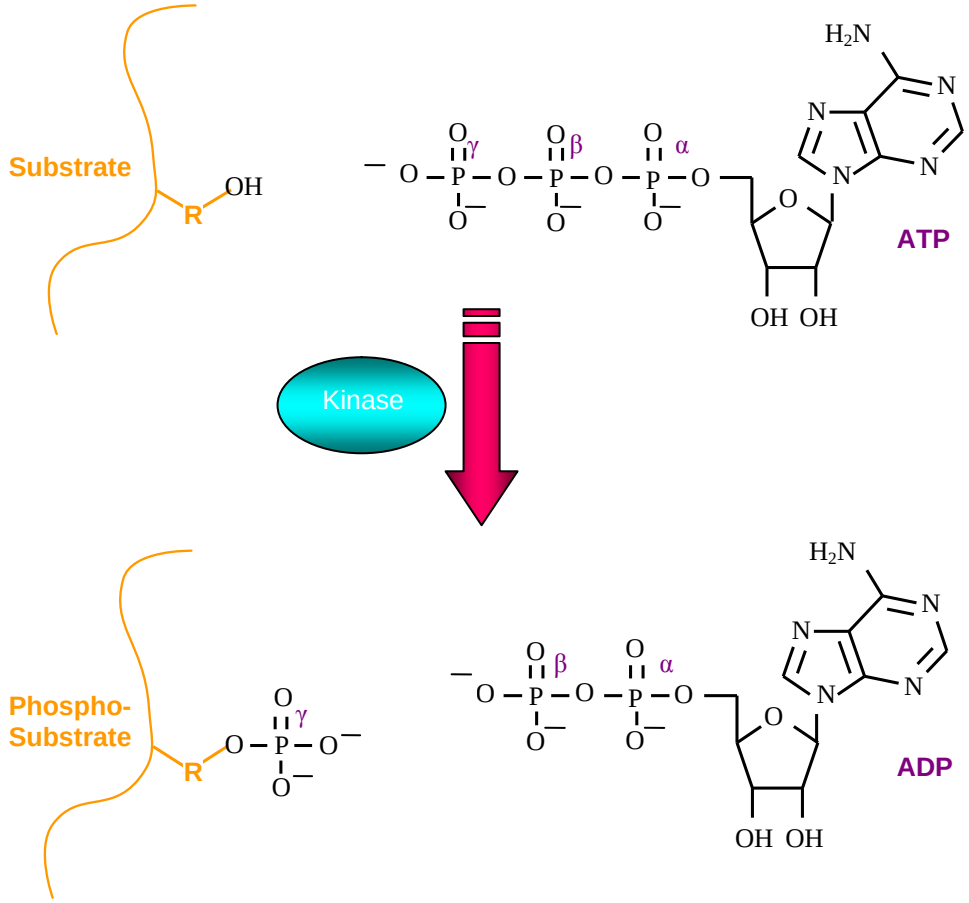

Figure 4.1 Phosphorylation by protein kinases

A protein kinase transfers the terminal phosphate of ATP to a hydroxyl group on a substrate protein.

Many AGC kinases have two common activation mechanisms mediated by highly conserved regulatory motifs (**Figure 4.2**). One is a key phosphorylation within their activation segment, known as the activation or T-loop, on a serine or threonine. The other is a phosphorylation in the conserved tail region C-terminal to the kinase domain, known as the hydrophobic motif. The activation loop is located adjacent to the ATP-binding site, usually in the C-lobe. It contains critical elements for catalytic activity including the DFG (Asp-Phe-Gly) motif that, with the glycine rich loop, positions the ATP for phospho-transfer. The aspartic acid of the DFG motif binds magnesium (Mg^{2+}) ions which in turn coordinate the β- and γ-phosphates of ATP while the glycine rich loop forms the ceiling of the active site (Johnson *et al.* 1996; Pearce *et al.* 2010). The activation loop is linked to the N-lobe through the αC helix that

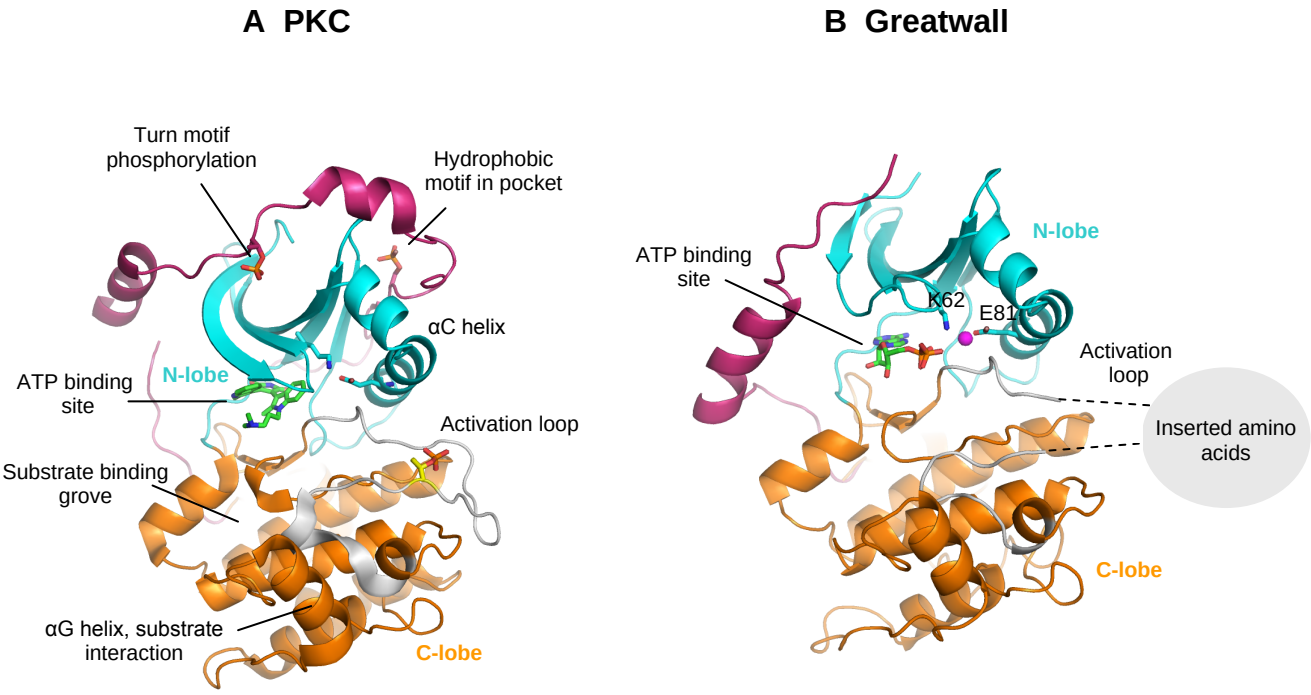

Figure 4.2 Modelling Greatwall kinase domain structure

(A) Structural model of PKCβII displaying the key structural features of AGC kinases. Here the small N-lobe (aqua), large C-lobe (orange), αC helix, activation loop (grey), C-terminal extension containing the turn motif and hydrophobic motif (pink), substrate binding grove and αG helix, are indicated. The three important regulatory phosphorylations are shown in ball-and-stick representation (red) and a competitive inhibitor of ATP is shown in the ATP-binding site in green. This and all other molecular graphics figures were produced with the help of Dr. Anthony Oliver using MacPyMOL (DeLano Scientific). **(B)** Structural model of Greatwall kinase. This model was generated using the modelling software PHYRE and coloured as for **(A)**. The C-terminal extension leading up to the hydrophobic motif could only be partially modelled and is shown in pink. One molecule of ADP is shown in the ATP-binding site in green. The activation loop is coloured grey, with the unmodelled region between the lobes where the large middle insertion of amino acids are likely looped out is indicated by the dashed lines and grey parenthesis. The active site magnesium ion is shown as a magenta sphere and the side chains for the conserved lysine and glutamic acid (K62 and E81) that position the γ-phosphate of ATP for phospho-transfer are indicated by ball-and-stick representation.

undergoes conformational changes upon phosphorylation for the activation loop. This allows a key glutamic acid residue in the αC helix to form an ion pair with a conserved lysine residue in the N-lobe. This creates a network of hydrogen bonds that are critical for catalytic activity and to allow positioning of the ATP γ-phosphate for phospho-

transfer. A hydrophobic pocket in the N-lobe, part of which is formed by the αC helix, mediates important regulatory interactions with the hydrophobic motif. The hydrophobic motif is formed by an extension from the C-lobe, in the C-terminal tail. In the active kinase this wraps around the N-lobe and stabilises the active conformation of the αC helix by inserting two aromatic residues into the hydrophobic motif pocket. In this manner the activation loop and the hydrophobic motif act together to help position the αC helix in the active conformation. In most AGC kinases a turn motif precedes the hydrophobic motif in the C-terminal tail. This assists the positioning of the C-terminal tail allowing it to correctly fold around the whole of the N-lobe and increases the local concentration of the hydrophobic motif at the hydrophobic motif pocket. For this reason phosphorylation of the turn motif and presence of the corresponding positively charged patch of the N-lobe are required for full kinase activity. AGC kinases can interact with their substrates in different ways but a grove close to the active site is known to be involved in binding the substrate. The residues forming this grove likely determine sequence specificity of the kinase. In addition, an αG helix that protrudes from the C-lobe has been implicated in substrate interactions (Knighton *et al.* 1991; Hanks *et al.* 1995; Biondi *et al.* 2002; Frodin *et al.* 2002; Yang *et al.* 2002; Biondi *et al.* 2003; Sano *et al.* 2003; Komander *et al.* 2005; Pearce *et al.* 2010).

Many AGC kinases have two common activation mechanisms mediated by highly conserved regulatory motifs. One is a key phosphorylation within their activation segment, known as the activation or T-loop, on a serine or threonine. The other is a phosphorylation in the conserved tail region C-terminal to the kinase domain, known as the hydrophobic motif. The activation loop is located adjacent to the ATP-binding site, usually in the C-lobe. It contains critical elements for catalytic activity including the DFG (Asp-Phe-Gly) motif that, with the glycine rich loop, positions the ATP for phospho-transfer. The aspartic acid of the DFG motif binds magnesium (Mg^{2+}) ions which in turn coordinate the β- and γ-phosphates of ATP while the glycine rich loop forms the ceiling of the active site (Johnson *et al.* 1996; Pearce *et al.* 2010). The activation loop is linked to the N-lobe through the αC helix that undergoes conformational changes upon phosphorylation for the activation loop. This allows a key glutamic acid residue in the αC helix to form an ion pair with a conserved lysine residue in the N-lobe. This creates a network of hydrogen bonds that are critical for catalytic activity and to allow positioning of the ATP γ-phosphate for phospho-transfer. A hydrophobic pocket in the N-lobe, part of which is formed by the αC helix, mediates

important regulatory interactions with the hydrophobic motif. The hydrophobic motif is formed by an extension from the C-lobe, in the C-terminal tail. In the active kinase this wraps around the N-lobe and stabilises the active conformation of the αC helix by inserting two aromatic residues into the hydrophobic motif pocket. In this manner the activation loop and the hydrophobic motif act together to help position the αC helix in the active conformation. In most AGC kinases a turn motif precedes the hydrophobic motif in the C-terminal tail. This assists the positioning of the C-terminal tail allowing it to correctly fold around the whole of the N-lobe and increases the local concentration of the hydrophobic motif at the hydrophobic motif pocket. For this reason phosphorylation of the turn motif and presence of the corresponding positively charged patch of the N-lobe are required for full kinase activity. AGC kinases can interact with their substrates in different ways but a grove close to the active site is known to be involved in binding the substrate. The residues forming this grove likely determine sequence specificity of the kinase. In addition, an αG helix that protrudes from the C-lobe has been implicated in substrate interactions (Knighton *et al.* 1991; Hanks *et al.* 1995; Biondi *et al.* 2002; Frodin *et al.* 2002; Yang *et al.* 2002; Biondi *et al.* 2003; Sano *et al.* 2003; Komander *et al.* 2005; Pearce *et al.* 2010).

The importance of the phosphorylation-dependant interactions in allowing kinase integrity and activity has been highlighted by the inactive conformations of these kinases. Once active, the kinase fold forms an ordered and conserved catalytic core unit. When the kinases are inactive, however, their conformations can be highly diverse. In the inactive state the hydrophobic motif pocket, the αC helix and most of the activation segment can be highly flexible and disordered. These differing inactive conformations allow individual AGC kinases to mediate interactions with various different cellular compartments, activators and substrates (Huse *et al.* 2002; Yang *et al.* 2002; Pearce *et al.* 2010).

4.3 Modelling Greatwall kinase

Little was known about the mechanisms promoting Greatwall activation when this work began. What was known was based on work in *Xenopus* that indicated that Greatwall was activated by phosphorylation in mitosis (Yu *et al.* 2006; Zhao *et al.* 2008). To build on this and increase our understanding of Greatwall's regulation a

structural model of human Greatwall was generated. All positions of amino acid residues refer to human Greatwall kinase and relate to this model, unless otherwise stated.

This model was created in collaboration with Dr Anthony Oliver at the Genome Damage and Stability Center (GDSC), University of Sussex. This was produced using the computational protein structure prediction engine, the Protein Homology/analogY Recognition Engine (PHYRE) (Kelley *et al.* 2009). This generates a 3-dimensional (3D) model based on protein threading (or fold recognition) and can be used to generate models for proteins that have no homologues with known structure. Structural prediction is made in this case by aligning, or 'threading', amino acids from the target sequence onto a template structure and then evaluating how well the target matches the template. In this manner a 'best-fit' template is selected from known structures and a model of the target sequences structure is built based on its alignment with this chosen template (Kelley *et al.* 2009). The catalytic core of Greatwall was modeled in this manner using the α isoform of PKC, another AGC family kinase, as the 'best-fit' template (**Figure 4.2 B**).

The amino acid sequence alignment revealed that active kinase core likely comprises the first 36 to 195 amino acid residues (N-lobe) and the last amino acid residues 737 to 849 (C-lobe) (**Figure 4.3**). These regions are highly conserved between human, *Drosophila* and *Xenopus* Greatwall kinases (for full alignment of these proteins see **Appendix C**). The two lobes then fold together effectively looping out the middle amino acids (residues 196 to 736). These residues between the N- and C-lobes represent a large insertion between the lobes of 540 amino acids with as yet unknown function. In this model the glycine rich loop (ISRGAFGKV) is formed by amino acids 41 to 49 and the DFG motif is formed by amino acids 174 to 176. The ion pair required to coordinate the Mg^{2+} ion and position the ATP γ-phosphate for phospho-transfer is formed by lysine 62 (K62) in the N-lobe and glutamic acid 81 (E81) from the αC helix. At the end of the C-lobe amino acids 854 to 878 form an AGC kinase C-terminal tail that contains the hydrophobic motif (residues 853 to 875).

Greatwall is not a conventional AGC kinase due to its large region of inserted amino acids between the two lobes of the kinase domain , between kinase subdomains VII and VIII (Burgess *et al.* 2010) where the activation loop is typically located. Our model indicates that part of this region forms the activation loop but much of this insertion could not be modelled. Structural prediction software indicates that it has no

Figure 4.3 Mapped features of Greatwall

The kinase domain lobes and hydrophobic motif are coloured as in **Figure 4.2 B**. The glycine rich loop, DFG motif, ion pair (K62 and E81) are indicated. Residues mutated in this investigation are indicated by diamond parentheses.

sequence similarity with any known protein folds and it is poorly conserved between human, *Drosophila* and *Xenopus* Greatwall kinases (see **Appendix C**). It is interesting

to note that a large majority (70%) of the insertion is encoded by a single large exon in the Greatwall (MASTL) gene (exon 8, residues 329 to 708, **Appendix D**). This leads us to postulate that it could represent a gene fusion event. The resulting protein, Greatwall, would therefore represent a hybrid gene product, although searches for sequences homologous to this exon sequence return no results. At present the origin of this unique type of bifurcated kinase structure and the functions of the large insertion remain obscure.

4.4 Identification of the activation loop

The structural model of Greatwall kinase allowed the identification of the activation loop and positioning of the DFG motif. Any threonine or serine after this motif might represent the phosphorylation of the activation loop critical for kinase activity. This phosphorylation is mediated by upstream kinases and begins AGC kinase activation. It serves to promote conformational changes that are critical for kinase activity as discussed in section **4.2** (Johnson *et al.* 1996; Pearce *et al.* 2010). A threonine at position 194 (T194) was identified that might represent the candidate phosphorylated residue. This was guided in part by phosphorylation site mapping analysis of Greatwall using PhosphoSitePlus (http://www.phosphosite.org). This is an online systems biology resource for the study of protein PTMs. It provides an extensive, manually curated database indicating phosphorylation sites and other PTMs that have been identified from both high-throughput and low-throughput articles and reports (Hornbeck *et al.* 2012). The output of this analysis is shown in **Figure 4.4**. This indicated that the first residue that is likely to be phosphorylated after the DFG motif is T194. This informed our prediction that T194 would be phosphorylated in the activation loop and therefore be critical for kinase activity.

In order to test this prediction, I mutated T194 to an alanine (T194A) by site-directed mutagenesis. The chemically inert methyl functional group of the alanine residue cannot be phosphorylated and allows the significance of the phosphorylation of this residue on the activity of the kinase to be assessed. T194 lies adjacent to another threonine residue, T193, that might also be phosphorylated and contribute to kinase activation. This was also mutated to alanine (T193A) and a double mutant in which both of these residues were mutated to alanines (T193/4A) was also generated. The non-

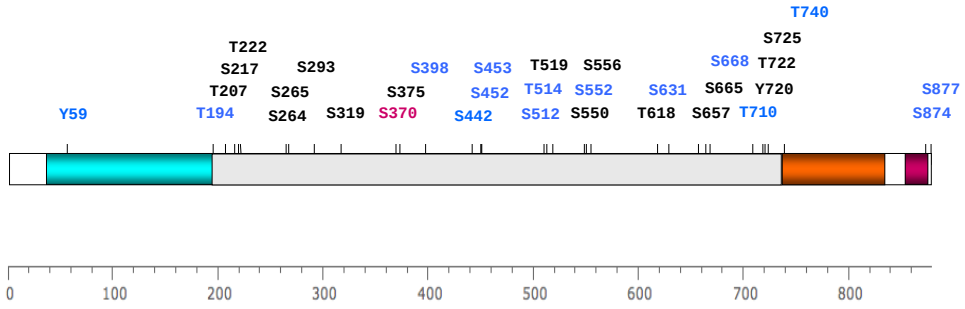

Figure 4.4 Phosphorylation site mapping of Greatwall

Phosphorylation site mapping analysis of Greatwall using PhosphoSitePlus. Sites with only one mass spectrometry (MS)/high-throughput (HTP) reference are shown in black. Sites with more than one MS/HTP reference are shown in blue and a site with more than five MS/HTP references is indicated in pink. The kinase domain lobes and hydrophobic motif are indicated coloured as in **Figure 4.2 B**.

phosphorylatable mutants T193A, T194A and T193/4A were flag-tagged and transfected into human HEK 293 cells. Wildtype flag-Greatwall (WT Greatwall) was also transfected into these cells to provide a bench mark for full kinase activity. The cells were then allowed to express the tagged proteins for 24 hours. After this, the media was then replaced with media containing the spindle poison Nocodazole and the cells incubated for a further 16 hours. This served to arrest the cells in mitosis at the time when Greatwall is maximally active as determined in **Chapter 3** (**Figure 3.3**). The cells were harvested and the flag-tagged active protein immunoprecipitated using magnetic beads coated with an anti-flag antibody. The purified kinase was then taken into an *in vitro* kinase assay using recombinant MBP as an arbitrary substrate. The lysates and immunoprecipitates were assessed for flag-Greatwall expression by immunoblotting and Greatwall kinase activity against MBP was visualised on an autoradiograph (**Figure 4.5 A**). No band-shift of active Greatwall is observed on the resulting immunoblots as the exposure shown is relatively short and indicates the main bands of Greatwall only. In longer (but overexposed) images a band-shift can be seen. This suggests that only a proportion of Greatwall is in the highly active (up-shifted) state at any one time while in mitosis. The T194A mutant had severely reduced activity with only 32% of WT Greatwall's kinase activity (normalised for protein amount) while T193A had around 70% activity (that varied up to 95% of WT activity). The double mutant had 27% of WT kinase activity and is not significantly different to that of T194A. These results

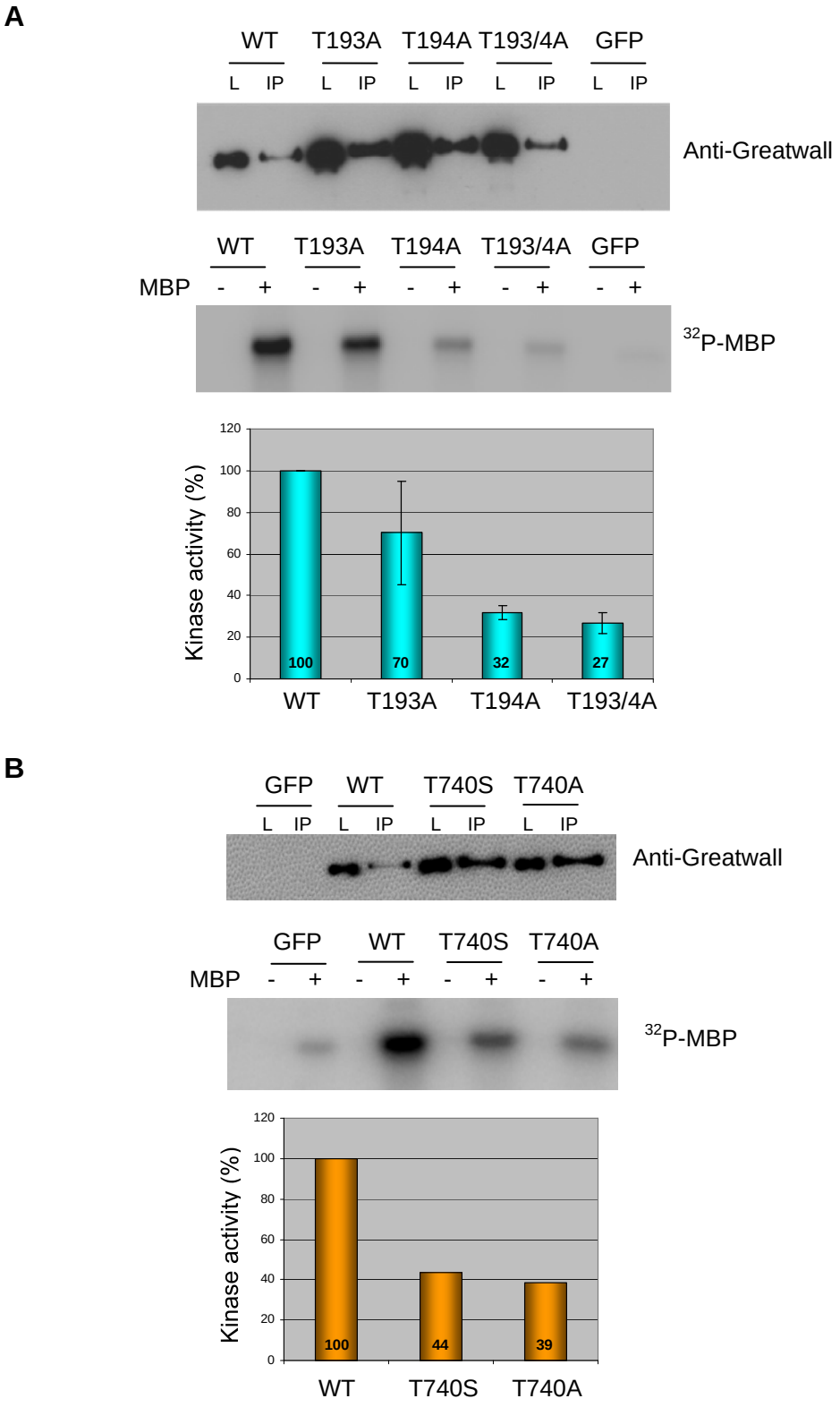

Figure 4.5 Determination of the phosphorylation events that begin Greatwall kinase activation

(A) Flag-tagged Greatwall or non-phosphorylatable mutants T193A, T194A and T193/4A were expressed in human HEK 293T cells. Cells transfected with a GFP control were analysed as well. After 24 hours the cells were treated with Nocodazole. The flag-tagged proteins were then immunoprecipitated using anti-

flag magnetic beads. An *in vitro* kinase assay was then performed using MBP as a substrate for the kinase. The top panel shows the results of SDS-PAGE analysis indicating the expression of the flag-tagged protein in the cell lysates (L) and the immunoprecipitate (IP) detected using the anti-Greatwall antibody. The autoradiograph is shown in the second panel. Quantification of the kinase activity of the mutant kinases relative to the wildtype is shown in the graph beneath. This represents results averaged from three independent experiments and the standard deviation is represented by the error bars. **(B)** Flag-tagged Greatwall or mutants T741S and T741A were expressed in HEK 293T cells, immunoprecipitated and taken into a kinase assay as described for **(A)**.

imply that T193 does not significantly contribute to kinase activation and its mutation does not synergise with the loss of activity seen when T194 is mutated in combination with this residue. This indicates that T194 is a phosphorylated residue that is important for Greatwall kinase activity and is likely part of the kinase activation loop as predicted.

This was further supported by a recent publication in which this residue, T194, was also found to be essential for Greatwall kinase activation (Blake-Hodek *et al.* 2012). Here they carried out mutagenesis of *Xenopus* Greatwall. They also concluded that T194 (T193 in *Xenopus*) formed part of the kinase activation loop of Greatwall. The authors reported the same result as obtained here, that mutation of T194 to an A severely disrupted kinase activity and furthermore its function. In *Xenopus* CSF extracts expression of the A mutant led to failure to sustain M phase when endogenous Greatwall had been depleted (Blake-Hodek *et al.* 2012). Together, this provides evidence that T194 is an important phosphorylated residue of the Greatwall kinase activation loop and is required for kinase activity in mitosis.

4.5 Identification of a second site important for Greatwall activity

Threonine 740 (T740) was identified by phospho-site mapping and structural analysis to also be a potentially significant residue that requires phosphorylation for full activation of Greatwall (**Figure 4.4**). In order to test this proposal, I mutated T740 to an A, expressed it with a flag-tag and immunoprecipitated the protein from human cells arrested in mitosis. A kinase assay was then performed to assess its activity as described previously (in section **4.4**). The mutant, T740A, again severely disrupted Greatwall kinase activity and displayed only 44% of WT kinase activity (**Figure 4.5 B**). This was

not rescued by mutation of this site to another phosphorylatable residue, in this case to a serine (S). The T740S mutant displayed a similar reduction in kinase activity (39%) as T740A when compared to WT Greatwall. The failure of this phosphorylatable mutation to restore kinase activity might reflect a specific structural requirement of the kinase for a T at this position rather than a direct requirement for this site to be phosphorylated.

T740 was identified as an important phospho-residue in Greatwall in three studies published during the course of this work. Each of these found that mutation of this residue to an A disrupted kinase activity to a similar degree as reported here and that this led to failure to support M phase in *Xenopus* egg extracts after endogenous Greatwall depletion (Yu *et al.* 2006; Vigneron *et al.* 2011; Blake-Hodek *et al.* 2012). This implies that this residue is necessary for Greatwall function and might represent a critical element of the P+1 loop rather than forming part of the activation loop itself. The P+1 loop is a small motif that usually resides immediately downstream of the activation loop. It is implicated in substrate sequence recognition and is thought to bind a substrate residue C-terminal of the residue to be phosphorylated. A phospho-mimetic mutant of this residue, T740E, in *Xenopus* displayed no function, further supporting the proposal that this site does not represent an important activation loop phosphorylation (Blake-Hodek *et al.* 2012). It indicates an intolerance of Greatwall activity for amino acid substitutions at this position. This is therefore likely to be because it is an important residue in the P+1 loop and represents a site critical for substrate interaction (Nolen *et al.* 2004; Hauge *et al.* 2007; Vigneron *et al.* 2011; Blake-Hodek *et al.* 2012).

4.6 Other structural features of Greatwall kinase

The primary aim of this work was to understand the mechanisms involved in Greatwall activation and we began our investigation by attempting to determine key activating phosphorylations of the kinase, based on those described for other AGC kinases. As mentioned earlier, as this work was coming to fruition, another paper was published by Vigneron *et al.* (2011) also detailing Greatwall's activation mechanisms. In this paper they investigated human Greatwall kinase by mutating residues that are highly conserved in other eukaryotic serine/threonine kinases to assess if Greatwall could function as a typical AGC kinase. Initially they mutated a conserved glycine residue (G44) found in the glycine rich loop (**Figure 4.3**) to a serine and analysed the

mutant for kinase activity. The glycine rich loop covers and anchors the nontransfered α- and β-phosphates of the ATP leaving the γ-phosphate exposed and positioned appropriately for phospho-transfer (Hanks *et al.* 1995; Pearce *et al.* 2010). In their study they over expressed HA-tagged human Greatwall or mutant Greatwall in *Xenopus* CSF extracts and carried out *in vitro* kinase assays using MBP as a substrate (Vigneron *et al.* 2011). They also performed rescue experiments, in which they introduced the HA-tagged mutant Greatwall into *Xenopus* CSF extracts that had been depleted of endogenous Greatwall. They then assessed the ability of the mutants to sustain the mitotic phenotype in these extracts. Analysis of the G44S mutant showed that it exhibited only 5% of WT Greatwall activity and was incapable of maintaining M phase in CSF extracts, indicating that the glycine rich loop is critical for Greatwall kinase activity. They also mutated lysine 62 (K62) that forms the ion pair with the glutamic acid in the αC helix to coordinate a network of hydrogen bonds required for catalytic activity (**Figure 4.2** and **4.3**) (Hanks *et al.* 1995; Pearce *et al.* 2010). Mutation of this residue to an alanine resulted in only 8% of kinase activity remaining as compared with WT Greatwall. The mutant was not able to support the mitotic state in CSF extracts and thus rendered the kinase non-functional (Hanks *et al.* 1995; Pearce *et al.* 2010; Vigneron *et al.* 2011). The importance of these two key residues for Greatwall activity indicate the conservation of key AGC kinase structural features in Greatwall kinase, in agreement with the results presented already in this work.

4.7 Identification of the hydrophobic motif

The hydrophobic motif is characterised by three aromatic residues surrounding a phosphorylated serine or threonine residue. This can be phosphorylated by another kinase or result from autophosphorylation by the kinase itself. Once phosphorylated, in addition to contributing to kinase activity itself, it can serve as a docking site for other kinases that when bound, enhance or mediate the catalytic activity of the kinase (Frodin *et al.* 2002; Pearce *et al.* 2010).

The AGC C-terminal tail of Greatwall is somewhat unconventional and seems to lack elements seen in other AGC kinases. Despite this, sequence alignments with the tail regions of the other MAST kinases and the AGC kinase PKC (**Figure 4.6 A**) combined with phospho-site mapping (**Figure 4.4**) of this region highlighted two

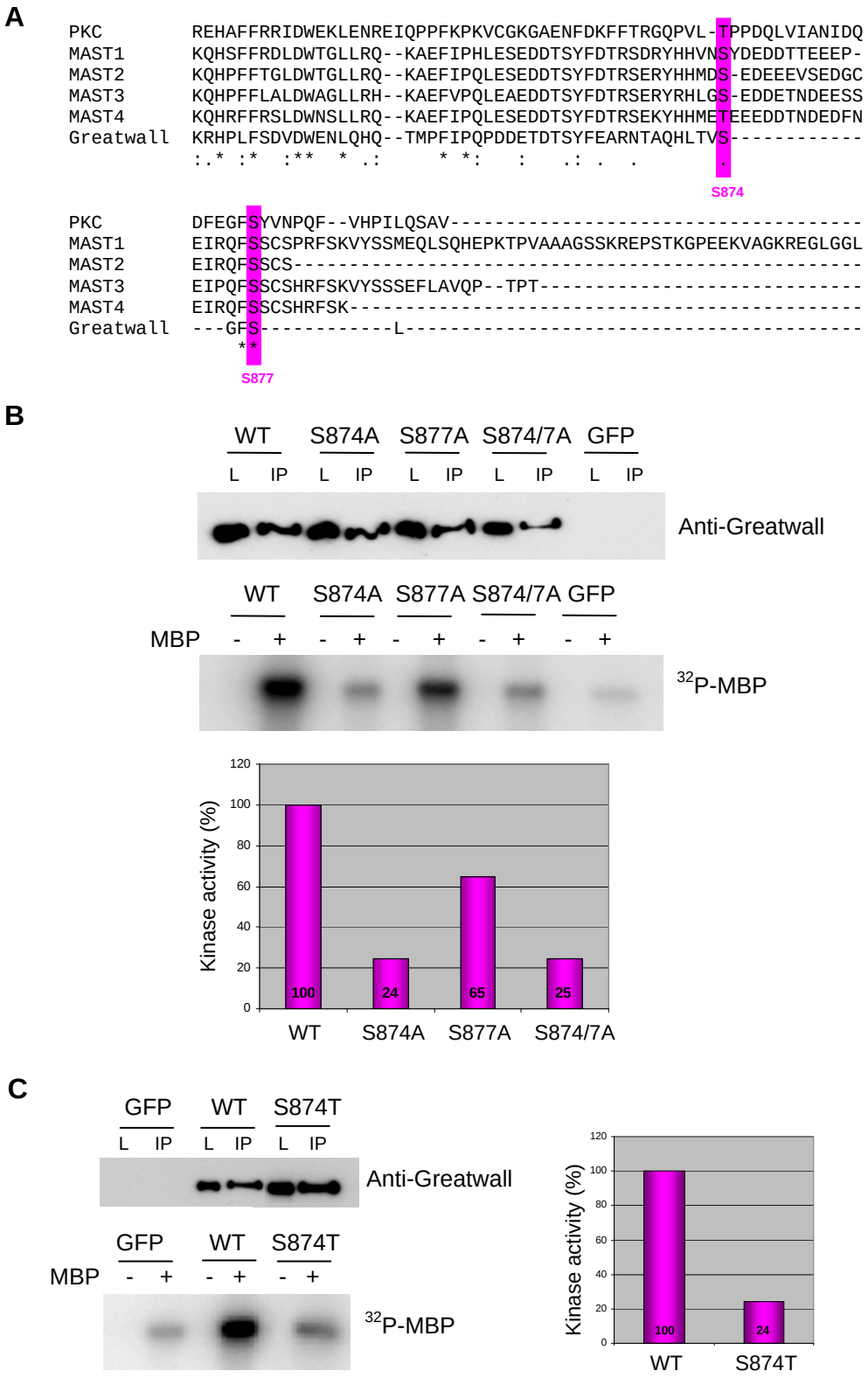

Figure 4.6 Identifying the hydrophobic motif of Greatwall

(A) Sequence alignments of Greatwall C-terminal tail region with those of the other AGC kinases. Alignments with the MAST kinases and PKC are shown. Serine 874 (S874) and serine 877 (S877) are

highlighted with pink parentheses. These residues might represent important phospho-sites for Greatwall activation as they are well conserved in the tail region of these kinases. **(B)** Flag-tagged Greatwall or non-phosphorylatable mutants S874A, S877A and S874/7A were expressed in HEK 293T cells, immunoprecipitated and taken into a kinase assay as described for **Figure 4.5**. **(C)** Flag-tagged Greatwall or the phosphorylatable mutant T874S were assessed as described for **(B)**.

residues that might represent important phospho-sites for Greatwall activation. These residues that might represent important phospho-sites for Greatwall activation. These sites, serine 874 (S874) and serine 877 (S877), are well conserved in the tail region of these AGC kinases. We hypothesised that one of these residues might represent the hydrophobic motif phosphorylation of the C-terminal tail of Greatwall. Once this site is phosphorylated on the last serine (or threonine) it then wraps around the N-lobe and anchors the two aromatic residues in the hydrophobic motif pocket. This allows the phosphate of the serine or threonine to bind an arginine residue of the αC helix, stabilising it and enhancing phospho-transferase activity. Thus, phosphorylation of the hydrophobic motif acts in concert with the activation loop to stabilise the active form of the kinase and is required for full activity of AGC kinases (Yang *et al.* 2002; Pearce *et al.* 2010).

In order to determine which, if either, of these residues were phosphorylated and important for Greatwall kinase activity, I mutated these residues to alanines separately or in combination. I then analysed these mutants for kinase activity as described previously (**Figure 4.6 B**). The S874A mutant displayed much reduced activity with only 24% of WT kinase activity. This was the same for the double mutant, while the S877A mutant showed less disruption of kinase activity with 65% of WT kinase activity remaining. We concluded from this data that the key phosphorylated residue of the hydrophobic motif is S874, and that S877 does not contribute to kinase activity.

At the time of analysis of these results Vigneron *et al.* (2011) published their analysis of the same sites. They also found that S874 when mutated to an A resulted in reduction of kinase activity to only 31% of WT activity. When tested in *Xenopus* CSF extracts this mutation resulted in complete loss of functionality, as judged by its inability to sustain M phase in these depleted extracts. In contrast, and in keeping with my conclusions, they found that mutation of S877 did not affect kinase activity (with 85% activity remaining) nor did its mutation affect Greatwall functionality (Vigneron *et*

al. 2011). These results were subsequently further confirmed by Blake-Hodek *et al.* (2012) who also reported the same effects when S874 was mutated in *Xenopus* Greatwall (S883 in *Xenopus*).

Conclusion that this residue therefore represented the key activating phosphorylated residue of the hydrophobic motif, however, proved premature. Vigneron *et al.* (2009; 2011) reported that sequence alignment of AGC kinase C-terminal tails with that of the Greatwall kinase indicated that the C-terminal tail is truncated in Greatwall (something also noted here) (**Figure 4.6 A**). This, they hypothesised, represented a lack of a true hydrophobic motif in this kinase. Instead they found that addition of a synthetic peptide encompassing the carboxy-terminal hydrophobic motif of another AGC kinase, Rsk2, stimulated kinase activity of Greatwall that was dependant on prior phosphorylation of S784. This led them to propose that S874 in fact represents phosphorylation of what would be more similar to the typical turn motif of AGC kinases. The turn motif precedes the hydrophobic motif and allows the correct orienting of the C-terminal tail to allow it to fold around the N-lobe and thus increases the local concentration of the hydrophobic motif in hydrophobic motif pocket. For this reason, phosphorylation of the turn motif is required for full kinase activity (Hauge *et al.* 2007; Kannan *et al.* 2007; Vigneron *et al.* 2011).

Seemingly in contradiction to this, however, they also confirmed that Greatwall does posses a functional hydrophobic motif binding pocket (Vigneron *et al.* 2011). When they mutated arginine 82 (R82) and tyrosine 98 (Y98) to alanines, both Greatwall kinase activity and functionality were lost with only 13% and 7% kinase activity remaining respectively. These residues are conserved with the hydrophobic motif binding pockets of other AGC kinases. The first residue binds the phosphorylated residue of the hydrophobic motif and the second binds the last phenylalanine of the motif to mediate the stabilisation of the active catalytic core (Biondi *et al.* 2003; Kannan *et al.* 2007; Pearce *et al.* 2010). It is strange that Greatwall should require a hydrophobic motif binding pocket while not actually possessing a true hydrophobic motif. It is known that membrane-localised 3-phosphoinositide-dependant kinase 1 (PDK1), another unconventional AGC kinase, binds via its hydrophobic motif binding pocket to the phosphorylated hydrophobic motifs of its substrates (Biondi *et al.* 2000; Biondi *et al.* 2002; Biondi *et al.* 2003; Kannan *et al.* 2007). This binding facilitates conformational changes in its catalytic core that increase its activity. Thus, the authors proposed a model in which Greatwall kinase activation is completed via the interaction

of another AGC kinase inserting its phosphorylated hydrophobic motif into the hydrophobic motif binding pocket of Greatwall (Vigneron *et al.* 2011). In this model the phosphorylation of S874 would act as the turn motif and would be predicted to act by mediating the interaction of the hydrophobic motif with the pocket. This seems a logical conclusion, but in a final twist, Blake-Hodek *et* al. (2012) suggest that the C-terminal tail of Greatwall is insufficiently long to promote such an interaction. Thus, the true nature of the mechanism of S874 phosphorylation in mediating Greatwall kinase activity still remains to be fully elucidated.

This also leads to speculation on the reason that mutation of this site to another phosphorylatable residue (to a threonine, S874T) failed to even partially rescue Greatwall activity (with the T mutant displaying 24% of WT kinase activity, as was the same for the A mutant) (**Figure 4.6 C**). Indicating that, rather than this representing an important phosphorylation event, it is a structural requirement of the catalytic core to have a serine residue at this position. This result was considered anomalous in the face of the report by Vigneron *et al.* (2011) until recently (when the report by Blake-Hodek *et al.* (2012) was published as this was being written up) and further analysis is required to clarify these issues.

4.8 Making a constitutively active kinase

The important T194 and S874 sites were also altered to an aspartic acid (D), both separately and in combination, to mimic a phosphorylated T or S. The purpose of making these phospho-mimetic mutants was primarily to make a Greatwall kinase that was constitutively active. Unfortunately none of these mutant kinases exhibited constitutive activity; rather they all showed reduced activity as compared to the WT kinase whether the cells were in mitosis or not (**Figure 4.7 A and B**). T194D had only 26% activity in asynchronous cells and only 28% of WT activity in mitotic cells arrested with Nocodazole. S874D had only 30% and 26% activity in asynchronous and mitotic cells respectively. In both cases the reduction in activity is similar to that seen for the original A mutants. The double mutant displayed very similar reductions in kinase activity, with 24% activity in asynchronous cells and 16% activity in mitotic cells. This suggests that these phospho-mimetic mutants were not sufficient to restore kinase activity. I also tried mutating these sites to glutamic acid, E, in case this should

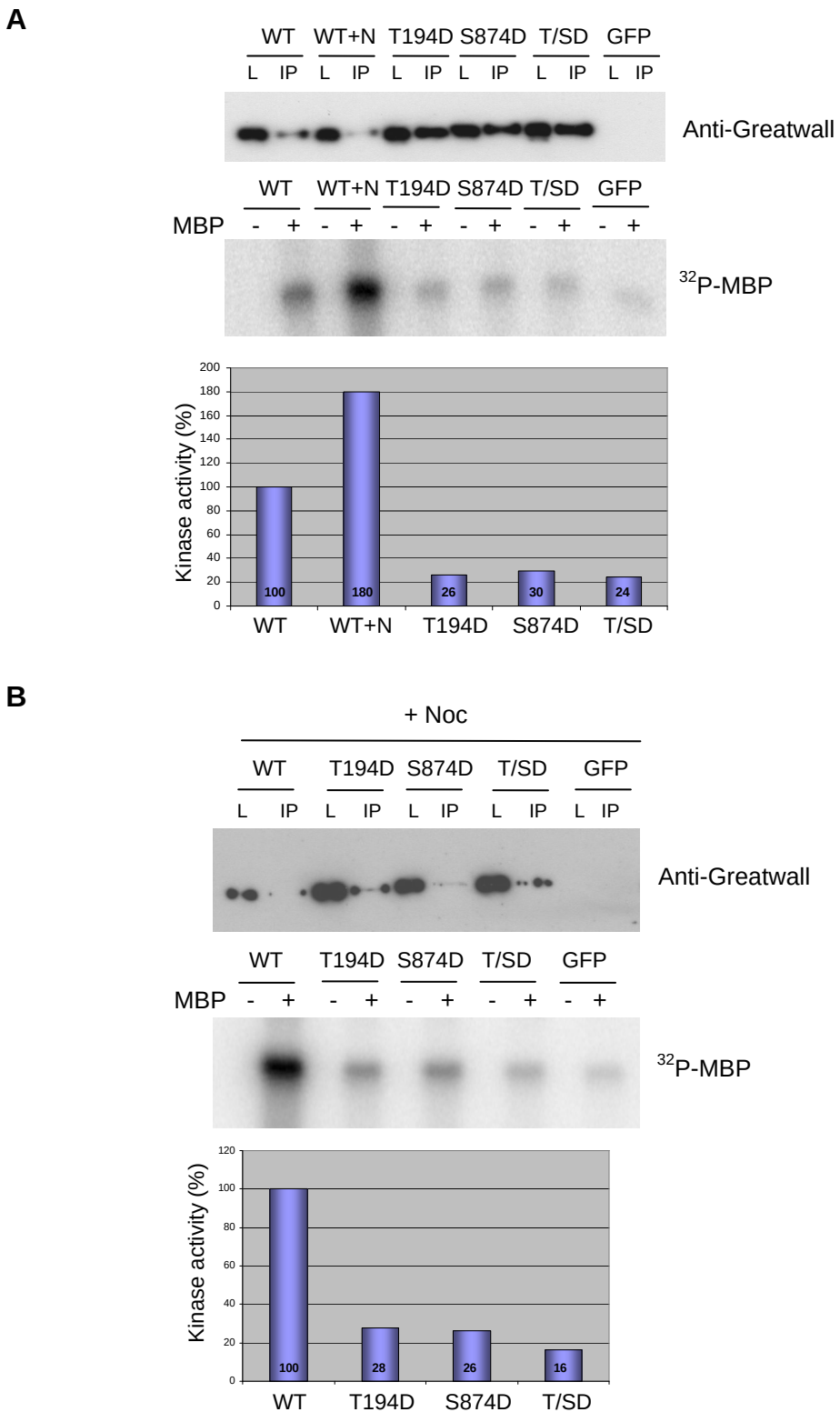

Figure 4.7 Making a constitutively active Greatwall

(A) Flag-tagged Greatwall or phospho-mimetic mutants T194D, S874D and double mutant T914D/S874D (T/SD) were expressed in HEK 293T cells, immunoprecipitated and taken into a kinase assay as described for **Figure 4.5**. Here only one lot of cells transfected with the wildtype kinase were

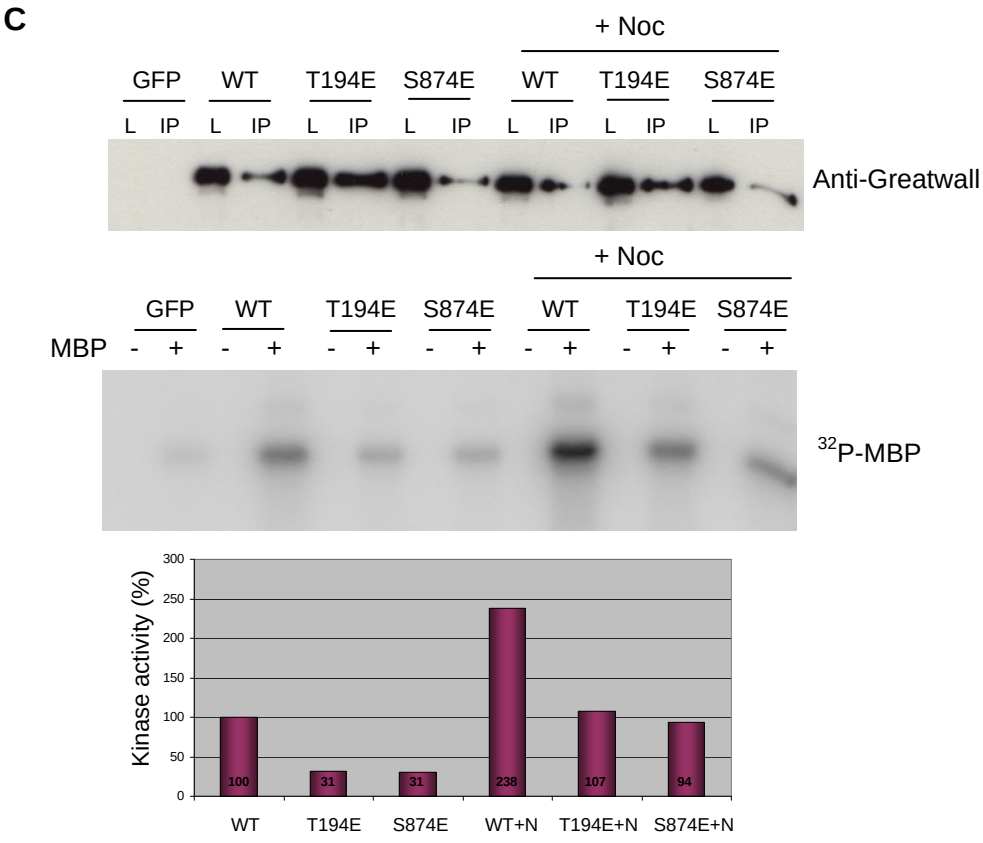

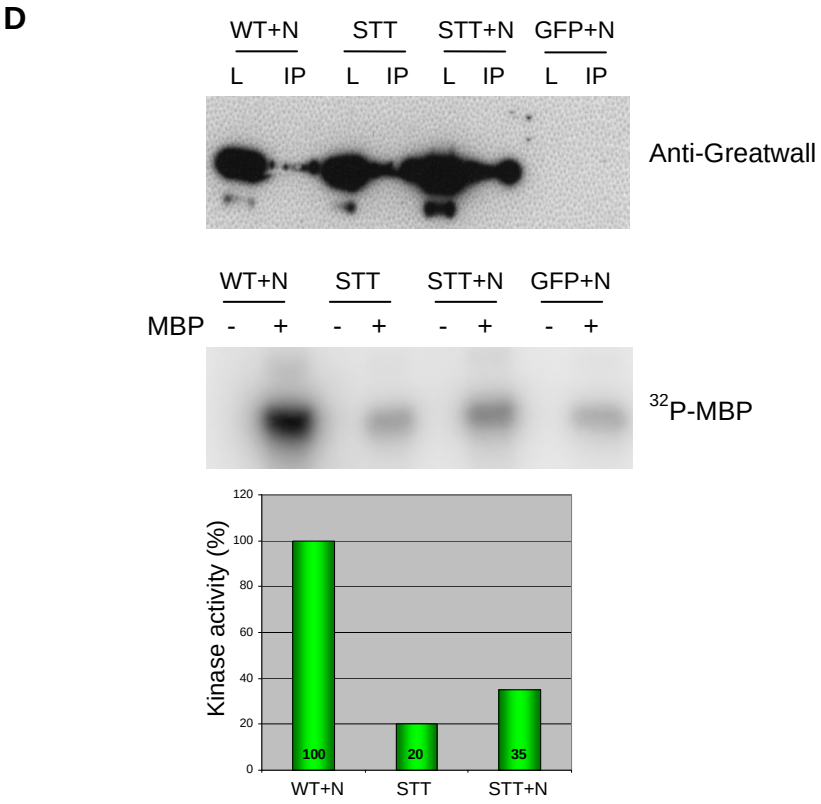

treated with Nocodazole (+N). **(B)** Flag-tagged Greatwall or phospho-mimetic mutants T194D, S874D and double mutant T914D/S874D (T/SD) were expressed in HEK 293T cells, immunoprecipitated and

taken into a kinase assay as described for **(A)**. All cells were treated with Nocodazole (+Noc) as indicated. **(C)** Flag-tagged Greatwall or phospho-mimetic mutants T194E and S874E were expressed in HEK 293T cells, immunoprecipitated and taken into a kinase assay as described for **(A)**. Where indicated cells were treated with Nocodazole (+Noc). **(D)** Flag-tagged Greatwall or the triple mutant S102D/T194E/T207E (STT) were expressed in HEK 293T cells, immunoprecipitated and taken into a kinase assay as described for **(A)**. Where indicated cells were treated with Nocodazole (+N).

prove more successful (**Figure 4.7 C**). The results were again disappointing with both the T194E and S874E mutant displaying reduced activity as compared to the WT kinase. Both displayed only 31% activity in asynchronous cells. The activity shown by these mutants was slightly increased by the addition of Nocodazole to arrest the cells in mitosis. This still did not increase the activity of the mutants to that of the mitotic WT kinase; T194E had only 45% activity and S874E had only 40% activity. This suggested that mutation of these sites to an E was slightly less disruptive to kinase activity but was insufficient to produce a fully active or constitutively active kinase.

Vigneron *et al.* (2011), however, reported that in their experiments when S874 is mutated to a D it showed only a 38% decrease in activity when compared to mitotic WT kinase activity. This mutant was also able to completely rescue the mitotic exit phenotype in *Xenopus* egg extracts. This supported their conclusion that this is an important phospho-site. Recently, Blake-Hodek *et al.* (2012) reported the same result. In their experiments the mutation of S874 to a D resulted in less than 50% activity as compared with the WT kinase but again was functional in *Xenopus* egg extracts. Further, they reported that mutation of T194 to an E resulted in a reduction in kinase activity to below 50% of that of WT kinase activity but that this mutant was fully functional in egg extracts. This is in conflict with the results discussed here that neither mutation of these residues to a phospho-mimetic (D or E) nor another phosphorylatable mutant (T/S) could induce kinase activity. However, in human cells we have so far been unable to test the mutant kinases for functionality and must defer to these analyses. Taking into account the reports described here it seems that although mutation of these sites to phospho-mimetic residues reduces kinase activity, they do restore Greatwall functionality.

4.9 A novel mechanism for Greatwall activation

A novel mechanism for Greatwall activation was proposed recently in the work published by Blake-Hodek *et al.* (2012). Here they found that more than 20 tryptic phospho-peptides result after Greatwall activation and hyperphosphorylation in M phase of *Xenopus* egg extracts. At least 15 were found to result from autophosphorylation by Greatwall itself. They found that ^{32}P was almost exclusively incorporated into active Greatwall with first-order kinetics typical of unimolecular reactions, indicating that Greatwall autophosphorylation is intramolecular (Blake-Hodek *et al.* 2012).

To investigate how Greatwall is activated by phosphorylation in mitosis they mutated all conserved T and S residues outside of the non-conserved middle region (NCMR) of inserted amino acid residues. In this manner they identified five phospho-sites by mass spectral analysis that were conserved between *Xenopus* and human Greatwall. Mutation of these residues to an A severely compromised Greatwall function. Three of these sites were T194, T740 and S874 (that were also identified in this work). The two further sites identified in this study were T207 (T206 in *Xenopus*) and S213 (S212 in *Xenopus*). Phospho-mimetic mutations of T194E, T207E and S874D rescue Greatwall activity in extracts while T740E and S212D do not. This implies a structural role for the residues S212 and T470 in Greatwall activation but that residues T194, T207 and S874 represent important phosphorylated residues (Blake-Hodek *et al.* 2012).

Blake-Hodek *et al.* (2012) found that a peptide containing S874 was phosphorylated *in vitro* by active Greatwall. They proposed a mechanism for activation of Greatwall based on the activation mechanism of PKA. Previous studies have shown that activation of PKA occurs via a two-step mechanism. Activation is begun by a priming phosphorylation of the activation loop on T197 by PDK1. It then autophosphorylates S338 in the turn motif of its C-terminal tail to mediate full activation (Frodin *et al.* 2002; Iyer *et al.* 2005). Blake-Hodek *et al*. (2012) suggest that Greatwall might be activated by a similar mechanism. In this model, residues T194 and T207 are initially phosphorylated in the presumptive activation loop by an upstream activating kinase. These two residues are found in a position analogous to that of the activating phosphorylation of PKAs activation loop on T197. This then allows the primed Greatwall to autophosphorylate on residue S874. As mentioned previously, this phosphorylation of the turn motif would possibly then allow it to mediate interaction

with/or the binding of an exogenous hydrophobic motif to complete Greatwall activation.

4.10 Other mutagenesis

Another residue, S102 (S101 in *Xenopus*), was reported by Blake-Hodek *et al*. (2012) to severely disrupt Greatwall function when mutated to an A, while its mutation to a D conferred limited constitutive activity. They found no evidence for the phosphorylation of this site and concluded that the mutation of this residue to a D must instead stabilise a partially active conformation of Greatwall by as yet unknown structural interactions. This constitutive activity synergises when combined with T207E and T194E mutations (Blake-Hodek *et al.* 2012). Correspondence from the authors prior to publication of this paper had informed us that this was the case for *Xenopus* Greatwall and the same mutagenesis was performed to try to produce a constitutively active human Greatwall kinase (**Figure 4.7 B**). Expression of the triple human Greatwall mutant, S102D, T194E and T207E (STT), did not restore kinase activity. The activity of the mutant remained far below that of WT kinase activity, with only 20% activity in asynchronous cells that increased to only 30% in mitotically arrested cells. The disruption to kinase activity is equivalent to that seen for the individual A mutants and suggests no constitutive activation. It is important to point out that it is possible that Greatwall function has been preserved or increased in this mutant. It has not been possible to test this, although the very low activity seen for the STT mutant Greatwall suggests that this is unlikely.

In addition, S370 was of interest early on in this study. Its possible involvement in Greatwall activation was suggested by phospho-site mapping of Greatwall (**Figure 4.4**). It was thought that this residue could potentially form an important interaction with T194. Both these residues were initially mutated to an A. The results of this are shown in **Figure 4.8 A**. While T194 mutation severely disrupted Greatwall kinase activity, S370 mutation had no effect. It was therefore concluded that this residue was not significant for Greatwall activity.

Another mutant was made in which lysine at position 72 (K72) was mutated to a methionine (M). This K72M mutant (K71M in *Xenopus*) is equivalent to the *Drosophila Scant* mutation (Archambault *et al.* 2007) and was reported to show reduced but

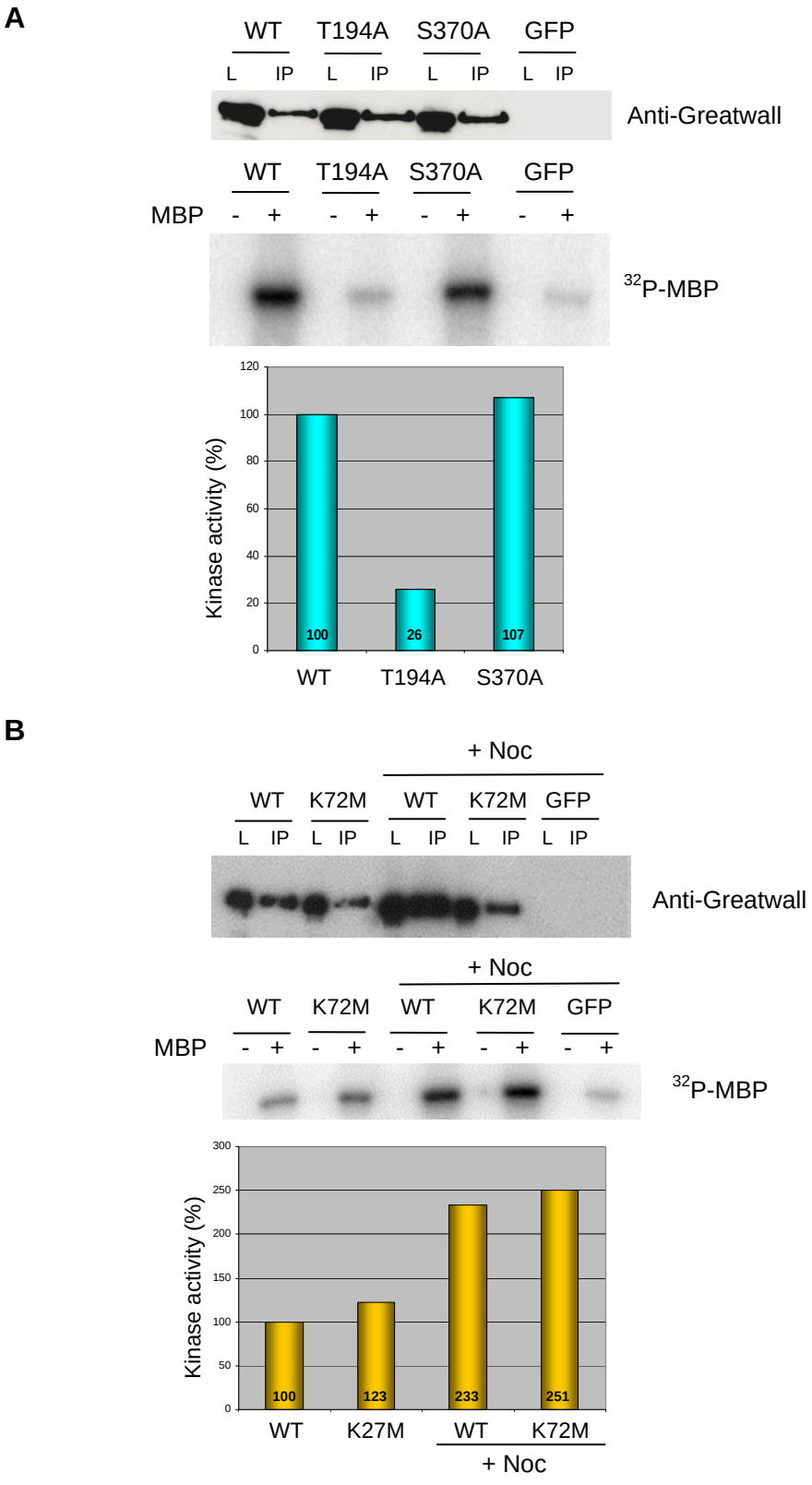

Figure 4.8 Other Greatwall mutants

(A) Flag-tagged Greatwall or non-phosphorylatable mutants T194A and S370A were expressed in HEK 293T cells, immunoprecipitated and taken into a kinase assay as described for **Figure 4.5**. **(B)** Flag-

tagged Greatwall or mutant K72M were expressed in HEK 293T cells, immunoprecipitated and taken into a kinase assay as described for **(A)**. The cells were treated with Nocodazole (+Noc) as indicated.

constitutive gain of activity against Ensa in *Xenopus* (Yamamoto *et al.* 2011). Kinases assays revealed that *Scant* Greatwall but not WT Greatwall showed interphase activity toward Ensa. It was able to promote M phase in oocytes but only with a significant delay, suggesting its low level of activity is limiting. In *Xenopus* only a two-fold increase in activity (at best) was reported and the authors suggested that the increased activity seen in *Drosophila Scant* might have resulted from the cell cycle arrest of the cultured cells leading to a high concentration of protein in the preparation (Yamamoto *et al.* 2011). They reported that the addition of a proteasome inhibitor (MG132) caused increased protein levels and accelerated M phase entry. This suggested that *Scant* Greatwall has partial constitutive activity but with reduced stability. We were interested to see what effects this mutation might have on the activity of human Greatwall. The results of the kinase assay are shown in **Figure 4.8 B**. The K72M mutant appears to have slightly increased activity in both interphase and mitosis (with 123% activity in asynchronous cells and 108% in mitotic cells as compared to that of WT). The functionality of this mutant in human cells has not yet been tested but it seems promising that this might also have increased activity.

4.11 Making a minimal kinase

An obvious question when looking at the structure of Greatwall kinase is what is the function, if any, of the large non-conserved middle region (NCMR) of inserted amino acids? Is it dispensable for kinase activity? In order to address these questions we created two different minimal kinases or artificially spliced variants of Greatwall; artificial splice transcript I (SPI) and artificial splice transcript II (SPII). To determine where the kinase domain boundaries might fall we aligned the kinase domain sequences of other AGC kinases PKC isoforms and MAST1, 2, and 3 kinases with that of Greatwall (**Figure 4.9 A**). Greatwall showed homology and aligned with the kinase domains of PKC and in particular with the α isoform. Based on this we created the artificially spliced variants of Greatwall in which the kinase domain sequence that

A

```
                1                                                  43
     PKCalpha   DFGMCKEHMM D--------- ------GVTT RTFCGTPDYI APE
      PKCbeta   DFGMCKENIW D--------- ------GVTT KTFCGTPDYI APE
     PKCgamma   DFGMCKENVF P--------- ------GTTT RTFCGTPDYI APE
   PKCepsilon   DFGMCKEGIL N--------- ------GVTT TTFCGTPDYI APE
     PKCdelta   DFGMCKENIF G--------- ------ESRA STFCGTPDYI APE
        MAST1   DFGLSKMGLM SLTTNLYEGH IEKDAREFLD KQVCGTPEYI APE
        MAST2   DFGLSKIGLM SLTTNLYEGH IEKDAREFLD KQVCGTPEYI APE
        MAST3   DFGLSKIGLM SMATNLYEGH IEKDAREFID KQVCGTPEYI APE
     Greatwall  DFGLSKVTL- NRDINMMD-- ------ILTT PXILGTPDYL APE
     Consensus  DFG$cKe... .......... ........tt .tfcGTP#Yi APE

                1                                    34
     PKCalpha   DFGMCKE--- ---HMMDGVT TRTFCGTPDY IAPE
      PKCbeta   DFGMCKE--- ---NIWDGVT TKTFCGTPDY IAPE
     PKCgamma   DFGMCKE--- ---NVFPGTT TRTFCGTPDY IAPE
   PKCepsilon   DFGMCKE--- ---GILNGVT TTTFCGTPDY IAPE
     PKCdelta   DFGMCKE--- ---NIFGESR ASTFCGTPDY IAPE
     Greatwall  DFGLSKVTLN RDINMMDILT TPXILGTPDY LAPE
     Consensus  DFG$cKe... ...n..d..t t.tfcGTPDY iAPE

                1                                                  43
        MAST1   DFGLSKMGLM SLTTNLYEGH IEKDAREFLD KQVCGTPEYI APE
        MAST2   DFGLSKIGLM SLTTNLYEGH IEKDAREFLD KQVCGTPEYI APE
        MAST3   DFGLSKIGLM SMATNLYEGH IEKDAREFID KQVCGTPEYI APE
     Greatwall  DFGLSKVTL- NRDINMMD-- ------ILTT PXILGTPDYL APE
     Consensus  DFGLSK.gLm s..tN$y#gh iekdaref.d kq!cGTP#Yi APE

                1                        *|          34
     PKCalpha   DFGMCKE--- ---HMMDGVT TRTFCGTPDY IAPE
     Greatwall  DFGLSKVTLN RDINMMDILT TPXILGTPDY LAPE
     Consensus  DFG$cKe... ...nMMDglT TrticGTPDY iAPE
                           * *
```

B

Greatwall

```
   1 MDPTAGSKKEPGGGAATEEGVNRIAVPKPPSIEEFSIVKPISRGAFGKVY
  51 LGQKGGKLYAVKVVKKADMINKNMTHQVQAERDALALSKSPFIVHLYYSL
 101 QSANNVYLVMEYLIGGDVKSLLHIYGYFDEEMAVKYISEVALALDYLHRH
 151 GIIHRDLKPDNMLISNEGHIKLTDFGLSKVTLNRDINMMDILTTPSMAKP
 201 RQDYSRTPGQVLSLISSLGFNTPIAEKNQDPANILSACLSETSQLSQGLV
 251 CPMSVDQKDTTPYSSKLLKSCLETVASNPGMPVKCLTSNLLQSRKRLATS
 301 SASSQSHTFISSVESECHSSPKWEKDCQESDEALGPTMMSWNAVEKLCAK
 351 SANAIETKGFNKKDLELALSPIHNSSALPTTGRSCVNLAKKCFSGEVSWE
 401 AVELDVNNINMDTDTSQLGFHQSNQWAVDSGGISEEHLGKRSLKRNFELV
 451 DSSPCKKIIQNKKTCVEYKHNEMTNCYTNQNTGLTVEVQDLKLSVHKSQQ
 501 NDCANKENIVNSFTDKQQTPEKLPIPMIAKNLMCELDEDCEKNSKRDYLS
 551 SSFLCSDDDRASKNISMNSDSSFPGISIMESPLESQPLDSDRSIKESSFE
 601 ESNIEDPLIVTPDCQEKTSPKGVENPAVQESNQKMLGPPLEVLKTLASKR
 651 NAVAFRSFNSHINASNNSEPSRMNMTSLDAMDISCAYSGSYPMAITPTQK
 701 RRSCMPHQTPNQIKSGTPYRTPKSVRRGVAPVDDGRILGTPDYLAPELLL
 751 GRAHGPAVDWWALGVCLFEFLTGIPPFNDETPQQVFQNILKRDIPWPEGE
 801 EKLSDNAQSAVEILLTIDDTKRAGMKELKRHPLFSDVDWENLQHQTMPFI
 851 PQPDDETDTSYFEARNTAQHLTVSGFSL
```

Figure 4.9 Making a minimal Greatwall kinase

(A) Alignment of the kinase domains and bridging activation loop sequences from the DFG motif of PKC isoforms and MAST1-3 with that of Greatwall (with the insertion between the N- and C-lobes removed).

C

Greatwall SPI

```
  1 MDPTAGSKKEPGGGAATEEGVNRIAVPKPPSIEEFSIVKPISRGAFGKVY
 51 LGQKGGKLYAVKVVKKADMINKNMTHQVQAERDALALSKSPFIVHLYYSL
101 QSANNVYLVMEYLIGGDVKSLLHIYGYFDEEMAVKYISEVALALDYLHRH
151 GIIHRDLKPDNMLISNEGHIKLTDFGLSKVTLNRDINMMDILTTPTILGT
201 PDYLAPELLLGRAHGPAVDWWALGVCLFEFLTGIPPFNDETPQQVFQNIL
251 KRDIPWPEGEEKLSDNAQSAVEILLTIDDTKRAGMKELKRHPLFSDVDWE
301 NLQHQTMPFIPQPDDETDTSYFEARNTAQHLTVSGFSL
```

Greatwall SPII

```
  1 MDPTAGSKKEPGGGAATEEGVNRIAVPKPPSIEEFSIVKPISRGAFGKVY
 51 LGQKGGKLYAVKVVKKADMINKNMTHQVQAERDALALSKSPFIVHLYYSL
101 QSANNVYLVMEYLIGGDVKSLLHIYGYFDEEMAVKYISEVALALDYLHRH
151 GIIHRDLKPDNMLISNEGHIKLTDFGLSKVTLNRDINMMDILTTPRTFCI
201 LGTPDYLAPELLLGRAHGPAVDWWALGVCLFEFLTGIPPFNDETPQQVFQ
251 NILKRDIPWPEGEEKLSDNAQSAVEILLTIDDTKRAGMKELKRHPLFSDV
301 DWENLQHQTMPFIPQPDDETDTSYFEARNTAQHLTVSGFSL
```

D

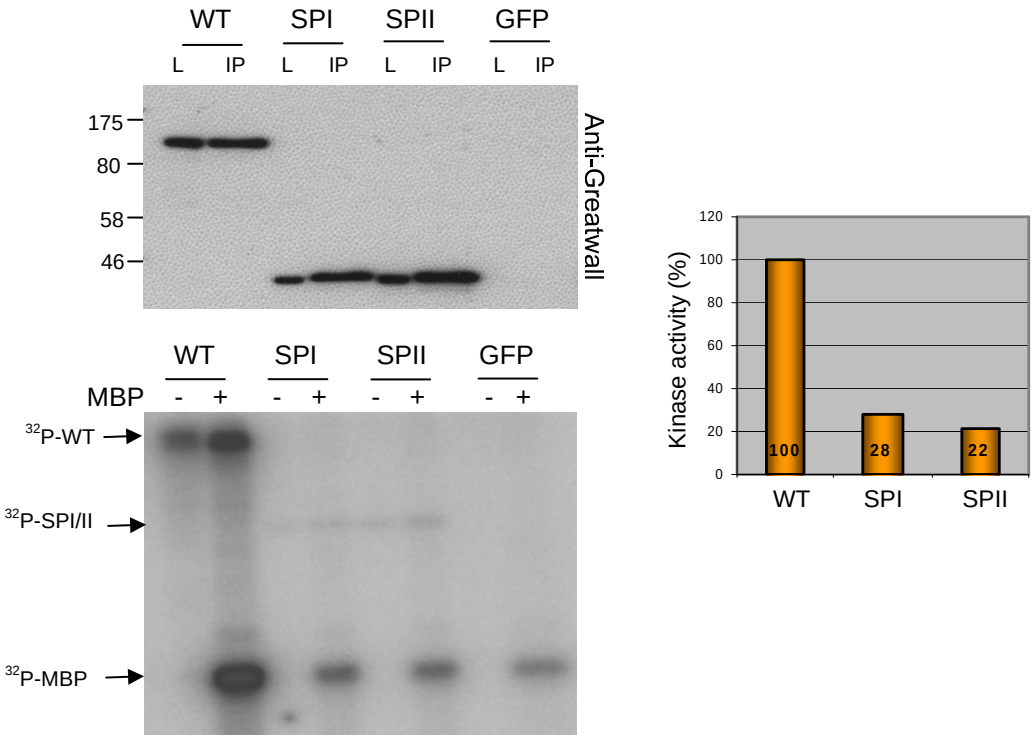

The sequence alignment was created using Multalin version 5.4. The N- and C-lobes of the Greatwall kinase domain are indicated coloured in **Figure 4.2 B**. The alignment of Greatwall with the kinase domain of PKCα is shown in the bottom alignment. **(B)** Mapped Greatwall. The two halves of the kinase domain are shown coloured as in **(A)**. The purple font indicates the NCMR. **(C)** Artificial splice variants of Greatwall. The two different variants, SPI and SPII, are shown. The two halves of the kinase domain are coloured as in **(A)**. The purple font indicates residues introduced between the two halves of the kinase catalytic core. **(D)** Flag-tagged Greatwall or mutants SPI and SPII were expressed in HEK 293T cells, immunoprecipitated and taken into a kinase assay as described for **Figure 4.5**. The phosphorylation of MBP and autophosphorylation of the WT and mutant kinases are indicated by arrows.

aligned with PKCα was preserved with the intervening NCMR removed. These variants contained amino acid residues 1-195 and 737-878 which encompasses the presumptive N- and C-lobes of the kinase domain as well as any important N- or C-terminal extensions (**Figure 4.9 B and C**). Between the two halves of the kinase domain a single T was inserted to form the first variant, SPI. The second variant, SPII, contained the short sequence RTFC between the two halves of the kinase domain making the sequence between the halves equivalent to that of PKCα. These two variants were then expressed with a flag-tag in human cells and immunoprecipitation and subsequent kinase assays performed to assess their activity (**Figure 4.9 D**). Disappointingly they seemed to be relatively inactive, retaining only 28% and 22% of mitotic WT kinase activity for SPI and SPII respectively. We did, however, see some evidence of autophosphorylation of the Greatwall SPI and SPII proteins themselves (**Figure 4.9 D**). This is perhaps surprising in light of the proposed mechanism of Greatwall activation discussed in section **4.9** here. It might suggest that phosphorylation of T194, in the absence of T207 is sufficient to induce autophosphorylation of the C-terminal tail motif and activate Greatwall, even if only weakly. This could mean that these variants are at least partially functionally active. Further investigation is required to establish if these variants have functional activity and this work is currently ongoing.

Two groups that recently mechanistically investigated Greatwall performed similar deletions. Vigneron *et al*. (2011) deleted residues 195-735 (without inserting any bridging sequence) and found the resulting minimal kinase had a 95% decrease in activity as compared to the WT kinase and a complete loss of functionality. A shorter deletion of residues 254-640 produced the same results. However, by performing a series of shorter deletions within this region they established that no specific sequence between residues 254-640 were required for activity. Moreover, the point mutation or deletion of all phospho-residues within the region did not perturb the kinase activity or functionality. Instead they suggest that this might represent a requirement of a minimal length of sequence to allow structural rearrangements required for kinase activity. By deleting various regions of the NCMR in *Xenopus* Greatwall the same conclusion was reached by Blake-Hodek *et al.* (2012). They also found that the *Drosophila* Greatwall NCMR, despite having no sequence homology to that of *Xenopus*, could functionally substitute for the *Xenopus* enzyme in CSF extracts, further supporting the conclusion that its presence is required for kinase functionality but that the NCMR sequence is nonessential.

4.12 Conclusions and discussion

Greatwall is an atypical AGC kinase. The two lobes of its kinase domain are separated by a large insertion of non-conserved amino acids of unknown function. The predicted structural model produced was validated and the activation loop, P+1 loop, and turn motif were identified here. These findings determine that Greatwall conserves many of the basic structural features of other eukaryotic serine/threonine kinases. Although, it appears to be regulated by unique mechanisms that do not conform to those seen for other AGC kinases. The production of a constitutive kinase, however, has not been successful so far.

The use of structural modeling, phosphorylation site mapping and mutagenic analysis has allowed an insight into the mechanisms that regulate human Greatwall. This, in combination with the investigations carried out in two other studies, has led to the emergence of a novel three-step mechanism for its activation (Vigneron *et al.* 2011; Blake-Hodek *et al.* 2012). In this model, Greatwall's activation begins with the priming phosphorylations of its activation loop on two threonines, T194 and T207. It then becomes partially active and autophosphorylates its turn motif in the C-terminal tail, on S874. Finally, this then likely mediates the docking and/or interaction of the hydrophobic motif binding pocket with a phosphorylated hydrophobic motif of another AGC kinase. Once bound the kinase is fully active. This mechanism of activation best suits the data available and represents the culmination of work from all three studies. This surprising mechanism of activation is in keeping with the highly intricate mechanisms that control AGC kinase activities (Pearce *et al.* 2010). These are often aided by specific domains located in associated proteins. Moreover, Greatwall itself has been found to be an unconventional kinase from the start, when it was found not to phosphorylate and initiate mitosis but to counteract a phosphatase that otherwise prevents mitotic entry (Yu *et al.* 2004; Haccard *et al.* 2011). There are still more questions that arise from this model. The identity of the activating kinase that phosphorylates the activation loop and primes Greatwall activation will be discussed in the next chapter. Additionally, the identity of the hydrophobic motif-donating protein that is required for full activity remains unknown, as does the exact mechanism by which this interaction is mediated. It is likely that additional, non-essential phosphorylations elsewhere in the kinase fine tune this mechanism. The NCMR is likely to contribute to this despite the finding that no specific sequences within this region are

absolutely required for kinase activity.

The structural study presented, unfortunately, has several limitations. Primarily, the inability to test the functionality of the mutants *in vivo*. This is being addressed by the establishment of an siRNA resistant form of Greatwall that can subsequently be mutated and used to perform rescue experiments in human cells after Greatwall knockdown. At the time of writing this thesis, this system was still being established and will hopefully answer some of the outstanding questions regarding these mutants functionality in due course. Fortunately, many of the mutants discussed here were also analysed by other groups in *Xenopus* egg extracts (Yu *et al.* 2006; Vigneron *et al.* 2011; Blake-Hodek *et al.* 2012). These were mentioned where relevant and in many cases their reported data lent support to the results I presented here and the conclusions that were drawn. Another limitation is the lack of a true substrate with which to test Greatwall activity. The cellular substrates of Greatwall, Arpp19 and Ensa, were only established relatively late on in this project and it was felt that there was insufficient time remaining to try and express these *in vitro* and go back and repeat each kinase assay. Reassuringly this was addressed by the work of Blake-Hodek *et al.* (2012) who found that there was no difference *in vitro* between Greatwalls ability to phosphorylate Ensa or the MBP. In all cases they found that the levels of phosphorylation seen when either Ensa or MBP were used as a substrate for their kinase assays were the same (Blake-Hodek *et al.* 2012). This suggests that the activity of Greatwall can be reasonably assessed *in vitro* using MBP as a substrate. Although its *in vivo* activity could still differ and the functionality of the enzyme cannot be assumed to correlate with the *in vitro* activity seen. Additionally, in future work, it would also be informative to assess PP2A binding in all the phosphorylation site mutants to gain further insight to how they might be effecting Greatwall regulation and functionality.

Overall, an interesting mechanism for Greatwall activation has been uncovered that warrants further investigation to unravel the complexities of Greatwall *in vivo* activation mechanisms.

CHAPTER 5. Investigating Greatwall activation

5.1 Introduction

The mechanisms of Greatwall activity still remain to be fully elucidated and will likely require structural insight. Moreover, the precise dynamics of Greatwall activation and inactivation as well as characterisation of the upstream kinases and phosphatases that regulate this kinase also remain enigmatic. The work presented in this chapter focuses on gaining deeper understanding of this aspect of Greatwall regulation.

There is strong evidence from the studies carried out in frog egg extracts that *Xenopus* Greatwall is activated by MPF in mitosis. The MPF (the cyclin B-CDK1 complex) is an obvious candidate for the upstream activating kinase of Greatwall. Once MPF becomes active at the end of G2 it is known to phosphorylate and activate kinases (Wee1) and phosphatases (Cdc25) that then in turn propagate its own activation and mediate changes to promote mitotic entry. Conceivably, CDK1 also acts upstream of Greatwall, integrating it in the general MPF activation feedback loop (**Figure 5.1 A**). In this way, activation of Greatwall by MPF phosphorylation would then mediate inhibition of PP2A, via phosphorylation of Arpp19/Ensa, allowing CDK phosphorylations to persist promoting further activation of MPF and mitotic entry. It has been shown that Greatwall becomes hyperphosphorylated and active at the same point in the cell cycle at which the MPF becomes active, at the G2/M transition. It then remains active in mitosis until mitotic exit, also the time in which MPF becomes inactive (Zhao *et al.* 2008). Thus, the cyclic rise and fall of Greatwall activation follows closely with that of MPF and corresponds inversely to that of PP2A activity (Mochida *et al.* 2009). The addition of purified MPF to Greatwall immunoprecipitated from interphase egg extracts leads to phosphorylation of Greatwall. Moreover, when recombinant Greatwall was pre-treated with MPF it exhibited autophosphorylation and phosphorylated MBP *in vitro*. The addition of the MPF pre-treated Greatwall into Greatwall depleted CSF extracts rescued the loss of M phase while a non-treated (unphosphorylated) or kinase dead Greatwall could not (Yu *et al.* 2006).

Greatwall has numerous potential CDK phosphorylated sites (S/TP). Yu *et al.* (2006) found that mass spectral analysis of *Xenopus* Greatwall revealed seven sites phosphorylated in recombinant Greatwall that had been treated with MPF, and five of

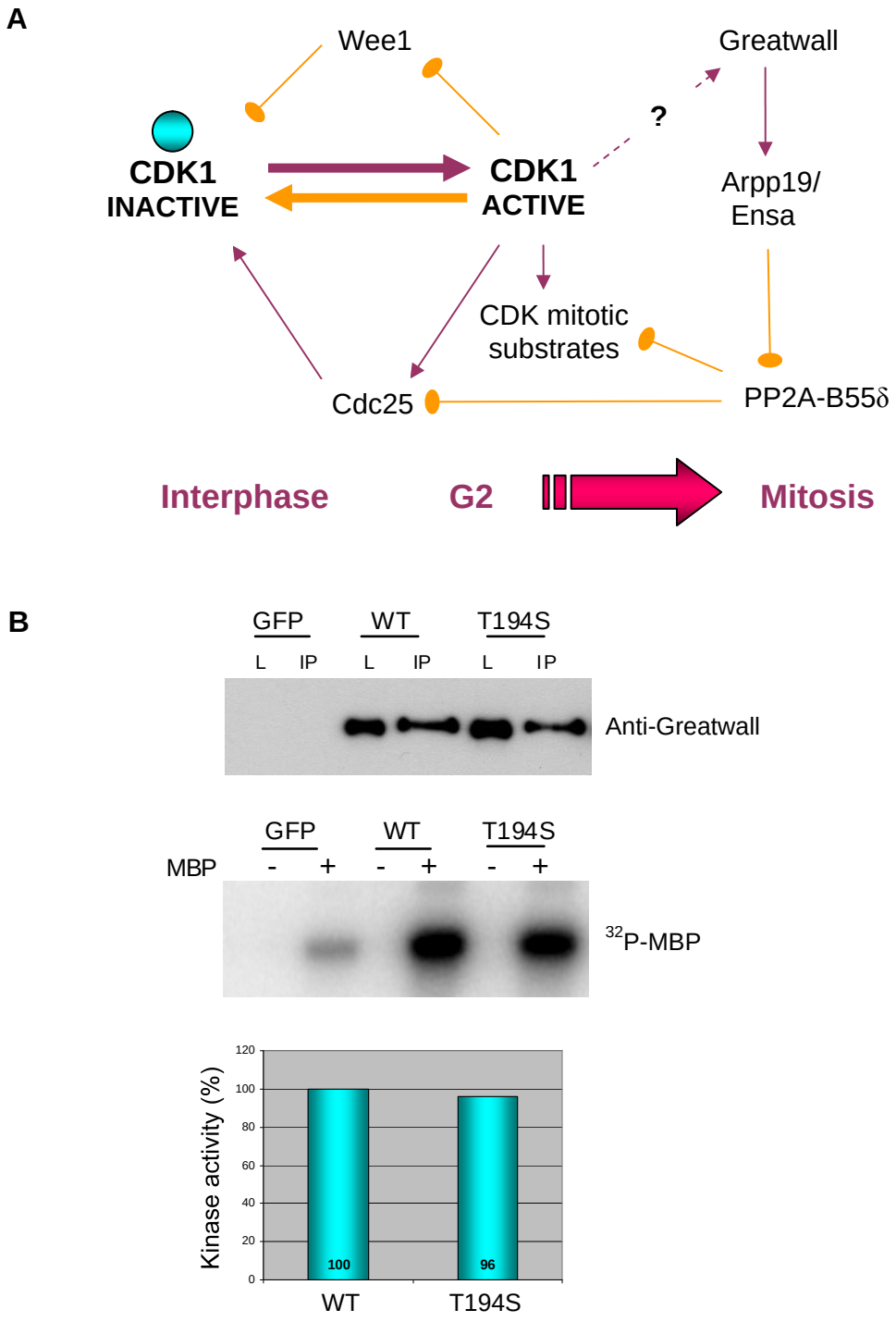

Figure 5.1 Is human Greatwall activated by CDK1?

(A) Schematic representation of the Greatwall pathway. Once Greatwall is active in late G2 it then phosphorylates its targets, Ensa and/or Arpp19, inactivating PP2A-B55δ. This allows CDK1 mitotic phosphorylations to accumulate on targets, including Cdc25, and activation of the CDK positive feedback loop to drive cells into mitosis. Activating modifications are shown as purple arrows and all inhibitory modifications are shown in orange. The potential activation of human Greatwall by CDK1 is indicated by a question mark and dashed arrow. **(B)** Flag-tagged WT Greatwall (WT) or phosphorylatable mutant T194S (T194S) were expressed in human HEK 293T cells. Cells transfected with a GFP control were analysed as

well. After 24 hours the cells were treated with Nocodazole. The flag-tagged proteins were then immunoprecipitated using anti-flag magnetic beads. An *in vitro* kinase assay was then performed using MBP as a substrate for the kinase. The top panel shows the results of SDS-PAGE analysis indicating the expression of the flag-tagged protein in the cell lysates (L) and the immunoprecipitate (IP) detected using the anti-Greatwall antibody. The autoradiograph is shown in the second panel. Quantification of the kinase activity of the mutant kinase relative to the wildtype is shown in the graph beneath.

these were conserved. Sequential mutation of these five residues (from a serine or threonine to alanine) revealed only one mutation, T748A that was unable to rescue the CSF extracts to M phase. This is not that surprising in light of later studies, discussed in **Chapter 4**, as the other residues they identified were all in the NCMR. They did not investigate this residue further but concluded that there is likely at least one CDK1 phosphorylation site in Greatwall that is important for its activation. Additionally, Blake-Hodek *et al.* (2012) found that one or more phospho-sites of M phase Greatwall were epitopes recognised by the Mitotic Protein Monoclonal 2 (MPM-2) antibody that reacts with mitotic phospho-proteins phosphorylated on serine or threonine residues followed by a proline. As mentioned, these sites are often phosphorylated by CDKs (Wu *et al.* 2010). Further proof that Greatwall activation in *Xenopus* might depend on the prior activation and subsequent phosphorylation by MPF came from a later report by Zhao *et al.* (2008). They found that microinjection of CDK inhibitor, p21, into oocytes or treatment of cycling extracts with the CDK inhibitor Roscovitine prevented Greatwall phosphorylation. This leads to the conclusion that MPF is an important activator of *Xenopus* Greatwall.

There is also data that supports the activation of human Greatwall by cyclin B-CDK1. Human Greatwall localises to centrosomes during G2 where cyclin B-CDK1 is also first activated (Burgess *et al.* 2010). There are 18 potential CDK phospho-sites (T/SP) in human Greatwall, although the majority of these (all but five) lie inside the NCMR (**Appendix C**). Human Greatwall is also maximally active only in mitosis, as reported here and by Voets *et al.* (2010). This group observed a mitotic mobility shift that was concomitant with the phosphorylation of APC/C subunit APC3, was diminished by treatment with λ phosphatase and was enhanced by treatment with okadaic acid. Correspondingly, they found that the addition of okadaic acid at any other stage of the cell cycle did not elicit this mobility shift. This suggests that Greatwall is subject to an activating phosphorylation event in mitosis similar to that seen for *Xenopus* Greatwall. Moreover, CDK inhibition (using Flavopiridol), but not Aurora B

inhibition (using AZD1152), reverted Greatwall phosphorylation in cells released from a Nocodazole arrest but held in mitosis by MG132-mediated proteasome inhibition. Thus, suggesting that mitotic phosphorylation of Greatwall requires CDK activity (Voets *et al.* 2010).

Despite this body of evidence, the precise activating residues that are phosphorylated by CDK1 have not yet been identified and the dynamics of Greatwall activation at the G2/M transition have yet to be established. Additionally, the inactivating phosphatase(s) that act on Greatwall and its substrates, and on CDK substrates in general, at mitotic exit have still to be determined. Without a clear understanding of these pathways, that play critical roles in cell cycle progression, an adequate model of cell cycle control cannot be compiled. Throughout this chapter these questions will be addressed.

5.2 Creating a phospho-specific antibody to monitor Greatwall kinase activation

The threonine at position 194 (T194) was identified in **Chapter 4** as a key phosphorylated site required for human Greatwall activation. To confirm this as a phosphorylation event that allows Greatwall activity, this residue was mutated to another phosphorylatable residue, a serine. Its mutation to a serine should allow this site to still be phosphorylated and propagate Greatwall activation. The results are shown in **Figure 5.1 B**. The mutant T194S was clearly still a functional kinase and displayed full activity (96%) in mitotic cells as compared to WT Greatwall. This finding supports the importance of phosphorylation of this residue for Greatwall activation.

A phospho-specific antibody was generated in rabbit by Eurogentec to target this phosphorylation site in human Greatwall using the peptide sequence CMMDILTT(PO_3H_2)PSMAK. The purified antibody sera was tested using human HEK 293T cell lysates produced from cells that were transiently overexpressing a flag-tagged WT Greatwall and the nonphosphorylatable T194A Greatwall mutant (**Figure 5.2 A**). The phospho-specific anti-pT194 Greatwall antibody detected the presence of T194 phosphorylated Greatwall in Nocodazole arrested mitotic cells lysates and immunoprecipitate. Despite the clear presence of the T194A mutant Greatwall in the mitotic cell lysates and immunoprecipitate (detected using the total anti-Greatwall antibody), none was detected by the phospho-specific anti-pT194 Greatwall antibody. It

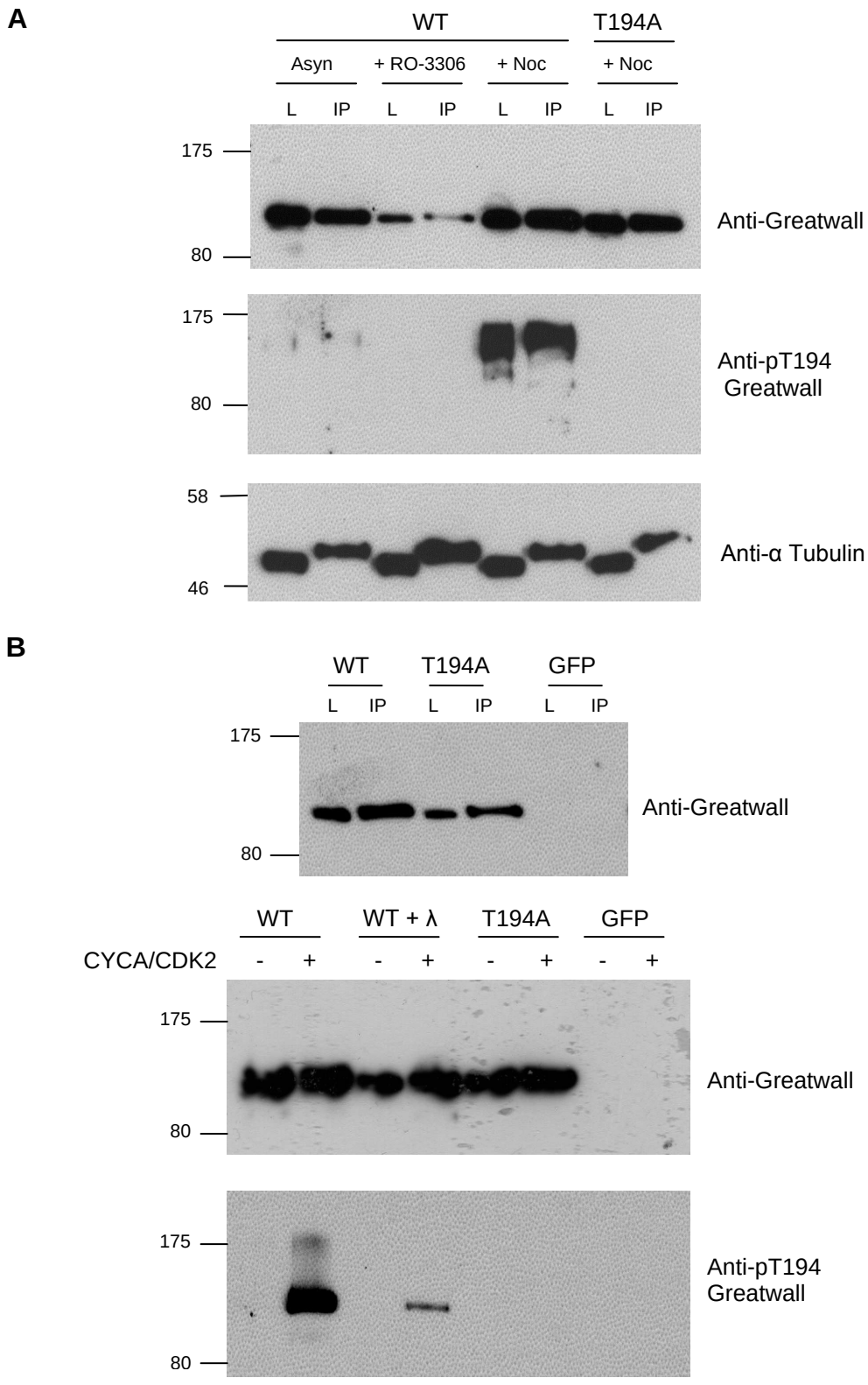

Figure 5.2 Investigating Greatwall activation by CDK in human cells

(A) Immunoprecipitation of flag-tagged WT Greatwall or the non-phosphorylatable mutant Greatwall T194A from HEK 293T cells. Cells were untreated (Asyn) or treated with RO-3306 (+RO-3306) or

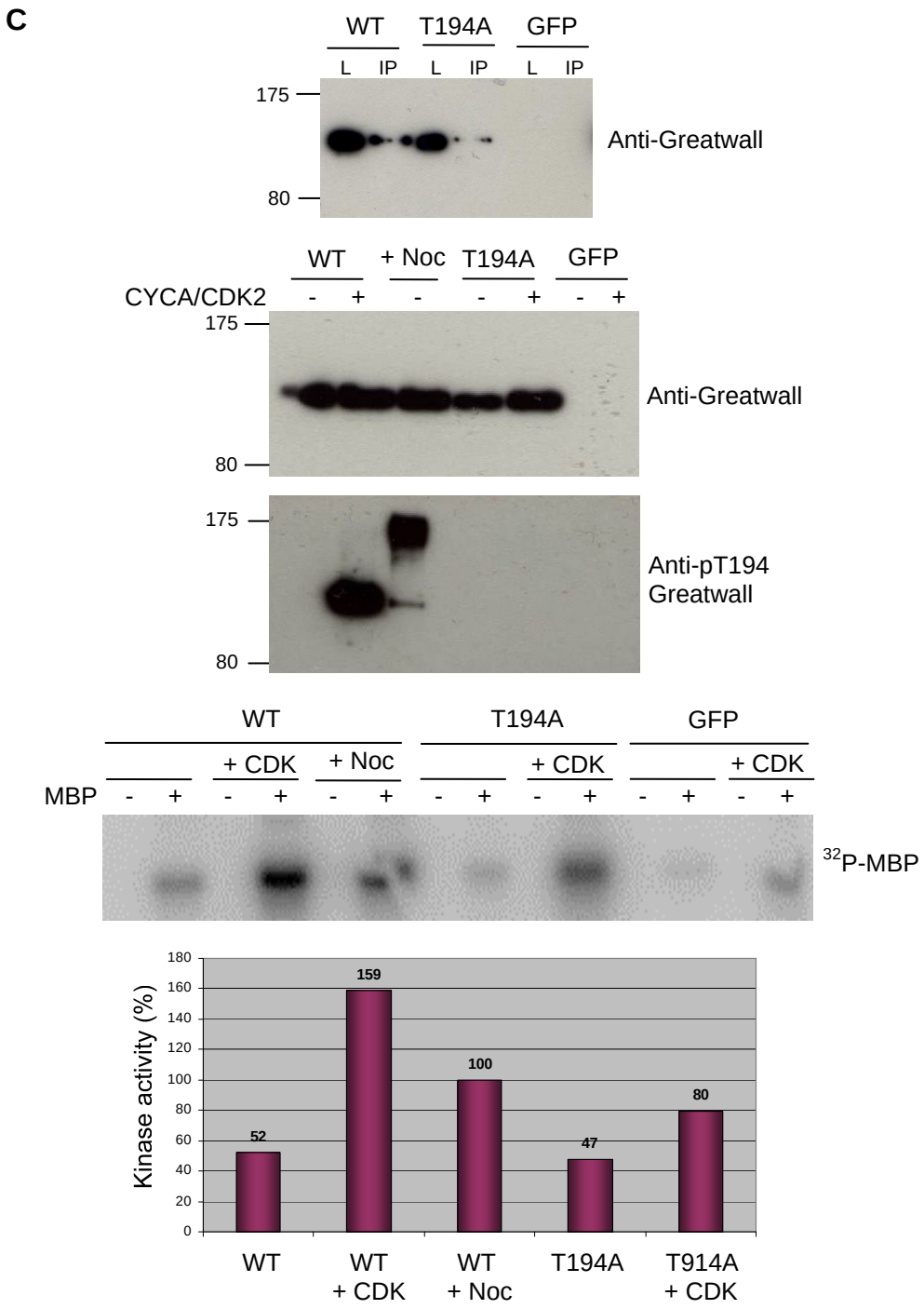

Nocodazole (+ Noc). The top panel shows the results of SDS-PAGE analysis indicating the expression of the flag-tagged protein in the cell lysates (L) and the immunoprecipitate (IP) detected using the anti-Greatwall antibody to probe for total human Greatwall protein levels (top panel) and the anti-pT194 antibody was used to probe for the presence of Greatwall phosphorylated on T194 (middle panel) in these different conditions, while an anti-α Tubulin antibody (bottom panel) was used as a loading control. **(B)** Kinase assay of flag-tagged WT Greatwall (WT) or the non-phosphorylatable mutant Greatwall T194A (T194A) from HEK 293T cells. Cells transfected with a GFP control (GFP) were analysed as well. The *in vitro* kinase assay was performed using recombinant cyclin A-CDK2 (CYCA/CDK2) in which the immunoprecipitated Greatwall was the substrate. A sample of cyclin A-CDK2-treated WT Greatwall was

then subsequently treated with λ phosphatase (+ λ). The top panel shows the results of SDS-PAGE analysis indicating the expression of the flag-tagged protein in the cell lysates (L) and the immunoprecipitate (IP) detected using the anti-Greatwall antibody to probe for total human Greatwall protein levels. The *in vitro* kinase assays were also analysed by SDS-PAGE analysis using the anti-Greatwall antibody to probe for total human Greatwall protein levels (middle panel) and the anti-pT194 antibody to probe for the presence of Greatwall phosphorylated on T194 (bottom panel). **(C)** Flag-tagged WT Greatwall (WT) or the non-phosphorylatable mutant Greatwall T194A (T194A) were expressed in HEK 293T cells. Cells transfected with a GFP control (GFP) were analysed as well. Cells were treated with Nocodazole (+ Noc) and the flag-tagged proteins then immunoprecipitated. These were then taken into an *in vitro* kinase assay with recombinant cyclin A-CDK2 (CYCA/CDK2) using the immunoprecipitated Greatwall as a substrate. All samples were then washed to remove cyclin A-CDK2 and taken into an *in vitro* kinase assay with MBP as a substrate for Greatwall. The top panel shows the results of SDS-PAGE analysis indicating the expression of the flag-tagged protein in the cell lysates (L) and the immunoprecipitate (IP) detected using the anti-Greatwall antibody to probe for total human Greatwall protein levels (top panel). The cyclin A-CDK2 *in vitro* kinase assays were analysed by SDS-PAGE analysis using the anti-Greatwall antibody to probe for total human Greatwall protein levels (second panel) and the anti-pT194 antibody to probe for the presence of Greatwall phosphorylated on T194 (third panel). Finally the autoradiograph from the *in vitro* kinase assays using MBP as a substrate for Greatwall is shown in the bottom panel with or without pre-treatment with cyclin A-CDK2 (+ CDK). Quantification of the kinase activities from the autoradiograph is shown relative to the untreated WT Greatwall kinase activity in the graph beneath.

can be concluded that in this mutant the site could not be phosphorylated and was therefore not detected. This indicates that the anti-pT194 Greatwall antibody generated is highly specific for the phosphorylation of this residue in human Greatwall. Furthermore, this site is phosphorylated when Greatwall is known to be active in mitosis.

5.3 Confirmation of CDK as an activator of Greatwall kinase

T194 is found in a CDK phosphorylation consensus motif (T/SP). Its potential as a proline-directed CDK phospho-site was supported by the lack of signal detected by the anti-pT194 Greatwall antibody from WT Greatwall in HEK 293T cells that had been treated with the CDK1 inhibitor, RO-3306 (**Figure 5.2 A**). Although, once again, the levels of the Greatwall protein expressed in the presence of this inhibitor appeared

lower than for the other lysates. This was the case despite the tubulin loading control indicating that total protein levels in all lysates were equal.

To test if human Greatwall can be phosphorylated *in vitro* on T194 by CDK, WT and T194A mutant Greatwall were purified from asynchronous HEK 293T cells and incubated with recombinant cyclin A-CDK2. The results are shown in **Figure 5.2 B**. WT Greatwall that was not incubated with cyclin A-CDK2 shows no phosphorylation of T194 while Greatwall incubated with cyclin A-CDK2 is clearly phosphorylated at this site. Moreover, the signal seen from WT Greatwall incubated with cyclin A-CDK2 is severely diminished after treatment with λ phosphatase. This indicates that the signal seen from the anti-pT194 Greatwall antibody is a result of phosphorylation of this site in Greatwall by cyclin A-CDK2. This conclusion is further supported by the lack of any detectable signal seen from the incubation of the mutant T194A Greatwall with cyclin A-CDK2. However, only a small proportion of the phosphorylated WT Greatwall is shifted up in the gel after incubation with cyclin A-CDK2. This suggests that phosphorylation of Greatwall by cyclin A-CDK2 does not trigger phosphorylation of the kinase to mediate the modifications of the protein to the extent noted for Greatwall from mitotic extracts. Therefore, CDK phosphorylation of Greatwall might not fully activate Greatwall or other phosphorylations/PTMs might occur to correctly activate and localise it allowing it to promote proper mitotic entry.

To address if the phosphorylation of Greatwall by cyclin A-CDK2 on T194 can activate Greatwall, immunoprecipitated WT and T194A Greatwall were incubated with or without cyclin A-CDK2. The beads were then washed to remove the cyclin A-CDK2 (if present) and the CDK pre-treated (or not) Greatwall was then incubated in a kinase assay with MBP (**Figure 5.2 C**). The incubation of Greatwall with cyclin A-CDK2 activated the kinase, as judged by the phosphorylation of MBP. The high level of Greatwall kinase activity produced after incubation with cyclin A-CDK2 exceeded that of the WT Greatwall immunoprecipitated from Nocodazole-arrested mitotic cells, with 159% kinase activity comparatively. This large increase in kinase activity is likely a result of incomplete removal of the cyclin A-CDK2 from the sample. This is probable as the phosphorylation of MBP was also increased in the negative GFP control sample after cyclin A-CDK2 incubation. However, the increases in the controls are relatively minor and it is conceivable that CDK is sufficient to fully activate Greatwall *in vitro* to levels comparable to, or even exceeding, those of Greatwall purified from mitotic cells. These assays will have to be repeated in the presence of a CDK inhibitor, such as the

Roscovitine, to rule out contamination of CDK activity in the observed MBP phosphorylation.

The significance of the activity of the CDK pre-treated T194A mutant may also be a result of incomplete removal of cyclin A-CDK2. If this result were shown to be robust however, it might suggest that upon incubation with cyclin A-CDK2 phosphorylations elsewhere in the kinase are sufficient to render it partially active, at least *in vitro*. This is possible given that *Xenopus* Greatwall can be phosphorylated on its T-loop at two predicted CDK phospho-sites, T194 and T207 (Blake-Hodek *et al.* 2012). As discussed in **Chapter 4** in section **4.11** it is possible that a minimal Greatwall kinase lacking the T-loop phosphorylation site, T207, has some activity. This might mean that only one of these sites need be phosphorylated for partial kinase activity, at least *in vitro*. Further experiments with additional mutants and CDK inhibitors added to the reaction should serve to clarify these points.

These results clearly demonstrate that cyclin A-CDK2 can phosphorylate T194 in human Greatwall *in vitro*. It is relatively well established that *in vitro* all CDKs will phosphorylate target sites and exhibit similar substrate specificity (Hochegger *et al.* 2008). Moreover, when interphase recombinant *Xenopus* Greatwall was treated with MPF, cyclin A-CDK2 or cyclin E-CDK2 they were all equally efficient at activating Greatwall (Blake-Hodek *et al.* 2012). But which CDK activates human Greatwall *in vivo*? The fact that T194 is not phosphorylated in RO-3306-treated G2 arrested cells suggests that this site is a true mitotic CDK1 target. At the concentration (10 μM) used here, RO-3306 does not inhibit CDK2 and blocks cells at the end of G2 phase just prior to CDK1 activation (Vassilev *et al.* 2006). This observation is in agreement with work from other studies in *Xenopus* (Yu *et al.* 2006; Zhao *et al.* 2008) and allows the conclusion that human Greatwall is phosphorylated at the G2/M transition by CDK1 on T194.

5.4 Investigating Greatwall activation by CDK phosphorylation of T194 *in vivo*

The dynamics of Greatwall activation throughout the cell cycle in human cells was assessed using synchronised HeLa cells. These were synchronised by a double Thymidine block and then released and subsequently followed through their cell cycle for 12 hours. During this time, samples were taken every hour and analysed for

Greatwall levels by immunoblotting using the total anti-Greatwall antibody and the anti-pT194 Greatwall antibody (**Figure 5.3 A**). Greatwall expression remained relatively constant throughout the cell cycle as previously observed. However, Greatwall phosphorylation on T194, and thus its activation, fluctuated. No signal (activation) was seen in the cells until mitotic entry, as judged by the corresponding FACS analysis, at which point it peaked and remained high until the cell population began to return to G1 phase after mitotic exit when it decreased again. This pattern of Greatwall activation agrees with the reports from other studies and coincides with cyclin B-CDK1 activity, suggesting that Greatwall is activated by cyclin B-CDK1 phosphorylation at the G2/M transition. In addition, an unexpected peak of Greatwall activity was detected at the two hour time point once the cells had been released. This might correspond to a serge of Greatwall activity to restart the cell cycle in a similar manner as described after DNA damage (see **Chapter 1**, section **1.11**) (Peng *et al.* 2010; Peng *et al.* 2011) or hint at an as yet unknown function for Greatwall in S phase. This potentially interesting result falls outside the scope of this thesis but warrants further investigation to clarify.

Greatwall activation at different stages throughout the cell cycle was also assessed by immunoblotting in human HeLa, HCT116, HEK 293T and RPE cells (**Figure 5.3 B**). Lysates of asynchronous cells, S phase cells arrested using Thymidine, G2 phase cells arrested using RO-3306, and mitotic cells arrested using Nocodazole were analysed. RPE cells were not assessed in S phase as they do not exhibit a Thymidine-mediated cell cycle arrest, as previously discussed. For all cell lines Greatwall is not phosphorylated on T194 in the asynchronous cells or in the cells arrested in S phase. This supports the idea that Greatwall activity is required to restart the cell cycle after the Thymidine block is removed, rather than it being active in S phase blocked cells. Cells treated with RO-3306 all show apparently reduced expression of Greatwall, in keeping with results obtained previously. Greatwall activation by T194 phosphorylation in the RO-3306 arrested cells is not detected. A small amount of Greatwall is detected in the HEK 293T cells and is likely a result of slippage into mitosis during the G2 arrest in these cells. A strong signal is detected in all mitotic lysates and confirms that Greatwall is phosphorylated and active in these cells in mitosis. The strong signal of T194-phosphorylated Greatwall seen in the mitotic cells indicates that Greatwall is present despite it not being detected, or being detected only poorly, by the total anti-Greatwall antibody. This further supports the hypothesis that the activating phosphorylations/PTMs modifications of Greatwall in mitosis serve to

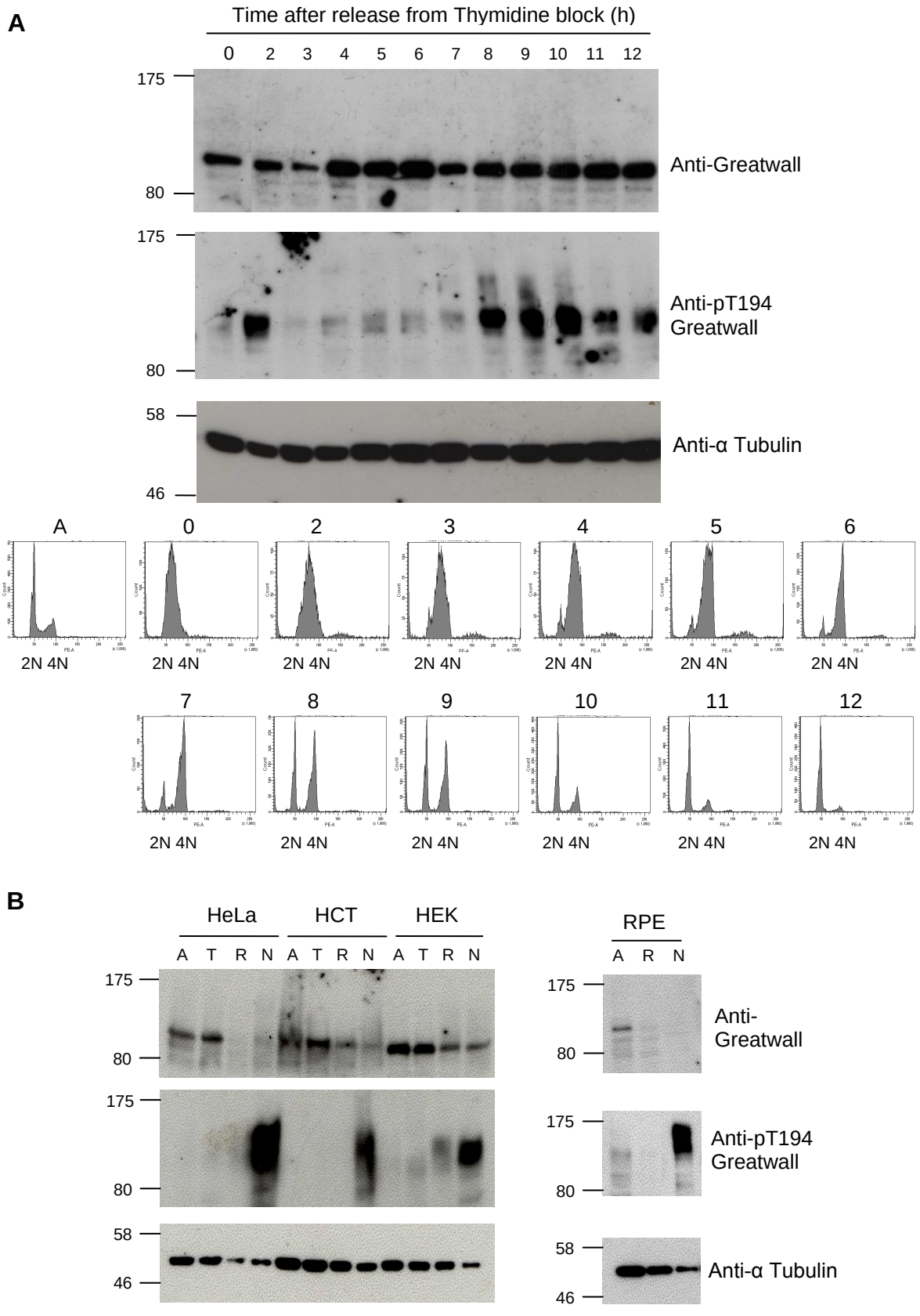

Figure 5.3 Investigating Greatwall activation by CDK *in vivo* in human cells

(A) SDS-PAGE analysis of HeLa cells synchronised by double Thymidine block and then released for 12

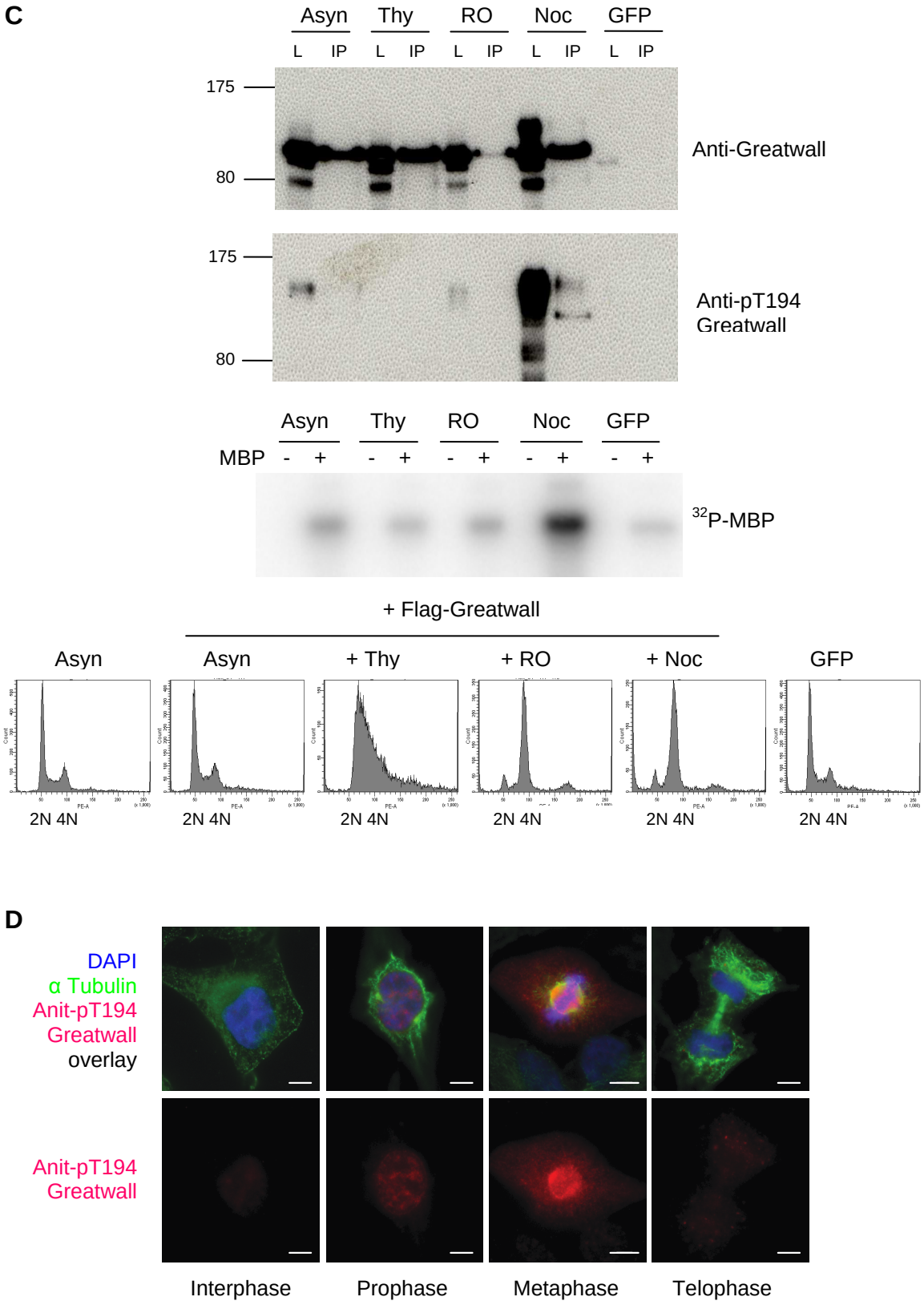

hours. Samples were taken every hour for a 12 hour period and analysed using the anti-Greatwall antibody to probe for total human Greatwall protein levels (top panel) and the anti-pT194 antibody to probe for the presence of Greatwall phosphorylated on T194 (middle panel). An anti-α Tubulin antibody (bottom panel) was used as a loading control. The cell cycle (FACS/PI) profiles for all the cell lysates are

shown beneath. Asynchronous (A) cell lysates were analysed as well for comparison. **(B)** SDS-PAGE analysis of HeLa, HEK 293T, HCT116 and RPE cell lysates from asynchronous (A) cells or cells that had been treated with Thymidine (T), RO-3306 (R), or Nocodazole (N). The anti-Greatwall antibody was used to probe for total human Greatwall protein levels (top panel) and the anti-pT194 antibody was used to probe for the presence of Greatwall phosphorylated on T194 (middle panel) in these different conditions, while an anti-α Tubulin antibody (bottom panel) was used as a loading control. **(C)** Flag-tagged WT Greatwall was expressed and immunoprecipitated from HEK 293T asynchronous (Asyn) cells or cells that had been treated with Thymidine (Thy), RO-3306 (RO) or Nocodazole (Noc). Asynchronous cell lysates transfected with GFP (GFP) were analysed as well for comparison. The top panel shows the immunoblot indicating the expression of the flag-tagged protein from the cell lysates (L) or the immunoprecipitate (IP) detected using the anti-Greatwall antibody. The middle panel shows the presence of Greatwall phosphorylated on T194 in these different conditions probed using the anti-pT194 antibody. *In vitro* kinase assays were performed using MBP as a substrate for the kinase. The autoradiograph is shown in the bottom panel. The cell cycle (FACS/PI) profiles for all the cell lysates are shown below. **(D)** Representative images of HeLa cells stained for T194 phosphorylated Greatwall in interphase and in different stages of mitosis. Fixed cells from an asynchronous population HeLa cells were stained with the anti-pT194 Greatwall antibody (cherry), an anti-α Tubulin antibody (green) and DAPI (blue). The maximum projection from 0.3μm Z-sections are shown with scale bars of 10 μm.

mask the protein from detection by the total anti-Greatwall antibody. Therefore, Greatwall levels are not decreased in mitosis but the presence of activating PTMs prevent its detection and the anti-pT194 Greatwall antibody indicates that high levels of active Greatwall are present in all cell lines in mitosis.

These findings are supported by results shown in **Figure 5.3 C**. Transient overexpression of flag-tagged Greatwall in human HEK 293T cells was used to analyse of the activity of Greatwall in different cell cycle phases. Some phosphorylated Greatwall was detected in the asynchronous cells, none was detected in S phase cells, a small amount was detected in the RO-3306 treated cells likely due to mitotic slippage, and a strong signal was detected in the mitotically arrested cells. The analysis of Greatwall activity in these cell cycle phases was also assessed using *in vitro* kinase assays. The results confirm the immunoblot analysis and indicate that in S phase Greatwall is not active while in the mitotic cells Greatwall had high activity. This further validates a model in which Greatwall is activated by CDK1 at mitosis. It is again difficult to conclude about Greatwall activity in late G2 because it is detected by the total anti-Greatwall antibody only at much reduced levels despite careful equalisation of total protein levels in the lysates.

Immunofluorescent staining using the anti-pT194 Greatwall antibody (**Figure 5.3 D**) revealed very little signal in interphase cells. G2 cells with separated centrosomes showed weak nuclear staining. At the end of G2 and in early prophase active Greatwall accumulated in the nucleus. It then moved to the spindle and emanated across the spindle microtubules and was concentrated at the poles. This signal peaked in metaphase and the progressively diminished until in telophase it had returned to background levels and was considered extinguished.

5.5 Investigating mitotic exit and Greatwall inactivation

Once active in mitosis, another key question regarding Greatwall regulation is how it is inactivated during mitotic exit? The current understanding of phosphatase regulation and activity during mitotic exit is relatively rudimentary. A recent study in *Drosophila* using siRNA screening found that ~ 20% of all phosphatases are required for proper cell cycle progression and/or mitosis (Chen *et al.* 2007). As entry into mitosis depends on the phosphorylation of numerous cyclin B-CDK1 substrates, to allow subsequent mitotic exit, these mitotic phospho-proteins must be dephosphorylated or degraded by the activity of phosphatases to return them to their interphase dephosphorylated forms (Wurzenberger *et al.* 2011). Consistent with this, persistent CDK activity prevents mitotic exit and CDK substrate dephosphorylation is considered a hallmark of mitotic exit (Queralt *et al.* 2008). The results of studies in *Xenopus* have been conflicting as to which phosphatase is the dominant CDK-antagonising phosphatase at mitotic exit. In *Xenopus*, PP2A complexed with the B55δ isoform was shown to prevent mitotic exit when depleted from cycling egg extracts but both PP1 and PP2A have been implicated in facilitating mitotic exit via the removal of these mitotic phosphorylations (Forester *et al.* 2007; Mochida *et al.* 2009; Wu *et al.* 2009). The precise mechanisms controlling mitotic exit are far from clear at present.

A recent study in Cdc20 null primary mouse embryonic fibroblasts found that Greatwall must be inactivated to promote cyclin B-CDK1 substrate dephosphorylation and mitotic exit (induced via CDK1 inhibition) (Manchado *et al.* 2010). They also determined that mitotic exit in these cells was mediated by activation of PP2A complexed with B55α and δ isoforms specifically, while siRNA depletion of the B55β isoform did not affect mitotic exit. However, the identity of the inactivating phosphatase

of Greatwall in human cells is still unknown.

In order to examine mitotic exit mechanisms in human cells, HeLa cells were arrested in mitosis using the Eg5 inhibitor, S-trityl-L-cysteine (STLC). A mitotic shake off was then performed and the mitotic cells incubated for 30 minutes with the CDK1 inhibitor, RO-3306, in the presence of STLC to induce mitotic exit. Samples were then taken at 0, 5, 10, 20 and 30 minutes after RO-3306 addition and analysed for their general CDK substrate phosphorylation state using immunoblotting and an antibody directed against phosphorylated serines of the CDK consensus motif. The results seen in **Figure 5.4 A**, show a strong signal, corresponding to phosphorylated CDK substrates, was present in the STLC-treated extracts before RO-3306 addition. This indicates that they were arrested in mitosis with high CDK activity. This signal decreased markedly following the addition of RO-3306 and was almost completely diminished after 30 minutes incubation with the CDK1 inhibitor. Thus, once CDK1 is inhibited, mitotic phosphatases rapidly dominate and dephosphorylate its substrates. These samples were also analysed for Greatwall levels and the presence of T194-phosphorylated Greatwall. Concurrent with the induction of mitotic exit Greatwall becomes rapidly dephosphorylated. The phosphorylation of T194 is diminished after only 5 minutes and is totally absent after 20 minutes of RO-3306 treatment. The protein itself is seen to shift down in the gel at each increasing time point as its mitotic modifications that retard its electrophoretic mobility are lost. The total protein levels of Greatwall do not appear to decrease suggesting that in these conditions it is not degraded, merely inactivated, as judged by the loss of the phosphorylation of T194 in its T-loop that is required for its kinase activity.

A key aspect of understanding Greatwall regulation is determination of the phosphatase(s) responsible for removing its mitotic activating phosphorylations during mitotic exit. Manchado *et al.* (2010) proposed that mitotic exit in mammalian cells required Greatwall inhibition and the activation of PP2A. They also found that the siRNA-mediated depletion of the PP1 inhibitor, Inhibitor 1, and resulting PP1 activation led to partial exit from mitosis when CDK activity was inhibited by Roscovitine. They suggested that PP1 could potentially have a role upstream of PP2A in inactivating Greatwall. This indicates a potential role for both PP1 and PP2A in promoting exit from mitosis as has been previously suggested in *Xenopus* (Mochida *et al.* 2009; Wu *et al.* 2009), although the precise mechanisms involved are still to be elucidated.

In order to address this, two phosphatase inhibitors were used: okadaic acid and

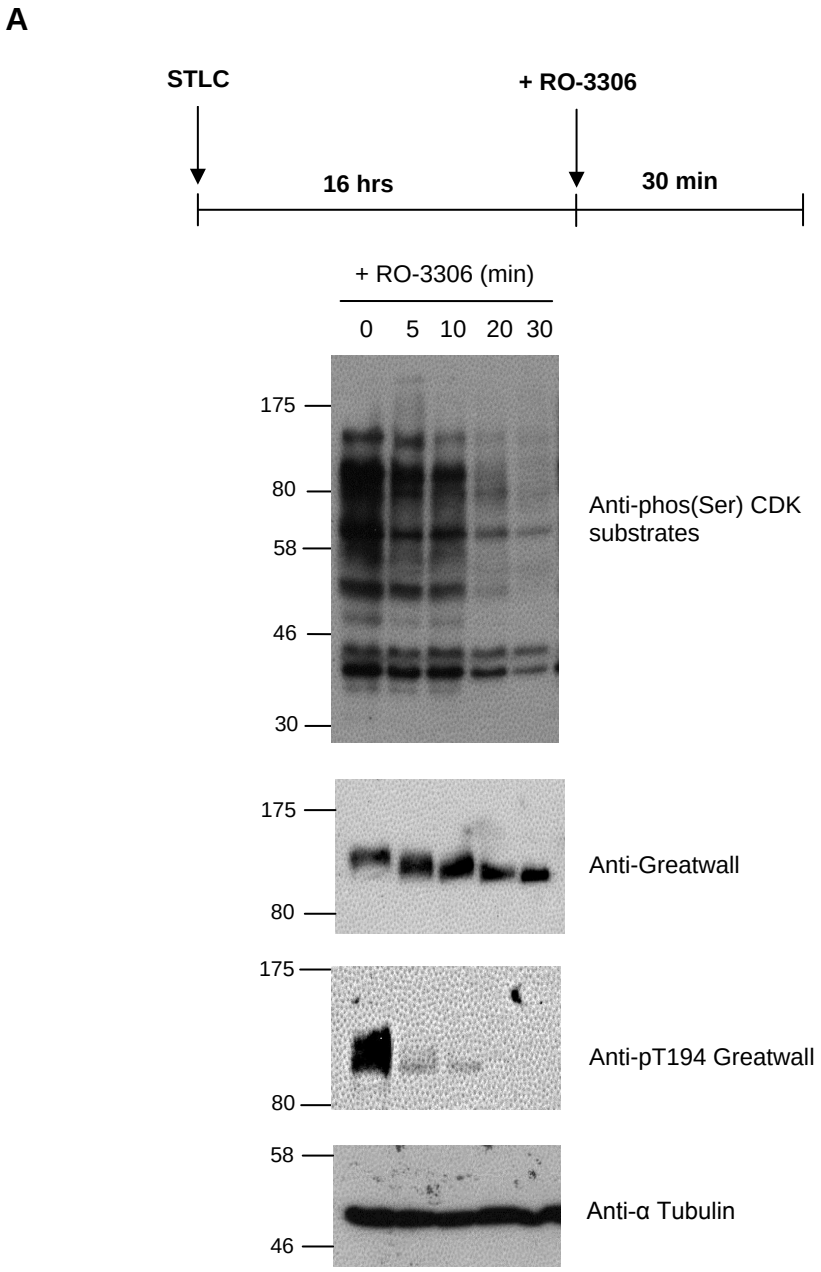

Figure 5.4 Investigating Greatwall inactivation in human cells

(A) Investigating Greatwall inactivation during mitotic exit. SDS-PAGE analysis of HeLa cells that were treated with STLC to arrest them in mitosis. A mitotic shake-off was performed and the cells treated with RO-3306 in the presence of STLC to induce mitotic exit. Samples were then taken at 0, 5, 10, 20 and 30 minutes after RO-3306 addition and analysed by immunoblot. The phosphorylation pattern of cyclin B-CDK1 substrates was assessed using an anti-phosphorylated serine CDK motif antibody (anti-phos(Ser) CDK substrates) (top panel). The anti-Greatwall antibody was used to probe for total human Greatwall protein levels (second panel) and the anti-pT194 antibody was used to probe for the presence of Greatwall phosphorylated on T194 (third panel) in these different conditions, while an anti-α Tubulin antibody (bottom panel) was used as a loading control.

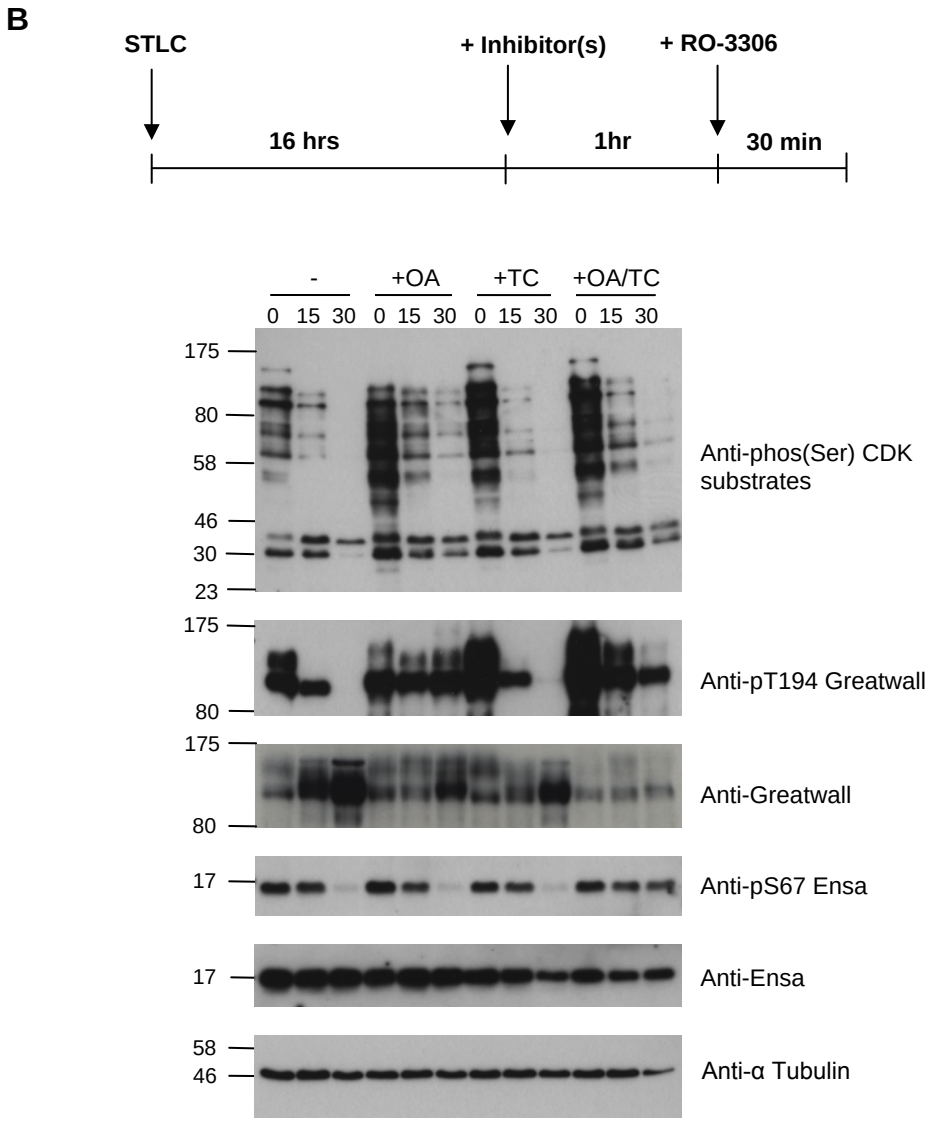

(B) Investigating Greatwall inactivation by phosphatases during mitotic exit. HeLa cells were treated with STLC to arrest them in mitosis. The cells were then treated for one hour with (+) or without (-) phosphatase inhibitors; okadaic acid (OA), Tautomycetin (TC), or both (OA/TC). A mitotic shake-off was performed and the cells treated with RO-3306 in the presence of STLC to induce mitotic exit. Samples were then taken at 0, 15 and 30 minutes after RO-3306 addition and analysed by immunoblot. The protein and phosphorylation status of the lysates were analysed as for **(A)** and additionally an anti-Ensa antibody was used to probe for total human Ensa protein levels and an anti-pS67 Ensa antibody was used to probe for the presence of Arpp19/Ensa phosphorylated on S67 in these different conditions.

Tautomycetin. At the concentrations used here okadaic acid is a potent inhibitor of PP2A but has little effect on PP1 (Felix *et al.* 1990), while Tautomycetin inhibits PP1 specifically (Cheng *et al.* 1989; Favre *et al.* 1997). The phosphatase inhibitors were

added to the STLC-treated cells separately or together for one hour prior to RO-3306 addition to allow the mitotic drug-targeted phosphatase(s) to be fully inhibited at the time of RO-3306-induced mitotic exit. Samples were then taken at 0, 15 and 30 minutes after RO-3306 addition and analysed as before (**Figure 5.4 B**).

A strong signal of CDK substrate phosphorylation was again seen before addition of RO-3306 which was severely diminished after 15 minutes and gone after 30 minutes in the absence of any phosphatase inhibitors. In the presence of okadaic acid, the initial amount of CDK phosphorylation was increased and the removal of CDK substrate phosphorylations was delayed but the majority of the signal was still gone after 30 minutes. In the presence of Tautomycetin, although the initial amount of CDK substrate phosphorylation was again increased, the signal was gone after 30 minutes the same as in the absence of any phosphatase inhibitors. The results of addition of both of the phosphatase inhibitors together were the same as for okadaic acid alone suggesting that PP2A could serve to initiate activity of the CDK counteracting phosphatases, but neither PP2A nor PP1 are required for removal of the majority of mitotic phosphorylations during mitotic exit in human cells. That the removal of CDK substrate phosphorylations is not blocked by inhibition of PP1 and PP2A indicates that other unknown phosphatases contribute to the removal of mitotic phosphorylations during mitotic exit to return cells to interphase.

Total Greatwall levels detected using the anti-Greatwall antibody tends towards an increased signal at later time points. This fits with the observation reported previously that the total anti-Greatwall antibody is unable to efficiently detect the presence of mitotically modified active Greatwall. Only once the protein has been dephosphorylated/its mitotic modifications have been removed as the cells exit mitosis, is the antibody able to detect the presence of the protein once more in these samples. The presence of T194-phosphorylated, and thus active, Greatwall is rapidly decreased after 15 minutes of RO-3306 treatment in the absence of phosphatase inhibitors or if PP1 only is inhibited (using Tautomycetin). In the presence of okadaic acid (when PP2A is inhibited), T194 phosphorylation of Greatwall persists and is still detected even after 30 minutes of incubation with the CDK1 inhibitor (**Figure 5.4 B**). This indicates that PP2A activity is required to dephosphorylate Greatwall at mitotic exit and that PP1 does not contribute to this. Interestingly, treatment with the PP2A inhibitor alone seemed to cause a decreased mobility shift of Greatwall on the immunoblot prior to CDK inhibition, suggesting that some of the mitotic modifications or phosphorylations

of Greatwall were removed in the absence of PP2A activity. The association of Greatwall directly with PP2A subunits, which could potentially serve to facilitate its PTMs required for full kinase activity, have been reported (Vigneron *et al.* 2009). This loss of electrophoretic mobility of Greatwall was not seen if both PP2A and PP1 were both inhibited. Further investigations by Dr. Nadia Hégarat in our laboratory have shown that Greatwall kinase activity levels are maintained up to 60% relative to WT mitotic Greatwall in *in vitro* kinases assays when PP2A is inhibited with okadaic acid in CDK1-inhibited mitotic cells. Therefore suggesting that PP2A contributes to the majority of Greatwall inactivation during mitotic exit but that the removal of other PTMs or phosphorylations (by other phosphatases, such as PP4 and PP6) likely also occur.

The total levels of the Ensa protein remained constant in the lysates indicating that it is not degraded, merely inactivated by dephosphorylation at mitotic exit. A phospho-specific anti-pS67 Ensa antibody was used to assess Greatwall substrate phosphorylation. However, the Greatwall phosphorylation motif recognised by this antibody (FDSGDY) is identical in both Arpp19 and Ensa and thus both are detectable with this antibody. Here I will refer to Arpp19/Ensa for simplicity because it is not possible to distinguish between the phosphorylation of the two proteins with specific antibodies. Greatwall phosphorylation of Arpp19/Ensa on serine 67 (S67) (Gharbi-Ayachi *et al.* 2010; Mochida *et al.* 2010) was detected in the mitotically arrested lysates prior to forced mitotic exit via CDK inhibition. This phosphorylation persisted 15 minutes after CDK inhibition but was gone after 30 minutes in the absence of a phosphatase inhibitor or in the presence of either okadaic acid or Tautomycetin alone. Only when both of these inhibitors were added together was Arpp19/Ensa dephosphorylation blocked. This indicates that to dephosphorylate Arpp19/Ensa and relieve its inhibition of PP2A at mitotic exit both PP2A and PP1 must be inhibited or that a separate phosphatase targets Arpp19/Ensa that is only sufficiently inhibited in the presence of both drugs. Further work by Dr. Nadia Hégarat in our laboratory has demonstrated that this phosphatase is the RNA polymerase II C-terminal domain phosphatase Fcp1 (a personal communication by Dr. Nadia Hégarat). SiRNA depletion of Fcp1 blocked Arpp19/Ensa dephosphorylation following CDK inhibition in STLC-synchronised mitotic HeLa cells. Fcp1 has been recently reported to be required in human cells at the end of mitosis for timely cyclin B-CDK1 inactivation (Visconti *et al.* 2012). Its crucial targets include Cdc20 and Wee1, and as a result of this work we now

add Arpp19/Ensa to this list.

5.6 Conclusions and discussion

The activation status of Greatwall has been implicated to play a critical role in mitotic entry, maintenance of the mitotic state, as well as in mitotic exit. Throughout this chapter the control of Greatwall activity has been examined.

A phospho-specific antibody that is highly specific for phosphorylation of human Greatwall at T194 was used to confirm that Greatwall is phosphorylated by CDK1 on T194 to activate it at the G2/M transition. Greatwall then remains phosphorylated and active in mitosis until mitotic exit. It is likely that activating phosphorylations of the T-loop by CDK1 are not the whole story of Greatwall regulation and it is probable that other PTMs/phosphorylations occur during mitosis. The work presented suggests that it is likely that CDK1 and not CDK2 activates Greatwall *in vivo*. This may be because of the activity of the Greatwall dephosphorylating phosphatase that counteracts Greatwall activation in interphase. This phosphatase may require the cyclin B-CDK1 activation loop for its inactivation, thereby integrating Greatwall activation in the larger G2/M feedback system. This chapter describes work that initiated characterisation of the phosphatase(s) that regulate Greatwall and its substrates.

Interestingly, the majority of WT Greatwall activated by cyclin A-CDK2 was not hyper-shifted in the gel while the mitotic WT Greatwall was (**Figure 5.2 C**). This has also been observed by other groups (Yu *et al.* 2006; Zhao *et al.* 2008). This can be interpreted to mean that Greatwall that has been activated is further modified in mitosis. This might point to a complex mechanism of activation to ensure Greatwall activity with correct timing and dynamics to promote and sustain mitosis.

Phosphorylation site mapping using PhosphoSitePlus (**Figure 5.5**) indicates that human Greatwall might be phosphorylated on as many as 33 different residues. Five of these sites lie outside of the NCMR (Y59, T194, T740, S874 and S877) the rest are all contained within it. Within the NCMR only one site is a tyrosine (Y720). The others are all serine or threonine residues and could therefore potentially be autophosphorylated by Greatwall itself after priming phosphorylation by CDK. Six of the indicated sites are also potential CDK phospho-sites (S/TP) and could be alternatively phosphorylated by

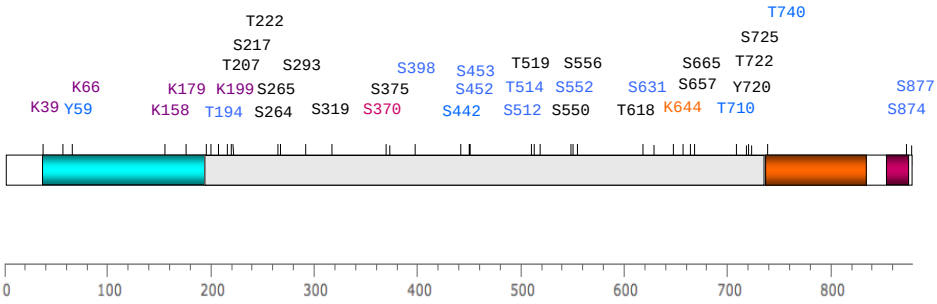

Figure 5.5 Phosphorylation/PTM site mapping of Greatwall

Phosphorylation/PTM site mapping analysis of Greatwall using PhosphoSitePlus. Sites with only one MS/HTP reference are shown in black. Sites with more than one MS/HTP reference are shown in blue and a site with more than five MS/HTP references is indicated in pink. The kinase domain lobes and hydrophobic motif are indicated coloured as in **Figure 4.2 B**. In addition, the sites that are potentially ubiquitinated are indicated in purple and the site, K644, which is potentially both ubiquitinated and acetylated is indicated in orange.

CDK itself (**Appendix C**). It has been speculated that both of these occur upon mitotic entry; CDKs phosphorylate Greatwall at multiple sites and Greatwall can in turn autophosphorylate itself at multiple sites (Blake-Hodek *et al.* 2012). PhosphoSitePlus analysis of Greatwall also revels that, in addition to multiple potential phosphorylated sites, there are six sites that might be ubiquitinated; lysines (K) 39, 66, 158, 179, 199, and 644. One of these sites, K644, is also potentially acetylated (**Figure 5.5**). The massive electrophoretic retardation of mitotic Greatwall in *Xenopus* was reduced by treatment with λ phosphatase (Yu *et al.* 2006) but in human Greatwall it was only partially diminished (Burgess *et al.* 2010). Also, Greatwall was reported to be ubiquitinated and excluded from the nucleus prior to NEBD in *Drosophila*, despite being enriched in the nucleus during interphase (Archambault *et al.* 2007). Here, human Greatwall pre-treated with recombinant cyclin A-CDK2 was fully active and phosphorylated in the T-loop on T194 and this activation allowed Greatwall to autophosphorylate but it did not display the full hyper-shift in the gel seen for mitotic Greatwall. This suggests that further modifications are acquired by Greatwall in mitosis. The insights provided from the analysis of potential PTMs of Greatwall using PhosphoSitePlus analysis indicate a possible explanation in which regulation of Greatwall activity could occur via a balance between phosphorylation, ubiquitination

and acetylation of the protein. These observations hint that Greatwall activation might require complex control mechanisms not yet understood.

Mechanisms in which protein activity is regulated by a balance between phosphorylation, ubiquitination and acetylation modifications are known. Another AGC kinase, p70 ribosomal S6 kinase (S6K), is known to be activated by phosphorylation on multiple serine and threonine residues. It is also targeted by acetylation on lysine 516 by the histone acetyltransferase (HAT) p300 which serves to modulate the functions of the kinase in response to growth factor signalling (Fenton *et al.* 2010). Furthermore, S6K ubiquitination has recently been shown to be an important regulatory event in S6K signalling and serves to control the steady state levels of this kinase in human cells (Wang *et al.* 2008). Additionally, the tumour suppressor p53 is activated by a phosphorylation-acetylation cascade in response to DNA damage. Phosphorylations in the N-terminus of the protein in response to DNA damage enhance its interaction with p300 and the p300/CBP-associated factor (PCAF) thereby driving acetylation of p53 in its C-terminus. Its acetylation on at least eight sites is essential for its dissociation from its repressor Mdm2 and activation. This serves to prevent ubiquitination preventing its export and degradation (Sakaguchi *et al.* 1998; Tang *et al.* 2008).

The analysis revealing potential ubiquitination and phosphorylation sites as well as a potential acetylation site within the protein indicate that a similar complex mode of regulation might apply to Greatwall. It is clear that a large electrophoretic mobility shift is seen for human Greatwall at the G2/M transition that persists until mitotic exit. It is conceivable that Greatwall activity is modulated via ubiquitination at one or all of the six potential ubiquitination sites, by acetylation and by multiple phosphorylations which could serve to facilitate the activation as well as stabilisation and/or localisation of Greatwall. Some of these modifications could potentially be mediated by CDK1-activated second messenger proteins. Alternatively, mitotic modification of the protein via ubiquitination, acetylation and/or phosphorylation might serve to promote its association with as yet unknown inhibitors or activating proteins required to modulate its activity in mitosis. This complex model of Greatwall activation remains to be elucidated but it would not be unprecedented considering the mechanisms controlling other proteins, such as S6K and p53.

The evidence presented in this chapter (**Figure 5.2 C**) indicates that CDK phosphorylation is capable of activating Greatwall to its full capacity. This activating phosphorylation of Greatwall is likely to occur via phosphorylation by CDK1 for the

reasons discussed previously. However, in RO-3306-treated cells, in which CDK1 activity was repressed, Greatwall has been repeatedly detected at seemingly low levels despite careful equalisation of total protein levels. This suggests that the PTMs that Greatwall acquires at mitotic entry may have already begun to be added to the kinase in this late G2 phase block. Therefore, preventing its detection by the anti-Greatwall antibody as has been noted for the active kinase in mitotic extracts. Alternatively, in the absence of CDK1 activity at the G2/M transition the protein might be unstable and possibly actively degraded. RO-3306 treatment is known to result in downregulation of anti-apoptotic genes such as Bcl-2, survivin and p21 in human cells (Kojima *et al.* 2009). Its mechanism of action is unknown but it is possible that Greatwall is affected in the same manner after treatment with RO-3306. Another explanation could be that, as discussed, CDKs other than CDK1 are able to phosphorylate Greatwall and activate it. Therefore, in the absence of CDK1 activity in late G2 it is destabilised/degraded to ensure early Greatwall activity is not triggered aberrantly by phosphorylation by other CDKs such as CDK2 which remains active in G2 (Hochegger *et al.* 2008). Further experiments with other CDK and proteasome inhibitors could clarify this observation.

Additionally, as mentioned previously, it is likely that Greatwall can autophosphorylate itself as well as being phosphorylated by additional kinases. Kinase autophosphorylation can occur via an intermolecular mechanism (when one kinase molecule phosphorylates another) or via an intramolecular mechanism (when a kinase molecule acts upon itself). Recently a paper published by Dodson *et al.* (2013) reported a biochemical method for testing an individual kinase to determine its activation mechanism via derivation of its kinetic signature. Future work might seek to explore the mechanism of Greatwall kinase autoactivation to gain further insights into the cellular regulation this novel kinase.

Once in mitosis, Greatwall and other mitotic CDK-substrates must then be dephosphorylated to allow proper mitotic exit (Queralt *et al.* 2008; Manchado *et al.* 2010). The results presented here suggest that PP1 and PP2A are not the main CDK-antagonising phosphatases that remove mitotic phospho-epitopes in human cells. These results indicate that PP2A is, however, required to dephosphorylate and inactivate Greatwall. Further recent work from our laboratory carried out by Dr. Nadia Hégarat has confirmed that the α and δ isoforms of the B55 subunit of PP2A are required in human cells to remove T194 phosphorylation in Greatwall. The siRNA-mediated depletion of the α and δ isoforms of the B55 subunit of PP2A following CDK inhibition

in STLC-synchronised mitotic HeLa cells significantly reduced dephosphorylation of T194 in Greatwall. It did not completely block this dephosphorylation, possibly due to incomplete depletion of the B55 subunits in the cells. This confirms that PP2A-B55 is required to inactivate Greatwall by targeting the T194 site, although, the removal of other PTMs/phosphorylations by an unknown okadaic-acid insensitive phosphatase likely also contributes. Furthermore, Arpp19/Ensa is targeted by another phosphatase and recent work from our laboratory suggests that this enzyme is Fcp1. This helps explain the observation that this phosphatase is required for mitotic exit (Visconti *et al.* 2012) and implicates it as yet another intrinsic element of the mitotic switch.

Intriguingly, neither PP1, PP2A nor Fcp1 are required for the majority of CDK substrate dephosphorylation (concluded from the results presented here and personal communication from Dr. Nadia Hégarat). In yeast this function is performed by the Cdc14 phosphatase (Stegmeier *et al.* 2004). Cdc14 is a dual-specificity phosphatase that belongs to a phosphatase family quite distinct from PP1 and PP2A and is insensitive to okadaic acid (Queralt *et al.* 2008). As discussed (**Chapter 1** section **1.13**) there are two orthologues of Cdc14 in human cells (termed Cdc14A and B). Both have been implicated to have a role in mitotic progression and exit (Bembenek *et al.* 2001; Kaiser *et al.* 2002; Dryden *et al.* 2003). To our knowledge a double deletion of these phosphatases has not been generated, but single knockout cells and mice and show only weak cell cycle phenotypes (Mocciaro *et al.* 2010; Guillamot *et al.* 2011). It could still be possible that this function is conserved between yeast and humans after all and that Cdc14 A and B play a redundant role in mitotic exit.

A manuscript reporting these findings is currently in revision for publication. Further work will be required to reveal the regulation and cross talk of these phosphatases. Moreover, biochemical assays will be required to prove that these enzymes act directly on the phosphorylation sites of their respective targets. Thus, the work presented here suggests a complex hierarchy of phosphatases acting during mitotic exit.

CHAPTER 6. Taking a chemical genetic approach to inhibit Greatwall kinase

6.1 Introduction

Using endogenous gene targeting to modify an individual gene, or part of it, is exquisitely specific. It offers a way in which to study the effect of a single gene product by its loss (a 'knockout') or by its replacement with an altered version (a 'knockin'). This targeting strategy is based on homologous recombination and is achieved through the careful design of a specific targeting vector to the gene of interest. Alterations that can be introduced in this manner can vary widely and can include the deletion of specific exons, introductions of specific point mutations, introduction of a specific tag or even the addition of a gene. Moreover, gene targeting can be permanent or conditional and it can be used for any gene regardless of its transcriptional activity or size.

The strength of this technique is evident, but despite its use with great success in bacteria and yeast, it traditionally has a very poor efficiency rate in mammalian cells. In general, the gene targeting efficiency for mammalian cells is only 10^{-5} to 10^{-7} targeted cells per transfected cell (Deng *et al.* 1992; Yanez *et al.* 1998; Khan *et al.* 2011). Moreover, the prevalence of non-homologous end joining in mammalian cells increases the chances of the targeting vector DNA being integrated randomly (Khan *et al.* 2011). This technique can also be very slow to exert its effects and cannot be titrated to induce variable levels of inactivation. Alternatively, small molecule inhibitors can be used to inhibit kinases and overcome these limitations (Vassilev *et al.* 2006; Lenart *et al.* 2007; Scutt *et al.* 2009). They can induce inhibition rapidly and in a dose-dependant manner. However, due to the conservation of catalytic kinase domains between cellular protein kinases completely specific drugs are rare and many existing 'specific' kinase inhibitors can have unforeseen impacts on other kinases (Davies *et al.* 2000; Tyler *et al.* 2007; Garske *et al.* 2011). This is highlighted by results obtained in which different phenotypes were observed from genetic and pharmaceutical approaches used to target the same kinase (Weiss *et al.* 2007).

Recently a range of new techniques have been developed to improve gene

targeting speed and efficiency in human cells. These include the use of simplified methods for construction of gene targeting vectors and the use of viruses to improve the efficiency of targeting (Iiizumi *et al.* 2006; Khan *et al.* 2011). Moreover, genetic targeting and the use of small molecule inhibitors has been combined via a comparatively new technique termed 'chemical genetics'. This encompasses the strengths of both techniques and has pioneered the inhibition of a single engineered kinase using small molecule inhibitors. Chemical genetics allows inhibition of a kinase with complete specificity to be achieved in a rapid, titratable and reversible manner. This technique takes advantage of the conserved structure of the ATP-binding site of protein kinases (Bishop *et al.* 1998; Bishop *et al.* 2000; Alaimo *et al.* 2005). Using this approach a critical conserved bulky hydrophobic residue found in the ATP-binding site, also known as the 'gatekeeper' residue or 'molecular gate', that restricts access to a pre-existing cavity within the ATP-binding pocket, is mutated at the gene level to a smaller amino acid. The resulting enlarged engineered kinase pocket is then able to accept a bulky ATP-analogue that blocks it, preventing binding of wildtype substrates thus rendering the kinase non-functional (**Figure 6.1 A**). Wildtype kinases are naturally resistant to inhibition as they are unable to accept the bulky ATP-analogue as a result of a steric clash with their natural larger gatekeeper residue. The mutant kinase is then expressed from the endogenous gene locus under normal transcriptional regulation overcoming the draw backs of off-target effects from inhibitors and eliminating doubt over specificity (Alaimo *et al.* 2005; Hochegger *et al.* 2007; Scutt *et al.* 2009; Garske *et al.* 2011; Hegarat *et al.* 2011).

In this chapter I attempt to use these techniques to adopt a chemical genetics approach to inhibit Greatwall kinase by creating a stable human cell line expressing an ATP-analogue sensitive (*as*) Greatwall.

6.2 Identification of the gatekeeper residue in Greatwall

In order to identify the gatekeeper residue in the ATP-binding pocket of Greatwall I aligned the amino acid sequence with that of another AGC kinase, PKA (**Figure 6.1 B** and **Appendix E** for the full alignment). In 2002, both the α and β isoforms of the catalytic subunit of PKA were engineered to modify their structures so that they acquired novel inhibitor sensitivity (Niswender *et al.* 2002). This was achieved

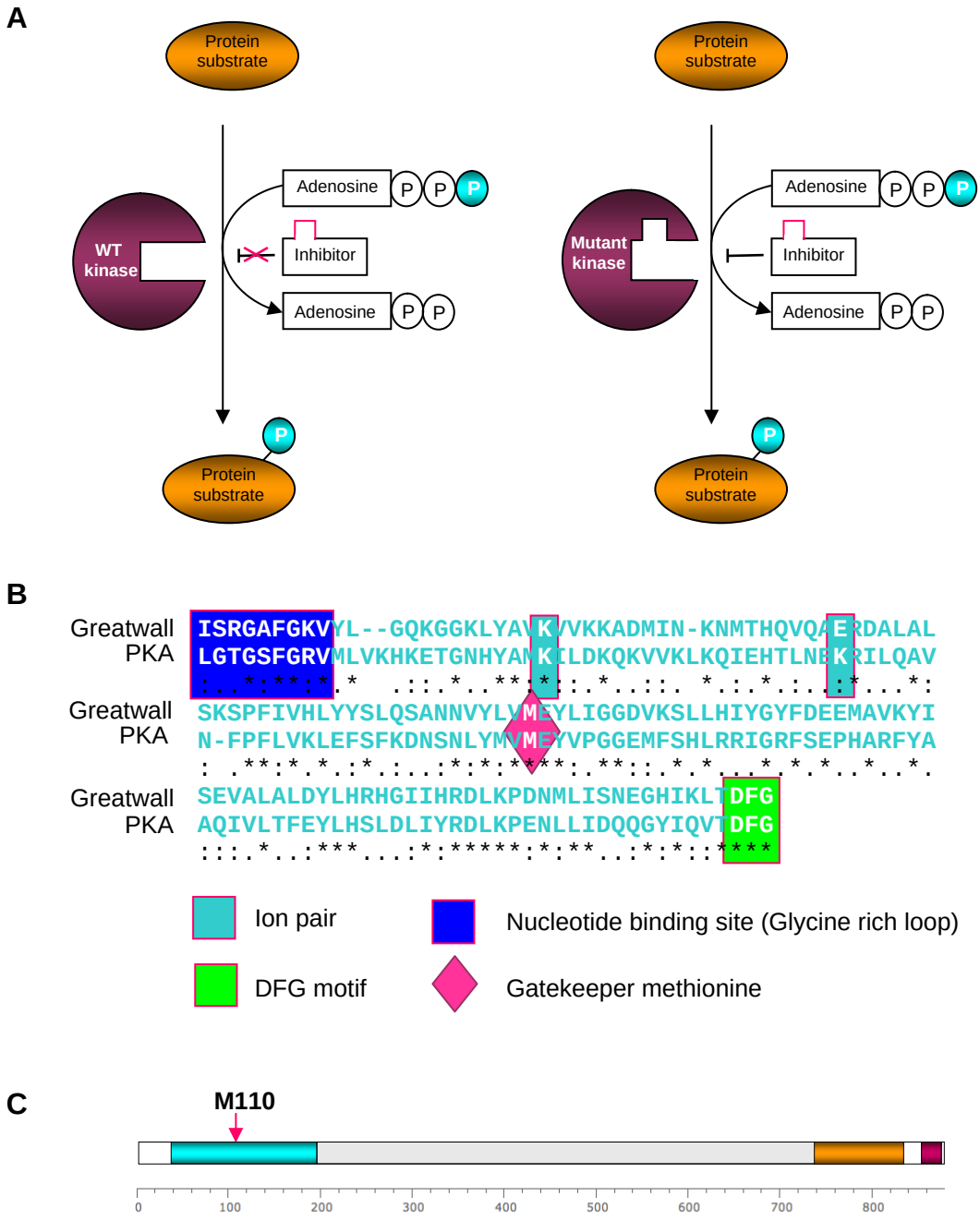

Figure 6.1 Identifying the gatekeeper residue of human Greatwall kinase

(A) Using a chemical genetic approach to inhibit a kinase. Only an engineered kinase with an enlarged ATP-binding pocket is able to accept the bulky ATP-analogue resulting in the inhibition of that kinase specifically. Adapted from Alaimo *et al*. (2005). **(B)** Sequence alignment of Greatwall with the α isoform of the catalytic subunit of PKA. The kinase N-terminal subdomain is shown in a CLUSTAL 2.1 multiple sequence alignment. An asterisk (*) indicates positions that have a single, fully conserved residue. A colon (:) indicates conservation between groups of strongly similar properties - scoring > 0.5 in the Gonnet PAM 250 matrix. A period (.) indicates conservation between groups of weakly similar properties - scoring =< 0.5 in the Gonnet PAM 250 matrix (Larkin *et al.* 2007; Goujon *et al.* 2010). Key features:

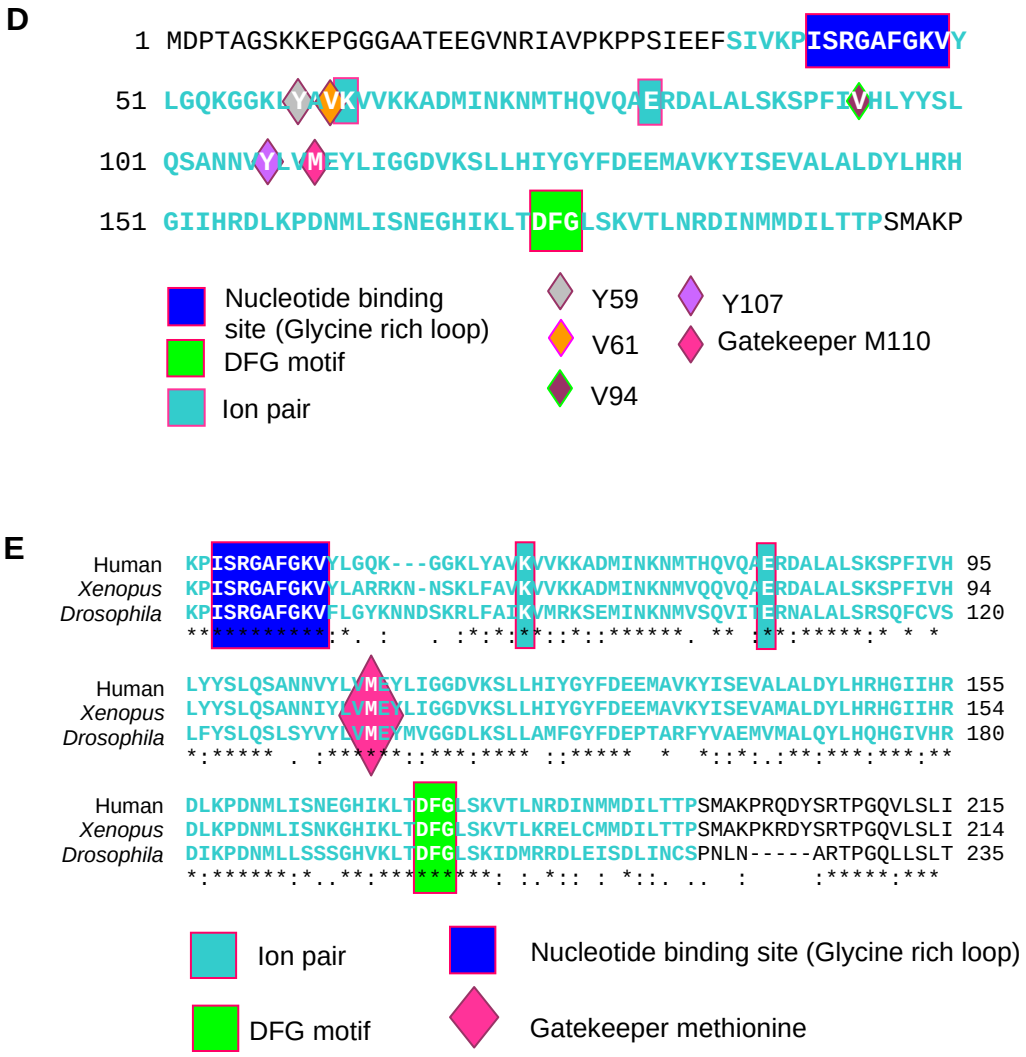

glycine rich loop, DFG motif, ion pair and the gatekeeper methionine are indicated. **(C)** Schematic representation of the Greatwall protein indicating the position of the gatekeeper methionine 110 in the kinase N-lobe. The kinase N-lobe (aqua) and C-lobe (orange) are indicated as well as the hydrophobic motif (pink). **(D)** Mapped features of Greatwall. The kinase N-lobe is indicated in aqua font and the glycine rich loop, DFG motif and ion pair (K62 and E81) are indicated. Residues mutated (including the gatekeeper methionine) in this investigation are indicated by diamond parentheses. **(E)** Sequence alignment of human, *Xenopus* and *Drosophila* Greatwalls. The kinase N-terminal subdomain is shown in a CLUSTAL 2.1 multiple sequence alignment as described for **(B)**. Coloured as for **(D)**. **(F)** Structural model of the ATP-binding pocket of Greatwall. Here the small N-lobe (aqua), large C-lobe (orange), and activation loop (grey) are indicated (as in **Figure 4.2**). One molecule of ADP is shown in the ATP-binding site in green. This was generated up the superposition of CHK2 (PDB: 2CN5) on the Greatwall model (introduced in **Chapter 4**). The gatekeeper M110 and V94 are shown in grey and the dotted surface indicates the van der waals radius of M110. **(G)** Structural model of the ATP-binding pocket of Greatwall targeted for engineering. This is coloured as for **(F)**. One molecule of the bulky ATP-analogue, 1NM-PP1, is shown in the ATP-binding site in yellow. This was generated by overlaying CHK2 (PDB:

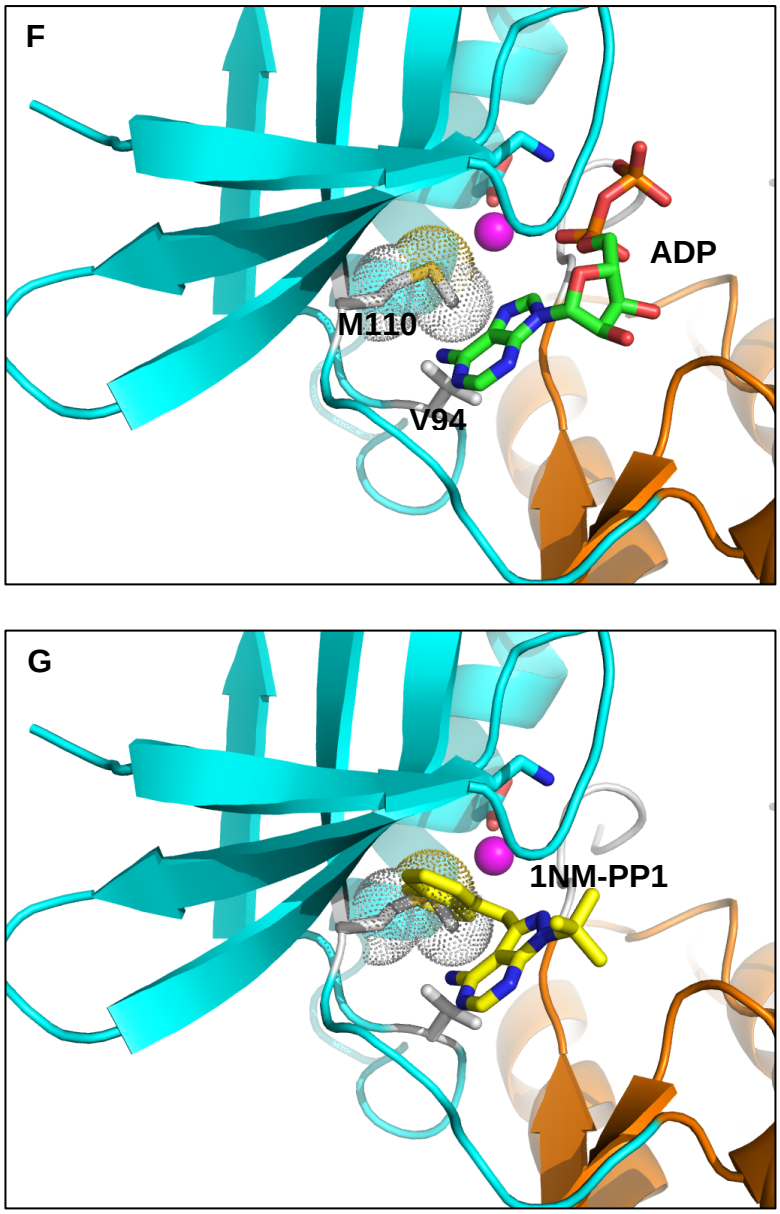

4LGH) on the Greatwall model. This clearly illustrates the steric clash that occurs between the ATP-analogue and the naturally occurring gatekeeper methionine that renders the wildtype kinase immune to inhibition with the ATP-analogue. It is this M110 that can be mutated to a smaller residue to allow the engineered kinase to accept the bulky ATP-analogue inhibitor.

by mutating the gatekeeper methionine at position 120 in the ATP-binding pocket to a smaller amino acid residue, either to an alanine or a glycine respectively. In this manner both the α and β isoforms were successfully rendered sensitive to specific bulky ATP-analogue inhibitors. These inhibitors did not inhibit the wildtype PKA but allowed

effective inhibition of the engineered isoforms separately and thus allowed the roles of the two isoforms to be better defined.

Comparison of the amino acid sequence of the ATP-binding pocket of PKA catalytic subunit α isoform with that of Greatwall indicates that they share the same methionine at the gatekeeper position in the ATP-binding pocket (**Figure 6.1 C** and **F**). The gatekeeper methionine at position 110 (M110) is located in the kinase N-terminal subdomain (**Figure 6.1 C, D** and **F**) at the beginning of exon 3 in the Greatwall gene locus and is conserved across *Drosophila*, *Xenopus* and humans (**Figure 6.1 E** and **Appendix C** for full alignment). Based on this we hypothesised that mutation of this gatekeeper methionine to a smaller alanine residue (M110A) should render it ATP-analogue sensitive. This space-creating substitution of the gatekeeper residue would alter the size of the ATP-binding pocket of the kinase allowing it to accept the bulky ATP-analogue (**Figure 6.1 G**). Thus, inducing sensitivity to bulky ATP-analogues in the same manner as for PKA (Niswender *et al.* 2002; Alaimo *et al.* 2005). This *as* Greatwall would then be able to be rapidly inhibited by the addition of a cell permeable bulky ATP-analogue in a titratable and reversible manner. Allowing the effects of the loss of Greatwall kinase activity specifically to be studied in an otherwise 'normal' cell.

6.3 Targeting vector construction

I used the MultiSite Gateway® system from Invitrogen to create a gene targeting vector to introduce the M110A mutation of the ATP-binding site into the Greatwall gene locus. This system provides a quick and simple method for the creation of gene targeting constructs (Iiizumi *et al.* 2006). For this method, the design of primers to allow the PCR amplification of genomic DNA fragments for homologous DNA arms is the critical step. Once these have been created there is no requirement for ligation reactions or extensive restriction site mapping that can be laborious and time consuming when using traditional techniques.

This cloning method is based on the bacteriophage λ site-specific recombination system which allows λ integration into the *E.coli* chromosome and for the switch between the lytic and lysogenic pathways. This system has been modified here in order to allow the rapid and efficient transfer of heterologous DNA sequences into multiple vector systems. The site-specific recombination occurs between attachment (*att*) sites in

a conservative manner such that there is no net gain or loss of bases and no DNA synthesis is required. The recombination is catalysed by a mix of enzymes that bind to the *att* sites, bringing the target sequences together and facilitating strand exchange and ligation of the DNA in a novel form. This results in the DNA segments flanking the *att* sites being switched in a manner so that the resultant *att* sites are hybrids of the sequences donated by each parental vector. The mixture of recombination enzymes used is dependant on whether the λ phage utilises the lytic (as for the BP recombination reaction between *attB* and *attP* sites) or the lysogenic pathway (as for the LR recombination reaction between the *attL* and *attR* sites) (also see **Chapter 2**, section **2.2.5 Figure 2.2.1**). For this purpose entry vectors are generated by PCR amplification of the genomic DNA for the homologous DNA arms flanked by appropriate *att* sites and assembled with the backbone of an entry vector via a site-specific recombination reaction (the BP reaction). This method then allows for the assembly of four DNA fragments; the destination vector backbone, a selection cassette and the two (subcloned) homologous DNA arms, together in a single step via independent site-specific recombination reactions (the LR reaction). This powerful new cloning technology allows for the replacement of endonucleases and ligase with site-specific recombination (Iiizumi *et al.* 2006) (for more information refer to the Gateway® Technology with Clonase™ II manual from Invitrogen).

The targeting strategy for the Greatwall gene locus (shown in **Figure 6.2 A**) involved the design of primers to generate a 1058 bp left (5') homology arm situated in exon 2 of the Greatwall gene and a 951 bp right (3') homology arm that included the beginning of exon 3 of the Greatwall gene. The M110A mutation was introduced at the beginning of exon 3 in the 3' homology arm by the 3' primer as indicated in **Figure 6.2 A**. These homology arms were amplified by PCR from genomic DNA extracted from human HeLa cells. Here the 5' homology arm contained an additional NdeI restriction site introduced by the 3' primer within the non-coding sequence for later screening by Southern blotting. Specific recombination *att* sequences were inserted at either end of the arms to allow the site-specific homologous recombination into the correct entry vectors via the BP recombination reaction. The resulting left homology arm and right homology arm entry vectors were confirmed by sequence analysis. These were then taken into a final recombination step involving a four way recombination reaction with a selection cassette entry vector (providing a drug resistance gene) and the backbone of the destination vector (pAAV-Dest) to create the final targeting vector using the LR

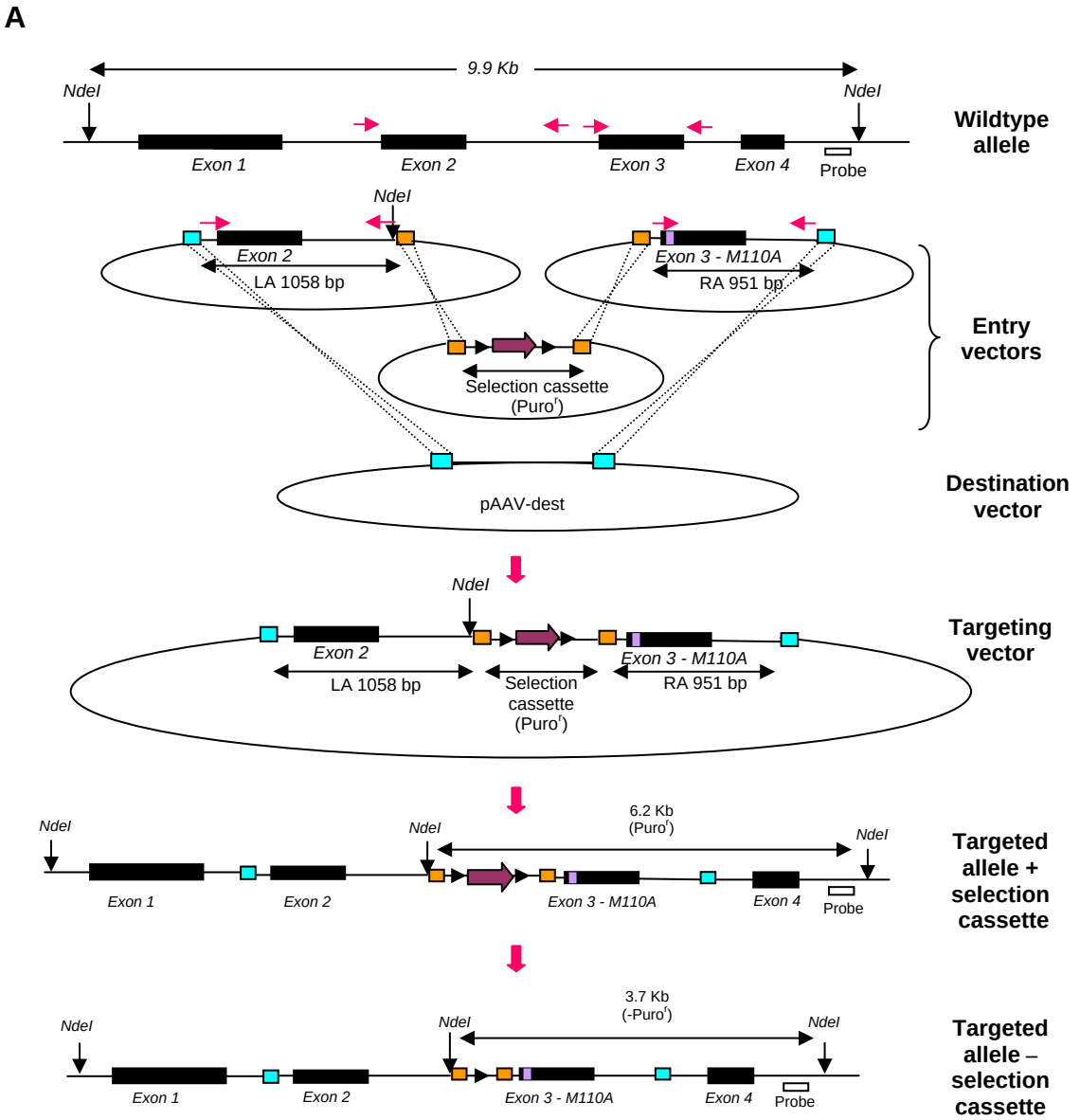

Figure 6.2 Strategy for creating an *as* Greatwall knockin human cell line

(A) A schematic representation of the targeting strategy to introduce the M110A mutation (indicated by a violet stripe in exon 3) into the ATP-binding pocket of Greatwall kinase. Here the primers (indicated by pink arrows) were used to amplify the left (5') and a right (3') homology arms (LA and RA respectively)

that were then incorporated into a destination vector (pAAV-Dest) with a puromycin resistance gene ($Puro^r$, indicated by the purple block arrow) in a four-way recombination reaction. The resulting targeting vector is indicated, containing the AAV vector backbone that allowed for viral infection in human HCT116 cells. The resulting targeted allele generated from homologous recombination with the targeting vector is shown, as are the expected fragments sizes from NdeI digestion of the targeted allele containing the incorporated selection cassette or with it deleted from this site by Cre. Exons are indicated by black rectangles, *att* sites are indicated with aqua and orange rectangles, loxP sites are indicated by black arrow heads, NdeI restriction sites are indicated by black arrows and the position of the probe used for Southern blotting is indicated by a clear rectangle. **(B)** NotI digestion of the final gene targeting vector. The expected bands are indicated: 951 bp for the 3' homology arm, 1058 bp for the 5' homology arm, 2460 bp for the puromycin resistance gene, and 2884 bp for the pAAV-Dest vector back bone.

recombination reaction. The selection cassette I used contained a gene to provide resistance to the antibiotic puromycin for selection of cells containing integrated constructs. The final gene targeting vector was confirmed by restriction digestion (**Figure 6.2 B**).

6.4 Targeting Greatwall in human cells to make a stable knockin cell line

Traditional methods for gene targeting have commonly had very low efficiency in human cells, as mentioned previously (Khan *et al.* 2011). To obtain higher frequencies of gene targeting of the Greatwall gene in a human cell line, I used novel adeno-associated viral (AAV) technology (Kohli *et al.* 2004). The pAAV-Dest destination vector backbone I used for the gene targeting vector contained the *att* recombination site-containing cassette, required for the site-specific recombination reaction, inserted into a pAAV-MCS vector that carried genes required for use in an AAV system. The adeno-associated viruses (AAVs) are replication-deficient parvoviruses that traditionally require co-infection with a helper adenovirus or herpes virus to allow effective infection. The system I used allows production of infectious recombinant human adeno-associated virus-2 virons without the need for a live helper virus. Instead, co-transfection of the pAAV-MCS with a pHelper plasmid provides most of the gene products required for the production of infectious AAV particles. The rest are supplied by the AAV-293 host cells that are derived from HEK-293 cells and have

been modified to produce higher viral titers. In the wildtype AAV-2 virus, the genome contains both *rep* genes (encoding genes for replication) and *cap* genes (encoding caspid genes) flanked by inverted terminal repeats (ITRs) containing the *cis*-acting elements required for viral replication and packaging. Here the *rep* and *cap* genes have been removed from the viral vector leaving the ITRs only which allows for the targeting sequence to be inserted into the viral genome. The *rep* and *cap* genes are instead supplied in *trans* on the pAAV-RC plasmid. Because the viral vector containing the AAV-2 ITRs (in this case pAAV-MCS) does not share any homology with the pAAV-RC plasmid, the wildtype virus cannot be regenerated through recombination, as can potentially happen in other systems. The pAAV-MCS target sequence-containing plasmid is thus co-transfected with the pHelper and pAAV-RC plasmids resulting in viral replication and packaging in the AAV-293 cells. The recombinant AVV-2 particles can then be prepared and used to infect any mammalian cell line of choice (Kohli *et al.* 2004) (for more information see the AAV Helper-Free System Instruction Manual from Agilent Technologies).

The advantage of using this system is that gene targeting rates of 1% to 13% can be achieved in human cell lines (Russell *et al.* 1998; Porteus *et al.* 2003; Kohli *et al.* 2004). Moreover, defined sequence changes to the chromosomal loci can be introduced with high fidelity and without genotoxicity (Khan *et al.* 2011). The targeting frequencies achieved are several logs higher than can be obtained using conventional transfection or electroporation techniques. The reasons for this high efficiency rate are not fully understood but likely results from the delivery of large numbers of single-stranded vector genomes to the cell nucleus. The large numbers of the genomes present in the nuclei serves to enhance the targeting efficiency and, while the vast majority of the vector genomes are transcriptionally inactive, they are available to participate in homologous pairing with chromosomal loci. That the vector genome is delivered as single-stranded DNA also likely promotes homologous recombination, and the formation of hairpin structures by the ITRs at the AAV vector termini further serve to stabilise the vector genomes and decrease random integration events (Russell *et al.* 1998; Khan *et al.* 2011).

I co-transfected the AAV-293 cells with the Greatwall gene targeting vector, the pHelper plasmid, and the pAAV-RC vector using calcium phosphate transfection and allowed 72 hours for the production of infectious recombinant AAV-2 virons (rAAVs). Viral stocks were then prepared and incubated with the human colorectal cancer cell

line; HCT116 cells. I selected this human cell line for genetic targeting of the Greatwall gene because it is known to have high gene targeting rates and has been successfully used to target a number of human genes previously (Waldman *et al.* 1995; Waldman *et al.* 1996; Bunz *et al.* 1998). Importantly, these cells are mismatch repair deficient and have been demonstrated to be amenable to successful gene targeting by homologous recombination (Waldman *et al.* 1995; Horiuchi *et al.* 2012). Selection for positive clones was carried out in puromycin-containing media for three to four weeks in 96-well plates. Once single colonies had formed, the clones were expanded into 6-well plates and allowed to grow up for an additional week. Each clone was then trypsinised and divided into two halves. One half of the cells from each clone were frozen down and stored. The second half of the cells were used to extract genomic DNA for screening for the presence of targeted alleles.

6.5 Screening to detect the first targeted allele

In order to detect the presence of locus-specific targeting events in these clones PCR screening was used. Genomic DNA from groups of five clones were pooled together in PCR reactions designed to allow screening for the presence of targeted Greatwall alleles. I designed a forward primer (primer C) that would anneal to a portion of the selection cassette sequence and the beginning of exon three containing the M110A inserted mutation. This was paired with a reverse primer (primer B) situated outside of the right homology arm in the unchanged exon four. As a positive control another forward primer (primer A) was designed that annealed only to the wildtype non-mutated beginning of exon three and could also be combined with reverse primer B. These primers are indicated in **Figure 6.3 A**. If a targeted allele is present in the genomic DNA from one of the clones in a particular pool then a PCR product of the correct size (~ 1.5 Kb) should been seen when the PCR reaction with primers A and C is run on an agarose gel. Thus, indicating a specific targeting event at the Greatwall gene. In order to determine that genomic DNA (containing wildtype alleles) was present in detectable quantities and that the PCR reactions were working correctly a PCR product (of ~1.5 Kb) should been seen from all the PCR reactions carried out using primers A and B.

Over 160 clones were picked and prepared. Fortunately however, the PCR

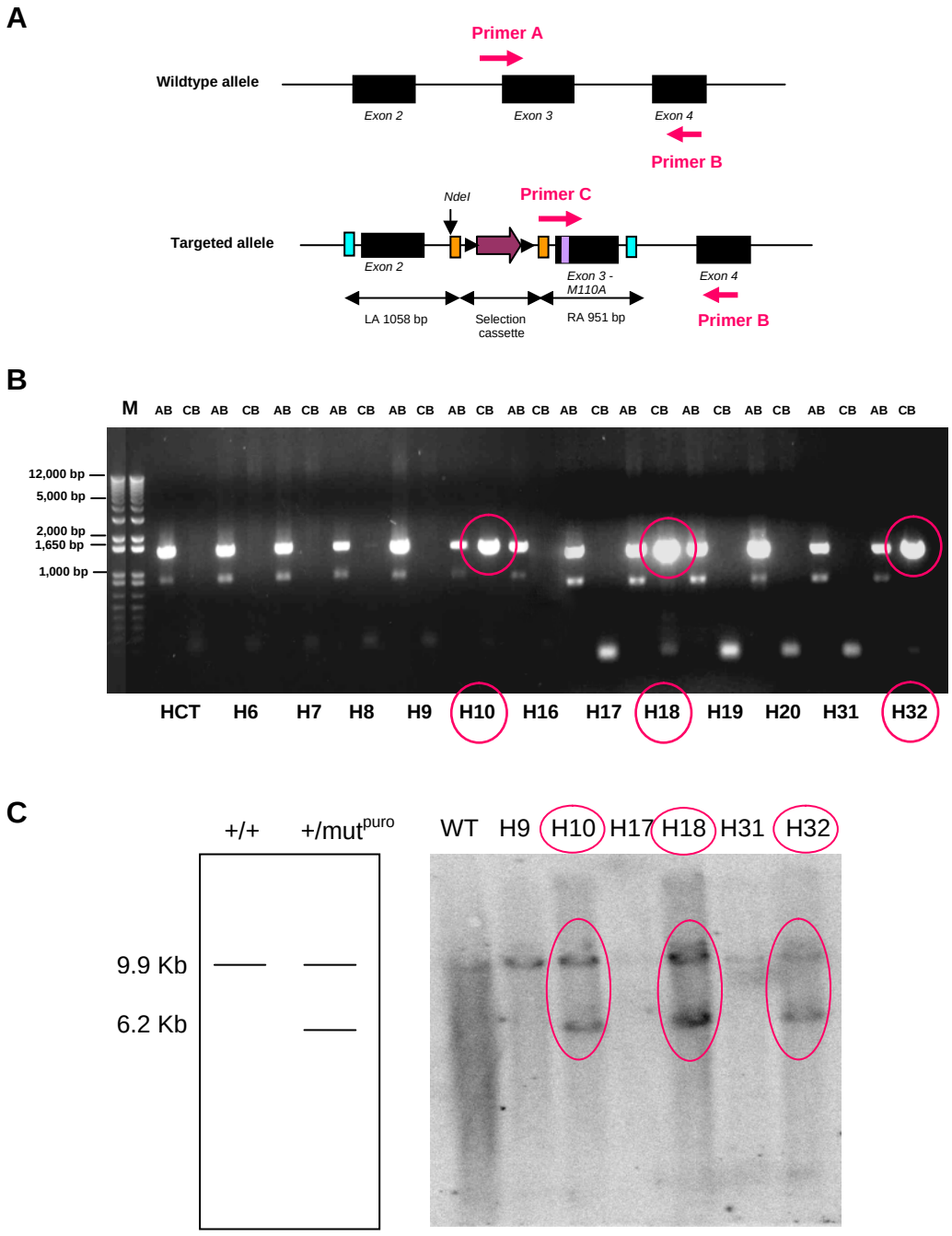

Figure 6.3 Detecting the first targeted *as* Greatwall allele

(A) Screening strategy for detection of the wildtype or targeted allele in clones. Coloured as described for **Figure 6.2 A**. PCR reactions with primer pair A and B amplify a ~ 1.5 Kb fragment from wildtype exon 3 to exon 4. PCR reactions with primer pair C and B amplify the inserted *att* sequence with the inserted M110A mutation of exon 3 producing a ~ 1.5 Kb fragment only when these extra and altered sequences are present at this gene locus. Thus allowing the presence of a targeted *as* Greatwall allele to be detected. **(B)** The results of the PCR screens using primer pairs A and B (AB) or C and B (CB). The first two lanes contain a molecular weight marker ladder (M). Run in the next lane is a PCR reaction with primer pair AB using genomic DNA from wildtype HCT116 cells (HCT) which shows the expected ~ 1.5 Kb product

from the wildtype alleles. Run in the lane after is a PCR reaction with primer pair C and B with wildtype HCT116 cell genomic DNA showing no product, indicating that they do not amplify any product from these cells DNA as no targeted allele is present. This pattern of loading is repeated for clones H6-10, H16-20 and H31-32. Positive clones are indicated by the presence of a product of ~ 1.5Kb in lanes loaded with PCR reactions using primer pair C and B. Pink circles indicate positive clones H10, H18 and H32. **(C)** Southern blot to confirm targeted alleles in the positive clones identified. The expected bands after NdeI digestion of genomic DNA are indicated schematically on the right. These are 9.9 Kb for wildtype alleles and 6.2 Kb for targeted alleles. The autoradiograph is shown on the left. The first lane shows the digestion of wildtype HCT116 cells (WT). This shows only the presence of the 9.9 Kb wildtype allele as expected, while clones H10, 18 and 32 show the presence of an additional targeted 6.2 Kb allele (circled in pink).

screening from the first eight pools (the first 40 clones) revealed the presence of a targeted allele in three of the pooled groups. Each clone from a positive pool was then screened individually (**Figure 6.3 B**). Three positive clones (H10, H18 and H32) were identified as potentially containing a targeted M110A mutant Greatwall allele as well as a wildtype Greatwall allele.

Southern blotting analysis was used to confirm the presence of a targeted allele in these three clones. The genomic DNA of the clones was digested with restriction enzyme NdeI. The PCR primers used to amplify the left homology arm for gene targeting were designed to introduce an additional NdeI site into targeted alleles (**Figure 6.2 A**). This meant that the Southern probe I had designed would anneal to a 9.9 Kb band of NdeI-digested genomic DNA downstream of the right homology arm (indicated in **Figure 6.2 A**) from wildtype alleles but would anneal to a shorter 6.2 Kb band of NdeI-digested genomic DNA in any targeted alleles. These bands could then be detected by running the digested DNA out on an agarose gel, probing with the radiolabeled probe and using an autoradiograph to visualise the band sizes. The presence of a targeted allele was confirmed in this manner in all three of the clones that had been indicated previously by PCR (**Figure 6.3 C**). That these targeted alleles carried the M110A mutation in exon three was subsequently also confirmed by sequence analysis.

6.6 Cre-mediated excision of the drug resistance gene in targeted cells

In order to recover puromycin sensitivity and ensure that the drug resistance gene did not interfere with expression of *as* Greatwall from the targeted allele, the resistance gene was excised using Cre recombinase. This then also allowed the use of the same procedure as had already been fine-tuned for these cells during the first round of targeting to target the second allele, to enable selection of homozygous targeted clones again using puromycin.

This was achieved using an adenovirus expressing Cre recombinase (Ad-CMV-Cre, Vector Labs) that mediated excision of the puromycin resistance gene by virtue of the flanking loxP sequences. Cre recombinase is a Type 1 topoisomerase from the P1 bacteriophage that catalyses site-specific recombination between loxP sites. The loxP sites comprise two inverted 13 bp repeats flanking an 18 bp spacer region that confers directionality (these sites are indicated in **Figure 6.2 A**). The presence of loxP sites in the same direction flanking the puromycin resistance gene causes it to be excised by Cre recombinase leaving a single loxP site (Park *et al.* 2001; Kohli *et al.* 2004).

To excise the puromycin resistance gene I chose to use clone H18. The cells were infected with virus with a multiplicity of infection (MOI) of 100. The cells were incubated with virus-containing media for 24 hours after which cells were plated in 96-well plates. Clones were then selected for deletion of the puromycin resistance gene by double selection in media with or without puromycin. Clones that died in puromycin but remained growing in media without puromycin were taken for analysis by Southern blotting. Five clones (H18-puro C1, 3, 4, 5, and 6) that no longer contained the puromycin resistance gene were identified by the presence of a 3.7 Kb band indicating that the gene had been excised (**Figure 6.4 A**).

6.7 Targeting the second allele

The next step was to carry out a second round of gene targeting to mutate the remaining wildtype Greatwall allele to obtain a homozygous cell line expressing the *as* Greatwall from the endogenous gene locus of both alleles.

For this I chose to use clone H18-puro C5. The cells were re-infected with freshly prepared viral stock and selection carried out in puromycin-containing media for

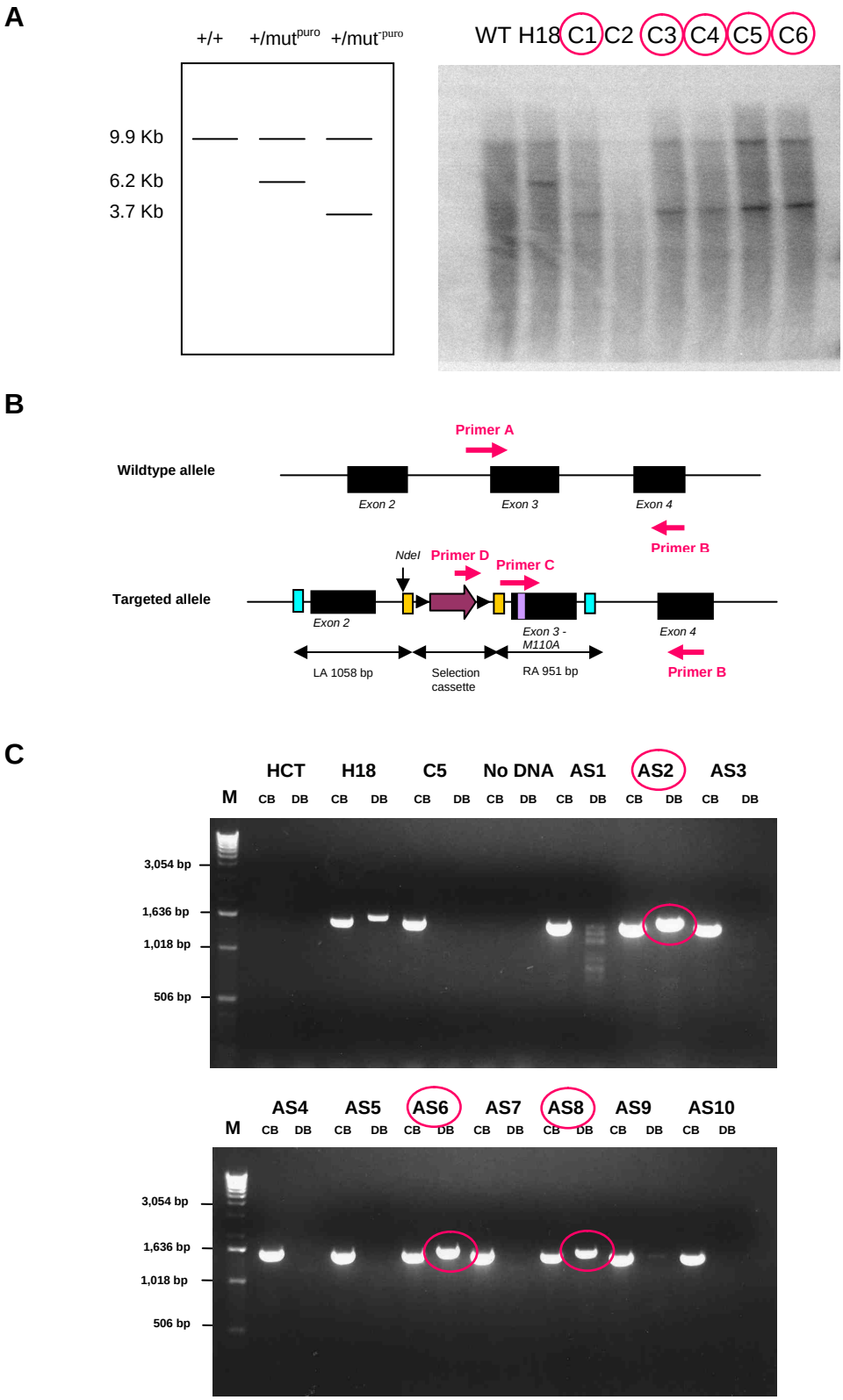

Figure 6.4 Targeting the second allele to create a homozygous *as* Greatwall knockin human cell line

(A) Southern blot to confirm the deletion of the puromycin resistance gene from targeted alleles in the positive clone H18. The expected bands after NdeI digestion of genomic DNA are indicated

schematically on the right: a 9.9 Kb for wildtype alleles (+/+), 6.2 Kb for targeted alleles (+/mut^{puro}), and a smaller 3.2. Kb band of targeted alleles with the puromycin resistance gene successfully deleted (+/mut^{-puro}). The autoradiograph is shown on the left. The first lane shows the digestion of the wildtype HCT116 cells (WT). Only the presence of the 9.9 Kb wildtype allele is detected as expected. The next lane shows the digestion of the clone H18 indicating a wildtype allele and a 6.2 Kb targeted allele containing the puromycin selection cassette as expected is present. The following lanes are digestions of genomic DNA from clones of H18 after infection with Ad-CMV-Cre that showed re-sensitisation to puromycin. The deletion of the puromycin resistance gene from the targeted allele in the clones C1, C3, C4, and C5 is indicated by the presence of the smaller 3.2 Kb band in these lanes (indicated by pink circles). **(B)** A screening strategy for detection of targeted alleles containing the puromycin resistance gene. The primer pair C and B detects the targeted alleles by amplifying DNA sequence that includes the inserted *att* sequence and M110A mutation of exon 3 producing a ~ 1.5 Kb fragment only when these extra and altered sequences are present at this gene locus. The primer pair DB anneal inside the puromycin resistance gene and will only produce a product of ~ 1.6 Kb if this gene is present in an allele. Thus, allowing newly targeted alleles to be identified. **(C)** The results of the PCR screens using primer pair C and B (CB) or D and B (DB) are shown. The first lane contains the molecular weight marker ladder (M). The next two lanes contain the PCR reactions of the wildtype HCT116 cells (HCT) with primers C and B and D and B. As expected no products are present due to the complete absence of any targeted alleles. The next two lanes show PCR reactions of the H18 clone with primers CB and DB and both show PCR products indicting the presence of a targeted allele containing the puromycin resistance gene as expected. The following two lanes contain PCR reactions with primers CB and DB with clone C5 genomic DNA in which the puromycin resistance gene has been deleted. Correspondingly only primers CB give an expected ~ 1.5 Kb product indicating a targeted allele with no puromycin resistance gene. The next two lanes indicate the control PCR reactions with no genomic DNA template added. Following these are the results of new (AS) clones generated from the second round of targeting. The clones that show products in PCR reactions with both primers CB and DB indicate the presence of a targeted allele containing the puromycin resistance gene. These clones AS2, 6, 8, and 28 are indicated circled in pink.

three to four weeks in 96-well plates. Once single colonies had formed over 200 clones were expanded into 6-well plates and allowed to grow up for a further week. Each clone was then frozen down and a sample of the cells used for genomic DNA extraction. The genomic DNA was again pooled in groups of five clones in PCR reactions using primers designed to detect the targeted allele as a positive control or the targeted allele containing the puromycin resistance gene, indicating a new targeting event (**Figure 6.4 B**). In order to detect any newly targeted alleles I designed a forward primer (primer D) situated within the puromycin resistance gene (indicated in **Figure 6.4 B**) that was again paired with the reverse primer B. If a newly targeted allele is present in the genomic

DNA from one of the clones in a particular pool then a PCR product of the correct size (~ 1.6 Kb) should been seen when the PCR reaction with primers D and B is run on an agarose gel. As a positive control a PCR product (of ~1.5 Kb) should been seen from all the PCR reactions carried out using primers C and B designed to detect the presence of the first targeted allele (as described in section **6.5**).

Each clone from positive pools was then screened individually. The first ten clones were screened in this manner and three potential positive clones (AS2, 6 and 8) were identified (**Figure 6.4 C**). The results of the PCR reactions with these clones showed a PCR product in the reaction with primers D and B as well as with primers C and B. This suggests the presence of newly targeted alleles containing the puromycin resistance gene as well as an original targeted allele, indicating that these clones were potentially homozygous clones expressing only the *as* Greatwall from both alleles. These promising results were soon proven to be flawed and further PCR analysis reveled that these clones additionally all contained a wildtype allele (**Figure 6.5 A**). This was indicated by the presence of a PCR product from a PCR reaction with primers A and B and confirmed that a wildtype allele remained at this gene locus in these clones. This disappointing result indicates that re-targeting of the original targeted allele occurred and the remaining wildtype allele was not targeted. This finding was repeated with all further clones screened.

6.8 *In vitro* analysis of *as* Greatwall activity

The result from the second round of gene targeting led me to question if mutating Greatwall at this site could render it inactive, thus causing this mutation to be lethal or severely growth inhibitory if both alleles are altered.

At the time that the results of the second round of targeting were obtained, I also completed development of a number of new tools that would allow me to investigate the *as* Greatwall mutant. I had cloned the human Greatwall cDNA and flag-tagged it (as described in **Chapter 3**). I had also finished validating the anti-Greatwall antibody. Furthermore, a paper describing an *in vitro* kinase assay using MBP as a substrate for human Greatwall was published by Burgess *et al*. (2010). They had also attempted to create an *as* Greatwall by mutation of the gatekeeper to a glycine and found that this rendered the kinase inactive (author communication). This supported my suspicion that

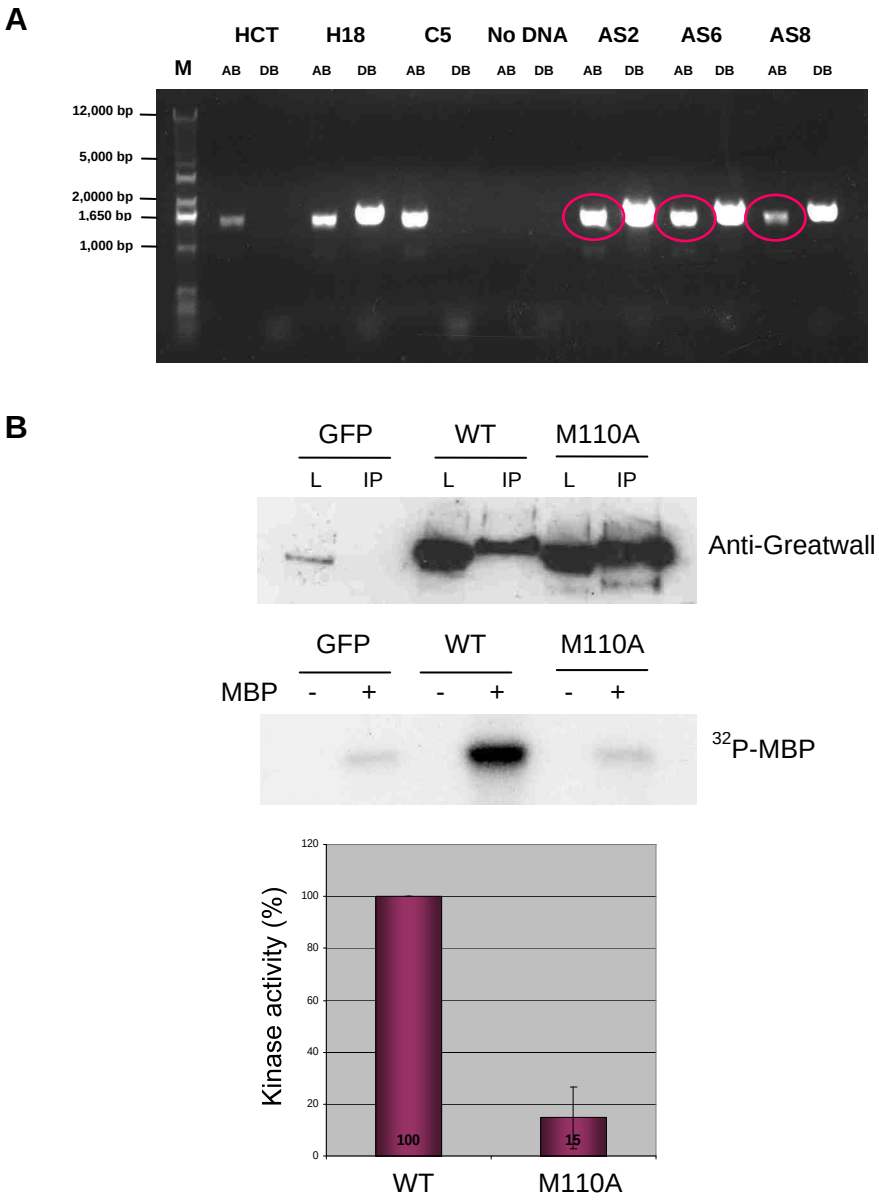

Figure 6.5 Analysis of *as* Greatwall cells

(A) The results of the PCR screening of the positive AS clones using primer pair A and B (AB) or D and B (DB) are shown (described in **Figure 6.4 B**). These AS clones should no longer contain a wildtype allele, only two targeted alleles: one with a puromycin resistance gene and one without. To test this, PCR reactions with primer pair AB (to detect the presence of a wildtype allele) and with the DB primers as a control (to detect the puromycin resistance gene containing-allele) were carried out using the potentially positive clones detected in **Figure 6.4 C**. As indicated by the presence of a product of ~ 1.5Kb in lanes loaded with PCR reactions using primers AB (indicated circled in pink), all the potentially positive clones contained a wildtype allele. This suggests that the original targeted allele is likely to have been re-targeted to produce a positive result when screened by PCR with primers DB. **(B)** Flag-tagged Greatwall or the M110A mutant was expressed in human HEK 293T cells. Cells transfected with a GFP control were analysed as well. After 24 hours the cells were treated with Nocodazole. The flag-tagged proteins were

then immunoprecipitated using anti-flag magnetic beads. An *in vitro* kinase assay was then performed using MBP as a substrate for the kinase. The top panel shows the results of SDS-PAGE analysis indicating the expression of the flag-tagged protein in the cell lysates (L) and the immunoprecipitate (IP) detected using the anti-Greatwall antibody. The autoradiograph is shown in the second panel. Quantification of the kinase activity of the mutant kinase relative to the wildtype is shown in the graph beneath. This represents results averaged from three independent experiments and the standard deviation is represented by the error bars.

the problem may lie in the mutation of the kinase and not the targeting strategy adopted. These factors prompted me to now test the kinase activity of the *as* Greatwall compared to the wildtype kinase.

I created the *as* Greatwall mutation (methionine 110 to alanine) in the flag-tagged cDNA by site-directed mutagenesis. The flag-tagged *as* and wildtype Greatwall were transfected into human HEK 293T cells and expression allowed for 24 hours. After this, the media was replaced with Nocodazole-containing media and the cells incubated for a further 16 hours to arrest the cells in mitosis, when Greatwall is maximally active. I then harvested the cells and immunoprecipitated the recombinant flag-tagged proteins using magnetic beads coated with an anti-flag antibody. The purified kinase was then taken into an *in vitro* kinase assay using MBP as a substrate. The lysates and immunoprecipitates were assessed for expression by immunoblotting and kinase activity against MBP was visualised on an autoradiograph (**Figure 6.5 B**). The *as* Greatwall showed severely reduced activity with only 15% of wildtype Greatwall kinase activity (on average, when normalised for protein amount). This result indicates that expressing two copies of *as* Greatwall would effectively render the cells Greatwall null and consequently non-viable.

6.9 Attempting to rescue the *as* kinase activity

It is known that the gatekeeper mutation renders a subset of kinases inactive, although the precise reasons for the intolerance to the mutation are not well understood (Zhang *et al.* 2005; Garske *et al.* 2011). This result unfortunately means that Greatwall falls into this 30% of kinases tested that will not tolerate the space-creating mutation of

the gatekeeper residue required for this type of chemical genetics approach to inhibit them (Zhang *et al.* 2005; Garske *et al.* 2011).

Recently, a method to rescue the activity of such intolerant kinases was described by Zhang *et al*. (2005) that should enable the chemical genetic methodology to be extended to render such kinases amenable to study using this approach. To rescue the kinase activity they attempted to identify second-site suppressor mutations that could rescue the activity of kinases that have suffered a severe loss of activity as a result of the introduction of the gatekeeper mutation. They termed these *sogg* mutations for 'suppressors of the glycine gatekeeper' (as the gatekeeper residue can be mutated to either a smaller alanine or glycine residue but glycine is most commonly used) (Zhang *et al.* 2005). Using structure-based sequence alignments of both tolerant and intolerant kinases they looked to distinguish key positions that could determine tolerant from intolerant kinases and allow second-site mutations to rescue kinase activity of intolerant kinases. The *sogg* mutations they identified were all located within the antiparallel β sheet of the kinase N-terminal subdomain, in a region that included the twelve residues of the three central β stands (the two edge strands - β1 and β4 - were excluded from the analysis as they are relatively exposed and often involved in protein-protein interactions). The single space-creating gatekeeper mutation likely destabilises this five-stranded antiparallel β sheet that contains numerous residues which are important for ATP binding and catalysis. It is therefore logical that targeted second-site mutations within this β sheet might correct the defects caused by the gatekeeper substitution. In this manner they identified successful *sogg* mutations for five highly divergent intolerant kinases that were able to suppress the loss of activity which had resulted from the single alanine or glycine gatekeeper substitution (Zhang *et al.* 2005).

A structure-based sequence alignment of Greatwall with the antiparallel β sheet in the N-terminal lobe of c-Src (a known substitution-tolerant kinase) indicated the twelve residues that comprised the central β strands which could be targets for rescuing *sogg* mutations in the *as* Greatwall (**Figure 6.6 A**). By comparison of successful *sogg* mutations introduced into the five other intolerant kinases (Cdc5, GRK2, MEKK1, Pto and APH(3')-IIIa) at these sites by Zhang *et al*. (2005), three residues were identified that could be potentially altered to restore kinase activity to the *as* Greatwall (**Figure 6.6 B**). These residues were tyrosine 59 (Y59), valine 61 (V61) and tyrosine 107 (Y107) (**Figure 6.1 D** and **Figure 6.6 B**).

These sites were mutated by site-directed mutagenesis in the wildtype kinase

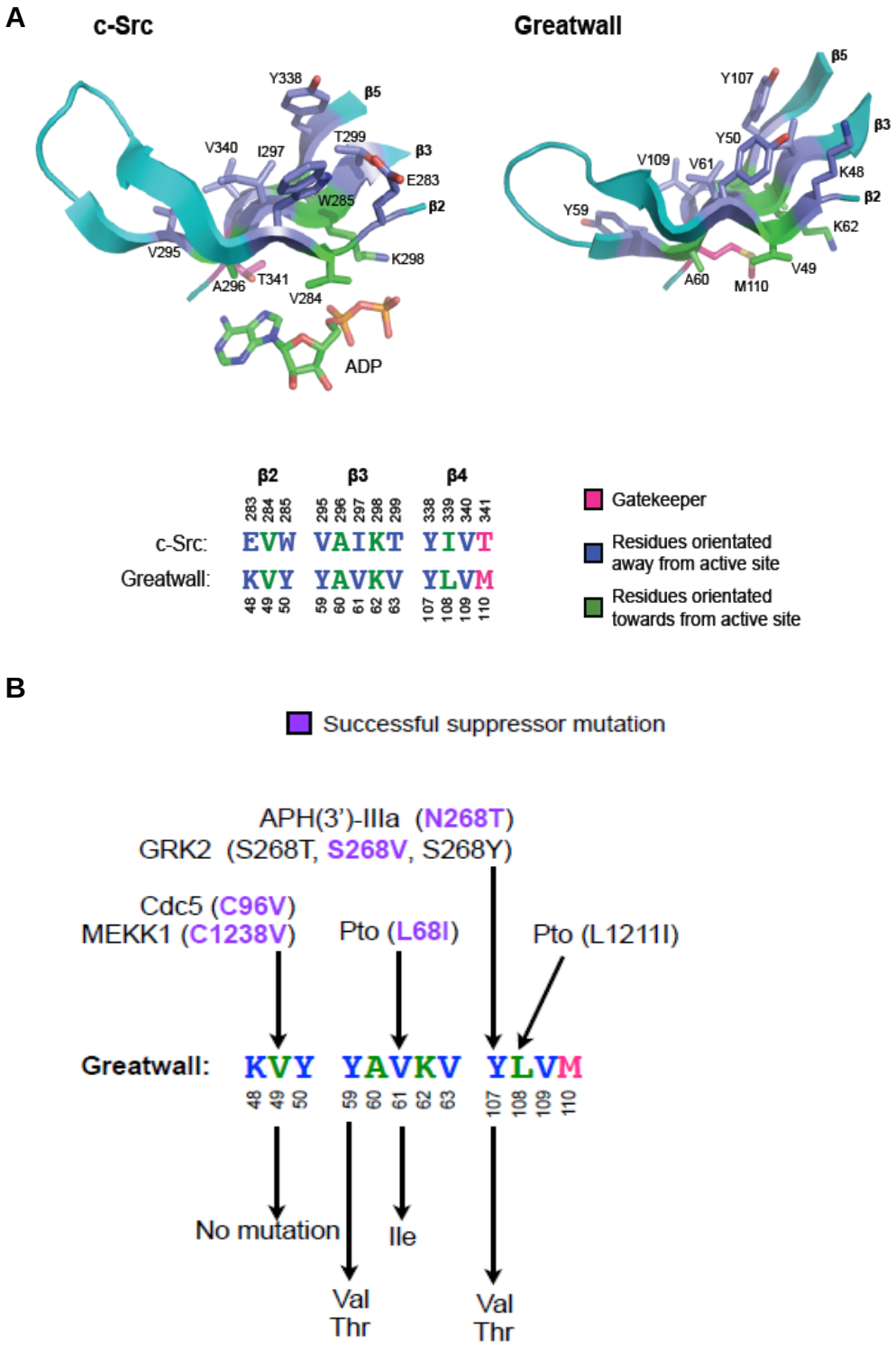

Figure 6.6 Creating second-site *sogg* mutants to rescue *as* kinase activity

(A) Structure-based sequence alignment of the antiparallel β sheet in the N-terminal lobe of Greatwall with that of c-Src. Indicated are the twelve residues that comprise the central β strands that could be targets for rescuing *sogg* mutations in the *as* Greatwall. Created by Dr. Anthony Oliver from the GDSC at the University of Sussex. **(B)** Central strands of the antiparallel β sheet in the N-terminal lobe of Greatwall with sites for potential rescuing *sogg* mutations indicated. This information is based on work

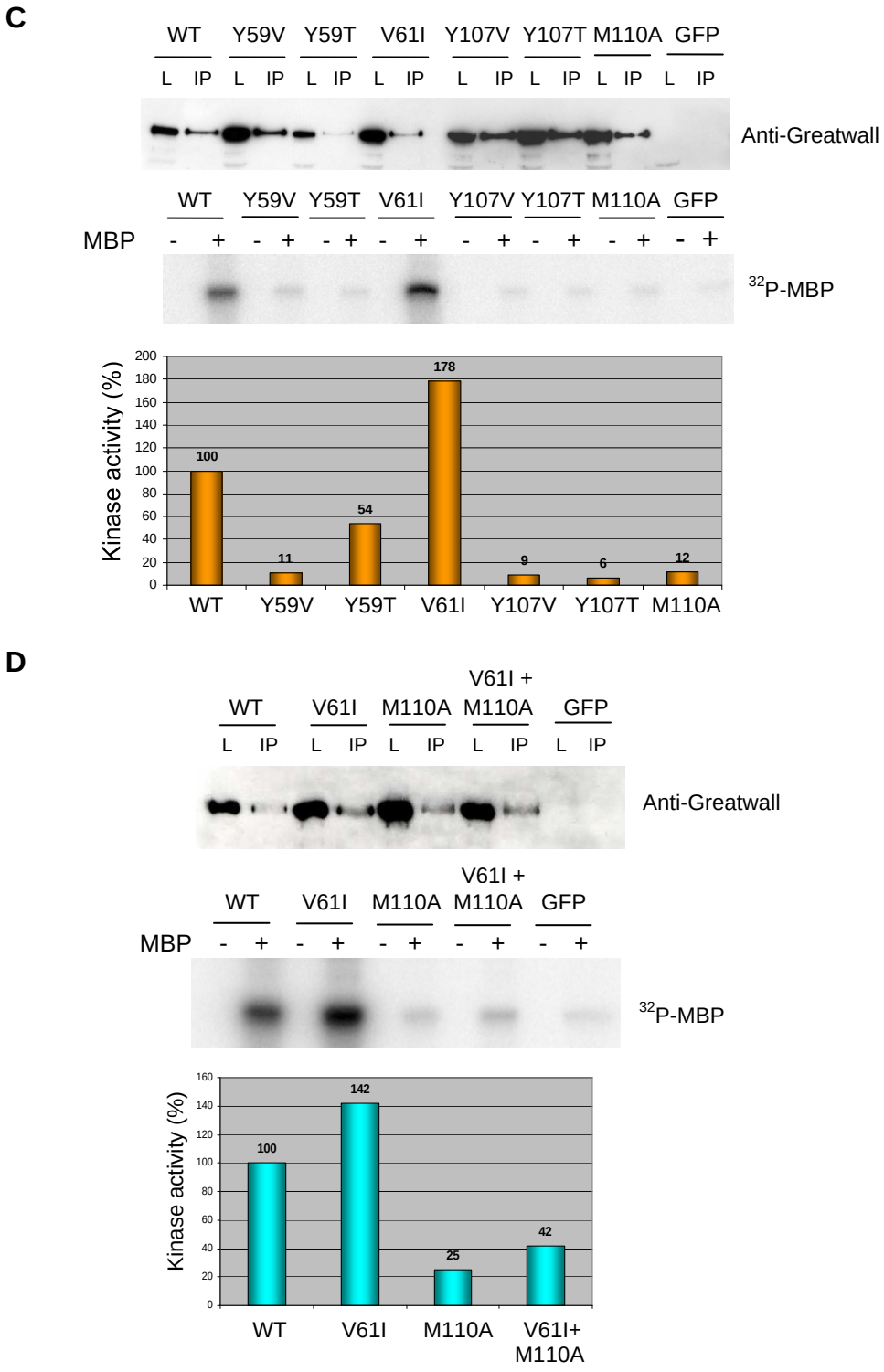

by Zhang *et al*. (2005). Again created by Dr. Anthony Oliver. **(C)** Flag-tagged Greatwall or mutants Y59V, Y59T, V61I, Y106V, Y107T and M110A were expressed in human HEK 293T cells, immunoprecipitated and taken into a kinase assay as described for **Figure 6.5 B**. **(D)** Flag-tagged Greatwall or mutants V61I, M110A and double mutant V61I+M110A were expressed in HEK 293T cells, immunoprecipitated and taken into a kinase assay as described for **(C)**.

initially to ensure that these mutations alone did not significantly alter the kinase activity or stability. Five mutants were made: Y59 was altered to either a valine (Y59V) or a threonine (Y59T), V61 was changed to an isoleucine (V61I) and Y107 was changed to either a valine (Y107V) or a threonine (Y107T). These mutants were then expressed with a flag-tag in HEK 293T cells and an *in vitro* kinase carried out (as described in section **6.8**). The results (**Figure 6.6 C**) indicate that mutation of Y107 to either a valine or threonine severely reduces kinase activity, with these mutants displaying only 6% and 9% of the activity of the wildtype kinase, respectively. Mutation of Y59 also reduced kinase activity, with threonine mutant displaying only 54% of wildtype kinase activity and the valine mutant having even less activity with only 11% of that of the wildtype kinase. This suggests that any mutation of the residues at these positions negatively effects kinase activity and would therefore be undesirable *sogg* mutations. Mutation of V61 to isoleucine, however, led to a significant increase in activity of the kinase (with 178% of that of wildtype kinase activity). This led me to attempt to rescue the *as* Greatwall kinase activity by mutating V61 to isoleucine (V61I) in the *as* Greatwall mutant. The results of the kinase assay carried out with the potential *sogg* mutant in the *as* Greatwall are shown in **Figure 6.6 D**. Unfortunately, the double V61I+M110A Greatwall mutant showed only 42% kinase activity as compared with the wildtype kinase. This is an increase in activity to that of the *as* Greatwall mutant alone, but is a long way from fully restoring the kinase activity to that of the native enzyme and is unlikely to be sufficient to support the cellular function *in vivo*.

6.10 Further mutagenesis to rescue kinase activity of *as* Greatwall

The mutation of M110 to a glycine instead of an alanine could have been attempted but, as mentioned previously, another group had reported to us that this was unsuccessful and rendered the kinase equally inactive (Burgess *et al.* 2010). These unpromising results from the *as* and *sogg* mutations of Greatwall led me to try a different approach. The Calcium-Dependant Protein Kinase 1 (CDPK1) is a naturally analogue sensitive kinase found in the parasite *Toxoplasma gondii* (Sugi *et al.* 2010). It has a glycine residue at the gatekeeper position in its ATP-binding pocket and is efficiently inhibited with the bulky ATP-analogue, 1NM-PP1. In fact, mutation of the gatekeeper residue from a glycine to a methionine has been shown to result in resistance

to the inhibitor (Sugi *et al.* 2010). By overlaying the structures of CDPK1 and the threaded Greatwall kinase domain, the residues involved in binding to the bulky ATP-analogue 1NM-PP1 (and related compounds) could be examined. Based on this sequence analysis performed by our collaborator, Dr. Anthony Oliver from the GDSC at the University of Sussex, I created a further mutant to try and achieve an *as* Greatwall with full kinase activity.

I mutated valine 94 to a methionine in combination with the M110A by site-directed mutagenesis. The mutation of the gatekeeper residue to a small amino acid can lead to attenuated kinase activity likely by disruption of a 'hydrophobic spine' which is required to stabilise the active conformation (Garske *et al.* 2011). This double mutant should have the effect of shifting the methionine from one side of the pocket to the other to restore the hydrophobic spine critical for the active conformation and thus for kinase activity as well as providing a stacking interaction with the bulky ATP-analogue inhibitor (**Figure 6.1 D**, **F** and **G**). This mutant was expressed flag-tagged in HEK 293T cells and their activity assessed by an *in vitro* kinase assay (**Figure 6.7 A**). The double mutant V94M+M110A did not show much improved kinase activity, with only 30% of wildtype kinase activity, which is unlikely to be sufficient to support kinase function *in vivo*.

6.11 Creating an *es* Greatwall

A paper published in 2011 described an alternative chemical genetic strategy for targeting protein kinases (Garske *et al.* 2011). This strategy aims to overcome the problems of kinase activity loss as a result of mutation of the gatekeeper residue to achieve specific inhibition via shape complementarity with a bulky ATP-analogue. This alternative strategy is based on covalent complementarity between an engineered gatekeeper cysteine and an electrophilic inhibitor. The introduction of a cysteine gatekeeper enables specific and potent inhibition with an electrophilic small molecule inhibitor by covalent complementarity without the need to enlarge the ATP-binding pocket. This cysteine gatekeeper also preserves the geometry and hydrophobicity of the ATP-binding pocket better than substitution to an alanine or glycine, allowing the native conformation to be retained as well as the kinase stability and activity. This is an important advantage as increasing evidence suggests that the conformation of the ATP-

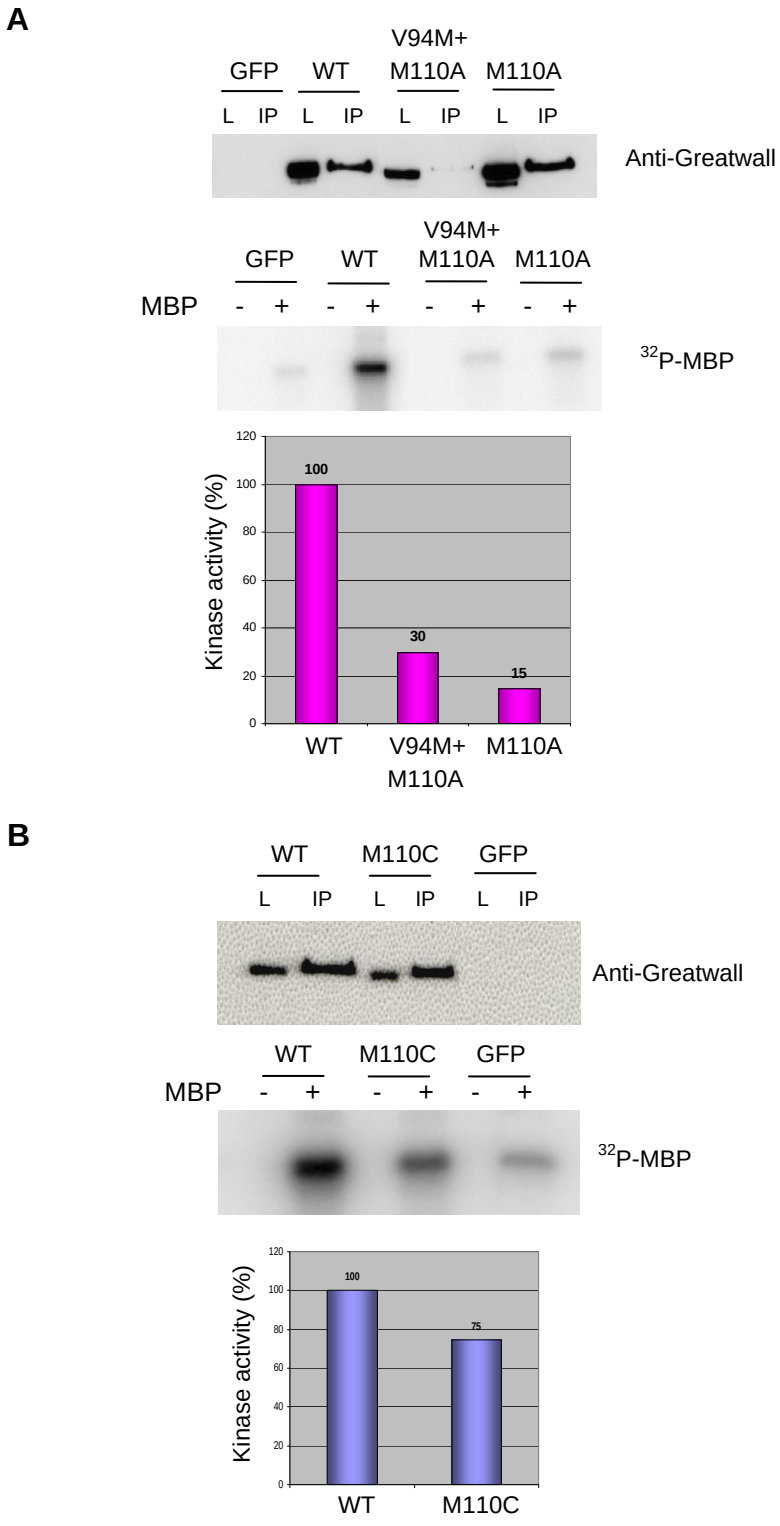

Figure 6.7 Creating other mutants to allow selective inhibition of Greatwall kinase

(A) Flag-tagged Greatwall or mutants M110A and V94M+M110A were expressed in human HEK 293T cells, immunoprecipitated and taken into a kinase assay as described for **Figure 6.5 B**. **(B)** Flag-tagged Greatwall or mutant M110C were expressed in HEK 293T cells, immunoprecipitated and taken into a kinase assay as described for **(A)**.

binding pocket has additional non-catalytic functional roles, such as in facilitating priming phosphorylation events and membrane recruitment (Cameron *et al.* 2009; Okuzumi *et al.* 2009; Garske *et al.* 2011). Kinases engineered with a cysteine gatekeeper are known as electrophile-sensitive (*es*) kinases (Garske *et al.* 2011).

Based on this work I attempted to create an *es* Greatwall by mutating the gatekeeper methionine to a cysteine by site-directed mutagenesis. I then expressed this *es* Greatwall with a flag-tag in HEK 293T cells and tested the mutant kinase activity in an *in vitro* kinase assay (**Figure 6.7 B**). The *es* Greatwall showed a promising 75% activity compared to the wildtype kinase. Investigation of the ability of this *es* Greatwall to support cellular function *in vivo* now needs to be determined and this work is currently underway.

6.12 Conclusions and discussion

My attempts to make a stable human cell line expressing an *as* Greatwall by substituting the gatekeeper methionine for a smaller alanine were unsuccessful. Despite this, the Gateway® cloning technology and AAV system utilised here were highly successful and were used to good effect to perform gene targeting in a human cell line. Furthermore, the PCR screening strategy developed to detect locus-specific targeting events was highly successful allowing for rapid and reliable screening of positive clones. The reason that this work failed was made clear by the finding that the loss of the methionine from the ATP-binding pocket likely caused the active conformation of the kinase to become inactive/unstable. The leads to the inevitable conclusion that any cells homozygous for an *as* Greatwall would have been rendered non-viable as they would have effectively been Greatwall null.

My attempts to rescue the stability of the active *as* kinase by creating a series of second-site *sogg* mutations in the antiparallel β sheet of the kinase N-terminal subdomain were also not successful. One mutant, V61I, seemed to achieve a slight increase in activity (to 42%) when combined with the *as* mutant but this improvement would not be sufficient to support the cellular function *in vivo*.

More encouragingly, the *es* mutant, created in a final attempt to produce a selectively inhibitable Greatwall kinase, showed a good level of kinase activity.

Furthermore, the *es* Greatwall might have sufficient activity remaining (with 75% kinase activity) to be functional *in vivo* and this is now being investigated.

In order to definitively determine if either of the gatekeeper residue substitutions (*as* or *es*) are sufficient to support cellular function *in vivo*, a siRNA rescue system would be invaluable. Creating these gatekeeper substitutions in a siRNA resistant Greatwall would allow them to be used to perform a rescue in human cells after Greatwall knockdown by RNAi. This system is currently in development and will ultimately allow the assessment of the gatekeeper substitutions functionality *in vivo*. Until such a system is available to validate these findings I can only draw conclusions based on the results reported here.

In general, it seems that for Greatwall kinase, substitution of the gatekeeper methionine with a glycine or alanine impacts negatively on its activity and is not a feasible method to engineer an inhibitable kinase. More encouraging are the results of substitution of the gatekeeper with a cysteine residue. The initial analysis of these mutants described here indicate that engineering the ATP-binding pocket with a cysteine residue may offer a promising future strategy for inhibiting human Greatwall using a chemical genetic approach.

CHAPTER 7. Investigation of Greatwall kinase as a target for cancer therapy

7.1 Introduction

Greatwall has been implicated to play a critical role in mitotic entry, maintenance of the mitotic state and mitotic exit in *Drosophila* larvae and tissue culture cells, *Xenopus* egg and CSF extracts, primary mouse embryonic fibroblasts, and transformed human cell lines (Yu *et al.* 2004; Yu *et al.* 2006; Burgess *et al.* 2010; Manchado *et al.* 2010; Voets *et al.* 2010). As a result, it is now generally accepted that Greatwall is an essential player in mitotic control that is conserved from flies to humans. These systems all represent early embryonic cell cycles or transformed unnatural cell cycles that have been manipulated and selected specifically for artificial or unnatural growth. That these systems have been extremely successful in the past at identifying and defining critical components of cell growth is undeniable. However, during my work on the human Greatwall, some of the results I obtained (that are presented here in the final results chapter of my thesis) have led me to question if Greatwall is truly the widespread regulator of normal cell growth that recent studies might suggest.

The only human disease that has been linked to a loss of Greatwall activity to date is a relatively mild autosomal dominant thrombocytopenia in which patients display defective megakaryocyte maturation (Gandhi *et al.* 2003). This results from a single inactivating point mutation of Greatwall (E167D). Clinically, this mild-moderate thrombocytopenia results in easy bruising but few serious complications from bleeding (Johnson *et al.* 2009). Additionally, its knockdown in zebrafish does not affect development but was associated with a reduction of platelet levels. Moreover, Johnson *et al*. (2009) reported that expression of Greatwall in human tissues is restricted to megakaryocytes and cancer cell lines. Greatwall mRNA was undetectable in all other human tissues tested, including: brain, thalamus, pituitary gland, spinal chord, heart, stomach, kidney, lung, testis, and ovary (Johnson *et al.* 2009). These data strongly contradict the concept that Greatwall is a cell cycle regulator required in all proliferating cells. As a consequence, it remains unclear whether Greatwall is essential for cell cycle

control in all cells and to what extent Greatwall inactivation effects survival of transformed and non-transformed cell lines. It is possible that human Greatwall is not widely expressed or required for the proliferation of normal somatic cells but is instead up-regulated and/or utilised specifically in rapidly dividing tumor cells. Thus, cancer cells could be exquisitely sensitive to Greatwall inactivation. This would make Greatwall an extremely attractive target for cancer therapy because its inactivation may have only very limited side effects in non-cancerous proliferating tissues leading to a wide therapeutic index.

The data presented in this chapter represents preliminary experimental evidence that this might indeed be the case, indicating that Greatwall has potential as a key clinical biomarker and an important target for cancer therapy.

7.2 Characterising Greatwall knockdown in HeLa and RPE cells

During my initial characterisation of Greatwall in human cells I worked with two cell lines: the well characterised transformed human cervical cancer HeLa cell line, and the non-transformed hTERT-immortalised human RPE cell line. Greatwall knockdown in HeLa cells led to severe mitotic phenotypes that ultimately resulted in a cell cycle arrest and apoptosis (described in depth in **Chapter 3**). In the RPE cells, however, I saw no apparent effects on their growth after Greatwall depletion (**Figure 7.1 A**). At 72 hours after Greatwall knockdown, all the HeLa cells were dead or dying while the RPE cells continued to grow and reach full confluency. That Greatwall had been fully depleted in both these cell lines was confirmed by western blot (**Figure 7.1 B**). An additional positive control siRNA that depleted the essential mitotic kinesin, Eg5, showed that it caused a cell cycle arrest as expected in both cell lines, further confirming that transfection and knockdown in these cells was successful (**Figure 7.1 A**). It also indicates that the knockdown of essential mitotic proteins in the RPE cells produces a phenotype.

In order to confirm that Greatwall knockdown has no effect on RPE cell growth, I depleted Greatwall in both cell lines again, this time using two different siRNA oligomers to target Greatwall mRNA transcripts. Again, the HeLa cells were arrested and died upon Greatwall knockdown in both cases while the RPE cells remained unaffected (**Figure 7.1 C**). Another knockdown was performed in the RPE cells using

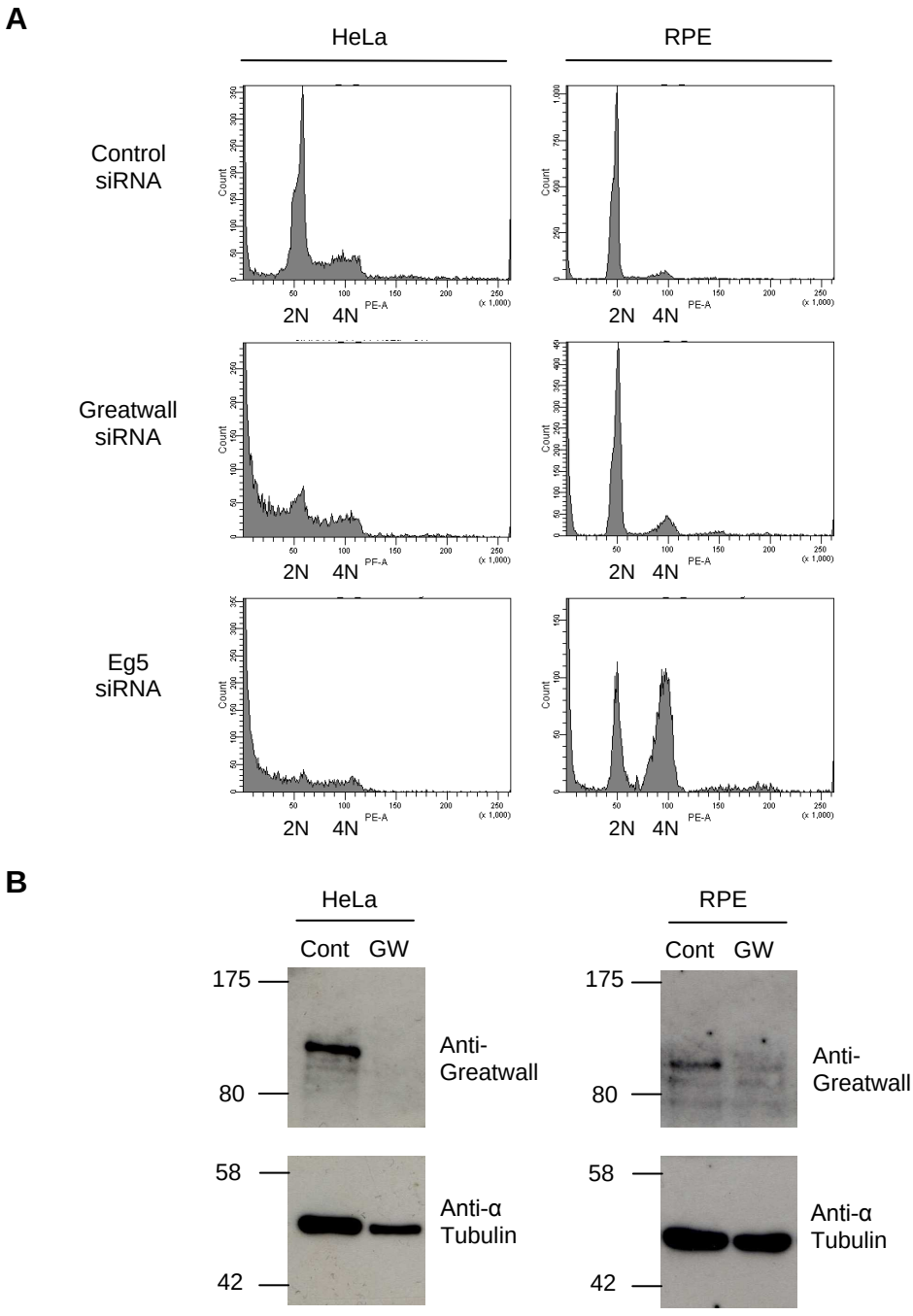

Figure 7.1 Greatwall depletion in HeLa and RPE cells

(A) Cell cycle (FACS/PI) profiles of HeLa and RPE cells that had been treated with 25 nM Greatwall siRNA for 72 hours. A negative control scrambled siRNA and positive control Eg5 siRNA were also used. **(B)** SDS-PAGE analysis of the HeLa and RPE cells that had been treated with 25 nM Greatwall siRNA (GW) for 72 hours. The negative control scrambled siRNA (Cont) was also used. In the top panel Greatwall levels were assessed using the anti-Greatwall antibody and it is clearly depleted in the samples treated with Greatwall siRNA but is detected in cells treated with the control siRNA. An anti-α Tubulin antibody was used to assess tubulin levels in the cells as a loading control, shown in the lower panel.

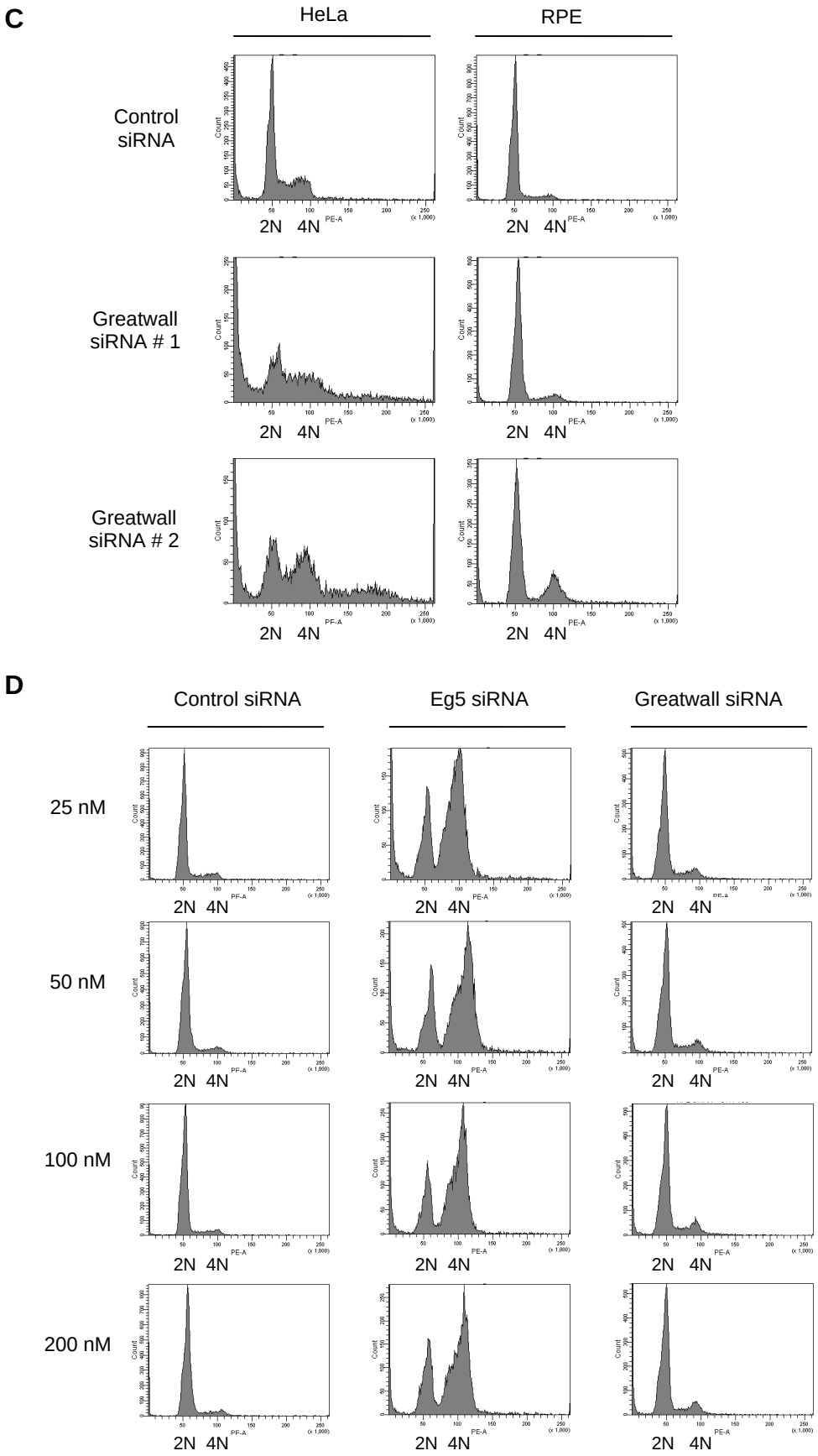

(C) Cell cycle (FACS/PI) profiles of HeLa and RPE cells that were treated with 25 nM Greatwall siRNA for 72 hours. The control scrambled siRNA was used as a negative control and two different Greatwall

siRNAs (#1 and #2) were used. **(D)** SiRNA titration in RPE cells. Cell cycle (FACS/PI) profiles are shown of RPE cells that had been treated with varying concentrations (from 25 nM to 200 nM, as indicated) of Greatwall siRNA for 72 hours. The negative control scrambled siRNA and positive control Eg5 siRNA were also used. The Eg5 siRNA phenotype seen indicates that knockdown of essential mitotic proteins leads to cell cycle arrest and cell death in RPE cells.

increasing concentrations (25 nM to 200 nM) of Greatwall siRNA (**Figure 7.1 D**). Even when 200 nM siRNA was used to deplete Greatwall in these cells, no effect was seen on their growth. These results were completely unexpected and led me to begin to question if Greatwall might in fact represent a kinase specifically utilised to license cell cycle progression only in certain cell types, rather than as a universal cell cycle regulator for all cells. When I looked back through the available literature concerning Greatwall and the types of systems used to study this kinase so far my suspicions were compounded, suggesting further investigation in other cell lines was warranted.

7.3 Evaluating Greatwall knockdown in other human cell lines

In order to further explore this observation, that HeLa and RPE cells respond very differently to Greatwall knockdown, I decided to examine if there are differences in the responses of other cell lines. HeLa cells are a transformed cancer cell line, while RPE cells are non-transformed and thus are considered to represent more ‘normal’ cells for studying growth. This led me to hypothesise that transformed and cancer cell lines, like those used to study human Greatwall thus far, might have up-regulated Greatwall expression in order to drive their cell cycles in a manner not utilised or required in normal non-transformed cells.

I obtained several transformed and non-transformed cell lines and tested the effect of Greatwall knockdown in these lines. I used the transformed cell lines; HeLa Kyoto cells (a derivative line of HeLa cells from Japan) and human colorectal cancer HCT116 cells. In addition, I used the non-transformed cell lines: human fibroblast 1BRhTERT cells and human fibroblast 48BRhTERT cells. I again used HeLa and RPE cells to act as control cell lines. The results obtained, as judged by FACS analysis (**Figure 7.2 A**), showed a similar trend that I observed for the HeLa and RPE cells. The

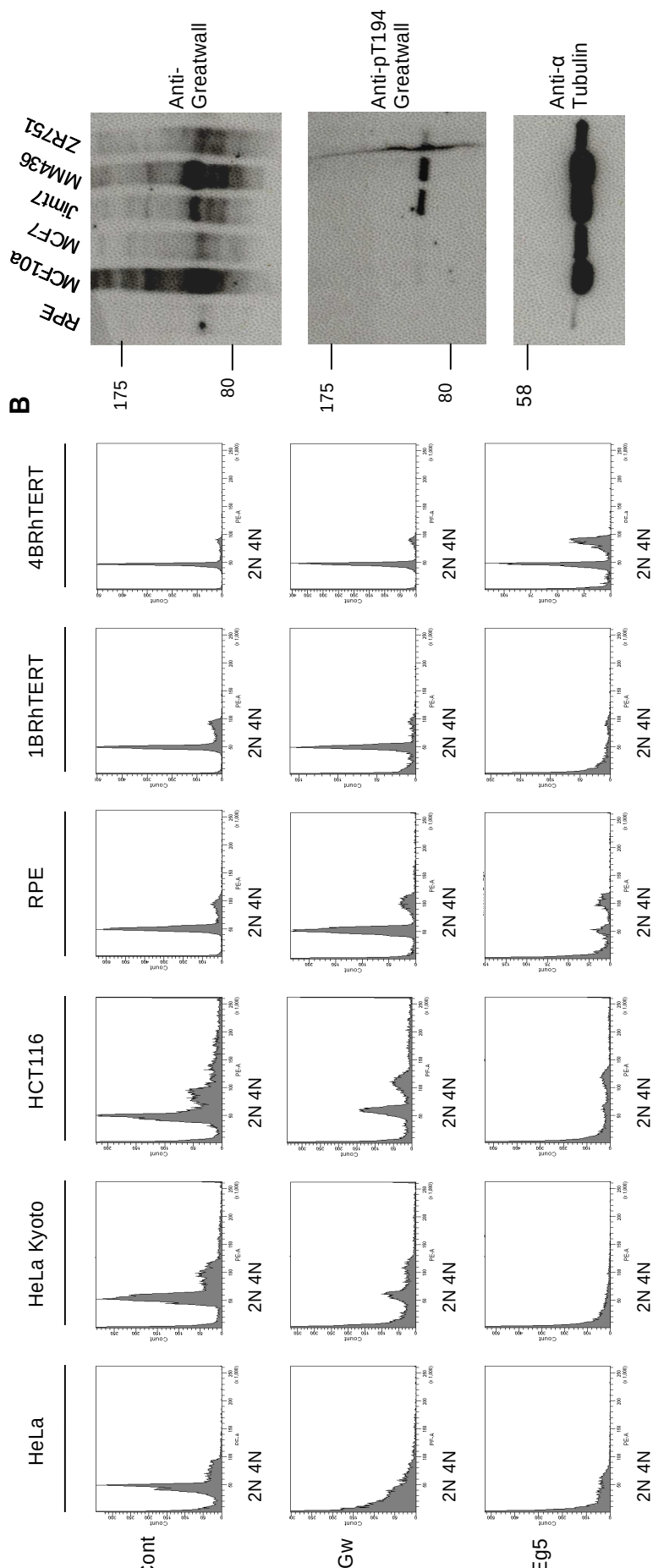

Figure 7.2 Evaluating Greatwall in other human cell lines

(A) Cell cycle (FACS/PI) profiles of cells that had been treated with 25 nM Greatwall siRNA (GW), a control scrambled siRNA (Cont), or with a positive control siRNA for Eg5 (Eg5) for 72 hours. **(B)** SDS-PAGE analysis of four breast cancer cell lines for Greatwall activation. Greatwall expression levels were detected using the anti-Greatwall antibody (top panel) and the anti-T194 antibody was used to probe for the presence of Greatwall phosphorylated on T194 (middle panel) in these different cell lines while an anti-α Tubulin antibody (bottom panel) was used as a loading control. The RPE cells and a normal human breast cell line (MCF10a) were also loaded for comparison.

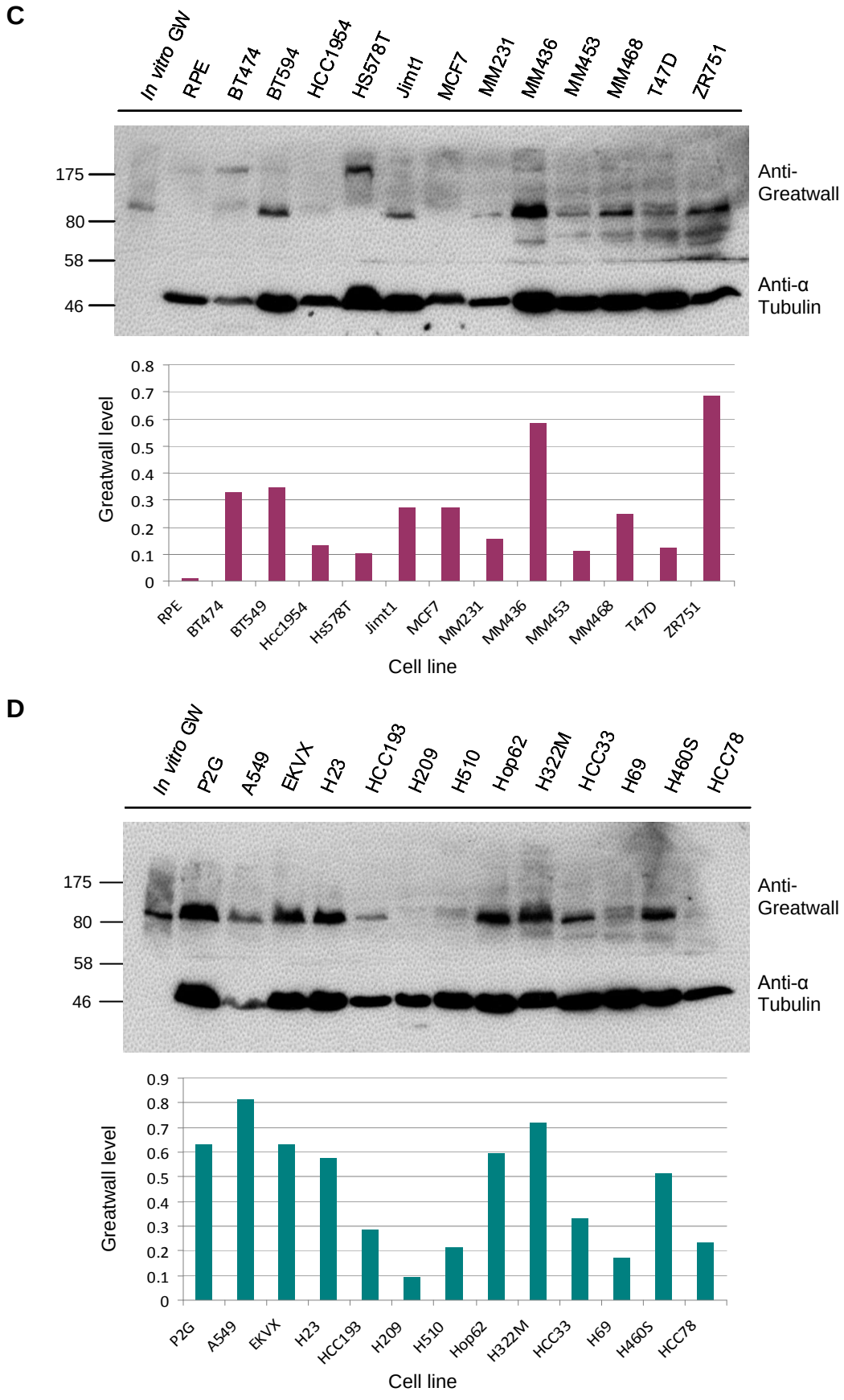

(C) SDS-PAGE analysis of a cohort of human breast cancer cell lines. Greatwall expression levels were detected using the anti-Greatwall antibody (top), and an anti-α Tubulin antibody (bottom) was used as a

loading control. The *in vitro* translated Greatwall (*In vitro* GW) and RPE cells were also loaded as controls. Quantification of the immunoblot (carried out by Dr. Victoria Haley from the Trafford Centre at the Brighton and Sussex Medical School) indicating Greatwall expression levels relative to tubulin are shown in the graph below. **(D)** SDS-PAGE analysis of a cohort of human lung cancer cell lines. Greatwall expression levels were detected and quantified as for **(C)**. The *in vitro* translated Greatwall (*In vitro* GW) and a normal human lung cell line (P2G) were also loaded for comparison.

non-transformed 1BRhTERT and 48BRhTERT cells showed no cell cycle arrest or cell death after Greatwall depletion, as also seen for the RPE cells. The transformed HeLa Kyoto and HCT116 cells showed a cell cycle arrest and apoptosis after Greatwall depletion, as also seen in the HeLa cells.

Although this is only a very small number of cell lines to have tested, the trend that Greatwall depletion results in cell cycle arrest and apoptosis in transformed cell lines but does not effect normal non-transformed cell lines holds true in this experiment. This finding is intriguing and clearly suggests further exploration of the effect is required. To this end, I decided to evaluate Greatwall kinase in a further cohort of human cancer cell lines.

7.4 Evaluating Greatwall expression in a cohort of cancer cell lines

In order to characterise Greatwall in human cancer cell lines I collaborated with Professor Peter Schmid's team in the Clinical Oncology Laboratory at the Brighton and Sussex Medical School. Together, we initiated a preliminary study of Greatwall in a cohort of breast and lung cancer cell lines.

I began by assessing the expression of Greatwall in these cancer cell lines by immunoblotting. A panel of twelve human breast cancer and twelve human lung cancer cell lines were used. For all cell lines, 1 x 10^5 cells were lysed in sample buffer and loaded. *In vitro* translated Greatwall and RPE cells were loaded as controls and a normal human lung cell line, P2G cells, was also loaded for comparison. The results of the immunoblot revealed that Greatwall expression varied widely across the different cell lines (**Figure 7.2 C and D**).

I then selected four of the breast cancer cell lines to begin to investigate if Greatwall activation varied between the cancer cell lines. For this, two cell lines

expressing high levels of Greatwall, and two medium level expressing cell lines were used. The RPE cells and a normal breast cancer cell line (MCF10a) that had been recently obtained were also loaded as controls. The results indicate that Greatwall activation levels also vary between breast cancer cell lines and may not necessarily correlate with the levels of Greatwall protein expression (**Figure 7.2 B**).

In order to determine the sensitivity of these cells to Greatwall knockdown using siRNA, colorimetric (MTT cell proliferation) and clonogenic (crystal violet) assays are currently in development. A limitation of this approach is that different cell lines have very different growth rates and transfection efficiencies as well as varying tolerance to transfection reagents, making it difficult to precisely quantify and compare the effects of Greatwall knockdown. It will of course be crucial to produce a clear and in-depth evaluation of these aspects of Greatwall in these cell lines before any conclusions about Greatwall as a potential biomarker or anti-cancer drug target can be drawn.

7.5 Conclusions and discussion

The preliminary work presented here supports the idea that Greatwall could potentially be an important prognostic biomarker and therapeutic target for cancer therapy. Greatwall knockdown causes cell cycle arrest and apoptosis in transformed cell lines but has little impact on survival of non-transformed cells. Moreover, the expression and activation of Greatwall varies greatly among breast and lung cancer cell lines. Intriguingly, this suggests that some cancer cells could be exquisitely and specifically sensitive to Greatwall inactivation. These data are clearly insufficient to definitively draw conclusions about the true nature of the role that Greatwall plays in cell cycle control in somatic or tumor cells. Further experiments will be necessary in order to confirm these findings and evaluate Greatwall as a therapeutic target.

While Greatwall is clearly critical for early embryonic cell cycles in *Xenopus* and *Drosophila* and is required for survival of at least some cancer cells, the findings discussed here suggest that it might not be an essential protein in all somatic cells. This could mean that the essential cell cycle control mechanisms have changed in specific tumor cells, reverting them back into a state similar to early embryonic cell cycles, that critically requires the activity of Greatwall. If this hypothesis is correct then Greatwall could be an ideal target for cancer therapy that shows high specificity for selective

tumors. If this hypothesis can be verified, further in depth work will be necessary to elucidate the precise mechanism of the switch from one state, in early embryogenesis, to the other in somatic cells.

Greatwall is a particularly promising therapeutic target because it combines an essential role in mitosis as well as a function in recovery from a DNA damage-induced cell cycle arrest (Peng *et al.* 2010; Voets *et al.* 2010). The development of new drugs and therapies to target cancer are a major focus of current endeavors to improve patient survival. Many of the most widely used chemotherapy agents target DNA damage checkpoints (e.g. Cisplatin, camptothecin) or the mitotic spindle checkpoint (e.g. Taxanes, Vinca Alkaloids) (Sudakin *et al.* 2007; Ljungman 2009). These chemotherapeutic agents are relatively non-specific and result in many unwanted side effects and a narrow therapeutic index. The development of more selective agents with a wide therapeutic index is highly desirable. DNA damage response factors and mitotic kinases have been at the vanguard of these endeavours (Girdler *et al.* 2006; Perez de Castro *et al.* 2008). Greatwall combines an essential role in mitosis and recovery from the DNA-damage response making it a novel target. This dual role for Greatwall in cell cycle control sets Greatwall apart from other kinases. This, combined with the evidence presented here that its role in cell cycle progression and proliferation is limited in somatic cells but may be essential for survival in certain cancer cells, strongly suggests that further investigations should be undertaken. It means that Greatwall could potentially represent an ‘Achilles heel’ for some tumors which could be exploited therapeutically for synthetic lethality strategies that might allow more selective killing of cancer cells with only limited effects on normal proliferating tissues.

CHAPTER 8. General discussion and future directions

8.1 General discussion

The work presented here has focused on elucidating the role of Greatwall kinase in human cells. The development of tools, including an anti-Greatwall antibody and a flag-tagged Greatwall, allowed the investigation of the kinase. Using these tools I determined that the human Greatwall protein is expressed at similar levels throughout the cell cycle and is activated by phosphorylations at the G2/M transition and remains phosphorylated until mitotic exit. The overexpression of the protein is well tolerated in human cells while its depletion, by siRNA, leads to problems at G2/M transition and numerous mitotic defects that correspond to the level of knockdown achieved. This data, in combination with other studies published during this work (Burgess *et al.* 2010; Voets *et al.* 2010), indicate that human Greatwall kinase's role in cells is likely equivalent to that of the *Drosophila* and *Xenopus* Greatwalls. It is required to inactivate PP2A, via phosphorylation of Ensa/Arpp19, at the G2/M transition to allow CDK1 mitotic phosphorylations to dominate and drive entry into mitosis.

The use of structural modeling, phosphorylation site mapping and mutagenic analysis has allowed the investigation of Greatwall's mechanism of activation. It is a particularly unusual kinase because it has a rare bifurcated kinase domain that is split by a large stretch of approximately 500 non-conserved amino acids. This initially led to scepticism about if this was a true protein kinase at all. It is now clear that this is a functional kinase and the work presented here has identified key features of the kinase fold. A model of the predicted kinase domain structure was produced using the computational protein structure prediction engine PHYRE by Dr. Anthony Oliver from the GDSC at the University of Sussex. This, combined with phosphorylation site mapping of the kinase using PhosSitePlus, allowed the identification of key residues that could contribute to Greatwall kinase activity. Production of mutant forms of Greatwall validated the predicted structural model and allowed identification of the activation loop, P+1 loop, and turn motif of Greatwall kinase. The work present when amalgamated with the investigations carried out in two other studies (Vigneron *et al.* 2011; Blake-Hodek *et al.* 2012), led to the proposal of a potential novel three-step

mechanism for Greatwall activation. In this model, activation is begun by priming phosphorylations of threonines, T194 and T207, in the activation loop. This results in initial low kinase activity that allows autophosphorylation of the turn motif on S874 in the C-terminal tail. This then likely mediates the docking and/or interaction of the hydrophobic motif binding pocket with a phosphorylated hydrophobic motif of another, as yet unknown, AGC kinase. Once bound Greatwall is then fully active. This mechanism of activation is somewhat unexpected but is supported by the experimental evidence and is in keeping with the highly intricate mechanisms that control other AGC kinase activities (Pearce *et al.* 2010). A crystal structure of the kinase would provide an invaluable insight into the exact mechanisms of activation of this novel kinase. The Greatwall artificial splicing variants that I generated as part of this work have subsequently been purified from *E.coli* and are currently in use for crystallography as well as for large-scale inhibitor screening.

The kinases and phosphatases governing Greatwall activity throughout the cell cycle were also investigated here. A critical phosphorylation on T194 was identified that is essential for Greatwall activity and is in a conserved CDK phosphorylation consensus motif. This led to the hypothesis that human Greatwall, like *Xenopus* Greatwall, is phosphorylated and activated by CDK1 at the G2/M transition. Subsequent experiments using a phospho-specific antibody that exclusively detects Greatwall only when it is phosphorylated at this residue confirmed this both *in vitro* and *in vivo* in human cells. The phosphorylation of T194 corresponds to Greatwall activation and occurs at the G2/M transition only in the presence of CDK1 activity and persists until mitotic exit. This site is phosphorylated by CDKs and is able to fully activate Greatwall *in vitro*. Thus, it can be concluded that Greatwall activation is begun at the G2/M transition by CDK1. However, this is unlikely to be the whole story concerning regulation of Greatwall activity in mitosis and other PTMs and possibly additional regulatory proteins likely participate as well.

The phosphatases that act to regulate mitotic exit and Greatwall inactivation to allow cells to return to interphase were also investigated. It was determined that PP2A is the phosphatase that is responsible for the majority of Greatwall dephosphorylation and inactivation at mitotic exit. Interestingly, it was found that Ensa dephosphorylation at mitotic exit was controlled by another phosphatase, the RNA polymerase II C terminal domain phosphatase Fcp1. Surprisingly, the results of this work indicate that neither PP1, PP2A nor Fcp1 are the major CDK-antagonising phosphatases that remove mitotic

phospho-epitopes in human cells and the identity of this phosphatase(s) remains unknown at present.

Another major part of this thesis work was dedicated to the pursuit of the generation of an ATP-analogue sensitive (*as*) Greatwall mutant using a chemical genetics approach in human cells. This would allow the specific, rapid and reversible inhibition of the kinase in an otherwise normal cell, enabling elegant studies of the function of this kinase in cells to be performed. A successful knockin targeting strategy in human cells was developed. Despite this, unfortunately, it was found that the *as* Greatwall mutant was not viable as a functional kinase. The mutation of the gatekeeper methionine residue within the ATP-binding pocket to an alanine was not tolerated by the kinase and subsequent mutations to rescue the kinase activity were unsuccessful. A final attempt to produce an analogue sensitive mutant by mutation of the gatekeeper residue to a cysteine, creating an electrophile-sensitive (*es*) kinase, proved promising with three quarters of the activity as compared to the wildtype kinase remaining. This chemical genetics work is currently being further developed as part of a Marie Curie Fellowship and the *es* Greatwall mutant will be used for target evaluation in xenograft experiments.

Finally, during this work inconsistencies were observed between the manner in which transformed cell lines and non-transformed immortalised cell lines responded to the siRNA-mediated knockdown of Greatwall. Greatwall knockdown causes cell cycle arrest and apoptosis in the transformed cancer cell lines but has little impact on survival of the non-transformed cells. It means that Greatwall could potentially represent an ‘Achilles heel’ for some tumors and, while its role in cell cycle progression and proliferation is limited in somatic cells, it may be essential for survival in certain cancer cells. The preliminary work presented here supports the idea that Greatwall could potentially be an important prognostic biomarker and therapeutic target for cancer therapy. This work has formed the foundation of a large collaborative drug discovery project at the University of Sussex to develop Greatwall as an anti-cancer drug target and potential clinical biomarker.

8.2 Greatwall kinase controlling mitotic progression – phosphatases come into focus

The emerging view of mitotic control as a delicate balance of kinases and their counteracting phosphatases is now becoming increasingly accepted and vigorously studied. Since the historic discovery of MPF, succeeding studies have revealed that entry into mitosis is regulated by the highly coordinated activities of multiple protein kinases and their opposing phosphatases (Bollen *et al.* 2009; Lindqvist *et al.* 2009). The phosphorylation of more than a thousand proteins by CDK and other mitotic kinases drive mitotic entry (Dephoure *et al.* 2008). These must then be subsequently removed by phosphatases as cells exit mitosis (Wurzenberger *et al.* 2011). This mitotic kinase and phosphatase activity is therefore inversely regulated to avoid futile cycles of phosphorylation and dephosphorylation (Domingo-Sananes *et al.* 2011; Medema *et al.* 2011). Furthermore, mitotic kinases are themselves regulated by phosphorylation and dephosphorylation, resulting in a complex feedback system of cell cycle control. This allows for these regulatory feedback circuits to act in a highly sensitive switch-like manner to ensure sharp phase transitions required for progression throughout mitosis (Domingo-Sananes *et al.* 2011; Krasinska *et al.* 2011). Moreover, it allows for bistability and hysteresis to exist within the system to further ensure a robust and efficient switch-like mechanism governs mitotic entry and exit (Domingo-Sananes *et al.* 2011).

In interphase, CDK1 is negatively regulated by phosphorylation at T14/Y15 by Wee1 and Myt1 kinases, and dephosphorylation of this site by Cdc25 constitutes the decision point to enter mitosis (Lindqvist *et al.* 2009). CDK1 then participates in its own activation by negatively regulating its inhibitor, Wee1, and activating its activator, Cdc25 (Hoffmann *et al.* 1993). This switch is counteracted by PP2A-B55δ which in turn is antagonised by Greatwall which phosphorylates and activates the PP2A-B55δ inhibitors Arpp19 and Ensa. Moreover, CDK1 can phosphorylate and activate Greatwall at multiple sites. This suggests a model by which CDK1 and Greatwall activation are locked in a complex feedback system at the G2/M transition. A recent paper that explored this relationship in frogs and starfish oocytes in depth concluded that cyclin B-CKD1 and Greatwall must now both be considered essential components of the MPF (Hara *et al.* 2012) as both are required for mitosis in these systems.

In order to gain a more precise understanding of this switch-like transition, identification of the phosphatases that target Greatwall itself and Arpp19/Ensa was

important. This thesis initiated work that led to the discovery that PP2A-B55 α and δ isoforms inactivate Greatwall at mitotic exit in human cells and that another phosphatase, Fcp1, serves to inactivate Arpp19/Ensa. These findings indicate a complex phosphatase regulation to mediate these transitions. This work is at the vanguard of our current progress in delineating mitotic entry and exit. Further focused work will be required to build on this emerging picture of these intricate and highly sensitive pathways.

8.3 Interactions with other key mitotic kinases and other emerging roles for Greatwall?

How does Greatwall interact with other key mitotic kinases, if indeed it does at all? There has been much conflicting data and hypotheses in the literature and work is ongoing to precisely define the interactions of Greatwall. In *Xenopus* Greatwall does not phosphorylate Plx1, Plx3, CDK1, cyclin B, Cdc25A, Cdc25C, Chk1, Wee1, Myt1 or Pin1 *in vitro* (Zhao *et al.* 2008). Moreover, the exact sequence phosphorylated by Greatwall in Arpp19 and Ensa is found only in these two proteins, although the stringency of the substrate recognition sequence is not known (Mochida *et al.* 2012).

Blake-Hodek *et al.* (2012) reported that in their hands Plx1, Aurora A, PKA, Nek2 and p42 MAPK do not contribute to Greatwall activation alone or synergistically with CDKs. Yu *et al*. (2006) found that Plx-treated Greatwall could not rescue the mitotic phenotype in Greatwall depleted extracts and showed no autophosphorylation or phosphorylation of MBP in *in vitro* kinase assays. Additionally, co-treatment of Greatwall with Plx and MPF again did not yield a synergistic increase in activity. In agreement with these studies, the results obtained here do not give reason to suspect the involvement of additional kinases, other than CDKs, in the activation of Greatwall to promote mitotic entry. However, other key mitotic kinases might serve to add phosphorylations to Greatwall during mitosis to facilitate its stabilisation or localisation.

That PLK1 was reported to activate Greatwall *in vitro* by Vigneron *et al.* (2011) seems not to fit with this analysis. It might be that PLK1 can phosphorylate human Greatwall in its NCMR and stabilise the kinase giving it the activity seen *in vitro* by this group. This might not represent a key mechanism for activation *in vivo* under normal cell cycle conditions but could suggest a role for PLK1 in the control of Greatwall

activation in circumstances other than normal mitotic entry. In this case, under certain circumstances, PKL1 would serve to activate Greatwall to inactivate phosphatases mediating specific cell cycle signalling to promote cell cycle progression. This has already been reported to occur after a DNA damage-mediated cell cycle arrest (Peng *et al.* 2011). This could be interpreted to mean that PLK1 is capable of activating the human Greatwall, at least partially, but that it does so only if a specific set of cellular conditions are present. A surge in Greatwall activity was observed here in human cells immediately after release from S phase following a cell cycle block induced by Thymidine. This requires further analysis but supports a role for Greatwall in restarting cell cycle progression in a manner similar to that described after a DNA damage cell cycle arrest (Peng *et al.* 2010; Peng *et al.* 2011). It would be interesting for future work to determine if this activation is PLK1 dependant.

In addition, a version of the Greatwall pathway has recently been reported to be conserved in budding yeast (Yu *et al.* 2004; Talarek *et al.* 2010; Bontron *et al.* 2013). In these yeast cells, instead of controlling mitotic entry and exit however, it appears to be involved in entry into the reversible quiescent or G0 state in response to limited nutrients to ensure maximum long-term survival; known as the chronological life span (Talarek *et al.* 2010). The proposed yeast Greatwall homologue, Rim15, is activated in response to nitrogen and/or carbon limitation. It then phosphorylates Igo1 and Igo2, the yeast orthologues of Arpp19 and Ensa, which directly inhibit yeast $PP2A^{Cdc55}$ preventing its dephosphorylation of certain transcription factors that are then able to be recruited too and activate transcription of genes that promote induction of the quiescence program (Bontron *et al.* 2013). Rim15 phosphorylated Igo1 can also directly interact with proteins at the 3’ UTR of mRNAs to protect them from degradation during the initiation of the quiescence state during which only certain genes remain expressed (Talarek *et al.* 2010). Loss of Rim15 or Igo1/2 prevents initiation of the G0 program. Human Arpp19 and Ensa were able to partially replace Igo1/2 function in the yeast cells suggesting an interesting potentially conserved role for Greatwall in the regulation of mRNA stability in higher eukaryotes (Talarek *et al.* 2010; Lorca *et al.* 2012). This thesis has specifically focused on examination of the role of Greatwall at the G2/M transition and in mitosis, but the potential for roles of the Greatwall pathway outside of this remit are fascinating and will provide important avenues for further investigations.

Another paper has recently described a study in which human Greatwall loss synergised with the loss of p53 in HCT116 cells (Krastev *et al.* 2011). They performed

an RNAi-based synthetic interaction screen and identified Greatwall as a gene whose knockdown selectively affected p53 knockout HCT116 cells. They found that Greatwall expression was required for efficient growth of the knockout cells and its loss slowed their rate of proliferation, raising the possibility that Greatwall acts in conjunction with p53 to maintain proliferation in these cells.

These studies point to possible functions and potential interactions of Greatwall that are as of yet relatively unexplored and will require further investigations to elucidate.

8.4 Greatwall and human diseases

There is a dilemma with the emerging role for Greatwall in control of the cell cycle. If it is essentially required for cell cycle progression how do organisms that lack Greatwall successfully progress through the cell cycle? It is only found in certain evolutionary lineages (Yu *et al.* 2006). In yeast Rim15 is nonessential and there are no close relatives of Greatwall known in *Caenorhabitis elegans* for example (Kim *et al.* 2012). Additionally, the available data in humans indicates that inactivating mutation of Greatwall (E167D) in patients only impacts mildly on platelets (Johnson *et al.* 2009). It is, therefore, conceivable that the Greatwall pathway is in fact not an essential component of the G2/M transition switch in normal somatic cells. The switch between interphase and mitosis is the result of many integrated inputs and could be differentially balanced so that Greatwall is not required in most cells. It might instead represent a subsidiary feedback loop that is only required under certain cell cycle conditions, such as in early development, and has been upregulated and become a ‘pathway addiction’ in artificially growing or tumour cells. In this case, Greatwall would normally only be required to reduce/inactivate PP2A-B55 when high levels of this phosphatase activity are present to drive (multiple) rapid cell cycle divisions/transitions, such as in gametes. It is possible that tumour cells have utilised this auxiliary pathway to drive their cell cycle artificially and that targeting this characteristic of their growth could represent a unique therapeutic intervention. Thus, allowing tumour cells to be specifically killed with relatively minor implications for other normal cells. The inhibition of several cell cycle protein kinases with small molecules are already being tested in phase I and II trials for cancer therapy (Girdler *et al.* 2006; Perez de Castro *et al.* 2008). Additionally,

inhibition of Greatwall might also act synergistically with other DNA damaging agents or mitotic inhibitors to further increase its efficacy and clinical applicability.

It is also important to note that a role for Greatwall in normal cells that are not somatic cells, such as the gametes, is not insignificant. As Adhikari *et al.* (2012a) point out, it is important for future work to determine if Greatwall regulates CDK1 phosphorylations at the resumption of meiosis in human oocytes. It is known that Ensa is expressed in these cells (Von Stetina *et al.* 2008). Determination of a role for Greatwall could therefore have significant implications for the treatment of female infertility that results from failure to resume normal meiotic maturation (Adhikari *et al.* 2012a).

There are tantalising hints that the full story of Greatwall kinase is not yet known and that further research is warranted to elucidate the true function(s) of Greatwall in human cells. Precise determination of the role of Greatwall kinase could potentially yield insights that could have important implications for treatments of human conditions that range from infertility to cancer.

REFERENCES

Abal, M., M. Piel, V. Bouckson-Castaing, M. Mogensen, J. B. Sibarita and M. Bornens (2002). "Microtubule release from the centrosome in migrating cells." J Cell Biol **159**(5): 731-737.

Abrieu, A., L. Magnaghi-Jaulin, J. A. Kahana, M. Peter, A. Castro, S. Vigneron, T. Lorca, D. W. Cleveland and J. C. Labbe (2001). "Mps1 is a kinetochore-associated kinase essential for the vertebrate mitotic checkpoint." Cell **106**(1): 83-93.

Acquaviva, C., F. Herzog, C. Kraft and J. Pines (2004). "The anaphase promoting complex/cyclosome is recruited to centromeres by the spindle assembly checkpoint." Nat Cell Biol **6**(9): 892-898.

Acquaviva, C. and J. Pines (2006). "The anaphase-promoting complex/cyclosome: APC/C." J Cell Sci **119**(Pt 12): 2401-2404.

Adhikari, D., K. Liu and Y. Shen (2012a). "Cdk1 drives meiosis and mitosis through two different mechanisms." Cell Cycle **11**(15): 2763-2764.

Adhikari, D., W. Zheng, Y. Shen, N. Gorre, Y. Ning, G. Halet, P. Kaldis and K. Liu (2012b). "Cdk1, but not Cdk2, is the sole Cdk that is essential and sufficient to drive resumption of meiosis in mouse oocytes." Hum Mol Genet **21**(11): 2476-2484.

Alaimo, P. J., Z. A. Knight and K. M. Shokat (2005). "Targeting the gatekeeper residue in phosphoinositide 3-kinases." Bioorg Med Chem **13**(8): 2825-2836.

Alberts, A. J., Julian Lewis, Martin Raff, Keith Roberts, and Peter Walter. (2002). Molecular Biology of the Cell, Fourth Edition: A Problems Approach Garland Publishing, Inc. New York & London.

Alonso, G., C. Ambrosino, M. Jones and A. R. Nebreda (2000). "Differential activation of p38 mitogen-activated protein kinase isoforms depending on signal strength." J Biol Chem **275**(51): 40641-40648.

Arata, Y., M. Fujita, K. Ohtani, S. Kijima and J. Y. Kato (2000). "Cdk2-dependent and -independent pathways in E2F-mediated S phase induction." J Biol Chem **275**(9): 6337-6345.

Arcadian. (2007). "Cyclinexpression waehrend Zellzyklus." 5 March 2007. from from Cyclinexpression_waehrend_Zellzyklus.png.

Archambault, V., X. Zhao, H. White-Cooper, A. T. Carpenter and D. M. Glover (2007). "Mutations in Drosophila Greatwall/Scant reveal its roles in mitosis and meiosis and interdependence with Polo kinase." PLoS Genet **3**(11): e200.

Baldin, V. and B. Ducommun (1995). "Subcellular localisation of human wee1 kinase is regulated during the cell cycle." J Cell Sci **108 (Pt 6)**: 2425-2432.

Baldin, V., K. Pelpel, M. Cazales, C. Cans and B. Ducommun (2002). "Nuclear localization of CDC25B1 and serine 146 integrity are required for induction of mitosis." J Biol Chem **277**(38): 35176-35182.

Bandara, L. R., J. P. Adamczewski, T. Hunt and N. B. La Thangue (1991). "Cyclin A and the retinoblastoma gene product complex with a common transcription factor." Nature **352**(6332): 249-251.

Barr, A. R. and F. Gergely (2007). "Aurora-A: the maker and breaker of spindle poles." J Cell Sci **120**(Pt 17): 2987-2996.

Bartek, J. and J. Lukas (2007). "DNA damage checkpoints: from initiation to recovery or adaptation." Curr Opin Cell Biol **19**(2): 238-245.

Beach, D., B. Durkacz and P. Nurse (1982). "Functionally homologous cell cycle control genes in budding and fission yeast." Nature **300**(5894): 706-709.

Bell, S. P. and A. Dutta (2002). "DNA replication in eukaryotic cells." Annu Rev Biochem **71**: 333-374.

Bembenek, J. and H. Yu (2001). "Regulation of the anaphase-promoting complex by the dual specificity phosphatase human Cdc14a." J Biol Chem **276**(51): 48237-48242.

Berthet, C., E. Aleem, V. Coppola, L. Tessarollo and P. Kaldis (2003). "Cdk2 knockout mice are viable." Curr Biol **13**(20): 1775-1785.

Biondi, R. M., P. C. Cheung, A. Casamayor, M. Deak, R. A. Currie and D. R. Alessi (2000). "Identification of a pocket in the PDK1 kinase domain that interacts with PIF and the C-terminal residues of PKA." EMBO J **19**(5): 979-988.

Biondi, R. M., D. Komander, C. C. Thomas, J. M. Lizcano, M. Deak, D. R. Alessi and D. M. van Aalten (2002). "High resolution crystal structure of the human PDK1 catalytic domain defines the regulatory phosphopeptide docking site." EMBO J **21**(16): 4219-4228.

Biondi, R. M. and A. R. Nebreda (2003). "Signalling specificity of Ser/Thr protein kinases through docking-site-mediated interactions." Biochem J **372**(Pt 1): 1-13.

Bishop, A. C., K. Shah, Y. Liu, L. Witucki, C. Kung and K. M. Shokat (1998). "Design of allele-specific inhibitors to probe protein kinase signaling." Curr Biol **8**(5): 257-266.

Bishop, A. C., J. A. Ubersax, D. T. Petsch, D. P. Matheos, N. S. Gray, J. Blethrow, E. Shimizu, J. Z. Tsien, P. G. Schultz, M. D. Rose, J. L. Wood, D. O. Morgan and K. M. Shokat (2000). "A chemical switch for inhibitor-sensitive alleles of any protein kinase." Nature **407**(6802): 395-401.

Blagden, S. P. and D. M. Glover (2003). "Polar expeditions--provisioning the centrosome for mitosis." Nat Cell Biol **5**(6): 505-511.

Blake-Hodek, K. A., B. C. Williams, Y. Zhao, P. V. Castilho, W. Chen, Y. Mao, T. M. Yamamoto and M. L. Goldberg (2012). "Determinants for Activation of the Atypical AGC Kinase Greatwall during M Phase Entry." Mol Cell Biol **32**(8): 1337-1353.

Blangy, A., H. A. Lane, P. d'Herin, M. Harper, M. Kress and E. A. Nigg (1995). "Phosphorylation by p34cdc2 regulates spindle association of human Eg5, a kinesin-related motor essential for bipolar spindle formation in vivo." Cell **83**(7): 1159-1169.

Boke, E. and I. M. Hagan (2011). "Polo, greatwall, and protein phosphatase PP2A Jostle for pole position." PLoS Genet **7**(8): e1002213.

Bolanos-Garcia, V. M. and T. L. Blundell (2011). "BUB1 and BUBR1: multifaceted kinases of the cell cycle." Trends Biochem Sci **36**(3): 141-150.

Bollen, M., D. W. Gerlich and B. Lesage (2009). "Mitotic phosphatases: from entry guards to exit guides." Trends Cell Biol **19**(10): 531-541.

Bolognese, F., M. Wasner, C. L. Dohna, A. Gurtner, A. Ronchi, H. Muller, I. Manni, J. Mossner, G. Piaggio, R. Mantovani and K. Engeland (1999). "The cyclin B2 promoter depends on NF-Y, a trimer whose CCAAT-binding activity is cell-cycle regulated." Oncogene **18**(10): 1845-1853.

Bontron, S., M. Jaquenoud, S. Vaga, N. Talarek, B. Bodenmiller, R. Aebersold and C. De Virgilio (2013). "Yeast endosulfines control entry into quiescence and chronological life span by inhibiting protein phosphatase 2A." Cell Rep **3**(1): 16-22.

Booher, R. N., P. S. Holman and A. Fattaey (1997). "Human Myt1 is a cell cycle-regulated kinase that inhibits Cdc2 but not Cdk2 activity." J Biol Chem **272**(35): 22300-22306.

Bornens, M. (2002). "Centrosome composition and microtubule anchoring mechanisms." Curr Opin Cell Biol **14**(1): 25-34.

Bousset, K. and J. F. Diffley (1998). "The Cdc7 protein kinase is required for origin firing during S phase." Genes Dev **12**(4): 480-490.

Boutros, R., C. Dozier and B. Ducommun (2006). "The when and wheres of CDC25 phosphatases." Curr Opin Cell Biol **18**(2): 185-191.

Brandeis, M., I. Rosewell, M. Carrington, T. Crompton, M. A. Jacobs, J. Kirk, J. Gannon and T. Hunt (1998). "Cyclin B2-null mice develop normally and are fertile whereas cyclin B1-null mice die in utero." Proc Natl Acad Sci U S A **95**(8): 4344-4349.

Brennan, I. M., U. Peters, T. M. Kapoor and A. F. Straight (2007). "Polo-like kinase controls vertebrate spindle elongation and cytokinesis." PLoS One **2**(5): e409.

Brown, N. R., M. E. Noble, A. M. Lawrie, M. C. Morris, P. Tunnah, G. Divita, L. N. Johnson and J. A. Endicott (1999). "Effects of phosphorylation of threonine 160 on cyclin-dependent kinase 2 structure and activity." J Biol Chem **274**(13): 8746-8756.

Brust-Mascher, I., G. Civelekoglu-Scholey, M. Kwon, A. Mogilner and J. M. Scholey (2004). "Model for anaphase B: role of three mitotic motors in a switch from poleward flux to spindle elongation." Proc Natl Acad Sci U S A **101**(45): 15938-15943.

Bunz, F., A. Dutriaux, C. Lengauer, T. Waldman, S. Zhou, J. P. Brown, J. M. Sedivy, K. W. Kinzler and B. Vogelstein (1998). "Requirement for p53 and p21 to sustain G2 arrest after DNA damage." Science **282**(5393): 1497-1501.

Burgess, A., S. Vigneron, E. Brioudes, J. C. Labbe, T. Lorca and A. Castro (2010). "Loss of human Greatwall results in G2 arrest and multiple mitotic defects due to deregulation of the cyclin B-Cdc2/PP2A balance." Proc Natl Acad Sci U S A **107**(28): 12564-12569.

Cameron, A. J., C. Escribano, A. T. Saurin, B. Kostelecky and P. J. Parker (2009). "PKC maturation is promoted by nucleotide pocket occupation independently of intrinsic kinase activity." Nat Struct Mol Biol **16**(6): 624-630.

Canepa, E. T., M. E. Scassa, J. M. Ceruti, M. C. Marazita, A. L. Carcagno, P. F. Sirkin and M. F. Ogara (2007). "INK4 proteins, a family of mammalian CDK inhibitors with novel biological functions." IUBMB Life **59**(7): 419-426.

Cardoso, M. C., H. Leonhardt and B. Nadal-Ginard (1993). "Reversal of terminal differentiation and control of DNA replication: cyclin A and Cdk2 specifically localize at subnuclear sites of DNA replication." Cell **74**(6): 979-992.

Carmena, M. and W. C. Earnshaw (2003). "The cellular geography of aurora kinases." Nat Rev Mol Cell Biol **4**(11): 842-854.

Carpten, J. D., A. L. Faber, C. Horn, G. P. Donoho, S. L. Briggs, C. M. Robbins, G. Hostetter, S. Boguslawski, T. Y. Moses, S. Savage, M. Uhlik, A. Lin, J. Du, Y. W. Qian, D. J. Zeckner, G. Tucker-Kellogg, J. Touchman, K. Patel, S. Mousses, M. Bittner, R. Schevitz, M. H. Lai, K. L. Blanchard and J. E. Thomas (2007). "A transforming mutation in the pleckstrin homology domain of AKT1 in cancer." Nature **448**(7152): 439-444.

Castilho, P. V., B. C. Williams, S. Mochida, Y. Zhao and M. L. Goldberg (2009). "The M phase kinase Greatwall (Gwl) promotes inactivation of PP2A/B55delta, a phosphatase directed against CDK phosphosites." Mol Biol Cell **20**(22): 4777-4789.

Cazales, M., E. Schmitt, E. Montembault, C. Dozier, C. Prigent and B. Ducommun (2005). "CDC25B phosphorylation by Aurora-A occurs at the G2/M transition and is inhibited by DNA damage." Cell Cycle **4**(9): 1233-1238.

Chaturvedi, P., V. Sudakin, M. L. Bobiak, P. W. Fisher, M. R. Mattern, S. A. Jablonski, M. R. Hurle, Y. Zhu, T. J. Yen and B. B. Zhou (2002). "Chfr regulates a mitotic stress pathway through its RING-finger domain with ubiquitin ligase activity." Cancer Res **62**(6): 1797-1801.

Chen, F., V. Archambault, A. Kar, P. Lio, P. P. D'Avino, R. Sinka, K. Lilley, E. D. Laue, P. Deak, L. Capalbo and D. M. Glover (2007). "Multiple protein phosphatases are required for mitosis in Drosophila." Curr Biol **17**(4): 293-303.

Chen, M. S., J. Hurov, L. S. White, T. Woodford-Thomas and H. Piwnica-Worms (2001). "Absence of apparent phenotype in mice lacking Cdc25C protein phosphatase." Mol Cell Biol **21**(12): 3853-3861.

Chen, R. H., J. C. Waters, E. D. Salmon and A. W. Murray (1996). "Association of spindle assembly checkpoint component XMAD2 with unattached kinetochores." Science **274**(5285): 242-246.

Cheng, X. C., T. Kihara, X. Ying, M. Uramoto, H. Osada, H. Kusakabe, B. N. Wang, Y. Kobayashi, K. Ko, I. Yamaguchi and et al. (1989). "A new antibiotic, tautomycetin." J Antibiot (Tokyo) **42**(1): 141-144.

Chevrier, V., M. Piel, N. Collomb, Y. Saoudi, R. Frank, M. Paintrand, S. Narumiya, M. Bornens and D. Job (2002). "The Rho-associated protein kinase p160ROCK is required for centrosome positioning." J Cell Biol **157**(5): 807-817.

Chin, C. F. and F. M. Yeong (2010). "Safeguarding entry into mitosis: the antephase checkpoint." Mol Cell Biol **30**(1): 22-32.

Cho, H., J. Mu, J. K. Kim, J. L. Thorvaldsen, Q. Chu, E. B. Crenshaw, 3rd, K. H. Kaestner, M. S. Bartolomei, G. I. Shulman and M. J. Birnbaum (2001). "Insulin resistance and a diabetes mellitus-like syndrome in mice lacking the protein kinase Akt2 (PKB beta)." Science **292**(5522): 1728-1731.

Cho, H. P., Y. Liu, M. Gomez, J. Dunlap, M. Tyers and Y. Wang (2005). "The dual-specificity phosphatase CDC14B bundles and stabilizes microtubules." Mol Cell Biol **25**(11): 4541-4551.

Ciccia, A. and S. J. Elledge (2010). "The DNA damage response: making it safe to play with knives." Mol Cell **40**(2): 179-204.

Cimini, D. (2007). "Detection and correction of merotelic kinetochore orientation by Aurora B and its partners." Cell Cycle **6**(13): 1558-1564.

Cimprich, K. A. and D. Cortez (2008). "ATR: an essential regulator of genome integrity." Nat Rev Mol Cell Biol **9**(8): 616-627.

Classon, M. and E. Harlow (2002). "The retinoblastoma tumour suppressor in development and cancer." Nat Rev Cancer **2**(12): 910-917.

Clemenson, C. and M. C. Marsolier-Kergoat (2009). "DNA damage checkpoint inactivation: adaptation and recovery." DNA Repair (Amst) **8**(9): 1101-1109.

Cohen, P. (2002). "Protein kinases--the major drug targets of the twenty-first century?" Nat Rev Drug Discov **1**(4): 309-315.

Cohen, P. and A. Knebel (2006). "KESTREL: a powerful method for identifying the physiological substrates of protein kinases." Biochem J **393**(Pt 1): 1-6.

Conklin, D. S., K. Galaktionov and D. Beach (1995). "14-3-3 proteins associate with cdc25 phosphatases." Proc Natl Acad Sci U S A **92**(17): 7892-7896.

Cowley, D. O., J. A. Rivera-Perez, M. Schliekelman, Y. J. He, T. G. Oliver, L. Lu, R. O'Quinn, E. D. Salmon, T. Magnuson and T. Van Dyke (2009). "Aurora-A

kinase is essential for bipolar spindle formation and early development." Mol Cell Biol **29**(4): 1059-1071.

Dabauvalle, M. C., M. Doree, R. Bravo and E. Karsenti (1988). "Role of nuclear material in the early cell cycle of Xenopus embryos." Cell **52**(4): 525-533.

Daub, H., J. V. Olsen, M. Bairlein, F. Gnad, F. S. Oppermann, R. Korner, Z. Greff, G. Keri, O. Stemmann and M. Mann (2008). "Kinase-selective enrichment enables quantitative phosphoproteomics of the kinome across the cell cycle." Mol Cell **31**(3): 438-448.

Davies, S. P., H. Reddy, M. Caivano and P. Cohen (2000). "Specificity and mechanism of action of some commonly used protein kinase inhibitors." Biochem J **351**(Pt 1): 95-105.

De Antoni, A., C. G. Pearson, D. Cimini, J. C. Canman, V. Sala, L. Nezi, M. Mapelli, L. Sironi, M. Faretta, E. D. Salmon and A. Musacchio (2005). "The Mad1/Mad2 complex as a template for Mad2 activation in the spindle assembly checkpoint." Curr Biol **15**(3): 214-225.

De Bondt, H. L., J. Rosenblatt, J. Jancarik, H. D. Jones, D. O. Morgan and S. H. Kim (1993). "Crystal structure of cyclin-dependent kinase 2." Nature **363**(6430): 595-602.

De Wulf, P., F. Montani and R. Visintin (2009). "Protein phosphatases take the mitotic stage." Curr Opin Cell Biol **21**(6): 806-815.

Delmolino, L. M., P. Saha and A. Dutta (2001). "Multiple mechanisms regulate subcellular localization of human CDC6." J Biol Chem **276**(29): 26947-26954.

Deng, C. and M. R. Capecchi (1992). "Reexamination of gene targeting frequency as a function of the extent of homology between the targeting vector and the target locus." Mol Cell Biol **12**(8): 3365-3371.

Dephoure, N., C. Zhou, J. Villen, S. A. Beausoleil, C. E. Bakalarski, S. J. Elledge and S. P. Gygi (2008). "A quantitative atlas of mitotic phosphorylation." Proc Natl Acad Sci U S A **105**(31): 10762-10767.

Dieterich, K., R. Soto Rifo, A. K. Faure, S. Hennebicq, B. Ben Amar, M. Zahi, J. Perrin, D. Martinez, B. Sele, P. S. Jouk, T. Ohlmann, S. Rousseaux, J. Lunardi and P. F. Ray (2007). "Homozygous mutation of AURKC yields large-headed polyploid spermatozoa and causes male infertility." Nat Genet **39**(5): 661-665.

Diffley, J. F. (2004). "Regulation of early events in chromosome replication." Curr Biol **14**(18): R778-786.

Diril, M. K., C. K. Ratnacaram, V. C. Padmakumar, T. Du, M. Wasser, V. Coppola, L. Tessarollo and P. Kaldis (2012). "Cyclin-dependent kinase 1 (Cdk1) is essential for cell division and suppression of DNA re-replication but not for liver regeneration." Proc Natl Acad Sci U S A **109**(10): 3826-3831.

Dodson, C. A., S. Yeoh, T. Haq and R. Bayliss (2013). "A kinetic test characterizes kinase intramolecular and intermolecular autophosphorylation mechanisms." Sci Signal **6**(282): ra54.

Domingo-Sananes, M. R., O. Kapuy, T. Hunt and B. Novak (2011). "Switches and latches: a biochemical tug-of-war between the kinases and phosphatases that control mitosis." Philos Trans R Soc Lond B Biol Sci **366**(1584): 3584-3594.

Doree, M. and T. Hunt (2002). "From Cdc2 to Cdk1: when did the cell cycle kinase join its cyclin partner?" J Cell Sci **115**(Pt 12): 2461-2464.

Drachman, J. G., G. P. Jarvik and M. G. Mehaffey (2000). "Autosomal dominant thrombocytopenia: incomplete megakaryocyte differentiation and linkage to human chromosome 10." Blood **96**(1): 118-125.

Dryden, S. C., F. A. Nahhas, J. E. Nowak, A. S. Goustin and M. A. Tainsky (2003). "Role for human SIRT2 NAD-dependent deacetylase activity in control of mitotic exit in the cell cycle." Mol Cell Biol **23**(9): 3173-3185.

Duensing, A., Y. Liu, M. Tseng, M. Malumbres, M. Barbacid and S. Duensing (2006). "Cyclin-dependent kinase 2 is dispensable for normal centrosome duplication but required for oncogene-induced centrosome overduplication." Oncogene **25**(20): 2943-2949.

Dunphy, W. G., L. Brizuela, D. Beach and J. Newport (1988). "The Xenopus cdc2 protein is a component of MPF, a cytoplasmic regulator of mitosis." Cell **54**(3): 423-431.

Dunphy, W. G. and A. Kumagai (1991). "The cdc25 protein contains an intrinsic phosphatase activity." Cell **67**(1): 189-196.

Dutcher, S. K. and L. H. Hartwell (1982). "The role of S. cerevisiae cell division cycle genes in nuclear fusion." Genetics **100**(2): 175-184.

Dutertre, S., M. Cazales, M. Quaranta, C. Froment, V. Trabut, C. Dozier, G. Mirey, J. P. Bouche, N. Theis-Febvre, E. Schmitt, B. Monsarrat, C. Prigent and B. Ducommun (2004). "Phosphorylation of CDC25B by Aurora-A at the centrosome contributes to the G2-M transition." J Cell Sci **117**(Pt 12): 2523-2531.

Elia, A. E., L. C. Cantley and M. B. Yaffe (2003a). "Proteomic screen finds pSer/pThr-binding domain localizing Plk1 to mitotic substrates." Science **299**(5610): 1228-1231.

Elia, A. E., P. Rellos, L. F. Haire, J. W. Chao, F. J. Ivins, K. Hoepker, D. Mohammad, L. C. Cantley, S. J. Smerdon and M. B. Yaffe (2003b). "The molecular basis for phosphodependent substrate targeting and regulation of Plks by the Polo-box domain." Cell **115**(1): 83-95.

Elledge, S. J. (1996). "Cell cycle checkpoints: preventing an identity crisis." Science **274**(5293): 1664-1672.

Evans, T., E. T. Rosenthal, J. Youngblom, D. Distel and T. Hunt (1983). "Cyclin: a protein specified by maternal mRNA in sea urchin eggs that is destroyed at each cleavage division." Cell **33**(2): 389-396.

Eyers, P. A., E. Erikson, L. G. Chen and J. L. Maller (2003). "A novel mechanism for activation of the protein kinase Aurora A." Curr Biol **13**(8): 691-697.

Fang, G., H. Yu and M. W. Kirschner (1998a). "The checkpoint protein MAD2 and the mitotic regulator CDC20 form a ternary complex with the anaphase-promoting complex to control anaphase initiation." Genes Dev **12**(12): 1871-1883.

Fang, G., H. Yu and M. W. Kirschner (1998b). "Direct binding of CDC20 protein family members activates the anaphase-promoting complex in mitosis and G1." Mol Cell **2**(2): 163-171.

Fattaey, A. and R. N. Booher (1997). "Myt1: a Wee1-type kinase that phosphorylates Cdc2 on residue Thr14." Prog Cell Cycle Res **3**: 233-240.

Favre, B., P. Turowski and B. A. Hemmings (1997). "Differential inhibition and posttranslational modification of protein phosphatase 1 and 2A in MCF7 cells treated with calyculin-A, okadaic acid, and tautomycin." J Biol Chem **272**(21): 13856-13863.

Felix, M. A., P. Cohen and E. Karsenti (1990). "Cdc2 H1 kinase is negatively regulated by a type 2A phosphatase in the Xenopus early embryonic cell cycle: evidence from the effects of okadaic acid." EMBO J **9**(3): 675-683.

Felix, M. A., J. Pines, T. Hunt and E. Karsenti (1989). "Temporal regulation of cdc2 mitotic kinase activity and cyclin degradation in cell-free extracts of Xenopus eggs." J Cell Sci Suppl **12**: 99-116.

Fenton, T. R., J. Gwalter, R. Cramer and I. T. Gout (2010). "S6K1 is acetylated at lysine 516 in response to growth factor stimulation." Biochem Biophys Res Commun **398**(3): 400-405.

Ferguson, A. M., L. S. White, P. J. Donovan and H. Piwnica-Worms (2005). "Normal cell cycle and checkpoint responses in mice and cells lacking Cdc25B and Cdc25C protein phosphatases." Mol Cell Biol **25**(7): 2853-2860.

Flynn, P., H. Mellor, A. Casamassima and P. J. Parker (2000). "Rho GTPase control of protein kinase C-related protein kinase activation by 3-phosphoinositide-dependent protein kinase." J Biol Chem **275**(15): 11064-11070.

Forester, C. M., J. Maddox, J. V. Louis, J. Goris and D. M. Virshup (2007). "Control of mitotic exit by PP2A regulation of Cdc25C and Cdk1." Proc Natl Acad Sci U S A **104**(50): 19867-19872.

Fotedar, R. and J. M. Roberts (1991). "Association of p34cdc2 with replicating DNA." Cold Spring Harb Symp Quant Biol **56**: 325-333.

Freire, R., M. A. van Vugt, I. Mamely and R. H. Medema (2006). "Claspin: timing the cell cycle arrest when the genome is damaged." Cell Cycle **5**(24): 2831-2834.

Frodin, M., T. L. Antal, B. A. Dummler, C. J. Jensen, M. Deak, S. Gammeltoft and R. M. Biondi (2002). "A phosphoserine/threonine-binding pocket in AGC kinases and PDK1 mediates activation by hydrophobic motif phosphorylation." EMBO J **21**(20): 5396-5407.

Frodin, M., C. J. Jensen, K. Merienne and S. Gammeltoft (2000). "A phosphoserine-regulated docking site in the protein kinase RSK2 that recruits and activates PDK1." EMBO J **19**(12): 2924-2934.

Fu, Z., L. Malureanu, J. Huang, W. Wang, H. Li, J. M. van Deursen, D. J. Tindall and J. Chen (2008). "Plk1-dependent phosphorylation of FoxM1 regulates a transcriptional programme required for mitotic progression." Nat Cell Biol **10**(9): 1076-1082.

Fung, T. K., H. T. Ma and R. Y. Poon (2007). "Specialized roles of the two mitotic cyclins in somatic cells: cyclin A as an activator of M phase-promoting factor." Mol Biol Cell **18**(5): 1861-1873.

Fung, T. K. and R. Y. Poon (2005). "A roller coaster ride with the mitotic cyclins." Semin Cell Dev Biol **16**(3): 335-342.

Furuno, N., N. den Elzen and J. Pines (1999). "Human cyclin A is required for mitosis until mid prophase." J Cell Biol **147**(2): 295-306.

Gabrielli, B. G., C. P. De Souza, I. D. Tonks, J. M. Clark, N. K. Hayward and K. A. Ellem (1996). "Cytoplasmic accumulation of cdc25B phosphatase in mitosis triggers centrosomal microtubule nucleation in HeLa cells." J Cell Sci **109 (Pt 5)**: 1081-1093.

Gandhi, M. J., C. L. Cummings and J. G. Drachman (2003). "FLJ14813 missense mutation: a candidate for autosomal dominant thrombocytopenia on human chromosome 10." Hum Hered **55**(1): 66-70.

Garcia, V., K. Furuya and A. M. Carr (2005). "Identification and functional analysis of TopBP1 and its homologs." DNA Repair (Amst) **4**(11): 1227-1239.

Garland, P., S. Quraishe, P. French and V. O'Connor (2008). "Expression of the MAST family of serine/threonine kinases." Brain Res **1195**: 12-19.

Garske, A. L., U. Peters, A. T. Cortesi, J. L. Perez and K. M. Shokat (2011). "Chemical genetic strategy for targeting protein kinases based on covalent complementarity." Proc Natl Acad Sci U S A **108**(37): 15046-15052.

Gautier, J., J. Minshull, M. Lohka, M. Glotzer, T. Hunt and J. L. Maller (1990). "Cyclin is a component of maturation-promoting factor from Xenopus." Cell **60**(3): 487-494.

Gavet, O. and J. Pines (2010a). "Activation of cyclin B1-Cdk1 synchronizes events in the nucleus and the cytoplasm at mitosis." J Cell Biol **189**(2): 247-259.

Gavet, O. and J. Pines (2010b). "Progressive activation of CyclinB1-Cdk1 coordinates entry to mitosis." Dev Cell **18**(4): 533-543.

Geng, Y., Q. Yu, E. Sicinska, M. Das, J. E. Schneider, S. Bhattacharya, W. M. Rideout, R. T. Bronson, H. Gardner and P. Sicinski (2003). "Cyclin E ablation in the mouse." Cell **114**(4): 431-443.

Gharbi-Ayachi, A., J. C. Labbe, A. Burgess, S. Vigneron, J. M. Strub, E. Brioudes, A. Van-Dorsselaer, A. Castro and T. Lorca (2010). "The substrate of Greatwall kinase, Arpp19, controls mitosis by inhibiting protein phosphatase 2A." Science **330**(6011): 1673-1677.

Girault, J. A., A. Horiuchi, E. L. Gustafson, N. L. Rosen and P. Greengard (1990). "Differential expression of ARPP-16 and ARPP-19, two highly related cAMP-regulated phosphoproteins, one of which is specifically associated with dopamine-innervated brain regions." J Neurosci **10**(4): 1124-1133.

Girdler, F., K. E. Gascoigne, P. A. Eyers, S. Hartmuth, C. Crafter, K. M. Foote, N. J. Keen and S. S. Taylor (2006). "Validating Aurora B as an anti-cancer drug target." J Cell Sci **119**(Pt 17): 3664-3675.

Goris, J., J. Hermann, P. Hendrix, R. Ozon and W. Merlevede (1989). "Okadaic acid, a specific protein phosphatase inhibitor, induces maturation and MPF formation in Xenopus laevis oocytes." FEBS Lett **245**(1-2): 91-94.

Goujon, M., H. McWilliam, W. Li, F. Valentin, S. Squizzato, J. Paern and R. Lopez (2010). "A new bioinformatics analysis tools framework at EMBL-EBI." Nucleic Acids Res **38**(Web Server issue): W695-699.

Guillamot, M., E. Manchado, M. Chiesa, G. Gomez-Lopez, D. G. Pisano, M. P. Sacristan and M. Malumbres (2011). "Cdc14b regulates mammalian RNA polymerase II and represses cell cycle transcription." Sci Rep **1**: 189.

Guse, A., M. Mishima and M. Glotzer (2005). "Phosphorylation of ZEN-4/MKLP1 by aurora B regulates completion of cytokinesis." Curr Biol **15**(8): 778-786.

Haccard, O. and C. Jessus (2011). "Greatwall kinase, ARPP-19 and protein phosphatase 2A: shifting the mitosis paradigm." Results Probl Cell Differ **53**: 219-234.

Hagan, I. M. (2008). "The spindle pole body plays a key role in controlling mitotic commitment in the fission yeast Schizosaccharomyces pombe." Biochem Soc Trans **36**(Pt 5): 1097-1101.

Hagting, A., C. Karlsson, P. Clute, M. Jackman and J. Pines (1998). "MPF localization is controlled by nuclear export." EMBO J **17**(14): 4127-4138.

Hanisch, A., A. Wehner, E. A. Nigg and H. H. Sillje (2006). "Different Plk1 functions show distinct dependencies on Polo-Box domain-mediated targeting." Mol Biol Cell **17**(1): 448-459.

Hanks, S. K. and T. Hunter (1995). "Protein kinases 6. The eukaryotic protein kinase superfamily: kinase (catalytic) domain structure and classification." FASEB J **9**(8): 576-596.

Hanks, S. K. and A. M. Quinn (1991). "Protein kinase catalytic domain sequence database: identification of conserved features of primary structure and classification of family members." Methods Enzymol **200**: 38-62.

Hara, K., P. Tydeman and M. Kirschner (1980). "A cytoplasmic clock with the same period as the division cycle in Xenopus eggs." Proc Natl Acad Sci U S A **77**(1): 462-466.

Hara, M., Y. Abe, T. Tanaka, T. Yamamoto, E. Okumura and T. Kishimoto (2012). "Greatwall kinase and cyclin B-Cdk1 are both critical constituents of M-phase-promoting factor." Nat Commun **3**: 1059.

Harbour, J. W., R. X. Luo, A. Dei Santi, A. A. Postigo and D. C. Dean (1999). "Cdk phosphorylation triggers sequential intramolecular interactions that progressively block Rb functions as cells move through G1." Cell **98**(6): 859-869.

Harrison, J. C. and J. E. Haber (2006). "Surviving the breakup: the DNA damage checkpoint." Annu Rev Genet **40**: 209-235.

Hartley, J. L., G. F. Temple and M. A. Brasch (2000). "DNA cloning using in vitro site-specific recombination." Genome Res **10**(11): 1788-1795.

Hartwell, L. H. (1978). "Cell division from a genetic perspective." J Cell Biol **77**(3): 627-637.

Hartwell, L. H., J. Culotti and B. Reid (1970). "Genetic control of the cell-division cycle in yeast. I. Detection of mutants." Proc Natl Acad Sci U S A **66**(2): 352-359.

Hartwell, L. H. and T. A. Weinert (1989). "Checkpoints: controls that ensure the order of cell cycle events." Science **246**(4930): 629-634.

Hauf, S., E. Roitinger, B. Koch, C. M. Dittrich, K. Mechtler and J. M. Peters (2005). "Dissociation of cohesin from chromosome arms and loss of arm cohesion during early mitosis depends on phosphorylation of SA2." PLoS Biol **3**(3): e69.

Hauge, C., T. L. Antal, D. Hirschberg, U. Doehn, K. Thorup, L. Idrissova, K. Hansen, O. N. Jensen, T. J. Jorgensen, R. M. Biondi and M. Frodin (2007). "Mechanism for activation of the growth factor-activated AGC kinases by turn motif phosphorylation." EMBO J **26**(9): 2251-2261.

Hegarat, N., E. Smith, G. Nayak, S. Takeda, P. A. Eyers and H. Hochegger (2011). "Aurora A and Aurora B jointly coordinate chromosome segregation and anaphase microtubule dynamics." J Cell Biol **195**(7): 1103-1113.

Hewitt, L., A. Tighe, S. Santaguida, A. M. White, C. D. Jones, A. Musacchio, S. Green and S. S. Taylor (2010). "Sustained Mps1 activity is required in mitosis to recruit O-Mad2 to the Mad1-C-Mad2 core complex." J Cell Biol **190**(1): 25-34.

Hirai, T. J., I. Tsigelny and J. A. Adams (2000). "Catalytic assessment of the glycine-rich loop of the v-Fps oncoprotein using site-directed mutagenesis." Biochemistry **39**(43): 13276-13284.

Hochegger, H., D. Dejsuphong, E. Sonoda, A. Saberi, E. Rajendra, J. Kirk, T. Hunt and S. Takeda (2007). "An essential role for Cdk1 in S phase control is revealed via chemical genetics in vertebrate cells." J Cell Biol **178**(2): 257-268.

Hochegger, H., A. Klotzbucher, J. Kirk, M. Howell, K. le Guellec, K. Fletcher, T. Duncan, M. Sohail and T. Hunt (2001). "New B-type cyclin synthesis is required between meiosis I and II during Xenopus oocyte maturation." Development **128**(19): 3795-3807.

Hochegger, H., S. Takeda and T. Hunt (2008). "Cyclin-dependent kinases and cell-cycle transitions: does one fit all?" Nat Rev Mol Cell Biol **9**(11): 910-916.

Hoffmann, I., P. R. Clarke, M. J. Marcote, E. Karsenti and G. Draetta (1993). "Phosphorylation and activation of human cdc25-C by cdc2--cyclin B and its involvement in the self-amplification of MPF at mitosis." EMBO J **12**(1): 53-63.

Hoffmann, I., G. Draetta and E. Karsenti (1994). "Activation of the phosphatase activity of human cdc25A by a cdk2-cyclin E dependent phosphorylation at the G1/S transition." EMBO J **13**(18): 4302-4310.

Horiuchi, D., N. E. Huskey, L. Kusdra, L. Wohlbold, K. A. Merrick, C. Zhang, K. J. Creasman, K. M. Shokat, R. P. Fisher and A. Goga (2012). "Chemical-genetic analysis of cyclin dependent kinase 2 function reveals an important role in cellular transformation by multiple oncogenic pathways." Proc Natl Acad Sci U S A **109**(17): E1019-1027.

Hornbeck, P. V., J. M. Kornhauser, S. Tkachev, B. Zhang, E. Skrzypek, B. Murray, V. Latham and M. Sullivan (2012). "PhosphoSitePlus: a comprehensive resource for investigating the structure and function of experimentally determined post-translational modifications in man and mouse." Nucleic Acids Res **40**(Database issue): D261-270.

Hornig, N. C. and F. Uhlmann (2004). "Preferential cleavage of chromatin-bound cohesin after targeted phosphorylation by Polo-like kinase." EMBO J **23**(15): 3144-3153.

Howard, A. and S. R. Pelc (1951). "Synthesis of nucleoprotein in bean root cells." Nature **167**(4250): 599-600.

Howell, B. J., B. F. McEwen, J. C. Canman, D. B. Hoffman, E. M. Farrar, C. L. Rieder and E. D. Salmon (2001). "Cytoplasmic dynein/dynactin drives kinetochore protein transport to the spindle poles and has a role in mitotic spindle checkpoint inactivation." J Cell Biol **155**(7): 1159-1172.

Hunt, T. (1989). "Maturation promoting factor, cyclin and the control of M-phase." Curr Opin Cell Biol **1**(2): 268-274.

Hunt, T. (2004). "The discovery of cyclin (I)." Cell **116**(2 Suppl): S63-64, 61 p following S65.

Hunt, T., F. C. Luca and J. V. Ruderman (1992). "The requirements for protein synthesis and degradation, and the control of destruction of cyclins A and B in the meiotic and mitotic cell cycles of the clam embryo." J Cell Biol **116**(3): 707-724.

Hunter, T. and G. D. Plowman (1997). "The protein kinases of budding yeast: six score and more." Trends Biochem Sci **22**(1): 18-22.

Huse, M. and J. Kuriyan (2002). "The conformational plasticity of protein kinases." Cell **109**(3): 275-282.

Hutterer, A., D. Berdnik, F. Wirtz-Peitz, M. Zigman, A. Schleiffer and J. A. Knoblich (2006). "Mitotic activation of the kinase Aurora-A requires its binding partner Bora." Dev Cell **11**(2): 147-157.

Iiizumi, S., Y. Nomura, S. So, K. Uegaki, K. Aoki, K. Shibahara, N. Adachi and H. Koyama (2006). "Simple one-week method to construct gene-targeting vectors: application to production of human knockout cell lines." Biotechniques **41**(3): 311-316.

Infante, A., U. Laresgoiti, J. Fernandez-Rueda, A. Fullaondo, J. Galan, R. Diaz-Uriarte, M. Malumbres, S. J. Field and A. M. Zubiaga (2008). "E2F2 represses cell cycle regulators to maintain quiescence." Cell Cycle **7**(24): 3915-3927.

Iyer, G. H., M. J. Moore and S. S. Taylor (2005). "Consequences of lysine 72 mutation on the phosphorylation and activation state of cAMP-dependent kinase." J Biol Chem **280**(10): 8800-8807.

Izawa, D. and J. Pines (2011). "How APC/C-Cdc20 changes its substrate specificity in mitosis." Nat Cell Biol **13**(3): 223-233.

Jackman, M., C. Lindon, E. A. Nigg and J. Pines (2003). "Active cyclin B1-Cdk1 first appears on centrosomes in prophase." Nat Cell Biol **5**(2): 143-148.

Jackson, P. K. (2006). "Climbing the Greatwall to mitosis." Mol Cell **22**(2): 156-157.

Janssens, V., S. Longin and J. Goris (2008). "PP2A holoenzyme assembly: in cauda venenum (the sting is in the tail)." Trends Biochem Sci **33**(3): 113-121.

Jeffrey, P. D., A. A. Russo, K. Polyak, E. Gibbs, J. Hurwitz, J. Massague and N. P. Pavletich (1995). "Mechanism of CDK activation revealed by the structure of a cyclinA-CDK2 complex." Nature **376**(6538): 313-320.

Jeffrey, P. D., L. Tong and N. P. Pavletich (2000). "Structural basis of inhibition of CDK-cyclin complexes by INK4 inhibitors." Genes Dev **14**(24): 3115-3125.

Jelluma, N., T. B. Dansen, T. Sliedrecht, N. P. Kwiatkowski and G. J. Kops (2010). "Release of Mps1 from kinetochores is crucial for timely anaphase onset." J Cell Biol **191**(2): 281-290.

Jinno, S., K. Suto, A. Nagata, M. Igarashi, Y. Kanaoka, H. Nojima and H. Okayama (1994). "Cdc25A is a novel phosphatase functioning early in the cell cycle." EMBO J **13**(7): 1549-1556.

Joaquin, M. and R. J. Watson (2003a). "The cell cycle-regulated B-Myb transcription factor overcomes cyclin-dependent kinase inhibitory activity of p57(KIP2) by interacting with its cyclin-binding domain." J Biol Chem **278**(45): 44255-44264.

Joaquin, M. and R. J. Watson (2003b). "Cell cycle regulation by the B-Myb transcription factor." Cell Mol Life Sci **60**(11): 2389-2401.

Johnson, H. J., M. J. Gandhi, E. Shafizadeh, N. B. Langer, E. L. Pierce, B. H. Paw, D. M. Gilligan and J. G. Drachman (2009). "In vivo inactivation of MASTL kinase results in thrombocytopenia." Exp Hematol **37**(8): 901-908.

Johnson, L. N., M. E. Noble and D. J. Owen (1996). "Active and inactive protein kinases: structural basis for regulation." Cell **85**(2): 149-158.

Kaiser, B. K., Z. A. Zimmerman, H. Charbonneau and P. K. Jackson (2002). "Disruption of centrosome structure, chromosome segregation, and cytokinesis by misexpression of human Cdc14A phosphatase." Mol Biol Cell **13**(7): 2289-2300.

Kaldis, P., A. A. Russo, H. S. Chou, N. P. Pavletich and M. J. Solomon (1998). "Human and yeast cdk-activating kinases (CAKs) display distinct substrate specificities." Mol Biol Cell **9**(9): 2545-2560.

Kallio, M. J., V. A. Beardmore, J. Weinstein and G. J. Gorbsky (2002). "Rapid microtubule-independent dynamics of Cdc20 at kinetochores and centrosomes in mammalian cells." J Cell Biol **158**(5): 841-847.

Kannan, N., N. Haste, S. S. Taylor and A. F. Neuwald (2007). "The hallmark of AGC kinase functional divergence is its C-terminal tail, a cis-acting regulatory module." Proc Natl Acad Sci U S A **104**(4): 1272-1277.

Karlsson-Rosenthal, C. and J. B. Millar (2006). "Cdc25: mechanisms of checkpoint inhibition and recovery." Trends Cell Biol **16**(6): 285-292.

Kastan, M. B. and J. Bartek (2004). "Cell-cycle checkpoints and cancer." Nature **432**(7015): 316-323.

Katula, K. S., K. L. Wright, H. Paul, D. R. Surman, F. J. Nuckolls, J. W. Smith, J. P. Ting, J. Yates and J. P. Cogswell (1997). "Cyclin-dependent kinase activation and S-phase induction of the cyclin B1 gene are linked through the CCAAT elements." Cell Growth Differ **8**(7): 811-820.

Kelley, L. A. and M. J. Sternberg (2009). "Protein structure prediction on the Web: a case study using the Phyre server." Nat Protoc **4**(3): 363-371.

Kelly, A. E. and H. Funabiki (2009). "Correcting aberrant kinetochore microtubule attachments: an Aurora B-centric view." Curr Opin Cell Biol **21**(1): 51-58.

Khan, I. F., R. K. Hirata and D. W. Russell (2011). "AAV-mediated gene targeting methods for human cells." Nat Protoc **6**(4): 482-501.

Kim, M. Y., E. Bucciarelli, D. G. Morton, B. C. Williams, K. Blake-Hodek, C. Pellacani, J. R. Von Stetina, X. Hu, M. P. Somma, D. Drummond-Barbosa and M. L. Goldberg (2012). "Bypassing the Greatwall-Endosulfine pathway: plasticity of a pivotal cell-cycle regulatory module in Drosophila melanogaster and Caenorhabditis elegans." Genetics **191**(4): 1181-1197.

Kim, S. Y. and J. E. Ferrell, Jr. (2007). "Substrate competition as a source of ultrasensitivity in the inactivation of Wee1." Cell **128**(6): 1133-1145.

Kimmins, S., C. Crosio, N. Kotaja, J. Hirayama, L. Monaco, C. Hoog, M. van Duin, J. A. Gossen and P. Sassone-Corsi (2007). "Differential functions of the Aurora-B and Aurora-C kinases in mammalian spermatogenesis." Mol Endocrinol **21**(3): 726-739.

Kitajima, T. S., T. Sakuno, K. Ishiguro, S. Iemura, T. Natsume, S. A. Kawashima and Y. Watanabe (2006). "Shugoshin collaborates with protein phosphatase 2A to protect cohesin." Nature **441**(7089): 46-52.

Klotzbucher, A., E. Stewart, D. Harrison and T. Hunt (1996). "The 'destruction box' of cyclin A allows B-type cyclins to be ubiquitinated, but not efficiently destroyed." EMBO J **15**(12): 3053-3064.

Knighton, D. R., J. H. Zheng, L. F. Ten Eyck, V. A. Ashford, N. H. Xuong, S. S. Taylor and J. M. Sowadski (1991). "Crystal structure of the catalytic subunit of cyclic

adenosine monophosphate-dependent protein kinase." Science **253**(5018): 407-414.

Knudsen, E. S. and K. E. Knudsen (2006). "Retinoblastoma tumor suppressor: where cancer meets the cell cycle." Exp Biol Med (Maywood) **231**(7): 1271-1281.

Kobayashi, T. and P. Cohen (1999). "Activation of serum- and glucocorticoid-regulated protein kinase by agonists that activate phosphatidylinositide 3-kinase is mediated by 3-phosphoinositide-dependent protein kinase-1 (PDK1) and PDK2." Biochem J **339 (Pt 2)**: 319-328.

Kohli, M., C. Rago, C. Lengauer, K. W. Kinzler and B. Vogelstein (2004). "Facile methods for generating human somatic cell gene knockouts using recombinant adeno-associated viruses." Nucleic Acids Res **32**(1): e3.

Kojima, K., M. Shimanuki, M. Shikami, M. Andreeff and H. Nakakuma (2009). "Cyclin-dependent kinase 1 inhibitor RO-3306 enhances p53-mediated Bax activation and mitochondrial apoptosis in AML." Cancer Sci **100**(6): 1128-1136.

Komander, D., G. Kular, M. Deak, D. R. Alessi and D. M. van Aalten (2005). "Role of T-loop phosphorylation in PDK1 activation, stability, and substrate binding." J Biol Chem **280**(19): 18797-18802.

Kozar, K., M. A. Ciemerych, V. I. Rebel, H. Shigematsu, A. Zagozdzon, E. Sicinska, Y. Geng, Q. Yu, S. Bhattacharya, R. T. Bronson, K. Akashi and P. Sicinski (2004). "Mouse development and cell proliferation in the absence of D-cyclins." Cell **118**(4): 477-491.

Kramer, A., C. P. Carstens, W. W. Wasserman and W. E. Fahl (1997). "CBP/cycA, a CCAAT-binding protein necessary for adhesion-dependent cyclin A transcription, consists of NF-Y and a novel Mr 115,000 subunit." Cancer Res **57**(22): 5117-5121.

Krasinska, L., M. R. Domingo-Sananes, O. Kapuy, N. Parisis, B. Harker, G. Moorhead, M. Rossignol, B. Novak and D. Fisher (2011). "Protein phosphatase 2A controls the order and dynamics of cell-cycle transitions." Mol Cell **44**(3): 437-450.

Krastev, D. B., M. Slabicki, M. Paszkowski-Rogacz, N. C. Hubner, M. Junqueira, A. Shevchenko, M. Mann, K. M. Neugebauer and F. Buchholz (2011). "A systematic RNAi synthetic interaction screen reveals a link between p53 and snoRNP assembly." Nat Cell Biol **13**(7): 809-818.

Krek, W. and E. A. Nigg (1991). "Mutations of p34cdc2 phosphorylation sites induce premature mitotic events in HeLa cells: evidence for a double block to p34cdc2 kinase activation in vertebrates." EMBO J **10**(11): 3331-3341.

Kumagai, A. and W. G. Dunphy (1991). "The cdc25 protein controls tyrosine dephosphorylation of the cdc2 protein in a cell-free system." Cell **64**(5): 903-914.

Kumagai, A. and W. G. Dunphy (1992). "Regulation of the cdc25 protein during the cell cycle in Xenopus extracts." Cell **70**(1): 139-151.

Kumagai, A., A. Shevchenko and W. G. Dunphy (2010). "Treslin collaborates with TopBP1 in triggering the initiation of DNA replication." Cell **140**(3): 349-359.

La Terra, S., C. N. English, P. Hergert, B. F. McEwen, G. Sluder and A. Khodjakov (2005). "The de novo centriole assembly pathway in HeLa cells: cell cycle progression and centriole assembly/maturation." J Cell Biol **168**(5): 713-722.

LaBaer, J., M. D. Garrett, L. F. Stevenson, J. M. Slingerland, C. Sandhu, H. S. Chou, A. Fattaey and E. Harlow (1997). "New functional activities for the p21 family of CDK inhibitors." Genes Dev **11**(7): 847-862.

Labbe, C., P. Goyette, C. Lefebvre, C. Stevens, T. Green, M. K. Tello-Ruiz, Z. Cao, A. L. Landry, J. Stempak, V. Annese, A. Latiano, S. R. Brant, R. H. Duerr, K. D. Taylor, J. H. Cho, A. H. Steinhart, M. J. Daly, M. S. Silverberg, R. J. Xavier and J. D. Rioux (2008). "MAST3: a novel IBD risk factor that modulates TLR4 signaling." Genes Immun **9**(7): 602-612.

Labbe, J. C., M. G. Lee, P. Nurse, A. Picard and M. Doree (1988). "Activation at M-phase of a protein kinase encoded by a starfish homologue of the cell cycle control gene cdc2+." Nature **335**(6187): 251-254.

Lane, H. A. and E. A. Nigg (1996). "Antibody microinjection reveals an essential role for human polo-like kinase 1 (Plk1) in the functional maturation of mitotic centrosomes." J Cell Biol **135**(6 Pt 2): 1701-1713.

Langan, T. A., J. Gautier, M. Lohka, R. Hollingsworth, S. Moreno, P. Nurse, J. Maller and R. A. Sclafani (1989). "Mammalian growth-associated H1 histone kinase: a homolog of cdc2+/CDC28 protein kinases controlling mitotic entry in yeast and frog cells." Mol Cell Biol **9**(9): 3860-3868.

Laoukili, J., M. R. Kooistra, A. Bras, J. Kauw, R. M. Kerkhoven, A. Morrison, H. Clevers and R. H. Medema (2005). "FoxM1 is required for execution of the mitotic programme and chromosome stability." Nat Cell Biol **7**(2): 126-136.

Larkin, M. A., G. Blackshields, N. P. Brown, R. Chenna, P. A. McGettigan, H. McWilliam, F. Valentin, I. M. Wallace, A. Wilm, R. Lopez, J. D. Thompson, T. J. Gibson and D. G. Higgins (2007). "Clustal W and Clustal X version 2.0." Bioinformatics **23**(21): 2947-2948.

Lee, M. G. and P. Nurse (1987). "Complementation used to clone a human homologue of the fission yeast cell cycle control gene cdc2." Nature **327**(6117): 31-35.

Lenart, P., M. Petronczki, M. Steegmaier, B. Di Fiore, J. J. Lipp, M. Hoffmann, W. J. Rettig, N. Kraut and J. M. Peters (2007). "The small-molecule inhibitor BI 2536 reveals novel insights into mitotic roles of polo-like kinase 1." Curr Biol **17**(4): 304-315.

Lens, S. M., E. E. Voest and R. H. Medema (2010). "Shared and separate functions of polo-like kinases and aurora kinases in cancer." Nat Rev Cancer **10**(12): 825-841.

Li, C. J. and M. L. DePamphilis (2002). "Mammalian Orc1 protein is selectively released from chromatin and ubiquitinated during the S-to-M transition in the cell division cycle." Mol Cell Biol **22**(1): 105-116.

Li, L., M. Ljungman and J. E. Dixon (2000). "The human Cdc14 phosphatases interact with and dephosphorylate the tumor suppressor protein p53." J Biol Chem **275**(4): 2410-2414.

Li, M. and P. Zhang (2009). "The function of APC/CCdh1 in cell cycle and beyond." Cell Div **4**: 2.

Lindqvist, A., H. Kallstrom, A. Lundgren, E. Barsoum and C. K. Rosenthal (2005). "Cdc25B cooperates with Cdc25A to induce mitosis but has a unique role in activating cyclin B1-Cdk1 at the centrosome." J Cell Biol **171**(1): 35-45.

Lindqvist, A., V. Rodriguez-Bravo and R. H. Medema (2009). "The decision to enter mitosis: feedback and redundancy in the mitotic entry network." J Cell Biol **185**(2): 193-202.

Littlepage, L. E., H. Wu, T. Andresson, J. K. Deanehan, L. T. Amundadottir and J. V. Ruderman (2002). "Identification of phosphorylated residues that affect the activity of the mitotic kinase Aurora-A." Proc Natl Acad Sci U S A **99**(24): 15440-15445.

Liu, D., M. Vleugel, C. B. Backer, T. Hori, T. Fukagawa, I. M. Cheeseman and M. A. Lampson (2010). "Regulated targeting of protein phosphatase 1 to the outer kinetochore by KNL1 opposes Aurora B kinase." J Cell Biol **188**(6): 809-820.

Liu, F., J. J. Stanton, Z. Wu and H. Piwnica-Worms (1997). "The human Myt1 kinase preferentially phosphorylates Cdc2 on threonine 14 and localizes to the endoplasmic reticulum and Golgi complex." Mol Cell Biol **17**(2): 571-583.

Ljungman, M. (2009). "Targeting the DNA damage response in cancer." Chem Rev **109**(7): 2929-2950.

Lobjois, V., D. Jullien, J. P. Bouche and B. Ducommun (2009). "The polo-like kinase 1 regulates CDC25B-dependent mitosis entry." Biochim Biophys Acta **1793**(3): 462-468.

Lohka, M. J., M. K. Hayes and J. L. Maller (1988). "Purification of maturation-promoting factor, an intracellular regulator of early mitotic events." Proc Natl Acad Sci U S A **85**(9): 3009-3013.

Lolli, G. and L. N. Johnson (2005). "CAK-Cyclin-dependent Activating Kinase: a key kinase in cell cycle control and a target for drugs?" Cell Cycle **4**(4): 572-577.

Lorca, T., C. Bernis, S. Vigneron, A. Burgess, E. Brioudes, J. C. Labbe and A. Castro (2010). "Constant regulation of both the MPF amplification loop and the Greatwall-PP2A pathway is required for metaphase II arrest and correct entry into the first embryonic cell cycle." J Cell Sci **123**(Pt 13): 2281-2291.

Lorca, T. and A. Castro (2012). "The Greatwall kinase: a new pathway in the control of the cell cycle." Oncogene.

Lu, L. Y., J. L. Wood, K. Minter-Dykhouse, L. Ye, T. L. Saunders, X. Yu and J. Chen (2008). "Polo-like kinase 1 is essential for early embryonic development and tumor suppression." Mol Cell Biol **28**(22): 6870-6876.

Lundberg, A. S. and R. A. Weinberg (1998). "Functional inactivation of the retinoblastoma protein requires sequential modification by at least two distinct cyclin-cdk complexes." Mol Cell Biol **18**(2): 753-761.

Luo, X., Z. Tang, J. Rizo and H. Yu (2002). "The Mad2 spindle checkpoint protein undergoes similar major conformational changes upon binding to either Mad1 or Cdc20." Mol Cell **9**(1): 59-71.

Macaluso, M., M. Montanari and A. Giordano (2006). "Rb family proteins as modulators of gene expression and new aspects regarding the interaction with chromatin remodeling enzymes." Oncogene **25**(38): 5263-5267.

Macurek, L., A. Lindqvist, D. Lim, M. A. Lampson, R. Klompmaker, R. Freire, C. Clouin, S. S. Taylor, M. B. Yaffe and R. H. Medema (2008). "Polo-like kinase-1

is activated by aurora A to promote checkpoint recovery." Nature **455**(7209): 119-123.

Mailand, N., C. Lukas, B. K. Kaiser, P. K. Jackson, J. Bartek and J. Lukas (2002a). "Deregulated human Cdc14A phosphatase disrupts centrosome separation and chromosome segregation." Nat Cell Biol **4**(4): 317-322.

Mailand, N., A. V. Podtelejnikov, A. Groth, M. Mann, J. Bartek and J. Lukas (2002b). "Regulation of G(2)/M events by Cdc25A through phosphorylation-dependent modulation of its stability." EMBO J **21**(21): 5911-5920.

Makela, T. P., J. P. Tassan, E. A. Nigg, S. Frutiger, G. J. Hughes and R. A. Weinberg (1994). "A cyclin associated with the CDK-activating kinase MO15." Nature **371**(6494): 254-257.

Malumbres, M. (2010). "Marcos Malumbres on CDK Inhibitors in Cancer Therapy." ScienceWatch.com, July 2010, from http://sciencewatch.com/dr/fmf/2010/10julfmf/10julfmfMalu/.

Malumbres, M. (2011). "Physiological relevance of cell cycle kinases." Physiol Rev **91**(3): 973-1007.

Malumbres, M. and M. Barbacid (2001). "To cycle or not to cycle: a critical decision in cancer." Nat Rev Cancer **1**(3): 222-231.

Malumbres, M. and M. Barbacid (2009a). "Cell cycle, CDKs and cancer: a changing paradigm." Nat Rev Cancer **9**(3): 153-166.

Malumbres, M., E. Harlow, T. Hunt, T. Hunter, J. M. Lahti, G. Manning, D. O. Morgan, L. H. Tsai and D. J. Wolgemuth (2009b). "Cyclin-dependent kinases: a family portrait." Nat Cell Biol **11**(11): 1275-1276.

Malumbres, M., R. Sotillo, D. Santamaria, J. Galan, A. Cerezo, S. Ortega, P. Dubus and M. Barbacid (2004). "Mammalian cells cycle without the D-type cyclin-dependent kinases Cdk4 and Cdk6." Cell **118**(4): 493-504.

Mamely, I., M. A. van Vugt, V. A. Smits, J. I. Semple, B. Lemmens, A. Perrakis, R. H. Medema and R. Freire (2006). "Polo-like kinase-1 controls proteasome-dependent degradation of Claspin during checkpoint recovery." Curr Biol **16**(19): 1950-1955.

Manchado, E., M. Guillamot, G. de Carcer, M. Eguren, M. Trickey, I. Garcia-Higuera, S. Moreno, H. Yamano, M. Canamero and M. Malumbres (2010). "Targeting mitotic exit leads to tumor regression in vivo: Modulation by Cdk1, Mastl, and the PP2A/B55alpha,delta phosphatase." Cancer Cell **18**(6): 641-654.

Manning, G., D. B. Whyte, R. Martinez, T. Hunter and S. Sudarsanam (2002). "The protein kinase complement of the human genome." Science **298**(5600): 1912-1934.

Maresca, T. J. and E. D. Salmon (2009). "Intrakinetochore stretch is associated with changes in kinetochore phosphorylation and spindle assembly checkpoint activity." J Cell Biol **184**(3): 373-381.

Marumoto, T., T. Hirota, T. Morisaki, N. Kunitoku, D. Zhang, Y. Ichikawa, T. Sasayama, S. Kuninaka, T. Mimori, N. Tamaki, M. Kimura, Y. Okano and H. Saya (2002). "Roles of aurora-A kinase in mitotic entry and G2 checkpoint in mammalian cells." Genes Cells **7**(11): 1173-1182.

Masai, H., E. Matsui, Z. You, Y. Ishimi, K. Tamai and K. Arai (2000). "Human Cdc7-related kinase complex. In vitro phosphorylation of MCM by concerted actions of Cdks and Cdc7 and that of a criticial threonine residue of Cdc7 bY Cdks." J Biol Chem **275**(37): 29042-29052.

Masui, Y. and C. L. Markert (1971). "Cytoplasmic control of nuclear behavior during meiotic maturation of frog oocytes." J Exp Zool **177**(2): 129-145.

Matsusaka, T. and J. Pines (2004). "Chfr acts with the p38 stress kinases to block entry to mitosis in mammalian cells." J Cell Biol **166**(4): 507-516.

Maurer, M., T. Su, L. H. Saal, S. Koujak, B. D. Hopkins, C. R. Barkley, J. Wu, S. Nandula, B. Dutta, Y. Xie, Y. R. Chin, D. I. Kim, J. S. Ferris, S. K. Gruvberger-Saal, M. Laakso, X. Wang, L. Memeo, A. Rojtman, T. Matos, J. S. Yu, C. Cordon-Cardo, J. Isola, M. B. Terry, A. Toker, G. B. Mills, J. J. Zhao, V. V. Murty, H. Hibshoosh and R. Parsons (2009). "3-Phosphoinositide-dependent kinase 1 potentiates upstream lesions on the phosphatidylinositol 3-kinase pathway in breast carcinoma." Cancer Res **69**(15): 6299-6306.

Mazia, D. (1961). "How cells divide." Sci Am **205**: 100-120.

McGuinness, B. E., T. Hirota, N. R. Kudo, J. M. Peters and K. Nasmyth (2005). "Shugoshin prevents dissociation of cohesin from centromeres during mitosis in vertebrate cells." PLoS Biol **3**(3): e86.

Medema, R. H. (2010). "Greatwall in control of recovery." Cell Cycle **9**(21): 4264-4265.

Medema, R. H. and A. Lindqvist (2011). "Boosting and suppressing mitotic phosphorylation." Trends Biochem Sci **36**(11): 578-584.

Mendez, J. and B. Stillman (2000). "Chromatin association of human origin recognition complex, cdc6, and minichromosome maintenance proteins during the cell cycle: assembly of prereplication complexes in late mitosis." Mol Cell Biol **20**(22): 8602-8612.

Mendez, J. and B. Stillman (2003). "Perpetuating the double helix: molecular machines at eukaryotic DNA replication origins." Bioessays **25**(12): 1158-1167.

Mikhailov, A., M. Shinohara and C. L. Rieder (2005). "The p38-mediated stress-activated checkpoint. A rapid response system for delaying progression through antephase and entry into mitosis." Cell Cycle **4**(1): 57-62.

Mimura, S. and H. Takisawa (1998). "Xenopus Cdc45-dependent loading of DNA polymerase alpha onto chromatin under the control of S-phase Cdk." EMBO J **17**(19): 5699-5707.

Minshull, J., J. J. Blow and T. Hunt (1989a). "Translation of cyclin mRNA is necessary for extracts of activated xenopus eggs to enter mitosis." Cell **56**(6): 947-956.

Minshull, J., R. Golsteyn, C. S. Hill and T. Hunt (1990). "The A- and B-type cyclin associated cdc2 kinases in Xenopus turn on and off at different times in the cell cycle." EMBO J **9**(9): 2865-2875.

Minshull, J., J. Pines, R. Golsteyn, N. Standart, S. Mackie, A. Colman, J. Blow, J. V. Ruderman, M. Wu and T. Hunt (1989b). "The role of cyclin synthesis, modification and destruction in the control of cell division." J Cell Sci Suppl **12**: 77-97.

Mocciaro, A., E. Berdougo, K. Zeng, E. Black, P. Vagnarelli, W. Earnshaw, D. Gillespie, P. Jallepalli and E. Schiebel (2010). "Vertebrate cells genetically deficient for Cdc14A or Cdc14B retain DNA damage checkpoint proficiency but are impaired in DNA repair." J Cell Biol **189**(4): 631-639.

Mochida, S. and T. Hunt (2007). "Calcineurin is required to release Xenopus egg extracts from meiotic M phase." Nature **449**(7160): 336-340.

Mochida, S. and T. Hunt (2012). "Protein phosphatases and their regulation in the control of mitosis." EMBO Rep **13**(3): 197-203.

Mochida, S., S. Ikeo, J. Gannon and T. Hunt (2009). "Regulated activity of PP2A-B55 delta is crucial for controlling entry into and exit from mitosis in Xenopus egg extracts." EMBO J **28**(18): 2777-2785.

Mochida, S., S. L. Maslen, M. Skehel and T. Hunt (2010). "Greatwall phosphorylates an inhibitor of protein phosphatase 2A that is essential for mitosis." Science **330**(6011): 1670-1673.

Morgan, D. O. (2007). The Cell Cycle: Principles of Control, New Science Press Ltd.

Morrison, D. K., M. S. Murakami and V. Cleghon (2000). "Protein kinases and phosphatases in the Drosophila genome." J Cell Biol **150**(2): F57-62.

Mueller, P. R., T. R. Coleman, A. Kumagai and W. G. Dunphy (1995). "Myt1: a membrane-associated inhibitory kinase that phosphorylates Cdc2 on both threonine-14 and tyrosine-15." Science **270**(5233): 86-90.

Murphy, M., M. G. Stinnakre, C. Senamaud-Beaufort, N. J. Winston, C. Sweeney, M. Kubelka, M. Carrington, C. Brechot and J. Sobczak-Thepot (1997). "Delayed early embryonic lethality following disruption of the murine cyclin A2 gene." Nat Genet **15**(1): 83-86.

Murray, A. W., M. J. Solomon and M. W. Kirschner (1989). "The role of cyclin synthesis and degradation in the control of maturation promoting factor activity." Nature **339**(6222): 280-286.

Murthy, K. and P. Wadsworth (2005). "Myosin-II-dependent localization and dynamics of F-actin during cytokinesis." Curr Biol **15**(8): 724-731.

Musacchio, A. and E. D. Salmon (2007). "The spindle-assembly checkpoint in space and time." Nat Rev Mol Cell Biol **8**(5): 379-393.

Nakajima, H., F. Toyoshima-Morimoto, E. Taniguchi and E. Nishida (2003). "Identification of a consensus motif for Plk (Polo-like kinase) phosphorylation reveals Myt1 as a Plk1 substrate." J Biol Chem **278**(28): 25277-25280.

Nasheuer, H. P., A. Moore, A. F. Wahl and T. S. Wang (1991). "Cell cycle-dependent phosphorylation of human DNA polymerase alpha." J Biol Chem **266**(12): 7893-7903.

Nebreda, A. R. and A. Porras (2000). "p38 MAP kinases: beyond the stress response." Trends Biochem Sci **25**(6): 257-260.

Neef, R., U. Gruneberg, R. Kopajtich, X. Li, E. A. Nigg, H. Sillje and F. A. Barr (2007). "Choice of Plk1 docking partners during mitosis and cytokinesis is controlled by the activation state of Cdk1." Nat Cell Biol **9**(4): 436-444.

Nguyen, T. B., K. Manova, P. Capodieci, C. Lindon, S. Bottega, X. Y. Wang, J. Refik-Rogers, J. Pines, D. J. Wolgemuth and A. Koff (2002). "Characterization and

expression of mammalian cyclin b3, a prepachytene meiotic cyclin." J Biol Chem **277**(44): 41960-41969.

Nguyen, V. Q., C. Co and J. J. Li (2001). "Cyclin-dependent kinases prevent DNA re-replication through multiple mechanisms." Nature **411**(6841): 1068-1073.

Nigg, E. A. (2001). "Mitotic kinases as regulators of cell division and its checkpoints." Nat Rev Mol Cell Biol **2**(1): 21-32.

Nilsson, J., M. Yekezare, J. Minshull and J. Pines (2008). "The APC/C maintains the spindle assembly checkpoint by targeting Cdc20 for destruction." Nat Cell Biol **10**(12): 1411-1420.

Niswender, C. M., R. W. Ishihara, L. M. Judge, C. Zhang, K. M. Shokat and G. S. McKnight (2002). "Protein engineering of protein kinase A catalytic subunits results in the acquisition of novel inhibitor sensitivity." J Biol Chem **277**(32): 28916-28922.

Nolen, B., S. Taylor and G. Ghosh (2004). "Regulation of protein kinases; controlling activity through activation segment conformation." Mol Cell **15**(5): 661-675.

Nurse, P. and P. Thuriaux (1980). "Regulatory genes controlling mitosis in the fission yeast Schizosaccharomyces pombe." Genetics **96**(3): 627-637.

Nurse, P., P. Thuriaux and K. Nasmyth (1976). "Genetic control of the cell division cycle in the fission yeast Schizosaccharomyces pombe." Mol Gen Genet **146**(2): 167-178.

O'Farrell, P. H. (2001). "Triggering the all-or-nothing switch into mitosis." Trends Cell Biol **11**(12): 512-519.

Okuzumi, T., D. Fiedler, C. Zhang, D. C. Gray, B. Aizenstein, R. Hoffman and K. M. Shokat (2009). "Inhibitor hijacking of Akt activation." Nat Chem Biol **5**(7): 484-493.

Ortega, S., I. Prieto, J. Odajima, A. Martin, P. Dubus, R. Sotillo, J. L. Barbero, M. Malumbres and M. Barbacid (2003). "Cyclin-dependent kinase 2 is essential for meiosis but not for mitotic cell division in mice." Nat Genet **35**(1): 25-31.

Pacek, M. and J. C. Walter (2004). "A requirement for MCM7 and Cdc45 in chromosome unwinding during eukaryotic DNA replication." EMBO J **23**(18): 3667-3676.

Pardee, A. B. (1974). "A restriction point for control of normal animal cell proliferation." Proc Natl Acad Sci U S A **71**(4): 1286-1290.

Parisi, T., A. R. Beck, N. Rougier, T. McNeil, L. Lucian, Z. Werb and B. Amati (2003). "Cyclins E1 and E2 are required for endoreplication in placental trophoblast giant cells." EMBO J **22**(18): 4794-4803.

Park, B. H., B. Vogelstein and K. W. Kinzler (2001). "Genetic disruption of PPARdelta decreases the tumorigenicity of human colon cancer cells." Proc Natl Acad Sci U S A **98**(5): 2598-2603.

Park, J., M. L. Leong, P. Buse, A. C. Maiyar, G. L. Firestone and B. A. Hemmings (1999). "Serum and glucocorticoid-inducible kinase (SGK) is a target of the PI 3-kinase-stimulated signaling pathway." EMBO J **18**(11): 3024-3033.

Parker, L. L. and H. Piwnica-Worms (1992). "Inactivation of the p34cdc2-cyclin B complex by the human WEE1 tyrosine kinase." Science **257**(5078): 1955-1957.

Pearce, L. R., D. Komander and D. R. Alessi (2010). "The nuts and bolts of AGC protein kinases." Nat Rev Mol Cell Biol **11**(1): 9-22.

Peng, A., L. Wang and L. A. Fisher (2011). "Greatwall and Polo-like kinase 1 coordinate to promote checkpoint recovery." J Biol Chem **286**(33): 28996-29004.

Peng, A., T. M. Yamamoto, M. L. Goldberg and J. L. Maller (2010). "A novel role for greatwall kinase in recovery from DNA damage." Cell Cycle **9**(21): 4364-4369.

Perez de Castro, I., G. de Carcer, G. Montoya and M. Malumbres (2008). "Emerging cancer therapeutic opportunities by inhibiting mitotic kinases." Curr Opin Pharmacol **8**(4): 375-383.

Petri, E. T., A. Errico, L. Escobedo, T. Hunt and R. Basavappa (2007). "The crystal structure of human cyclin B." Cell Cycle **6**(11): 1342-1349.

Peyrollier, K., L. Heron, A. Virsolvy-Vergine, A. Le Cam and D. Bataille (1996). "Alpha endosulfine is a novel molecule, structurally related to a family of phosphoproteins." Biochem Biophys Res Commun **223**(3): 583-586.

Pfleger, C. M. and M. W. Kirschner (2000). "The KEN box: an APC recognition signal distinct from the D box targeted by Cdh1." Genes Dev **14**(6): 655-665.

Picard, A., J. P. Capony, D. L. Brautigan and M. Doree (1989). "Involvement of protein phosphatases 1 and 2A in the control of M phase-promoting factor activity in starfish." J Cell Biol **109**(6 Pt 2): 3347-3354.

Picard, A., J. C. Labbe, H. Barakat, J. C. Cavadore and M. Doree (1991). "Okadaic acid mimics a nuclear component required for cyclin B-cdc2 kinase microinjection to drive starfish oocytes into M phase." J Cell Biol **115**(2): 337-344.

Pines, J. and I. Hagan (2011). "The Renaissance or the cuckoo clock." Philos Trans R Soc Lond B Biol Sci **366**(1584): 3625-3634.

Pines, J. and T. Hunt (1987). "Molecular cloning and characterization of the mRNA for cyclin from sea urchin eggs." EMBO J **6**(10): 2987-2995.

Pines, J. and T. Hunter (1991). "Human cyclins A and B1 are differentially located in the cell and undergo cell cycle-dependent nuclear transport." J Cell Biol **115**(1): 1-17.

Pines, J. and C. L. Rieder (2001). "Re-staging mitosis: a contemporary view of mitotic progression." Nat Cell Biol **3**(1): E3-6.

Plowman, G. D., S. Sudarsanam, J. Bingham, D. Whyte and T. Hunter (1999). "The protein kinases of Caenorhabditis elegans: a model for signal transduction in multicellular organisms." Proc Natl Acad Sci U S A **96**(24): 13603-13610.

Pomerening, J. R., J. A. Ubersax and J. E. Ferrell, Jr. (2008). "Rapid cycling and precocious termination of G1 phase in cells expressing CDK1AF." Mol Biol Cell **19**(8): 3426-3441.

Porteus, M. H., T. Cathomen, M. D. Weitzman and D. Baltimore (2003). "Efficient gene targeting mediated by adeno-associated virus and DNA double-strand breaks." Mol Cell Biol **23**(10): 3558-3565.

Prosperi, E., A. I. Scovassi, L. A. Stivala and L. Bianchi (1994). "Proliferating cell nuclear antigen bound to DNA synthesis sites: phosphorylation and association with cyclin D1 and cyclin A." Exp Cell Res **215**(2): 257-262.

Qi, W., Z. Tang and H. Yu (2006). "Phosphorylation- and polo-box-dependent binding of Plk1 to Bub1 is required for the kinetochore localization of Plk1." Mol Biol Cell **17**(8): 3705-3716.

Queralt, E. and F. Uhlmann (2008). "Cdk-counteracting phosphatases unlock mitotic exit." Curr Opin Cell Biol **20**(6): 661-668.

Rane, S. G., P. Dubus, R. V. Mettus, E. J. Galbreath, G. Boden, E. P. Reddy and M. Barbacid (1999). "Loss of Cdk4 expression causes insulin-deficient diabetes and Cdk4 activation results in beta-islet cell hyperplasia." Nat Genet **22**(1): 44-52.

Rangone, H., E. Wegel, M. K. Gatt, E. Yeung, A. Flowers, J. Debski, M. Dadlez, V. Janssens, A. T. Carpenter and D. M. Glover (2011). "Suppression of scant identifies Endos as a substrate of greatwall kinase and a negative regulator of protein phosphatase 2A in mitosis." PLoS Genet **7**(8): e1002225.

Rao, P. N. and R. T. Johnson (1970). "Mammalian cell fusion: studies on the regulation of DNA synthesis and mitosis." Nature **225**(5228): 159-164.

Remus, D. and J. F. Diffley (2009). "Eukaryotic DNA replication control: lock and load, then fire." Curr Opin Cell Biol **21**(6): 771-777.

Rieder, C. L. (2011). "Mitosis in vertebrates: the G2/M and M/A transitions and their associated checkpoints." Chromosome Res **19**(3): 291-306.

Rieder, C. L. and R. Cole (2000). "Microscopy-induced radiation damage, microtubules, and progression through the terminal stage of G2 (prophase) in vertebrate somatic cells." Cold Spring Harb Symp Quant Biol **65**: 369-376.

Rieder, C. L., R. W. Cole, A. Khodjakov and G. Sluder (1995). "The checkpoint delaying anaphase in response to chromosome monoorientation is mediated by an inhibitory signal produced by unattached kinetochores." J Cell Biol **130**(4): 941-948.

Rieder, C. L., A. Schultz, R. Cole and G. Sluder (1994). "Anaphase onset in vertebrate somatic cells is controlled by a checkpoint that monitors sister kinetochore attachment to the spindle." J Cell Biol **127**(5): 1301-1310.

Robinson, D. R., S. Kalyana-Sundaram, Y. M. Wu, S. Shankar, X. Cao, B. Ateeq, I. A. Asangani, M. Iyer, C. A. Maher, C. S. Grasso, R. J. Lonigro, M. Quist, J. Siddiqui, R. Mehra, X. Jing, T. J. Giordano, M. S. Sabel, C. G. Kleer, N. Palanisamy, R. Natrajan, M. B. Lambros, J. S. Reis-Filho, C. Kumar-Sinha and A. M. Chinnaiyan (2011). "Functionally recurrent rearrangements of the MAST kinase and Notch gene families in breast cancer." Nat Med **17**(12): 1646-1651.

Rodier, G., P. Coulombe, P. L. Tanguay, C. Boutonnet and S. Meloche (2008). "Phosphorylation of Skp2 regulated by CDK2 and Cdc14B protects it from degradation by APC(Cdh1) in G1 phase." EMBO J **27**(4): 679-691.

Rosenberg, J. S., F. R. Cross and H. Funabiki (2011). "KNL1/Spc105 recruits PP1 to silence the spindle assembly checkpoint." Curr Biol **21**(11): 942-947.

Ruchaud, S., M. Carmena and W. C. Earnshaw (2007). "Chromosomal passengers: conducting cell division." Nat Rev Mol Cell Biol **8**(10): 798-812.

Russell, D. W. and R. K. Hirata (1998). "Human gene targeting by viral vectors." Nat Genet **18**(4): 325-330.

Russo, A. A., P. D. Jeffrey, A. K. Patten, J. Massague and N. P. Pavletich (1996a). "Crystal structure of the p27Kip1 cyclin-dependent-kinase inhibitor bound to the cyclin A-Cdk2 complex." Nature **382**(6589): 325-331.

Russo, A. A., P. D. Jeffrey and N. P. Pavletich (1996b). "Structural basis of cyclin-dependent kinase activation by phosphorylation." Nat Struct Biol **3**(8): 696-700.

Sabbattini, P., C. Canzonetta, M. Sjoberg, S. Nikic, A. Georgiou, G. Kemball-Cook, H. W. Auner and N. Dillon (2007). "A novel role for the Aurora B kinase in epigenetic marking of silent chromatin in differentiated postmitotic cells." EMBO J **26**(22): 4657-4669.

Sakaguchi, K., J. E. Herrera, S. Saito, T. Miki, M. Bustin, A. Vassilev, C. W. Anderson and E. Appella (1998). "DNA damage activates p53 through a phosphorylation-acetylation cascade." Genes Dev **12**(18): 2831-2841.

Salsi, V., G. Caretti, M. Wasner, W. Reinhard, U. Haugwitz, K. Engeland and R. Mantovani (2003). "Interactions between p300 and multiple NF-Y trimers govern cyclin B2 promoter function." J Biol Chem **278**(9): 6642-6650.

Sano, H., S. Kane, E. Sano, C. P. Miinea, J. M. Asara, W. S. Lane, C. W. Garner and G. E. Lienhard (2003). "Insulin-stimulated phosphorylation of a Rab GTPase-activating protein regulates GLUT4 translocation." J Biol Chem **278**(17): 14599-14602.

Santaguida, S., C. Vernieri, F. Villa, A. Ciliberto and A. Musacchio (2011). "Evidence that Aurora B is implicated in spindle checkpoint signalling independently of error correction." EMBO J **30**(8): 1508-1519.

Santamaria, D., C. Barriere, A. Cerqueira, S. Hunt, C. Tardy, K. Newton, J. F. Caceres, P. Dubus, M. Malumbres and M. Barbacid (2007). "Cdk1 is sufficient to drive the mammalian cell cycle." Nature **448**(7155): 811-815.

Sasai, K., H. Katayama, D. L. Stenoien, S. Fujii, R. Honda, M. Kimura, Y. Okano, M. Tatsuka, F. Suzuki, E. A. Nigg, W. C. Earnshaw, W. R. Brinkley and S. Sen (2004). "Aurora-C kinase is a novel chromosomal passenger protein that can complement Aurora-B kinase function in mitotic cells." Cell Motil Cytoskeleton **59**(4): 249-263.

Satyanarayana, A., C. Berthet, J. Lopez-Molina, V. Coppola, L. Tessarollo and P. Kaldis (2008). "Genetic substitution of Cdk1 by Cdk2 leads to embryonic lethality and loss of meiotic function of Cdk2." Development **135**(20): 3389-3400.

Sauvageau, M. and G. Sauvageau (2008). "Polycomb group genes: keeping stem cell activity in balance." PLoS Biol **6**(4): e113.

Schafer, K. A. (1998). "The Cell Cycle: A Review." Veterinary Pathology **35**(6): 461-478.

Schmitz, M. H., M. Held, V. Janssens, J. R. Hutchins, O. Hudecz, E. Ivanova, J. Goris, L. Trinkle-Mulcahy, A. I. Lamond, I. Poser, A. A. Hyman, K. Mechtler, J. M. Peters and D. W. Gerlich (2010). "Live-cell imaging RNAi screen identifies PP2A-B55alpha and importin-beta1 as key mitotic exit regulators in human cells." Nat Cell Biol **12**(9): 886-893.

Schulze, A., K. Zerfass, D. Spitkovsky, S. Middendorp, J. Berges, K. Helin, P. Jansen-Durr and B. Henglein (1995). "Cell cycle regulation of the cyclin A gene promoter is mediated by a variant E2F site." Proc Natl Acad Sci U S A **92**(24): 11264-11268.

Sciortino, S., A. Gurtner, I. Manni, G. Fontemaggi, A. Dey, A. Sacchi, K. Ozato and G. Piaggio (2001). "The cyclin B1 gene is actively transcribed during mitosis in HeLa cells." EMBO Rep **2**(11): 1018-1023.

Scolnick, D. M. and T. D. Halazonetis (2000). "Chfr defines a mitotic stress checkpoint that delays entry into metaphase." Nature **406**(6794): 430-435.

Scutt, P. J., M. L. Chu, D. A. Sloane, M. Cherry, C. R. Bignell, D. H. Williams and P. A. Eyers (2009). "Discovery and exploitation of inhibitor-resistant aurora and polo kinase mutants for the analysis of mitotic networks." J Biol Chem **284**(23): 15880-15893.

Seki, A., J. A. Coppinger, C. Y. Jang, J. R. Yates and G. Fang (2008). "Bora and the kinase Aurora a cooperatively activate the kinase Plk1 and control mitotic entry." Science **320**(5883): 1655-1658.

Sherr, C. J. and J. M. Roberts (1995). "Inhibitors of mammalian G1 cyclin-dependent kinases." Genes Dev **9**(10): 1149-1163.

Sherr, C. J. and J. M. Roberts (1999). "CDK inhibitors: positive and negative regulators of G1-phase progression." Genes Dev **13**(12): 1501-1512.

Shreeram, S., W. K. Hee and D. V. Bulavin (2008). "Cdc25A serine 123 phosphorylation couples centrosome duplication with DNA replication and regulates tumorigenesis." Mol Cell Biol **28**(24): 7442-7450.

Sif, S., P. T. Stukenberg, M. W. Kirschner and R. E. Kingston (1998). "Mitotic inactivation of a human SWI/SNF chromatin remodeling complex." Genes Dev **12**(18): 2842-2851.

Smith, E., N. Hegarat, C. Vesely, I. Roseboom, C. Larch, H. Streicher, K. Straatman, H. Flynn, M. Skehel, T. Hirota, R. Kuriyama and H. Hochegger (2011). "Differential control of Eg5-dependent centrosome separation by Plk1 and Cdk1." EMBO J **30**(11): 2233-2245.

Smith, L. D. and R. E. Ecker (1971). "The interaction of steroids with Rana pipiens Oocytes in the induction of maturation." Dev Biol **25**(2): 232-247.

Stegmeier, F. and A. Amon (2004). "Closing mitosis: the functions of the Cdc14 phosphatase and its regulation." Annu Rev Genet **38**: 203-232.

Sturgill, T. W., L. B. Ray, E. Erikson and J. L. Maller (1988). "Insulin-stimulated MAP-2 kinase phosphorylates and activates ribosomal protein S6 kinase II." Nature **334**(6184): 715-718.

Sudakin, V., G. K. Chan and T. J. Yen (2001). "Checkpoint inhibition of the APC/C in HeLa cells is mediated by a complex of BUBR1, BUB3, CDC20, and MAD2." J Cell Biol **154**(5): 925-936.

Sudakin, V. and T. J. Yen (2007). "Targeting mitosis for anti-cancer therapy." BioDrugs **21**(4): 225-233.

Sugi, T., K. Kato, K. Kobayashi, S. Watanabe, H. Kurokawa, H. Gong, K. Pandey, H. Takemae and H. Akashi (2010). "Use of the kinase inhibitor analog 1NM-PP1 reveals a role for Toxoplasma gondii CDPK1 in the invasion step." Eukaryot Cell **9**(4): 667-670.

Sugimoto, N., Y. Tatsumi, T. Tsurumi, A. Matsukage, T. Kiyono, H. Nishitani and M. Fujita (2004). "Cdt1 phosphorylation by cyclin A-dependent kinases negatively regulates its function without affecting geminin binding." J Biol Chem **279**(19): 19691-19697.

Sunkel, C. E. and D. M. Glover (1988). "polo, a mitotic mutant of Drosophila displaying abnormal spindle poles." J Cell Sci **89 (Pt 1)**: 25-38.

Takeda, D. Y. and A. Dutta (2005). "DNA replication and progression through S phase." Oncogene **24**(17): 2827-2843.

Takizawa, C. G. and D. O. Morgan (2000). "Control of mitosis by changes in the subcellular location of cyclin-B1-Cdk1 and Cdc25C." Curr Opin Cell Biol **12**(6): 658-665.

Talarek, N., E. Cameroni, M. Jaquenoud, X. Luo, S. Bontron, S. Lippman, G. Devgan, M. Snyder, J. R. Broach and C. De Virgilio (2010). "Initiation of the TORC1-

regulated G0 program requires Igo1/2, which license specific mRNAs to evade degradation via the 5'-3' mRNA decay pathway." Mol Cell **38**(3): 345-355.

Tamaskovic, R., S. J. Bichsel and B. A. Hemmings (2003). "NDR family of AGC kinases--essential regulators of the cell cycle and morphogenesis." FEBS Lett **546**(1): 73-80.

Tanaka, S. and H. Araki (2010). "Regulation of the initiation step of DNA replication by cyclin-dependent kinases." Chromosoma **119**(6): 565-574.

Tanaka, T., D. Knapp and K. Nasmyth (1997). "Loading of an Mcm protein onto DNA replication origins is regulated by Cdc6p and CDKs." Cell **90**(4): 649-660.

Tang, Y., W. Zhao, Y. Chen, Y. Zhao and W. Gu (2008). "Acetylation is indispensable for p53 activation." Cell **133**(4): 612-626.

Tang, Z., H. Shu, W. Qi, N. A. Mahmood, M. C. Mumby and H. Yu (2006). "PP2A is required for centromeric localization of Sgo1 and proper chromosome segregation." Dev Cell **10**(5): 575-585.

Tassan, J. P., S. J. Schultz, J. Bartek and E. A. Nigg (1994). "Cell cycle analysis of the activity, subcellular localization, and subunit composition of human CAK (CDK-activating kinase)." J Cell Biol **127**(2): 467-478.

Thompson, L. J., M. Bollen and A. P. Fields (1997). "Identification of protein phosphatase 1 as a mitotic lamin phosphatase." J Biol Chem **272**(47): 29693-29697.

Thornton, T. M. and M. Rincon (2009). "Non-classical p38 map kinase functions: cell cycle checkpoints and survival." Int J Biol Sci **5**(1): 44-51.

Toyoshima-Morimoto, F., E. Taniguchi and E. Nishida (2002). "Plk1 promotes nuclear translocation of human Cdc25C during prophase." EMBO Rep **3**(4): 341-348.

Toyoshima-Morimoto, F., E. Taniguchi, N. Shinya, A. Iwamatsu and E. Nishida (2001). "Polo-like kinase 1 phosphorylates cyclin B1 and targets it to the nucleus during prophase." Nature **410**(6825): 215-220.

Toyoshima, F., T. Moriguchi, A. Wada, M. Fukuda and E. Nishida (1998). "Nuclear export of cyclin B1 and its possible role in the DNA damage-induced G2 checkpoint." EMBO J **17**(10): 2728-2735.

Trunnell, N. B., A. C. Poon, S. Y. Kim and J. E. Ferrell, Jr. (2011). "Ultrasensitivity in the Regulation of Cdc25C by Cdk1." Mol Cell **41**(3): 263-274.

Tsutsui, T., B. Hesabi, D. S. Moons, P. P. Pandolfi, K. S. Hansel, A. Koff and H. Kiyokawa (1999). "Targeted disruption of CDK4 delays cell cycle entry with enhanced p27(Kip1) activity." Mol Cell Biol **19**(10): 7011-7019.

Tumurbaatar, I., O. Cizmecioglu, I. Hoffmann, I. Grummt and R. Voit (2011). "Human Cdc14B promotes progression through mitosis by dephosphorylating Cdc25 and regulating Cdk1/cyclin B activity." PLoS One **6**(2): e14711.

Turner, W. (1890). "The Cell Theory, Past and Present." J Anat Physiol **24**(Pt 2): 253-287.

Tyler, R. K., M. L. Chu, H. Johnson, E. A. McKenzie, S. J. Gaskell and P. A. Eyers (2009). "Phosphoregulation of human Mps1 kinase." Biochem J **417**(1): 173-181.

Tyler, R. K., N. Shpiro, R. Marquez and P. A. Eyers (2007). "VX-680 inhibits Aurora A and Aurora B kinase activity in human cells." Cell Cycle **6**(22): 2846-2854.

Vader, G., R. H. Medema and S. M. Lens (2006). "The chromosomal passenger complex: guiding Aurora-B through mitosis." J Cell Biol **173**(6): 833-837.

Vagnarelli, P., D. F. Hudson, S. A. Ribeiro, L. Trinkle-Mulcahy, J. M. Spence, F. Lai, C. J. Farr, A. I. Lamond and W. C. Earnshaw (2006). "Condensin and Repo-Man-PP1 co-operate in the regulation of chromosome architecture during mitosis." Nat Cell Biol **8**(10): 1133-1142.

Valiente, M., A. Andres-Pons, B. Gomar, J. Torres, A. Gil, C. Tapparel, S. E. Antonarakis and R. Pulido (2005). "Binding of PTEN to specific PDZ domains contributes to PTEN protein stability and phosphorylation by microtubule-associated serine/threonine kinases." J Biol Chem **280**(32): 28936-28943.

van Vugt, M. A., A. Bras and R. H. Medema (2004a). "Polo-like kinase-1 controls recovery from a G2 DNA damage-induced arrest in mammalian cells." Mol Cell **15**(5): 799-811.

van Vugt, M. A. and R. H. Medema (2004b). "Checkpoint adaptation and recovery: back with Polo after the break." Cell Cycle **3**(11): 1383-1386.

van Vugt, M. A., V. A. Smits, R. Klompmaker and R. H. Medema (2001). "Inhibition of Polo-like kinase-1 by DNA damage occurs in an ATM- or ATR-dependent fashion." J Biol Chem **276**(45): 41656-41660.

van Vugt, M. A., B. C. van de Weerdt, G. Vader, H. Janssen, J. Calafat, R. Klompmaker, R. M. Wolthuis and R. H. Medema (2004c). "Polo-like kinase-1 is required for bipolar spindle formation but is dispensable for anaphase promoting

complex/Cdc20 activation and initiation of cytokinesis." J Biol Chem **279**(35): 36841-36854.

Vanoosthuyse, V. and K. G. Hardwick (2009). "A novel protein phosphatase 1-dependent spindle checkpoint silencing mechanism." Curr Biol **19**(14): 1176-1181.

Vassilev, L. T., C. Tovar, S. Chen, D. Knezevic, X. Zhao, H. Sun, D. C. Heimbrook and L. Chen (2006). "Selective small-molecule inhibitor reveals critical mitotic functions of human CDK1." Proc Natl Acad Sci U S A **103**(28): 10660-10665.

Vigneron, S., E. Brioudes, A. Burgess, J. C. Labbe, T. Lorca and A. Castro (2009). "Greatwall maintains mitosis through regulation of PP2A." EMBO J **28**(18): 2786-2793.

Vigneron, S., A. Gharbi-Ayachi, A. A. Raymond, A. Burgess, J. C. Labbe, G. Labesse, B. Monsarrat, T. Lorca and A. Castro (2011). "Characterization of the mechanisms controlling Greatwall activity." Mol Cell Biol **31**(11): 2262-2275.

Virsolvy-Vergine, A., H. Leray, S. Kuroki, B. Lupo, M. Dufour and D. Bataille (1992). "Endosulfine, an endogenous peptidic ligand for the sulfonylurea receptor: purification and partial characterization from ovine brain." Proc Natl Acad Sci U S A **89**(14): 6629-6633.

Visconti, R., L. Palazzo, R. Della Monica and D. Grieco (2012). "Fcp1-dependent dephosphorylation is required for M-phase-promoting factor inactivation at mitosis exit." Nat Commun **3**: 894.

Visintin, R., K. Craig, E. S. Hwang, S. Prinz, M. Tyers and A. Amon (1998). "The phosphatase Cdc14 triggers mitotic exit by reversal of Cdk-dependent phosphorylation." Mol Cell **2**(6): 709-718.

Voets, E. and R. M. Wolthuis (2010). "MASTL is the human orthologue of Greatwall kinase that facilitates mitotic entry, anaphase and cytokinesis." Cell Cycle **9**(17): 3591-3601.

Von Stetina, J. R., S. Tranguch, S. K. Dey, L. A. Lee, B. Cha and D. Drummond-Barbosa (2008). "alpha-Endosulfine is a conserved protein required for oocyte meiotic maturation in Drosophila." Development **135**(22): 3697-3706.

Walden, P. D. and N. J. Cowan (1993). "A novel 205-kilodalton testis-specific serine/threonine protein kinase associated with microtubules of the spermatid manchette." Mol Cell Biol **13**(12): 7625-7635.

Waldman, T., K. W. Kinzler and B. Vogelstein (1995). "p21 is necessary for the p53-mediated G1 arrest in human cancer cells." Cancer Res **55**(22): 5187-5190.

Waldman, T., C. Lengauer, K. W. Kinzler and B. Vogelstein (1996). "Uncoupling of S phase and mitosis induced by anticancer agents in cells lacking p21." Nature **381**(6584): 713-716.

Walter, A. O., W. Seghezzi, W. Korver, J. Sheung and E. Lees (2000). "The mitotic serine/threonine kinase Aurora2/AIK is regulated by phosphorylation and degradation." Oncogene **19**(42): 4906-4916.

Wang, M. L., G. Panasyuk, J. Gwalter, I. Nemazanyy, T. Fenton, V. Filonenko and I. Gout (2008). "Regulation of ribosomal protein S6 kinases by ubiquitination." Biochem Biophys Res Commun **369**(2): 382-387.

Wang, P., X. Pinson and V. Archambault (2011). "PP2A-twins is antagonized by greatwall and collaborates with polo for cell cycle progression and centrosome attachment to nuclei in drosophila embryos." PLoS Genet **7**(8): e1002227.

Wasner, M., U. Haugwitz, W. Reinhard, K. Tschop, K. Spiesbach, J. Lorenz, J. Mossner and K. Engeland (2003). "Three CCAAT-boxes and a single cell cycle genes homology region (CHR) are the major regulating sites for transcription from the human cyclin B2 promoter." Gene **312**: 225-237.

Watanabe, N., H. Arai, J. Iwasaki, M. Shiina, K. Ogata, T. Hunter and H. Osada (2005). "Cyclin-dependent kinase (CDK) phosphorylation destabilizes somatic Wee1 via multiple pathways." Proc Natl Acad Sci U S A **102**(33): 11663-11668.

Watanabe, N., H. Arai, Y. Nishihara, M. Taniguchi, N. Watanabe, T. Hunter and H. Osada (2004). "M-phase kinases induce phospho-dependent ubiquitination of somatic Wee1 by SCFbeta-TrCP." Proc Natl Acad Sci U S A **101**(13): 4419-4424.

Weiss, W. A., S. S. Taylor and K. M. Shokat (2007). "Recognizing and exploiting differences between RNAi and small-molecule inhibitors." Nat Chem Biol **3**(12): 739-744.

Williams, M. R., J. S. Arthur, A. Balendran, J. van der Kaay, V. Poli, P. Cohen and D. R. Alessi (2000). "The role of 3-phosphoinositide-dependent protein kinase 1 in activating AGC kinases defined in embryonic stem cells." Curr Biol **10**(8): 439-448.

Woo, R. A. and R. Y. Poon (2003). "Cyclin-dependent kinases and S phase control in mammalian cells." Cell Cycle **2**(4): 316-324.

Wu, C. F., R. Wang, Q. Liang, J. Liang, W. Li, S. Y. Jung, J. Qin, S. H. Lin and J. Kuang (2010). "Dissecting the M phase-specific phosphorylation of serine-proline or threonine-proline motifs." Mol Biol Cell **21**(9): 1470-1481.

Wu, J. Q., J. Y. Guo, W. Tang, C. S. Yang, C. D. Freel, C. Chen, A. C. Nairn and S. Kornbluth (2009). "PP1-mediated dephosphorylation of phosphoproteins at mitotic exit is controlled by inhibitor-1 and PP1 phosphorylation." Nat Cell Biol **11**(5): 644-651.

Wurzenberger, C. and D. W. Gerlich (2011). "Phosphatases: providing safe passage through mitotic exit." Nat Rev Mol Cell Biol **12**(8): 469-482.

Xu, X., P. J. Rochette, E. A. Feyissa, T. V. Su and Y. Liu (2009). "MCM10 mediates RECQ4 association with MCM2-7 helicase complex during DNA replication." EMBO J **28**(19): 3005-3014.

Xu, Y., Y. Xing, Y. Chen, Y. Chao, Z. Lin, E. Fan, J. W. Yu, S. Strack, P. D. Jeffrey and Y. Shi (2006). "Structure of the protein phosphatase 2A holoenzyme." Cell **127**(6): 1239-1251.

Xu, Z., P. Vagnarelli, H. Ogawa, K. Samejima and W. C. Earnshaw (2010). "Gradient of increasing Aurora B kinase activity is required for cells to execute mitosis." J Biol Chem **285**(51): 40163-40170.

Yamamoto, T. M., K. Blake-Hodek, B. C. Williams, A. L. Lewellyn, M. L. Goldberg and J. L. Maller (2011). "Regulation of Greatwall kinase during Xenopus oocyte maturation." Mol Biol Cell **22**(13): 2157-2164.

Yamano, H., J. Gannon, H. Mahbubani and T. Hunt (2004). "Cell cycle-regulated recognition of the destruction box of cyclin B by the APC/C in Xenopus egg extracts." Mol Cell **13**(1): 137-147.

Yanez, R. J. and A. C. Porter (1998). "Therapeutic gene targeting." Gene Ther **5**(2): 149-159.

Yang, J., E. S. Bardes, J. D. Moore, J. Brennan, M. A. Powers and S. Kornbluth (1998). "Control of cyclin B1 localization through regulated binding of the nuclear export factor CRM1." Genes Dev **12**(14): 2131-2143.

Yang, J., P. Cron, V. Thompson, V. M. Good, D. Hess, B. A. Hemmings and D. Barford (2002). "Molecular mechanism for the regulation of protein kinase B/Akt by hydrophobic motif phosphorylation." Mol Cell **9**(6): 1227-1240.

Yazdi, P. T., Y. Wang, S. Zhao, N. Patel, E. Y. Lee and J. Qin (2002). "SMC1 is a downstream effector in the ATM/NBS1 branch of the human S-phase checkpoint." Genes Dev **16**(5): 571-582.

Yu, J., S. L. Fleming, B. Williams, E. V. Williams, Z. Li, P. Somma, C. L. Rieder and M. L. Goldberg (2004). "Greatwall kinase: a nuclear protein required for proper chromosome condensation and mitotic progression in Drosophila." J Cell Biol **164**(4): 487-492.

Yu, J., Y. Zhao, Z. Li, S. Galas and M. L. Goldberg (2006). "Greatwall kinase participates in the Cdc2 autoregulatory loop in Xenopus egg extracts." Mol Cell **22**(1): 83-91.

Yuan, J., F. Eckerdt, J. Bereiter-Hahn, E. Kurunci-Csacsko, M. Kaufmann and K. Strebhardt (2002). "Cooperative phosphorylation including the activity of polo-like kinase 1 regulates the subcellular localization of cyclin B1." Oncogene **21**(54): 8282-8292.

Zhang, C., D. M. Kenski, J. L. Paulson, A. Bonshtien, G. Sessa, J. V. Cross, D. J. Templeton and K. M. Shokat (2005). "A second-site suppressor strategy for chemical genetic analysis of diverse protein kinases." Nat Methods **2**(6): 435-441.

Zhao, H., X. Chen, M. Gurian-West and J. M. Roberts (2012). "Loss of cyclin-dependent kinase 2 (CDK2) inhibitory phosphorylation in a CDK2AF knock-in mouse causes misregulation of DNA replication and centrosome duplication." Mol Cell Biol **32**(8): 1421-1432.

Zhao, Y., O. Haccard, R. Wang, J. Yu, J. Kuang, C. Jessus and M. L. Goldberg (2008). "Roles of Greatwall kinase in the regulation of cdc25 phosphatase." Mol Biol Cell **19**(4): 1317-1327.

Zhou, B. B. and S. J. Elledge (2000). "The DNA damage response: putting checkpoints in perspective." Nature **408**(6811): 433-439.

Zhu, W., P. H. Giangrande and J. R. Nevins (2004a). "E2Fs link the control of G1/S and G2/M transcription." EMBO J **23**(23): 4615-4626.

Zhu, Y., C. Alvarez, R. Doll, H. Kurata, X. M. Schebye, D. Parry and E. Lees (2004b). "Intra-S-phase checkpoint activation by direct CDK2 inhibition." Mol Cell Biol **24**(14): 6268-6277.

Zou, L. and B. Stillman (2000). "Assembly of a complex containing Cdc45p, replication protein A, and Mcm2p at replication origins controlled by S-phase cyclin-dependent kinases and Cdc7p-Dbf4p kinase." Mol Cell Biol **20**(9): 3086-3096.

Appendix A – NCBI Greatwall and cloned Greatwall sequence alignment

```
NCBI_MASTL         1 MDPTAGSKKEPGGGAATEEGVNRIAVPKPPSIEEFSIVKPISRGAFGKVY     50
                     ||||||||||||||||||||||||||||||||||||||||||||||||||
Cloned_GW          1 MDPTAGSKKEPGGGAATEEGVNRIAVPKPPSIEEFSIVKPISRGAFGKVY     50

NCBI_MASTL        51 LGQKGGKLYAVKVVKKADMINKNMTHQVQAERDALALSKSPFIVHLYYSL    100
                     ||||||||||||||||||||||||||||||||||||||||||||||||||
Cloned_GW         51 LGQKGGKLYAVKVVKKADMINKNMTHQVQAERDALALSKSPFIVHLYYSL    100

NCBI_MASTL       101 QSANNVYLVMEYLIGGDVKSLLHIYGYFDEEMAVKYISEVALALDYLHRH    150
                     ||||||||||||||||||||||||||||||||||||||||||||||||||
Cloned_GW        101 QSANNVYLVMEYLIGGDVKSLLHIYGYFDEEMAVKYISEVALALDYLHRH    150

NCBI_MASTL       151 GIIHRDLKPDNMLISNEGHIKLTDFGLSKVTLNRDINMMDILTTPSMAKP    200
                     ||||||||||||||||||||||||||||||||||||||||||||||||||
Cloned_GW        151 GIIHRDLKPDNMLISNEGHIKLTDFGLSKVTLNRDINMMDILTTPSMAKP    200

NCBI_MASTL       201 RQDYSRTPGQVLSLISSLGFNTPIAEKNQDPANILSACLSETSQLSQGLV    250
                     ||||||||||||||||||||||||||||||||||||||||||||||||||
Cloned_GW        201 RQDYSRTPGQVLSLISSLGFNTPIAEKNQDPANILSACLSETSQLSQGLV    250

NCBI_MASTL       251 CPMSVDQKDTTPYSSKLLKSCLETVASNPGMPVKCLTSNLLQSRKRLATS    300
                     ||||||||||||||||||||||||||||||||||||||||||||||||||
Cloned_GW        251 CPMSVDQKDTTPYSSKLLKSCLETVASNPGMPVKCLTSNLLQSRKRLATS    300

NCBI_MASTL       301 SASSQSHTFISSVESECHSSPKWEKDCQESDEALGPTMMSWNAVEKLCAK    350
                     ||||||||||||||||||||||||||||||||||||||||||||||||||
Cloned_GW        301 SASSQSHTFISSVESECHSSPKWEKDCQESDEALGPTMMSWNAVEKLCAK    350

NCBI_MASTL       351 SANAIETKGFNKKDLELALSPIHNSSALPTTGRSCVNLAKKCFSGEVSWE    400
                     ||||||||||||||||||||||||||||||||||||||||||||||||||
Cloned_GW        351 SANAIETKGFNKKDLELALSPIHNSSALPTTGRSCVNLAKKCFSGEVSWE    400

NCBI_MASTL       401 AVELDVNNINMDTDTSQLGFHQSNQWAVDSGGISEEHLGKRSLKRNFELV    450
                     ||||||||||||||||||||||||||||||||||||||||||||||||||
Cloned_GW        401 AVELDVNNINMDTDTSQLGFHQSNQWAVDSGGISEEHLGKRSLKRNFELV    450

NCBI_MASTL       451 DSSPCKKIIQNKKTCVEYKHNEMTNCYTNQNTGLTVEVQDLKLSVHKSQQ    500
                     ||||||||||||||||||||||||||||||||||||||||||||||||||
Cloned_GW        451 DSSPCKKIIQNKKTCVEYKHNEMTNCYTNQNTGLTVEVQDLKLSVHKSQQ    500

NCBI_MASTL       501 NDCANKENIVNSFTDKQQTPEKLPIPMIAKNLMCELDEDCEKNSKRDYLS    550
                     ||||||||||||||||||||||||||||||||||||||||||||||||||
Cloned_GW        501 NDCANKENIVNSFTDKQQTPEKLPIPMIAKNLMCELDEDCEKNSKRDYLS    550

NCBI_MASTL       551 SSFLCSDDDRASKNISMNSDSSFPGISIMESPLESQPLDSDRSIKESSFE    600
                     ||||||||||||||||||||||||||||||||||||||||||||||||||
Cloned_GW        551 SSFLCSDDDRASKNISMNSDSSFPGISIMESPLESQPLDSDRSIKESSFE    600

NCBI_MASTL       601 ESNIEDPLIVTPDCQEKTSPKGVENPAVQESNQKMLGPPLEVLKTLASKR    650
                     ||||||||||||||||||||||||||||||||||||||||||||||||||
Cloned_GW        601 ESNIEDPLIVTPDCQEKTSPKGVENPAVQESNQKMLGPPLEVLKTLASKR    650

NCBI_MASTL       651 NAVAFRSFNSHINASNNSEPSRMNMTSLDAMDISCAYSGSYPMAITPTQK    700
                     ||||||||||||||||||||||||||||||||||||||||||||||||||
Cloned_GW        651 NAVAFRSFNSHINASNNSEPSRMNMTSLDAMDISCAYSGSYPMAITPTQK    700

NCBI_MASTL       701 RRSCMPHQTPNQIKSGTPYRTPKSVRRGVAPVDDGRILGTPDYLAPELLL    750
                     ||||||||||||||||||||||||||||||||||||||||||||||||||
Cloned_GW        701 RRSCMPHQTPNQIKSGTPYRTPKSVRRGVAPVDDGRILGTPDYLAPELLL    750

NCBI_MASTL       751 GRAHGPAVDWWALGVCLFEFLTGIPPFNDETPQQVFQNILKRDIPWPEGE    800
                     ||||||||||||||||||||||||||||||||||||||||||||||||||
Cloned_GW        751 GRAHGPAVDWWALGVCLFEFLTGIPPFNDETPQQVFQNILKRDIPWPEGE    800

NCBI_MASTL       801 EKLSDNAQSAVEILLTIDDTKRAGMKELKRHPLFSDVDWENLQHQTMPFI    850
                     ||||||||||||||||||||||||||||||||||||||||||||||||||
Cloned_GW        801 EKLSDNAQSAVEILLTIDDTKRAGMKELKRHPLFSDVDWENLQHQTMPFI    850

NCBI_MASTL       851 PQPDDETDTSYFEARNTAQHLTVSGFSL    878
                     ||||||||||||||||||||||||||||
Cloned_GW        851 PQPDDETDTSYFEARNTAQHLTVSGFSL    878
```

Appendix A – NCBI Greatwall and cloned Greatwall sequence alignment

An EMBOSS Needle-Pairwise Sequence Alignment (PROTEIN) of the mRNA sequence of human MASTL (NCBI, Accession NM_032844) with my cloned human Greatwall cDNA (Length: 878 Identity; 878/878 (100.0%); Similarity: 878/878 (100.0%); Gaps: 0/878 (0.0%); Score: 4582.0). This cloned sequence is also confirmed by the published amino acid sequence in Vigneron *et al*. (2011).

Appendix B – Growth data and ANOVA for HEK 293T, C1 and C7 cells

Hours	HEK 293T	Clone 1	Clone 7
0	1.59687	1.053019	1.51175
3	1.65987	1.247593	1.573518
6	1.882963	1.438333	1.774796
9	2.138463	1.634685	1.96337
12	2.43363	1.682426	2.225111
15	2.738	1.887444	2.464278
18.01666667	2.990111	2.114704	2.686815
21	3.370704	2.330704	2.955518
24	3.604574	2.555055	3.234
27	4.013148	2.784555	3.46963
30	4.416667	3.203667	3.724092
33	4.851296	3.49513	4.029704
36	5.387222	3.864685	4.371537
39	5.831667	4.253444	4.815018
42.01666667	6.405185	4.65413	5.247148
45	7.11	5.111778	5.939222
48	8.085741	5.705	6.553222
51	9.148149	6.491667	7.591852
54	10.42352	7.483334	8.482593
57	12.01352	8.45	9.509259
60	13.51685	9.613148	10.70352
63	15.14278	10.91	12.04889
66.01666667	17.1787	12.50167	13.77056
69	19.32667	14.03611	15.62352
72	21.97241	16.31389	17.71722
75	24.84222	18.25037	19.98611
78	28.18019	20.63889	22.35407
81	31.47074	23.40408	25.69093
84	34.84074	26.16296	28.98241

Hours	HEK 293T	Clone 1	Clone 7
87	38.59871	29.01389	32.59982
90.01666667	42.65148	32.37704	36.2187
93	46.35833	35.3737	40.16537
96	50.43556	39.01796	44.31166
99	54.16833	42.81741	48.76593
102	58.20555	46.27982	53.09723
105	61.57963	50.13074	57.3313
108	65.22222	53.25704	61.78704
111	68.56111	57.28519	65.50741
114.0166667	71.83889	61.35185	69.38519
117	74.14815	64.41111	72.69259
120	77.40741	67.92778	76.13148
123	80.09444	71.76296	79.36296
126	82.95741	75.45926	82.38889
129	85.17963	78.47222	84.92037
132	87.44259	81.24259	87.28333
135	89.37408	83.87037	89.27778
138.0166667	91.02408	86.53889	91.06482
141	92.38703	88.63333	92.48704
144	93.65	90.51111	93.77963
147	94.65926	92.16296	94.78889
150	95.39629	93.37222	95.63519
153	96.11297	94.3037	96.44445
156	96.49815	94.96111	97.09629
159	96.76481	95.64074	97.5037
162.0166667	97.15	96.38148	97.83518
165	97.49075	96.95556	98.12778
168	97.70926	97.38889	98.32963
171	97.99815	97.68148	98.40741

Hours	HEK 293T	Clone 1	Clone 7
174	98.1463	97.9389	98.48704
177	98.34074	98.18888	98.58148
180	98.43888	98.34259	98.65
183	98.57223	98.54444	98.67407
186.0166667	98.65371	98.5537	98.70741
189	98.70556	98.62222	98.73334
192	98.75	98.57963	98.7
195	98.8	98.62778	98.71296
198	98.77962	98.64445	98.67593
201	98.84074	98.62778	98.65
204	98.89075	98.64259	98.5611
207	98.87222	98.58704	98.56667
210.0166667	98.87408	98.5463	98.46481
213	98.8963	98.55927	98.41666
216	98.90186	98.50185	98.38889
219	98.89816	98.45926	98.33889
222	98.89075	98.40371	98.34074
225	98.88519	98.32593	98.2463
228	98.87963	98.30555	98.25555
231	98.90556	98.24075	97.98334
234.0166667	98.89629	98.23148	98.09444
237	98.92963	98.22408	97.93148
240	98.89259	98.06667	97.57963
243	98.92407	98.09259	97.82778
246	98.91296	97.97593	97.57037
249	98.88333	97.91111	97.4963
252	98.88333	97.8074	97.53889
255	98.86667	97.77038	97.23704

Anova: Single Factor

SUMMARY

Groups	*Count*	*Sum*	*Average*	*Variance*
HEK 293T	86	5353.758	62.253	1592.915
Clone 1	86	5071.0771	58.966013	1657.0034
Clone 7	86	5235.1378	60.873696	1652.2761

ANOVA

Source of Variation	*SS*	*df*	*MS*	*F*	*P-value*	*Fcrit*
Between Groups	468.58584	2	234.29292	0.1433804	0.866494	3.031203
Within Groups	416686.54	255	1634.0649			
Total	417155.12	257				

Growth data of the wildtype HEK 293T cells and cell lines, C1 and C7, used for the single factor ANOVA showing no significant main effect ($F(2, 255) = 0.14$, $p = 0.87$), indicating that there is no significant difference between the growth of the wildtype HEK 293T cells and the two cell lines' growth (**Chapter 3** section **3.5**). Data was collected using the IncuCyte system from Essen Biosciences.

Appendix C – Sequence alignment of Greatwall kinases

Appendix C – Sequence alignment of Greatwall kinases

A CLUSTAL 2.1 multiple sequence alignment of human, mouse, *Xenopus* and *Drosophila* Greatwalls. The key features and significant residues of the human kinase are indicated; the N-lobe is indicted in aqua font, the C-lobe is indicated in orange font, the hydrophobic motif is indicated in pink font, and significant residues are indicated with white font. All potential CDK phosphorylation (T/S-P) sites are highlighted in aqua with confirmed sites indicated by purple font and predicted sites (by PhosphoSitePlus analysis) indicated by orange font. Lysine 72, the residue reportedly altered in the *Drosophila Scant* mutation (K72M) (Archambault *et al.* 2007), is indicated highlighted in violet. E167, the residue reportedly mutated (E167D) and responsible for Thrombocytopenia in humans (Gandhi *et al.* 2003), is indicated highlighted in orange. The gatekeeper methionine 110 is highlighted in pink and the critical phosphorylated residue of the C-terminal tail of Greatwall (S874) is indicated in violet highlight. An asterisk (*) indicates positions that have a single, fully conserved residue. A colon (:) indicates conservation between groups of strongly similar properties - scoring > 0.5 in the Gonnet PAM 250 matrix. A period (.) indicates conservation between groups of weakly similar properties - scoring =< 0.5 in the Gonnet PAM 250 matrix.

Appendix D – Exon structure of Greatwall

```
  1 MDPTAGSKKEPGGGAATEEGVNRIAVPKPPSIEEFSIVKPISRGAFGKVY
 51 LGQKGGKLYAVKVVKKADMINKNMTHQVQAERDALALSKSPFIVHLYYSL
101 QSANNVYLVMEYLIGGDVKSLLHIYGYFDEEMAVKYISEVALALDYLHRH
151 GIIHRDLKPDNMLISNEGHIKLTDFGLSKVTLNRDINMMDILTTPSMAKP
201 RQDYSRTPGQVLSLISSLGFNTPIAEKNQDPANILSACLSETSQLSQGLV
251 CPMSVDQKDTTPYSSKLLKSCLETVASNPGMPVKCLTSNLLQSRKRLATS
301 SASSQSHTFISSVESECHSSPKWEKDCQESDEALGPTMMSWNAVEKLCAK
351 SANAIETKGFNKKDLELALSPIHNSSALPTTGRSCVNLAKKCFSGEVSWE
401 AVELDVNNINMDTDTSQLGFHQSNQWAVDSGGISEEHLGKRSLKRNFELV
451 DSSPCKKIIQNKKTCVEYKHNEMTNCYTNQNTGLTVEVQDLKLSVHKSQQ
501 NDCANKENIVNSFTDKQQTPEKLPIPMIAKNLMCELDEDCEKNSKRDYLS
551 SSFLCSDDDRASKNISMNSDSSFPGISIMESPLESQPLDSDRSIKESSFE
601 ESNIEDPLIVTPDCQEKTSPKGVENPAVQESNQKMLGPPLEVLKTLASKR
651 NAVAFRSFNSHINASNNSEPSRMNMTSLDAMDISCAYSGSYPMAITPTQK
701 RRSCMPHQTPNQIKSGTPYRTPKSVRRGVAPVDDGRILGTPDYLAPELLL
751 GRAHGPAVDWWALGVCLFEFLTGIPPFNDETPQQVFQNILKRDIPWPEGE
801 EKLSDNAQSAVEILLTIDDTKRAGMKELKRHPLFSDVDWENLQHQTMPFI
851 PQPDDETDTSYFEARNTAQHLTVSGFSL
```

The 12 exons that comprise translated human Greatwall kinase. The alternate black and purple font indicates alternate exons and blue font indicates amino acids encoded across a splice junction. The N-lobe of the kinase fold is indicted in aqua highlight, the C-lobe is indicated in orange highlight and the hydrophobic motif is indicated in pink highlight.

Appendix E – Sequence alignment of human PKA and Greatwall

```
Greatwall       MDPTAGSKKEPGG-------GAATEEGVNRIAVPKP--PSIEEFSIVKPISRGAFGKVYL 51
PKA             MGNAAAAKKGSEQESVKEFLAKAKEDFLKKWESPAQNTAHLDQFERIKTLGTGSFGRVML 60
                *. :*.:** .         . *.*: :::   *    . :::*. :*.:. *:**:* *

Greatwall       G--QKGGKLYAVKVVKKADMINKNMTHQVQAERDALALSKSPFIVHLYYSLQSANNVYLV 109
PKA             VKHKETGNHYAMKILDKQKVVKLKQIEHTLNEKRILQAVNFPFLVKLEFSFKDNSNLYMV 120
                   :: *: **:*::.* .::: :  .:.  *:  *   : **:*:* :*::. .*:*:*

Greatwall       MEYLIGGDVKSLLHIYGYFDEEMAVKYISEVALALDYLHRHGIIHRDLKPDNMLISNEGH 169
PKA             MEYVPGGEMFSHLRRIGRFSEPHARFYAAQIVLTFEYLHSLDLIYRDLKPENLLIDQQGY 180
                ***: **:: * *:  * *.*  *  * :::.*:::***  .:*:*****:*:**.::*:

Greatwall       IKLTDFGLSKVTLNRDINMMDILTTPSMAKPRQDYSRTPGQVLSLISSLGFNTPIAEKNQ 229
PKA             IQVTDFGFAKRVKGR---------------------------------------------- 195
                *::****::* . .*

Greatwall       DPANILSACLSETSQLSQGLVCPMSVDQKDTTPYSSKLLKSCLETVASNPGMPVKCLTSN 289
PKA             ------------------------------------------------------------

Greatwall       LLQSRKRLATSSASSQSHTFISSVESECHSSPKWEKDCQESDEALGPTMMSWNAVEKLCA 349
PKA             ------------------------------------------------------------

Greatwall       KSANAIETKGFNKKDLELALSPIHNSSALPTTGRSCVNLAKKCFSGEVSWEAVELDVNNI 409
PKA             ------------------------------------------------------------

Greatwall       NMDTDTSQLGFHQSNQWAVDSGGISEEHLGKRSLKRNFELVDSSPCKKIIQNKKTCVEYK 469
PKA             ------------------------------------------------------------

Greatwall       HNEMTNCYTNQNTGLTVEVQDLKLSVHKSQQNDCANKENIVNSFTDKQQTPEKLPIPMIA 529
PKA             ------------------------------------------------------------

Greatwall       KNLMCELDEDCEKNSKRDYLSSSFLCSDDDRASKNISMNSDSSFPGISIMESPLESQPLD 589
PKA             ------------------------------------------------------------

Greatwall       SDRSIKESSFEESNIEDPLIVTPDCQEKTSPKGVENPAVQESNQKMLGPPLEVLKTLASK 649
PKA             ------------------------------------------------------------

Greatwall       RNAVAFRSFNSHINASNNSEPSRMNMTSLDAMDISCAYSGSYPMAITPTQKRRSCMPHQT 709
PKA             ------------------------------------------------------------

Greatwall       PNQIKSGTPYRTPKSVRRGVAPVDDGRILGTPDYLAPELLLGRAHGPAVDWWALGVCLFE 769
PKA             ------------------------TWTLCGTPEYLAPEIILSKGYNKAVDWWALGVLIYE 231
                                       : ***:*****::*.:.:. ********* ::*

Greatwall       FLTGIPPFNDETPQQVFQNILKRDIPWPEGEEKLSDNAQSAVEILLTIDDTKRAG----- 824
PKA             MAAGYPPFFADQPIQIYEKIVSGKVRFP---SHFSSDLKDLLRNLLQVDLTKRFGNLKNG 288
                : :* ***  : * *::::*:. .: :*   .::*.: :. :. ** :* *** *

Greatwall       MKELKRHPLFSDVDWENLQH--QTMPFIPQPDDETDTSYFEARNTAQHLTVSGFSL---- 878
PKA             VNDIKNHKWFATTDWIAIYQRKVEAPFIPKFKGPGDTSNFDDYEEEEIRVSINEKCGKEF 348
                ::::*.*  *: .**  : :     ****: ..  *** *:  :  :  .  . .

Greatwall       ---
PKA             SEF 351
```

Appendix E – Sequence alignment of human PKA and Greatwall

A CLUSTAL 2.1 multiple sequence alignment of human PKA and Greatwall. The key features and significant residues are indicated; the N-lobe is indicted with aqua font, the C-lobe is indicated in light orange font, the hydrophobic motif is indicated in pink font and significant residues are indicated in white font. Important phosphorylated residues are indicated by purple font and highlighted in aqua, the gatekeeper methionine (M110) is indicated highlighted in pink. An asterisk (*) indicates positions that have a single, fully conserved residue. A colon (:) indicates conservation between groups of strongly similar properties - scoring > 0.5 in the Gonnet PAM 250 matrix. A period (.) indicates conservation between groups of weakly similar properties - scoring =< 0.5 in the Gonnet PAM 250